Common pesticides and the development of Parkinson's disease

Rizwan Nisar

Thesis submitted in partial fulfilment of the requirements
of the regulations for the degree of PhD
Newcastle University
Faculty of Medical Sciences
Institute of Cellular Medicine
April 2010

For my family

Contents

Abbreviations……xii
Acknowledgments……..xiv
Authors Declaration……..xv
Courses/Conferences attended……xvi
Abstract……..xvii

Chapter 1: Introduction

1.1 Pathogenesis of Parkinson's disease

***1.1.1 Parkinson's disease*.....2**
1.1.1.1 Clinical features of Parkinson's disease 2
1.1.1.2 Pathological features of Parkinson's disease 3
***1.1.2 Development of Parkinson's disease*.....6**
1.1.2.1 Mitochondrial Dysfunction in Parkinson's disease 6
1.1.2.2 Oxidative stress and Parkinson's disease.....8
1.1.2.3 Complex I deficiency 9
1.1.2.4 Mitochondrial DNA mutations in Parkinson's disease:.....10
***1.1.3 Models of Parkinson's disease* 11**
1.1.3.1 Toxin models of Parkinson's disease.....11
1.1.3.1.1 6-OHDA.....12
1.1.3.1.1a Toxicity of 6-OHDA 12
1.1.3.1.2 MPTP 13
1.1.3.1.2a MPTP- mechanism of action.....14
1.1.3.1.2b Cellular toxicity of MPP+.....14
1.1.3.1.2c MPTP and Intracellular changes 15
1.1.3.1.3 Rotenone 16
1.1.3.1.3a Cellular toxicity of rotenone 17
1.1.3.1.3b Neurotoxicity of rotenone.....17
1.1.3.1.3c Advantages and disadvantages of rotenone ..19
1.1.3.1.4 Paraquat.....19
1.1.3.2 Transgenic models of Parkinson's disease 21
1.1.3.3 Cell-models of Parkinson's disease 23

1.2 Biochemistry of Parkinson's disease

***1.2.1: Genetic Mutations linked with Parkinson's disease*.....25**
1.2.1.1: α-synuclein.....25
1.2.1.1.1 Mutations in α-synuclein 25
1.2.1.1.2 Transgenic models of α-synuclein 27
1.2.1.2 Parkin 27
1.2.1.2 .1 Parkin function.....27
1.2.1.2.2 Mutations in *PARKIN* 28
1.2.1.3 DJ-1:.....29
1.2.1.3.1 DJ-1 and Parkinson's disease.....30
1.2.1.3.2 Mutations in *DJ-1* 30
1.2.1.4 UCHL1.....30
1.2.1.5 PINK 1 31

1.2.1.5.1 Mutations in *PINK1* 31
1.2.1.5.2 Protective effect of PINK1 31
1.2.1.6 LRRK2 32
1.2.1. 6.1 Mutations in *LRRK2* 32
1.2.1.7 ATP13A2 33

1.3 Environmental factors and Parkinson's disease

1.3.1 *Review of meta-analyses linking Parkinson's disease and exposure to pesticides* 36
1.3.1.1 Pesticide Exposure 36
1.3.1.2 Paraquat exposure 37
1.3.1.3 Honolulu-Asia Aging Study 38
1.3.1.4 Rural living and well water drinking 39

1.4 Molecular pathways of cell death in Parkinson's disease

***1.4.1 Apoptosis*..... 42**
1.4.1.1 Apoptosis and Parkinson's disease 42
1.4.1.2 Experimental models and Apoptosis 44
***1.4.2 Autophagy*..... 45**
1.4.2.1 Autophagic-Lysosomal Pathways and Parkinson's disease 47
***1.4.3 Endoplasmic reticulum (ER) Stress and PD*..... 48**

Hypothesis..... 50
Aims and Project outline 50

Chapter 2: Materials and Methods

2.1 Cell Culture

***2.1.1.1 Materials for Cell Culture*..... 53**
2.1.1.1 Cell culture Methods 53
2.1.1.2 Differentiation of SH-SY5Y cells 53
***2.2.1 Cell Viability and Cytotoxicity Assessment* 53**
2.1.2.1Chemicals 54
2.2.1.2 Trypan blue exclusion assay 55
***2.3.1 Determination of cell viability in response to cell signalling /death inhibitors* 55**
***2.4.1 Determination of reactive oxygen species generation* 56**
***2.5.1 Analysis of mitochondrial membrane potential*..... 56**
***2.6.1 Statistical analysis*..... 56**

2.2 Protein Expression

2.2.1 Acute and chronic toxin exposure **57**
2.2.1.1 Western blotting 57
2.2.1.2 Primary antibodies 58
2.2.2 Immunofluorescence **58**

2.3 Atg5 knockdown

2.3.1 ATG5 siRNA transfection and toxin treatment **59**
2.3.2 ATG5 shRNA lentiviral particles transduction and toxin treatment **59**
2.3.3 Transfection of DJ-1, Parkin and wild-type α-synuclein plasmid DNA **59**
2.3.4 Immunofluorescence analysis of lysosomal aggregation **60**

2.4 Mitochondrial assays

2.4.1 Preparation of mitochondrial fraction from SH-SY5Y cells **60**
2.4.2 Buffer preparation **60**
2.4.3 Measurement of Complex I (NADH: ubiquinone oxidoreductase) Activity **61**
2.4.4 Measurement of mitochondrial complex II (succinate: ubiquinone oxidoreductase) activity **61**
2.4.5 Citrate synthase activity **62**
2.4.6 Immunofluorescence **62**

2.5 Polymerase Chain Reaction

2.5.1 RNA extraction **63**
2.5.2 DNAse Treatment **63**
2.5.3 RNA concentration **63**
2.5.4 Reverse transcription **63**
2.5.5 RT-PCR **63**
2.5.6 Statistical analysis **64**

2.6 Stem cell methods

2.6.1 Propagation of human neural precursor stem cell **64**
2.6.2 Differentiation of hNPSC and toxin treatment **65**
2.6.3 Immunocytochemistry **65**

2.7 General Statistics **66**

Chapter 3: Cytotoxicity measurement of agrochemicals in SH-SY5Y cells

3.1.1 Introduction **67**
3.1.1.1 Aims 68
3.1.2 Methods **68**
3.1.3 Results **69**
3.1.3.1 Effect of Toxin treatment on cell viability and cytotoxicity 69

3.1.3.2 Contribution of the organic, manganese-metal and zinc-metal components of EBDC fungicides to neuronal toxicity 79
3.1.3.3 Differentiation of SH-SY5Y 81
3.1.3.4 Effect of Dopamine Transporter inhibition on cell viability 85
3.1.3.5 Effect of cell-death inhibitors on cytotoxicity 90
3.1.3.6 Effect of cell-signalling inhibitors on cytotoxicity 98
3.1.3.7 Measurement of reactive oxygen species (ROS) in toxin treated cells 99
3.1.3.8 Effect of Antioxidants on toxin induced SH-SY5Y cell death .. 104
3.1.3.9 Measurement of mitochondrial transmembrane potential 104
***3.1.4 Discussion* 109**

Chapter Four: Intracellular protein expression in toxin treated SH-SY5Y cells

4.1.1 Introduction*..... *113
4.1.1.1 Aims 113
***4.1.2 Methods* 121**
***4.1.3 Results*..... 121**
4.1.3.1 Changes in protein expression after acute toxin exposure 121
4.1.3.1.1 PARP-1, Cytochrome c 121
4.1.3.1.2 Caspase-3 131
4.1.3.1.3 p53 132
4.1.3.1.4 RIP 137
4.1.3.1.5 α-synuclein 141
4.1.3.1.6 DJ-1 145
4.1.3.1.7 Tyrosine hydroxylase (TH) 148
4.1.3.1.8 Neurofilaments 150
4.1.4 Discussion* *152

Chapter Five: Toxin treatment and autophagy

5.1.1 Introduction*..... *160
5.1.1.1 Aims 162
***5.1.2 Methods* 162**
***5.1.3. Results*..... 163**
5.1.3.1 ATG5 siRNA transfection/Lentiviral Particles Transduction 163
5.1.3.2 ATG5 knockdown and toxin treatment 165
5.1.3.3 Changes in protein expression after acute toxin exposure 169
5.1.3.4 Toxin exposure and lysosomal aggregation 177
5.1.3.5 Transfection of DJ-1, Parkin and wild-type α-synuclein plasmid DNA 182
***5.1.4 Discussion* 184**

Chapter Six: Toxin treatment and Mitochondrial Dysfunction

***6.1.1 Introduction*..... 190**
6.1.1.1 Aims 190
***6.1.2 Methods* 191**
***6.1.3 Results*..... 191**
6.1.3.1 Acute toxin exposure and complex I-II activity 191

6.1.3.2 Toxin exposure and mitochondrial distribution.....200
6.1.4 Discussion **.....203**

Chapter Seven: RT-PCR gene analysis of toxin treated SH-SY5Y cells

7.1.1 Introduction**.....209**
7.1.1.1 Aims.....209
7.1.2 Methods **.....210**
7.1.3 Results**.....211**
7.1.3.1Gene expression profile of SH-SY5Y cells after acute toxin exposure.....212
7.1.3.2Gene expression profile of SH-SY5Y cells after chronic toxin exposure.....212
7.1.4 Discussion **.....216**

Chapter Eight: Differentiation of human embryonic neural precursor stem cells

8.1.1 Introduction**.....223**
8.1.1.1Aims.....223
8.1.2 Methods **.....224**
8.1.3 Results**.....224**
8.1.3.1 Differentiation of hNPSC into cells with dopaminergic-like phenotype.....224
8.1.3.2 Toxin treatment.....231
8.1.4 Discussion **.....234**

Chapter Nine: Discussion
Discussion……...238
Major limitations.....243
Future directions 244

References……..246

List of figures

Pages

Fig 1.1: Pathological hallmarks of PD…….4
Fig 1.2: Density of pigmented neurons in the SNpc……5
Fig 1.3: The Braak staging of Parkinson's disease……..…6
Fig 1.4: Result of mitochondrial dysfunction……..……9
Fig 1.5: Oxidation of 6-OHDA……...…13
Fig 1.6: Chemical structure of MPTP……14
Fig 1.7: MPTP/ MPP+ Intracellular Pathways……..15
Fig 1.8: Chemical structure of rotenone……16
Fig 1.9: Chronic rotenone exposure……...……...17
Fig 1.10: Electron micrograph of a cytoplasmic inclusion……..……19
Fig 1.11: Structural similarity of paraquat with MPTP and MPP+ ……20
Fig 1.12: α-synuclein immunoreactivity in transgenic mice……..…….21
Fig 1.13: α-synuclein immunoreactivity in transgenic drosophila……..……22
Fig 1.14: Genetic mutations linked with neurodegeneration in PD……...……24
Fig 1.15: α-Synuclein-positive LBs in the SN of idiopathic PD brain……25
Fig 1.16: α-synuclein protein motifs……...26
Fig 1.17: LRRK2 Gene with its functional domains and sequence changes…..33
Fig 1.18: Signalling cascade in apoptotic cell death……...43
Fig 1.19: Autophagic degradation of intracellular damaged and aberrant materials……...……46

Fig 3.1: Effect of toxin treatment for 24 h on viability in SH-SY5Y cells..…71
Fig 3.2: Effect of toxin treatment for 24 h on viability in SH-SY5Y cells…..72
Fig 3.3: Effect of toxin treatment for 24 h on viability in SH-SY5Y cells.....73
Fig 3.4: Trypan blue cell counts……74
Fig 3.5: Trypan blue cell counts……75
Fig 3.6: Trypan blue cell counts……76
Fig 3.7: Chemical composition of dithiocarbamate fungicides…….79
Fig 3.8: Dose–response effect of acute mancozeb, maneb, nabam and zineb on SH-SY5Y cell-viability……...…80
Fig 3.9: Time-course of SH-SYSY cell morphology changes…….....81
Fig 3.10: Microscopic images of immunohistochemical staining of undifferentiated SH-SY5Y neural cells……82
Fig 3.11: Toxin treatment of differentiated SH-SY5Y cells……83
Fig 3.12: Toxin treatment of differentiated SH-SY5Y cells……84
Fig 3.13: Western blot analyses of DAT in SH-SY5Y cells……...…85
Fig 3.14: Effect of DAT inhibitors GBR 12909 on cytotoxicity…….....86
Fig 3.15: Effect of DAT inhibitors GBR BTCP on cytotoxicity…….....87
Fig 3.16: Effect of GBR 12909 on cytotoxicity in differentiated SH-SY5Y cells…….……88
Fig 3.17: Effect on DAT inhibitors on dopamine hydrochloride induced toxicity……...……89
Fig 3.18: Effect of zVAD.fmk on cell viability in toxin-induced cytotoxicity...91
Fig 3.19: Effect of caspase-3 inhibitor on cell viability in toxin-induced cytotoxicity……...…92
Fig 3.20: Effect of caspase-9 inhibitor on cell viability in toxin-induced cytotoxicity……...…93

Fig 3.21: Effect of Necrostatin-1 on cell viability in toxin-induced cytotoxicity……..95
Fig 3.22 Effect of necrostatin-1 and zVAD.fmk on cell viability in staurosporine treated cells……96
Fig 3.23: Visual presentation of Nec-1 treated cells after toxin treatment……..97
Fig 3.24: Toxin induced ROS production in SH-SY5Y cells……100
Fig 3.25: Toxin induced ROS production in SH-SY5Y cells……101
Fig 3.26: Toxin induced ROS production in SH-SY5Y cells……102
Fig 3.27: Visual determination of ROS level in SH-SY5Y cells following toxin insult…….....103
Fig 3.28: Toxin-induced changes of mitochondrial membrane potential in SH-SY5Y cells……..….105
Fig 3.29: Toxin-induced changes of mitochondrial membrane potential in SH-SY5Y cells……..….106
Fig 3.30: Toxin-induced changes of mitochondrial membrane potential in SH-SY5Y cells……..….107
Fig 3.31: Toxin-induced changes of mitochondrial membrane potential in SH-SY5Y cells……..….108

Fig 4.1: Visual presentation of cleaved PARP-1 in toxin treated cells……123
Fig 4.2: Changes in nuclear morphology after toxin treatment……...…124
Fig 4.3: Effect of toxin treatment on the expression of apoptotic markers….126
Fig 4.4: Effect of toxin treatment on the expression of apoptotic markers….127
Fig 4.5: Effect of toxin treatment on the expression of apoptotic markers….128
Fig 4.6: Effect of diquat treatment on PARP-1 expression……..…129
Fig 4.7: Effect of diquat treatment on PARP-1 expression……130
Fig 4.8: Effect of chronic toxin treatment on the cleaved-PARP-1 expression……...131
Fig 4.9: Toxin induced changes in p53 levels……..…133
Fig 4.10: Effect of diquat treatment on p53 expression……..……135
Fig 4.11: Effect of diquat treatment on p53 expression……..…136
Fig 4.13: Toxin induced changes in RIP levels……..……139
Fig 4.14: Visual presentation of RIP in toxin treated cells……140
Fig 4.15: Expression of α-synuclein in toxin treated cells……..…142
Fig 4.16: Expression of α-synuclein in toxin treated cells……..…143
Fig 4.17: Visual presentation of α-synuclein in toxin treated cells……...144
Fig 4.18: Chronic toxin induced changes in α-synuclein levels……145
Fig 4.19: Toxin induced changes in DJ-1 levels……146
Fig 4.20: DJ-1 immunoreactivity following treatment with different toxins…147
Fig 4.21: Effect of 24-h toxin treatment on TH expression in SH-SY5Y cells……...148
Fig 4.22: SH-SY5Y cell morphology and tyrosine hydroxylase immunoreactivity following treatment with different toxins……...……149
Fig 4.23: Representative images showing neurofilament staining after toxin treatment……151

Fig 5.1: ATG5 knockdown efficiency in SH-SY5Y cells……...163
Fig 5.2: Alamar Blue reducing capacity of ATG5 KO SH-SY5Y cells…...…164
Fig 5.3: ATG5 knockdown and toxin treatment……..166
Fig 5.4: Atg5 siRNA treatment and cell-viability in toxin treated cells……..167

Fig 5.5: Atg5 siRNA treatment and cell-viability in toxin treated cells……..168
Fig 5.6: Toxin induced changes in ATG5 levels……..…169
Fig 5.7: Toxin induced changes in beclin-1 levels……..170
Fig 5.8: Toxin induced changes in beclin-1 levels……..171
Fig 5.9: Toxin induced changes in beclin-1 levels……..172
Fig 5.10: Toxin induced changes in LAMP-1 levels……..…173
Fig 5.11: Toxin induced changes in LAMP-1 levels……..…174
Fig 5.12: Toxin induced changes in LAMP-1 levels……..…175
Fig 5.13: Toxin induced changes in LAMP-2 levels……...…..175
Fig 5.14: Toxin induced changes in LAMP-2 levels……...…..176
Fig 5.15: Toxin induced changes in LAMP-2 levels……...…..177
Fig 5.16A: Localisation of lysosomal aggregates after toxin treatment……...…178
Fig 5.16B: Localisation of lysosomal aggregates after toxin treatment……...…179
Fig 5.17: Dose dependent increase in lysosomal aggregates after toxin treatment……..…180
Fig 5.18: Time dependent increase in lysosomal aggregates after toxin treatment……..…181
Fig 5.19: DJ-1 Transfection and cell-viability in toxin treated cells…..……183

Fig 6.1: Inhibition of NADH: quinone reductase (complex I) activity…...…193
Fig 6.2: Mean CI/II activity in MPP+ treated SH-SY5Y mitochondria……..196
Fig 6.3: Mean CI/II activity in Diquat treated SH-SY5Y mitochondria…….197
Fig 6.4: Mean CI/II activity in Diquat treated SH-SY5Y mitochondria…….198
Fig 6.5: Mitochondrial localisation after toxin treatment……201
Fig 6.6: Mitochondrial localisation after toxin treatment……202
Fig 6.7: Mitochondrial localisation after diquat treatment……..202

Fig 8.1: Cultivation of neural stem cells……..…226
Fig 8.2: Immunocytochemical analysis of neurospheres……..…227
Fig 8.3: Immunocytochemical analysis of differentiated N969 cells……..…228
Fig 8.4: Percentage of TH and Tuj1 positive cells……..229
Fig 8.5: Protein analysis showing tyrosine hydroxylase levels……...230
Fig 8.6: Effect of toxin treatment for 24 h on viability in differentiated midbrain precursor cells……..……231
Fig 8.7: Immunocytochemical staining of toxin treated cells……..…233

List of tables

Page

Table 1.1: Summary of Genetic mutations in PD……..34

Table 2.2: Properties and agricultural uses of selected chemicals to be used……..54

Table 2.2: Properties and agricultural uses of selected chemicals to be used…….…….55

Table 2.3: Details of primar antibodies used…….58

Table 3.1: Summary of cytotoxicity of selected toxins to SH-SY5Y cells (24 hour exposure), assessed using Alamar Blue reduction assay……..…77

Table 3.2: Estimation of LD_{50} values of SH-SY5Y cells (24 hour exposure)…...78

Table 3.3: Percentage increase/reduction in toxin treated cells after cell signalling inhibition……..……98

Table 3.4: Percentage increase/reduction in toxin treated cells after cell signalling inhibition……..…99

Table 6.1: Standard Assay measurements……...……191

Table 6.2: Complex I and II activity measurement in MPP+ treated SH-SY5Y cells……...…196

Table 6.3: Mean CI/II activity in diquat treated SH-SY5Y cells……198

Table 6.4: Chronic toxin exposure and complex I-II activity……..…199

Table 7.1: Symbol and title of selected genes analysed through RT-PCR…..…211

Table 7.2: Symbol and title of selected genes analysed through RT-PCR…..…212

Table 7.3, 7.4: Description of Significant Genes Identified by Whole Genome Expression after acute 24 hour toxin exposure……..…214

Table 7.5, 7.6: Description of Significant Genes Identified by Whole Genome Expression after chronic 4 week toxin exposure……...…215

Table 8.1: Percentage viability comparison between SH-SY5Y cells and hNPCs after 24 hours toxin exposure…….……232

Abbreviations

3-MA	3-Methyl adenine
6-OHDA	6-hydroxydopamine
AR-JP	Autosomal recessive-Juvenile parkinsonism
ATG	Autophagy-specific genes
AV	Autophagic vacuole
BBB	Blood brain barrier
BTCP	N-[1-(Benzo[b]thien-2-yl-cyclohexyl)] piperidine
CI	Complex I
CII	Complex II
CMA	Chaperone mediated autophagy
CURS	Columbia University Rating Scale
CSA	Cyclosporin A
DA	Dopaminergic
DAT	Dopamine transporter
dbcAMP	Dibutyryl cyclic AMP
DTC	Dithiocarbamate
DOPAC	3,4-dihydroxyphenylacetic acid
EPA	Environment protection agency
FPHM	Fluroxypyr methylheptyl ester
GBA	Glucocerebrosidase
GSHPx	Glutathione peroxidase
HVA	Homovanillic acid
LAMP	Lysosomal-associated membrane protein
LB	Lewy body
LDH	Lactate dehydrogenase
LRRK2	Leucine-rich repeat kinase 2
MAO-B	Monoamine oxidase-B
MAPK	Mitogen-activated protein kinase
Mn-EBDC	Manganese ethylene-bis-dithiocarbamate
MPTP	1-methyl 4-phenyl 1,2,3,6-tetrahydropyridine
MPP+	1-methyl 4-phenylpyridimium
mtDNA	Mitochondrial DNA
MTP	Mitochondrial transition pore
Na-EBDC	Nabam
NAC	N-acetyl-L-cysteine
NADPH	Nicotinamide adenine dinucleotide phosphate (reduced)
NET	Norepinephrine
NF	Neurofilament
NUDS	Northwestern University Disability Scale
OXPHOS	Oxidative phosphorylation system
PARP-1	Poly [ADP-ribose] polymerase 1
PINK1	PTEN induced kinase 1
PKC	Protein kinase C
PQ	Paraquat
PD	Parkinson's disease
iPD	Idiopathic Parkinson's Disease
POLG	Polymerase γ
RA	Retinoic acid

rAAV	Recombinant adeno-associated viral
RIP	Receptor interacting protein
ROS	Reactive oxygen species
SOD	Superoxide dismutase
SN	Substantia nigra
SNpc	Substantia nigra pars compacta
SNCA	alpha-synuclein
Tfam	Transcription factor A
TH	Tyrosine hydroxylase
UCHL1	Ubiquitin C-terminal hydrolase L1
UPS	Ubiquitin proteasome system
UPDRS	Unified Parkinson's Disease Rating scale
VMAT	Vesicular monoamine transporter
Tfam	Mitochondrial transcription factor A

Acknowledgments:

I would like to thank my supervisors Prof. Peter Blain and Dr. Chris Morris for their kind assistance and support throughout the course of this project. I very much appreciate the guidance provided by Dr. Morris and the relaxed attitude with which he mentored me and made the whole experience enjoyable and productive. He was always available for a brief or long chat and instantly provided very helpful and encouraging feedback. I benefited from his advice, directness and positive outlook. His helpful suggestions and critical comments contributed enormously to the production of this thesis. Without him this project could not have been completed. I also thank technicians, fellow PhD students and other members of staff at the Wolfson Unit who provided assistance in laboratories. I am grateful to Prof. Robert Taylor and Dr. Langping He from the NHS Mitochondrial Diagnostic Service for allowing me to use their facilities to measure the activity of mitochondrial respiratory chain complexes. Special thanks to Dr. Peter Hanson who provided generous help with Western blotting and RT-PCR and was always more than willing to listen to what I had to say! His support and assistance will always be appreciated. I must express my gratitude to Dr Hobab Galal and Dr Salem Fathalla who provided a much needed form of escape from work. Their uplifting presence made life inside and outside work so much more fun. Finally, I would like to thank my parents and family for their continued support and especially my wife, Javeria, for her patience, understanding and faith she had in me. Completing this work would have been all the more difficult were it not for their support.

Authors Declaration:

This thesis is submitted for the degree of Doctor of Philosophy to Newcastle University. The research described within was performed at the Medical Toxicology Centre within the Institute of Cellular Medicine and is my own work unless otherwise stated. The research was carried out under the supervision of Dr C.M. Morris and Professor P.G. Blain between October 2006 and October 2009.

I certify that none of the material offered in this thesis has been previously submitted by me for a degree or any other qualification at this or any other university.

Courses/Conferences attended:

- Health Protection 2009 Conference. HPA. University of Warwick (14-16 Sep 2009) (Poster Presentation)

- The British Toxicology Society Autumn Meeting, Durham University, (7-8 Sep 2009), (Oral/Poster Presentation)

- 25th International Neurotoxicology Conference, Rochester, New York. 12th - 17th Oct 08 (Poster Presentation)

- British Neuroscience Association-Young Neuroscientists' Day – Cardiff University, 22/10/08 (Oral/Poster Presentation)

- Health Protection Agency Chemical Hazards and Poisons Division Conference, May 2008 (Poster Presentation)

- In vitro models as tools for the study of neurological diseases. IIBB-CSIS – IDIBAPS, Barcelona, Spain – March 13-14, 2008 (Workshop)

Abstract

Parkinson's disease (PD) is an age-related neurodegenerative disorder, characterised by progressive degeneration of dopaminergic neurons in the substantia nigra, with the formation of α-synuclein rich, intracytoplasmic Lewy bodies. Several genetic and environmental factors, including pesticides are linked with sporadic PD. The aim of this study was to investigate the effect of selected pesticides on dopaminergic neuroblastoma SH-SY5Y cells and differentiated human neural precursor cells. Several parameters of toxicity were successfully measured including cell-viability in SH-SY5Y cells and estimation of sub-cytotoxic doses which were used to study the effects of signalling inhibitors, measurement of mitochondrial transmembrane potential, reactive oxygen species formation, inhibitory activity towards mitochondrial complex I/II, protein expression after acute and chronic toxin treatment and changes in gene expression. Twenty nine commonly used pesticides were screened for potential PD involvement, using cell viability and Alamar Blue reduction assay in SH-SY5Y cells. Most chemicals showed low toxicity using this system. Chemicals known (MPTP or MPP+) or thought to be involved with PD (e.g. paraquat) showed significant toxicity at the highest chosen dose i.e. 1mM (MPTP/MPP+ caused 20-30% reduction in cell-viability at 1mM whereas paraquat caused 60-70% reduction at 1mM). Significant toxicity was observed at concentrations as low as 0.01mM (60-70% reduction in cell-viability after maneb and mancozeb exposure) and 0.1mM (60%, 50%, 80% and 40% reduction in cell-viability after diquat, epoxiconazole, fluroxypyr-ester and mecoprop-methyl ester treatment respectively). Toxin exposure of human midbrain neurones (hNPCs) derived from embryonic neural stem cells showed that hNPCs were more vulnerable at 0.01mM and 0.1mM than SH-SY5Y cells (except maneb, mancozeb and fluroxypyr ester). Pharmacological inhibition of apoptosis showed a marginal but insignificant reduction in toxicity for most chemicals whereas macroautophagy inhibition had no effect. The absence of any effect of caspase inhibitors, with the exception of diquat, may indicate caspase independent induction of cell death markers like PARP-1 suggesting that toxin treatment seems to cause caspase independent cell death involving RIP. This was shown by using Necrostatin-1, a RIP1 and necroptosis inhibitor, which significantly increased viability (greater than 90% recovery vs. untreated cells) in diquat (0.1mM), mancozeb (0.05mM) and maneb (0.05mM) treated cells. Other results suggested possible involvement of chaperone-mediated autophagy (CMA)

with diquat, maneb and mancozeb toxicity which showed increased lysosomal accumulation. Mitochondrial energetics were not affected after acute and chronic toxin exposure which did not affect the mitochondrial complex I or II activities. Co-incidentally, cells exposed chronically to diquat appeared to down-regulate expression of autophagic and apoptotic response genes. It can be concluded that these agrochemicals exert their toxicity through distinct mechanisms including indirect energy depletion and direct damage to cell components and show significant toxicity possibly due to ROS generation causing necroptosis and CMA induction.

Chapter One: Introduction

Introduction

1.1 Pathogenesis of Parkinson's disease

1.1.1 Parkinson's disease

1.1.1.1 Clinical features of Parkinson's disease:

Parkinson's disease (PD) is an age-related neurodegenerative disorder. It affects 1% of people over 60 years of age in the west and has an incidence rate of 18 per 100000 per year (Twelves *et al.,* 2003). Classic signs of idiopathic PD (iPD) are resting tremor, rigidity, bradykinesia and postural instability. Additional symptoms include flexed posture, loss of postural reflexes and freezing phenomenon (Jankovic, 2008). At least two features must be identified for successful diagnosis with one being either tremor or bradykinesia. 70% of PD patients show a resting tremor of 3-5 Hz frequency (Samii *et al* 2004) but disease development does not follow a standard pattern and a variable deterioration rate is seen in early stages followed by severity in behavioural and cognitive disturbances like dementia. According to 'UK Parkinson's Disease Society Brain Bank' clinical diagnostic criteria, three or more supportive criteria are required for diagnosis. These include excellent response to levodopa and it lasting more than 5 years, clinical disease course longer than 10 years, resting tremor and progressive pattern (Gibb and Lees, 1988).

As the disease progresses, significant motor disability is seen in PD patients even when treated with symptomatic medications. Symptoms like hypomimia, dysphagia, sialorrhoea, microphagia, dystonia, are also noted. A number of different non-motor symptoms are gaining attention. These include cognitive (dementia) (Aarsland *et al.,* 2001), neuropsychiatric (depression, apathy, psychosis, anxiety and fatigue), sleep dysfunction (rapid eye movement sleep behaviour disorder, sleep attacks, daytime sleepiness, advanced sleep phase syndrome and early morning awakenings) (Fenelon, 2008), autonomic disturbances (constipation, nausea, orthostatic hypotension, urogenital problems) (Stacy, 2002) and sensory disturbances (restless legs syndrome, visual changes and decreased olfaction) (Park and Stacy, 2009). Increased mortality risk has been linked with both motor and non-motor features in newly diagnosed PD patients, especially with features like postural instability, hallucinations and cognitive impairment (Fénelon *et al.,* 2000).

Disease progression can be evaluated using a number of different rating scales. The 'Columbia University Rating Scale' (CURS), 'Northwestern University Disability Scale' (NUDS), and the 'Unified Parkinson's Disease Rating scale' (UPDRS) are the most valid and reliable scales currently used (Ramakar *et al.,* 2002).

Full PD diagnosis requires clinical and neuropathological confirmation. Clinical symptoms of PD are thought to be present when 50% of SN neurons have been lost (Fearnley and Lees, 1991). It is the most common cause of parkinsonism, accounting for nearly 80% of cases (Dauer & Przedborski, 2003).

1.1.1.2 Pathological features of Parkinson's disease:

Pathologic hallmarks of iPD include progressive degeneration of dopaminergic (DA) neurons in the substantia nigra pars compacta (SNpc) together with the formation of α-synuclein rich, proteinaceous inclusions called Lewy bodies (LBs) (fig 1.1) in the cytoplasm of surviving nigral neurons (Spillantini *et al.,* 1998). LBs have been observed in other regions like amygdala, cortex, vagal nucleus, locus coeruleus, and peripheral autonomic nervous system (Braak *et al.,* 2003). LBs can either have a spherical dense core surrounded by a halo or fully composed of oval or circular fibrillar material (Shults, 2006). Ultra-structural examination shows α-synuclein material in the periphery and central core (Arima *et al.,* 1998). In addition to α-synuclein, ubiquitin and neurofilaments make the majority of LB components along with other proteins. The widely reported morphology is obtained from end-stage PD patients but studies show that LB shape and structure changes with time and can have a variety of different shapes (Gómez-Tortosa *et al*., 2000; Sakamoto *et al*., 2002)

Fig 1.1: Pathological hallmarks of PD: Nerve cell with Lewy bodies double-stained for α-synuclein (positive core and halo staining) and ubiquitin (halo staining) (Taken from Spillantini *et al.,* 1998).

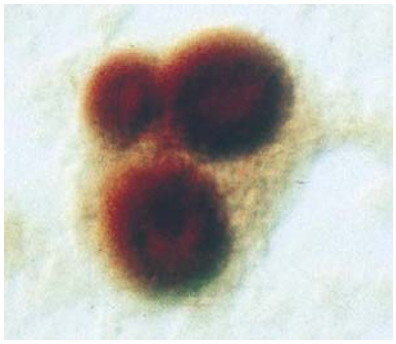

The loss of the pigmented cells in the SNpc in PD is not homogeneous and should be primarily assessed in the lateral and ventral regions of the SNpc to correlate with the level of motor symptoms (fig 1.2). Neurons with long, sparsely myelinated or unmyelinated axons are more likely to have α-synuclein inclusions. GABAergic, noradrenergic, serotonergic, histaminergic, cholinergic and glutamatergic cells may also be involved (Dickson *et al.,* 2009).

Fig 1.2: Density of pigmented neurons in the SNpc: (A) Distribution of pigmented neurons in healthy controls, (B) patients with mild PD, (C) moderate or (D) severe loss of pigmented neurons (×40 magnification, haematoxylin and eosin-stained sections, 3n=exiting 3rd nerve fibres, cp=cerebral peduncle, R=red nucleus) (Taken from Dickson *et al.,* 2009).

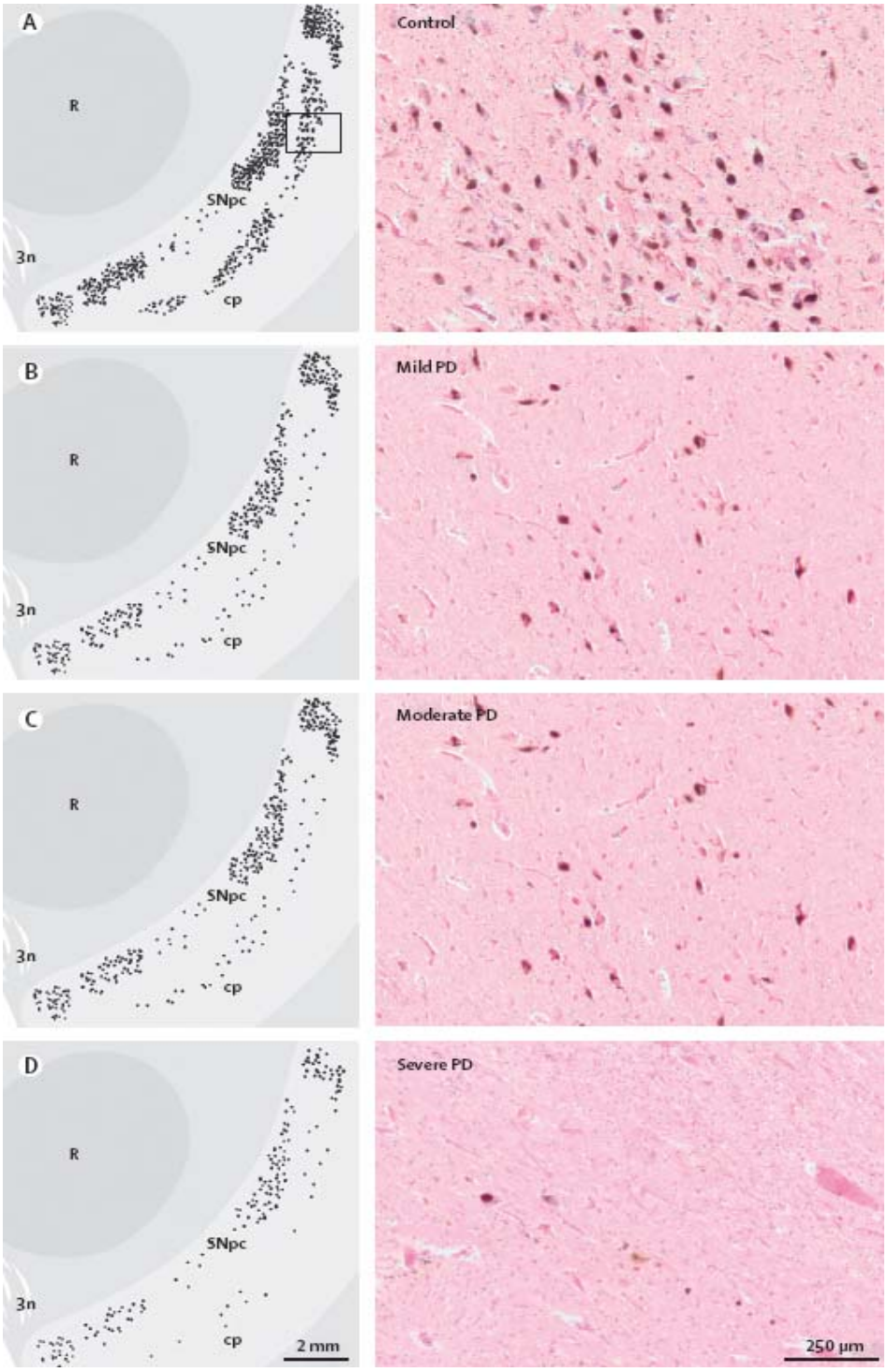

1.1.2 Development of Parkinson's disease:

A neuropathological staging scheme based on abnormal α-synuclein/Lewy body distribution and immunostaining has been proposed by Braak *et al* (2003) (fig 1.3). This scheme shows the pathological evolution of the disease from the brainstem to neocortex. Patients are pre-symptomatic in stages 1-2 and only in stages 3-4 are the substantia nigra, midbrain and basal forebrain affected, followed by the archicortex with clinical symptoms of parkinsonism appearing (Burke *et al.,* 2008). Stage 1 shows positive α-synuclein in medulla oblongata/pontine tegmentum or the olfactory bulb/anterior olfactory nucleus and neuronal loss in SNpc. Stages 3-4 show changes in the substantia nigra and areas of midbrain and basal forebrain. During stages 5-6, disease progresses into the mature neocortex (medial temporal lobe and association cortex) and clinical manifestations become clear (Braak *et al.,* 2004).

Fig 1.3: The Braak staging of Parkinson's disease: A) Disease progression involving Lewy body appearance to expansion into different brain regions. B) Disease sequence starting from the brainstem to other parts (Taken from Braak *et al.,* 2004).

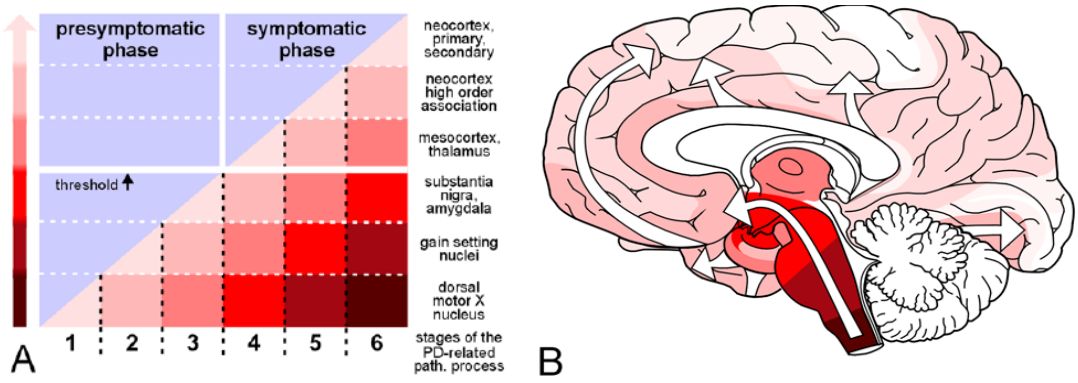

Clinical features of PD can be followed using this scheme from the early loss of olfactory function to the late development of cognitive problems like dementia, from the intracerebral formation of Lewy bodies and neurites at defined induction sites to damage to components of the autonomic, limbic, and somatomotor systems (Braak *et al.,* 2005).

1.1.2.1 Mitochondrial Dysfunction in Parkinson's disease:

Mitochondrial dysfunction has been linked with the pathogenesis of Parkinson's disease (Keeny *et al*., 2006; Schapira, 2006). Evidence from a high number of mitochondrial DNA (mtDNA) deletions in substantia nigra of PD patients

(Bender *et al.,* 2006) and inhibition of complex I activity (Schapira *et al*., 1998) suggests a key role of mitochondrial function in the pathogenesis of PD. The first case of mitochondrial involvement in PD was noticed in 1980s when intravenous administration of synthetic heroin containing 1-methyl 4-phenyl 1,2,3,6-tetrahydropyridine (MPTP) caused PD like symptoms. Further investigation showed that MPTP entered the brain and then converted into 1-methyl 4-phenylpyridimium ion (MPP+) by monoamine oxidase B in glial cells. MPP+ actively concentrated into the mitochondria where it inhibited complex I and caused mitochondrial dysfunction through increased oxidative stress and caused selective SN dopaminergic neuron death (Langston *et al.,* 1983). These findings led to more widespread use of MPTP in animal studies using mice and monkeys for investigating the neurophysiological and neuropathological aspects of PD. Accumulation of MPP+ has been observed in human platelets which also express DAT and high levels of MAO-B (Frankhauser *et al*., 2006). Evidence from several studies showed a reduced level of mitochondrial complex I activity in PD platelet mitochondria. However, the level of activity varied not just for complex I but for complex II (Haas *et al*., 1995), complex III (Benecke *et al*., 1993) and complex IV (Swerdlow *et al*., 2001). An equally high number of studies failed to find any ETC complex inhibition (Aomi *et al*., 2001; Blake *et al*., 1997; Mann *et al*., 1992). Similarly, studies showing a selective decrease in the quantity of complex I subunits in PD brain have been reported by some groups (Mizuno *et al*., 1989) with others suggesting no such change (Schapira *et al*., 1990).

Transgenic techniques involving knockout mice have shown that respiratory chain deficiency in DA neurons can lead to several symptoms of parkinsonism-like slow progressive degeneration of neurones, formation of (α-synuclein negative) intraneuronal inclusions and behavioural disturbances such as progressive impairment of motor function. These mice lacked mitochondrial transcription factor A (Tfam) in DA neurons and showed reduced mtDNA expression and the rate of cell death was higher in substantia nigra than in ventral tegmental area (Ekstrand *et al.,* 2007).

1.1.2.2 Oxidative stress and Parkinson's disease:

Elevated oxidative stress has been linked with neuronal loss and may play a role in the pathogenesis of Parkinson's disease (Halliwell, 1999). Increasingly the role of protein oxidation, reduced glutathione levels, generation of quinones through dopamine metabolism, lipid peroxidation and generation of reactive oxygen species (ROS) has been linked with oxidative damage (Alam *et al*., 1997; Sian *et al.*, 1991; Yoritaka *et al*., 1996). NADPH oxidase metabolises molecular oxygen, generates superoxide and appears to be present in all cell types including glial cells and neurons (Infanger *et al.,* 2006). Neurotoxic response to toxins like rotenone and MPTP is less in NADPH oxidase deficient mice (Sumimoto *et al.,* 2004) and studies have shown that its expression is up-regulated in the substantia nigra of PD patients (Infanger *et al.,* 2006).

Study of MPTP exposure shows generation of hydroxyl radicals in mice leading to oxidative stress (Chiueh *et al.,* 1992). Furthermore, oxidative stress may cause caspase-activation and apoptosis (Friedlander, 2003). Nikam et al (2009) have shown that levels of 'thiobarbituric acid reactive substances' (indicators of lipid peroxidation) and the rate of dopamine metabolism is significantly elevated in PD. Mitochondrial contents of oxidation products like TBARS and protein carbonyls are indicative of oxidative stress (Navarro *et al.,* 2009). Excessive MAO activity which can cause elevated formation of hydrogen peroxide has also been noted (Cohen, 1986). Increased nitric oxide synthase and reduction in superoxide dismutase (SOD) and glutathione peroxidase (GSHPx) activity, serum levels of vitamin E and C and selenium levels, have also been linked with PD (Nikam *et al*., 2009).

Further support to the idea that oxidative stress may lead to PD comes from presence of mutations in DJ-1 which abolish its neuroprotective effect against hydrogen peroxide and complex I inhibitor induced damage (Canet-Aviles *et al.,* 2004). Additionally, DJ-1 may play a role in preventing accumulation and misfolding of oxidised mitochondrial proteins in the same way it inhibits α-synuclein aggregation and toxicity (reviewed by Büeler, 2009).

1.1.2.3 Complex I deficiency:

The 13 proteins encoded by mitochondrial DNA act as the sub-units of various respiratory chain complexes of the oxidative phosphorylation system (OXPHOS) in the mitochondria (Wredenberg *et al*., 2002). Complex I is the largest of the OXPHOS complexes and its inhibition can lead to oxidative stress through free radical generation and ATP depletion (Fig 1.4) (Schapira, 2005). Excessive oxidative stress can in turn lead to the release of cytochrome c and induce caspase-mediated apoptosis (Stavrovskaya and Kristal, 2005).). Comparison of healthy and PD brain tissue has shown that several complex I subunits contain significantly higher protein carbonyl levels in PD which has been linked with complex I misassembly and dysfunction (Keeney *et al.,* 2006). The substantia nigra is more vulnerable to changes in complex I activity than other brain regions, possibly due to increased ROS generation and intracellular mechanisms like dopamine metabolism and iron content (Chinta and Andersen, 2008). The idea that a complex I defect causes elevation in ROS levels comes in part from rotenone exposure experiments using isolated mitochondria which showed a significant increase in ROS generation after toxin insult (Kushnareva *et al.,* 2002). Complex I activity has been reported to be reduced by up to 35% in PD SNpc region (Mann *et al.,* 1994) and ~30% in muscle and platelets of sporadic PD patients (Schapira *et al.,* 1990). Raised levels of malondialdehyde and 4-hydroxynonenal (lipid peroxidation marker) have been observed in SN and LBs in PD post-mortem brains (Andersen, 2004).

Fig 1.4: Result of mitochondrial dysfunction: Oxidative stress, complex I inhibition, ATP depletion, excitotoxicity leading to cell death (Taken from Sherer *et al.,* 2002).

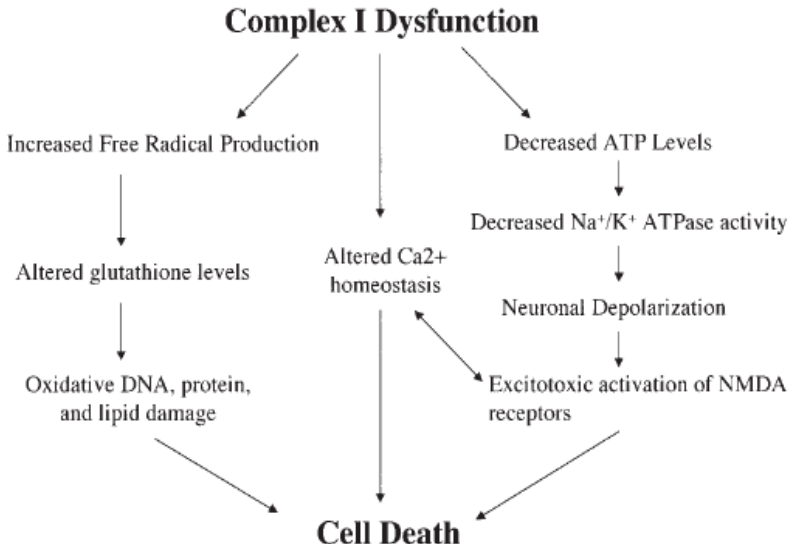

1.1.2.4 Mitochondrial DNA mutations in Parkinson's disease:

Deletions and mutations in nuclear encoded mitochondrial DNA can contribute to PD pathogenesis by causing mitochondrial dysfunction. mtDNA mutations, if accumulated over time, speed up the normal aging process with increased ROS production and oxidative damage (Petrozzi *et al.,* 2007). Respiratory chain function relies on a balanced expression of both mtDNA and nuclear genes, which is essential for the assembly of respiratory chain enzyme complexes. If mtDNA expression is suppressed it can lead to excess production of nuclear-encoded respiratory chain subunits resulting in an increased burden on the mitochondrial proteolytic system to degrade them (Ekstrand *et al.,* 2007).

Data from mtDNA haplotype studies suggests that some haplotypes can reduce PD risk and therefore mtDNA has a role in PD development (Pyle *et al.,* 2005). Mutations in the mtDNA polymerase γ (*POLG*) gene have been linked with parkinsonism associated with multiple mtDNA deletions. A significant cosegregation of *POLG* mutations and parkinsonism has been recorded with a reduction in dopaminergic neurons but without LB formation (Luoma *et al.,* 2004).

High levels of sporadic mtDNA deletions in SN neurons in aging and PD have been observed. It is also suggested that the accumulation of mtDNA deletions in SN can result in respiratory chain deficiency (Bender *et al.,* 2006). Large scale rearrangements (Chalmers, 2002) and point mutations have been found in some population groups (Petrozzi *et al.,* 2007). Sixty-eight homoplasmic and high-frequency heteroplasmic mtDNA mutations have been identified in PD but these fail to establish a link with the PD phenotype (Smigrodzki *et al.,* 2004). Cybrid studies transferring mitochondria from affected cells into normal mitochondria-less cells have proved inconclusive and failed to introduce a defect into these cells.

Genetic epidemiological studies show that lower complex I activity, increased ROS enzyme activities and increased ROS production can be inherited matrilineally (Swerdlow *et al.,* 1998) but the number of such documented cases is very limited. Case-control mutation studies have identified significant association of polymorphisms in several genes including N-acetyltransferase 2 (*NAT2*), monoamine

oxidase *(MAO-B*), glutathione transferase (*GSTT1*) and *tRNAGlu* with PD (Tan *et al.,* 2000) but a limitation of these studies is that they can easily give false positive or false negative results.

Haplogroup association studies, without identifying any specific mutations, have hinted that a relative excess of non-synonymous mutations in mtDNA encoded complex I genes may be linked with increased PD risk (Autere *et al.,* 2004). Other studies show that single nucleotide polymorphisms in Haplotype J and K reduce PD risk by 50% when compared with the most common haplogroup H (van der Walt *et al.,* 2003). Pyle et al (2005) have also reported a 22% reduction in population-attributable risk for PD in haplotype cluster UKJT (Pyle *et al*. 2005). Autere et al (2004) have linked the higher frequency of super cluster JTIWX in a population group with an increased risk of developing PD and PD with dementia. These findings show that polymorphisms within mtDNA can contribute to PD expression but the evidence for causative and risk alleles is still to be found.

1.1.3 Models of Parkinson's disease

A primary goal of animal models is to successfully exhibit PD features and mimic different stages so that the underlying mechanism can be studied in detail. Most commonly used animal models employ toxins such as MPTP, rotenone, paraquat or 6-hydroxydopamine (6-OHDA) but increasingly knock-out and transgenic models are being used. Most toxin models focus on the nigrostriatal pathway and DA neuronal loss without producing full PD pathology. This gap is being filled with the use of novel genetic models with the aim of reproducing the distribution, nature and progressive course of PD neuropathology.

1.1.3.1 Toxin models of Parkinson's disease:

Use of toxin models has filled major gaps in the understanding of cellular and molecular causes of PD. These models have not just provided invaluable information about the aetiology and pathogenesis of PD but also about the underlying biochemical processes in the cells. Use of neurotoxins is particularly favoured as they can produce both *in vivo* and *in vitro* selective neuronal death (Bove *et al.,* 2005).

Most commonly and widely used toxins include 1-methyl-4-phenyl-1,2,3,6-tetrahydropyridine (MPTP), 1-methyl-4-phenylpyridinium (MPP+), rotenone, 6-OHDA) and paraquat. These all have different mechanisms of actions, causing cytotoxic injury to the dopaminergic neurons (Przedborski & Ischiropoulos, 2005). Almost all neurotoxin induced models affect the mitochondria, some targeting specific targets such as complex I and III (Schober, 2004).

1.1.3.1.1 6-OHDA:

6-Hydroxydopamine (6-OHDA) has been used as a catecholaminergic neurotoxin for more than 30 years. It is a hydroxylated analogue of the neurotransmitter dopamine (Blum, 2001) and due to this structural similarity exhibits a high affinity for catecholaminergic membrane transporters like dopamine (DAT) and norepinephrine (NET) transporters. This allows it to damage both noradrenergic and dopaminergic neurons.

1.1.3.1.1a Toxicity of 6-OHDA:

Once inside the cell 6-OHDA can accumulate in the cytosol, damage catecholaminergic structures by causing oxidative stress or destroy adrenergic nerve terminals (Jeon *et al.,* 1995). It inhibits mitochondrial complex I and plays a part in the production of superoxide free radicals (Hasegawa *et al*., 1990). It easily oxidises producing para-quinone and hydrogen peroxide (fig 1.5) and can take part in reactions involving metabolic monoamine oxidation (Glinka, 1997).

6-OHDA does not cross the blood-brain barrier (BBB) and its systemic administration does not produce nigrostriatal lesions. This problem can be solved with stereotaxic injections at various sites in the brain. Injections into the SN and the medial forebrain bundle can cause dopaminergic degeneration within 12-24 hours and if injected into striatum it takes 2-3 days (Przedborski *et al.,* 1995). Intrastriatal injection of 6-OHDA causes a slow and progressive neuronal death which can last up to 2-3 weeks (Sauer & Oertel, 1994).

Fig 1.5: Oxidation of 6-OHDA producing hydrogen peroxide and para-quinone (Taken from Bove *et al.,* 2005)

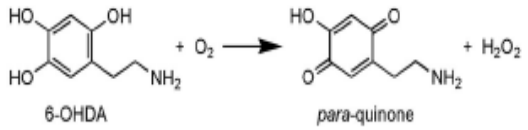

The majority of the 6-OHDA data comes from studies on rats, mice, and monkeys. The extent of lesion formation depends on the level of 6-OHDA, the site of injection and the species. The level of sensitivity to 6-OHDA varies in different parts of the brain. SN neurons are most sensitive, while tuberoinfundubular neurons are fully resistant (reviewed by Jonsson, 1980).

Most importantly, there is no convincing evidence of LB formation with 6-OHDA treatment and it does not affect all brain regions affected in PD. Locus coeruleus, olfactory structures and the lower brain stem are not affected by its actions (Betarbet *et al.,* 2002). It is not a potent inducer of motor abnormalities related to PD but occasional tremor, rigidity and akinesia have been reported (Cenci, 2002). Motor abnormalities observed after 6-OHDA treatment in both unilateral and bilateral-lesioned rats can be improved by dopaminergic stimulation (Olsson *et al.,* 1995) or drugs that stimulate dopaminergic receptors (Rodriguez *et al.,* 2001).

In summary, the 6-OHDA model induces acute and not the slowly progressive pathological and clinical features of PD. Nevertheless, it has proved to be a useful model of testing new transplantation and neuroprotective strategies (Bove *et al*., 2002; Aebisher *et al*., 1991; Bal *et al*., 1993; Venero *et al*., 1994). The main limitation of this model is its limited penetration across the BBB and induction of more permanent nigral lesions than dopamine depletors. However, despite this restriction many molecular changes caused by 6-OHDA are similar to those seen in PD and may prove useful in exploring neurodegeneration mechanisms of PD.

1.1.3.1.2 MPTP:

1-methyl-4-phenyl-1,2,3,6-tetrahydropyridine (MPTP) is an organic molecule (fig 1.6) that produces selective degeneration of the dopaminergic neurons of the substantia nigra in a variety of mammalian species (Burns *et al*., 1983; Heikkila *et al*.,

1984). It is the most frequently used toxin in animal models of PD and has been extensively used to elucidate numerous mechanisms of dopaminergic cell-death (Beal, 2001). It is structurally similar to a number of commonly used herbicides (e.g. paraquat) and pesticides (rotenone) that have shown evidence of dopaminergic cell degeneration (Bove *et al.,* 2005).

Fig 1.6: Chemical structure of MPTP (Taken from Bove *et al.,* 2005)

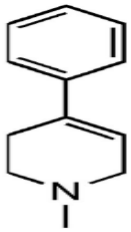

MPTP administration successfully reproduces most PD symptoms like bradykinesia, tremor, rigidity and postural instability (Tetrud *et al.,* 1986) and the sequence of degeneration that occurs after MPTP administration in animals produces pathologies similar to those seen in humans (Burns *et al*., 1985).

1.1.3.1.2a MPTP- mechanism of action:

MPTP is routinely used in experimental models due to its ability to induce PD like symptoms when intravenously injected. It is a highly lipophilic molecule and easily crosses the BBB. Once across, it is converted to 1-methyl-4-phenyl-2, 3-dihydropyridinium (MPDP+) by MAO-B in non-dopaminergic cells (serotonergic neurons and glial cells) (reviewed by Dauer & Przedborski, 2003) (fig 1.7). There it is converted into its active form MPP+ by an unknown mechanism. MPP+ is then released into the extracellular space where it is taken up into the dopaminergic neurons by DAT. Mice with DAT inhibitor or DAT genetic deletion have shown reduced toxicity of MPTP (Bezard *et al.,* 1999) but it has been far more difficult to show this effect in primates (Kopin, 1992).

1.1.3.1.2b Cellular toxicity of MPP+:

Once accumulated within the mitochondria, MPP+ inhibits complex I, III and IV of the electron transport chain where it decreases ATP production which can lead to partial depolarisation of cell membrane ionic gradients (Kopin, 1992). It disturbs cytosolic calcium homeostasis since energy is required to maintain calcium

concentrations in balance, as abnormally elevated calcium can lead to cell death (Bondy, 1989). Vesicular monoamine transporter (VMAT) incorporates MPP+ into 'dopamine containing synaptic vesicles' and can protect cells against toxic effects of MPP+ (Takahashi *et al.,* 1997) although translocation of MPP+ into synaptic vesicles stimulates excess release of cytosolic dopamine which, after undergoing auto-oxidation, generates ROS (Lotharius *et al*., 2000).

Fig 1.7: MPTP/ MPP+ Intracellular Pathways: MPP+ either concentrates within mitochondria, sequesters into synaptic vesicles or interacts with cytosolic enzymes (Taken from Smeyne & Jackson-Lewis, 2005)

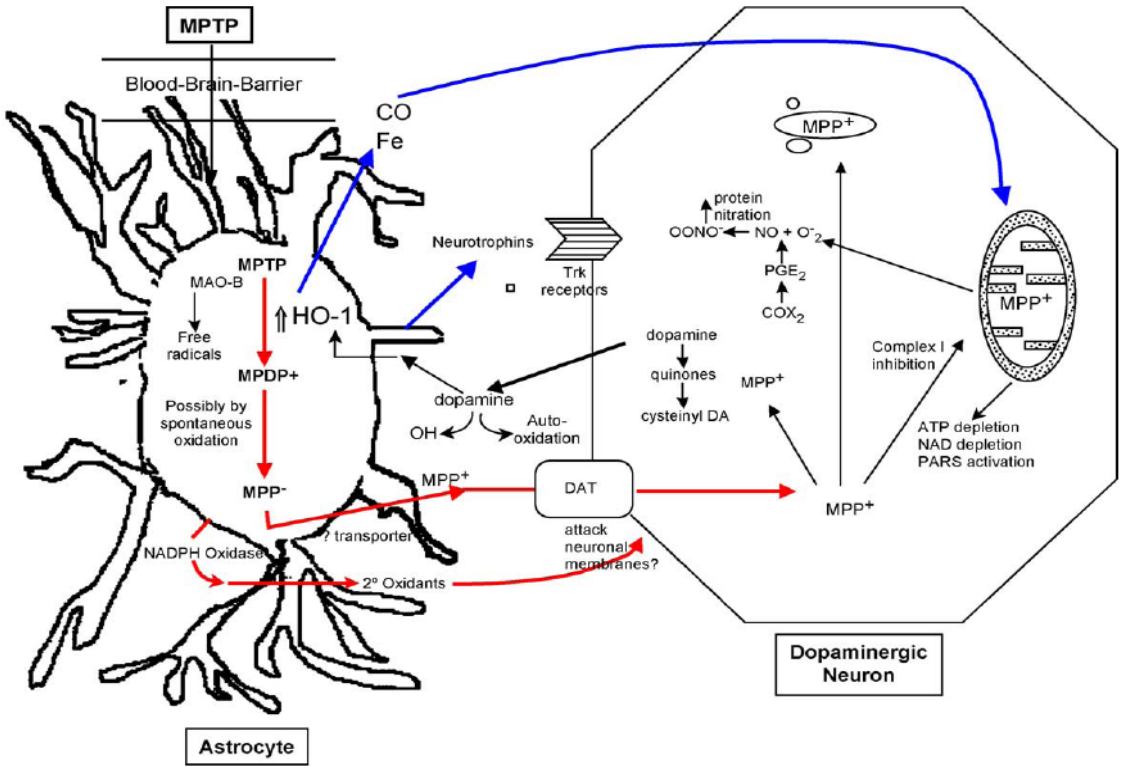

1.1.3.1.2c MPTP and Intracellular changes:

Acute MPTP exposure in mice significantly decreases intrastriatal levels of DA and its metabolites (DOPAC, HVA) as well as tyrosine hydroxylase (TH). Additionally, it significantly decreases the gene expression of DA, VMAT and TH (Xu *et al.,* 2005). Inhibition of MAO activity and a decrease in DA and its metabolites have also been observed in SH-SY5Y neuroblastoma cells exposed to MPTP (Song & Ehrich, 1997).

MPTP sensitivity levels are different for different species. Rodents are less sensitive than non-human primates. This may be due to differences in MAO-B localisation in the brain. In primates, highest MAO-B concentration is present in astrocytes in the substantia nigra and basal ganglia, whereas in rats, they are present in cells lining the blood vessels and ventricles (Kopin, 1992).

There is limited evidence of classical LB formation with the MPTP model. α-synuclein positive aggregates have been identified in continuously administered MPTP mice (Fornai *et al.,* 2004) and chronic treatment in baboons has produced α-synuclein positive aggregates (Kowall *et al*., 2000) but post-mortem investigation of human drug users exposed to MPTP in the 1980s did not show any such inclusions (Langston *et al.,* 1999). Przedborski et al (2001) have shown that sub-acute MPTP administration in mice and primates can up-regulate α-synuclein and accumulate it in cytosol. But such aggregates do not fully resemble LBs, as they are larger in size and lack a central core or filamentous halo (Kowall *et al.,* 2000).

1.1.3.1.3 Rotenone:

Rotenone is a commonly used cytotoxic retinoid extracted from some plants of Leguminosae family like *Derris elliptica*, *Derris mallaccensis*, *Lonchocarpus urucu* and *Lonchocarpus utilis* (fig 1.8) (Ray, 1991). It is widely used as an insecticide and to kill fish. Rotenone, being hydrophobic, can easily cross biological membranes without a transporter (Hatcher *et al.,* 2008). Like MPTP, it is highly lipophilic and can easily cross the BBB followed by accumulation within organelles such as mitochondria, where it inhibits complex I of the ETC (Talpade *et al.,* 2000; Uversky, 2004).

Fig 1.8: Chemical structure of rotenone (Taken from Bove *et al.,* 2005).

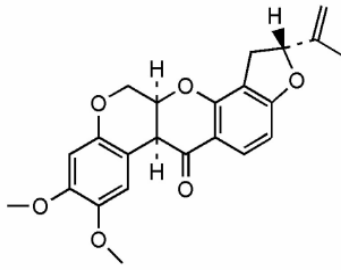

1.1.3.1.3a Cellular toxicity of rotenone:

Markers of Complex I inhibition, ROS production, acute ATP deficiency and oxidative stress have been observed in *in vivo* rotenone models (Bashkatova *et al.,* 2004). Indeed, oxidative damage has been shown in both *in vivo* and dissociated cell systems (Testa *et al.,* 2005). Rotenone causes oxidative damage in a time and dose-dependent manner with increased protein oxidation (Sherer *et al.,* 2002). Similar to the oxidative damage in PD, DA loss due to rotenone exposure is accompanied by an increase in oxidative protein damage (Testa *et al.,* 2005). Chronic rotenone toxicity causes a delayed depletion of glutathione accompanied by oxidative damage to proteins and DNA (Sherer *et al.,* 2002).

1.1.3.1.3b Neurotoxicity of rotenone:

Rotenone induces changes in the rat brain including neurodegeneration of DA neurons, inhibition and up-regulation of ubiquitin proteasome system (UPS) in the ventral midbrain, α-synuclein aggregation in striatum and ventral midbrain, complex I inhibition and DJ-1 oxidation in all brain regions (Betarbet *et al.,* 2006) (fig 1.9)

Fig 1.9: Chronic rotenone exposure inhibits complex I, causing oxidative stress which leads to UPS dysfunction and α-synuclein aggregation (Taken from Betarbet *et al.,* 2006).

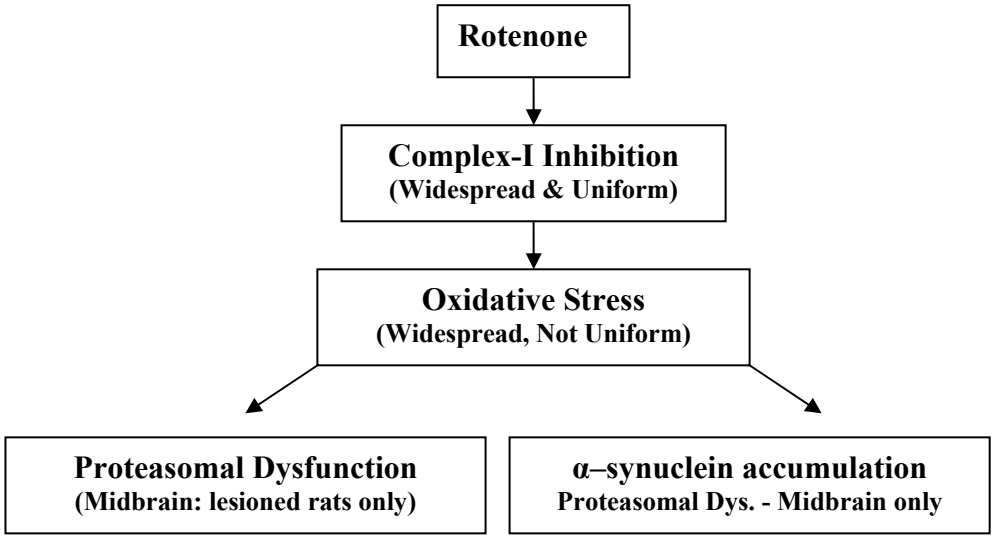

Rotenone causes neurotoxicity in nigrostriatal pathway and reduces SN DA neuron number in rats by up to 30% of the vehicle controls without exhibiting effects on the mesolimbic dopaminergic neurons. It shows a marked decrease in

dopaminergic fibres in striatum, as observed in PD. As with PD, rotenone damage is not limited to the dopaminergic system; it reduces the density of serotonin transporter up to 35%, cholinergic neurons up to 29% and noradrenergic neurons up to 26% (Hoglinger *et al.,* 2003).

Chronic systemic rotenone infusion in rats produces behavioural symptoms like flexed posture, bradykinesia and rigidity (Betarbet *et al.,* 2000). Spontaneous motor activity can be reduced to more than 70% in rats infused with rotenone for up to 4 weeks (Hoglinger *et al.,* 2003). However, this motor disability is not always accompanied with the formation of nigrostriatal dopaminergic lesions (Sherer *et al.,* 2003).

Inhibition of microtubule formation from tubulin has also been reported after rotenone exposure (Marshall & Himes, 1978). Excess tubulin monomers can be toxic to cells and may provide a link with neurodegeneration. Indeed, parkin can bind to tubulin, boosting degradation of misfolded tubulins (Ren *et al.,* 2003). Microglia protect against a number of insults but they may also release some cytotoxic substances causing neurodegeneration. Microglial activation has been observed in PD (McGreer *et al.,* 1988) and rotenone treated rats show microglial activation in the nigrostriatal tract. The exact relationship between the two is not clearly known yet and it remains unclear whether rotenone itself causes microglial activation or the activated microglia clear the way for rotenone to exert its cytotoxic effects (Gao *et al.,* 2002).

Unlike 6-OHDA and MPTP, rotenone causes the formation of proteinaceous aggregates in surviving dopaminergic neurons. Its chronic administration in rodent models has successfully produced LB like cytoplasmic aggregates that are ubiquitin and α-synuclein positive (fig 1.10) accompanied with DA neuron loss (Betarbet *et al.,* 2000). There is also evidence of rotenone accelerating α-synuclein fibrillation (Uversky *et al.,* 2001). Some studies have shown the formation of insoluble α-synuclein in rotenone treated rats (Sherer *et al.,* 2002). PD brains also show the presence of insoluble α-synuclein aggregates which are oxidatively modified. It is not clear whether the oxidative damage caused by rotenone leads to α-synuclein aggregation.

Fig 1.10: Electron micrograph of a cytoplasmic inclusion in the rotenone model (Taken from Meredith *et al.,* 2004)

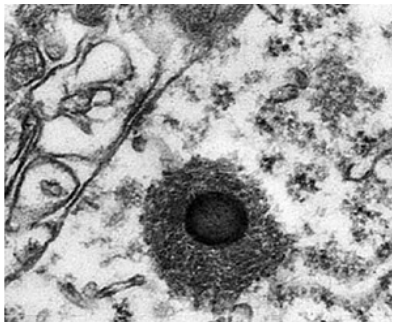

1.1.3.1.3c Advantages and disadvantages of rotenone:

Rotenone treatment produces α-synuclein positive inclusions and it kills nigrostriatal dopaminergic neurons in a highly variable manner in rats suggesting that genetic variability of individuals may be responsible for the difference in susceptibility observed (Betarbet *et al*. 2000). It causes systemic and chronic complex I inhibition decreasing UPS function and does not appear to possess a specific transport system to enter the cells (Drechsel & Patel, 2008). On the other hand, rotenone exposure leads to behavioural defects in rats without any nigrostriatal dopaminergic damage. It significantly reduces non-DAergic striatal neuronal populations (Hoglinger *et al.,* 2003). Rotenone linked striatal dopaminergic deficiency is not improved after dopamine-agonist or L-dopa administration (Betarbet *et al*. 2000)

1.1.3.1.4 Paraquat:

Paraquat (N, N'-Dimethyl-4,4'-bipyridinium dichloride) (PQ) is a widely used cationic non-selective herbicide that is consistently linked with PD. It has shown a dose-dependent effect with the incidence of PD (Liou *et al.,* 1997). This strong correlation and the reason that it has a very similar structure to MPTP and MPP+ (fig 1.11) has prompted researchers to label it as a risk factor for PD and therefore it is increasingly being used in cell-culture and animal studies. This coupled with the fact that rotenone and MPTP do not greatly contribute to the occurrence of PD as MPTP is not naturally present in the environment and rotenone has very limited uses and poor bioavailability (Richardson *et al.,* 2005).

Fig 1.11: Structural similarity of paraquat with MPTP and MPP+ (Taken from Shimizu *et al.,* 2001)

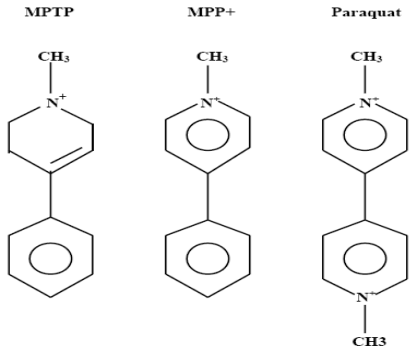

A PQ rat model has shown DA neuron death accompanied with α-synuclein aggregation (McCormack *et al.,* 2002). Brain levels of α-synuclein also significantly increase after PQ exposure accompanied by α-synuclein-positive lesions in SNpc (Manning-Bog *et al*., 2002). However, the details of these mechanisms are not clear.

PQ does not efficiently cross the BBB (requires a neutral amino acid transporter; McCormack *et al*., 2003; Shimizu *et al*., 2001) but many cases of mortalities due to PQ toxicity have shown significant damage to the brain (Hughes *et al*. 1988). Although PQ and MPP+ have similar structures, their mechanisms of neurotoxicity are quite distinct. Unlike MPP+, PQ is not a substrate of DAT and its toxicity is independent of DAT expression. It is not actively accumulated in mitochondria and there is no direct evidence of PQ inhibition of complex I (Richardson *et al.,* 2005). Contrary to earlier thinking PQ uses system L carrier (LAT-1) instead of DAT for transport through cells (Shimizu *et al.,* 2001) but this uptake mechanism has not been fully proven yet.

One proposed mode of PQ toxicity is the generation of ROS and resulting oxidative stress. One such process of generating ROS through redox cycling involving nitric oxide synthase has been suggested (Day *et al.,* 1999). It is thought that causing oxidative damage in the most vulnerable DA neurons in SN may be the prime source of its neurotoxicity rather than its action on mitochondria, complex I inhibition or uptake into DA neurons (Richardson *et al.,* 2005).

1.1.3.2 Transgenic models of Parkinson's disease:

Transgenic models of PD have used deletions and over-expression of PD related genes through conventional or virally mediated means (Kahle *et al.,* 2000; Lo Bianco *et al*., 2002). Transgenic mice generated by Masliah et al (2000) have expressed wild-type human α-synuclein and show ubiquitin and α-synuclein positive inclusions in substantia nigra, hippocampus and neocortex (fig 1.12). Similarly, drosophila models expressing wild and mutant α-synuclein can produce certain PD features like DA cell degeneration, inclusion-body formation and mobility dysfunction (Feany and Bender, 2000) (fig 1.13).

Deletion of genes required for neuronal maintenance and development has shown reduction in DA cell number e.g. Pitx3-deficient aphakia (ak) mice show L-DOPA reversible motor deficits with a reduction in SN DA neurons (Hwang *et al.,* 2005). Pitx3 deletion has no effect on mesolimboic DA neurons like PD (Fuchs *et al.,* 2009). Homozygous null mice for developmental genes 'homeobox transcription factors' Engrailed 1/2 have shown progressive degeneration of dopaminergic neurons with cerebellar pathology (Sgado *et al.,* 2006) but both models lack Lewy body formation and cell loss occurs much earlier than with sporadic PD pathology.

Fig 1.12: α-synuclein immunoreactivity in transgenic mice: Comparison of non-transgenic (A, D) and transgenic mice (B, E, G, J) showed positive reactivity with human (A-C) and murine α-synuclein antibodies (D-F). SN labelling showed that α-synuclein positive inclusions were visible in the transgenic substantia nigra (H) and hippocampus (I). (J= also ubiquitin-positive inclusions [green]; C, F = brain sections from a human Lewy body disease patient) (Taken from Masliah *et al.,* 2000).

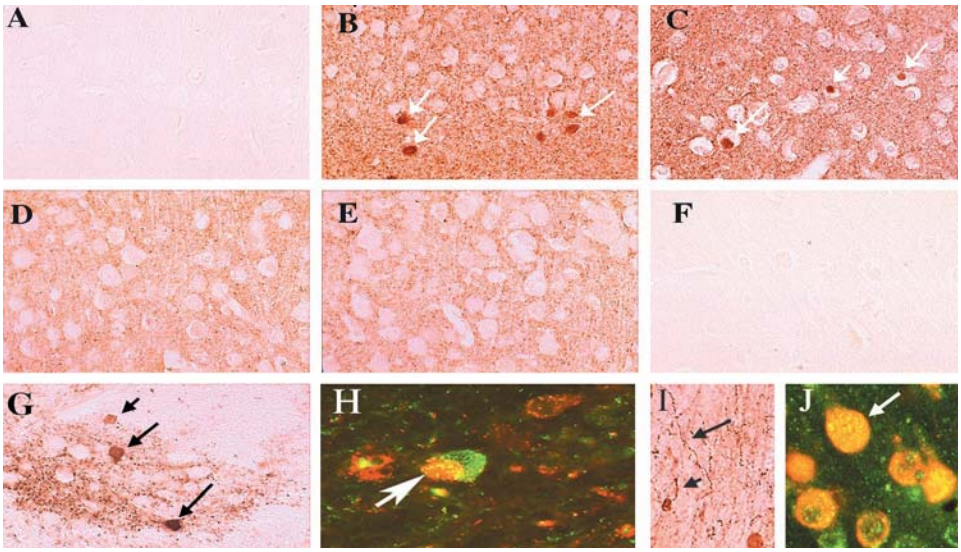

Fig 1.13: α-synuclein immunoreactivity in transgenic drosophila: A) α-synuclein positive inclusion in a 25-day-old α -synuclein transgenic fly. Punctate pattern of α -synuclein staining (B) suggested aggregate formation. Number of tyrosine hydroxylase positive neuronal cluster was low in 30±60 day-old flies (D) compared with young adult flies (C) (Feany and Bender, 2000).

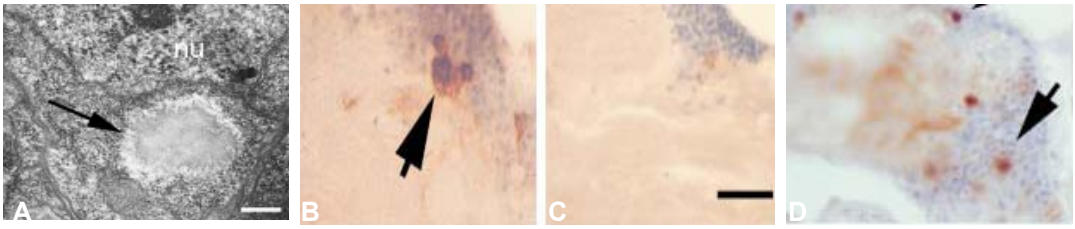

Over-expression of genes such as α-synuclein in mice has shown symptoms including reduced olfaction and deficits in motor skills as early as 2 months of age (Fleming *et al.,* 2006) as well as accumulation of insoluble α-synuclein (Fleming *et al.,* 2007) and widespread proteinase K resistant alpha-synuclein aggregates (Fernagut *et al.,* 2007). Other factors such as synaptic dysfunction, lower levels of noradrenalin in the cerebral cortex and changes in gene expression of ion channels in DA neurons have also been observed (reviewed by Meredith *et al.,* 2008). Several lines of mice over-expressing α-synuclein have been generated but issues regarding increased α-synuclein toxicity, abnormal motor deficits and production of LBs remain.

Similarly parkin, PINK1 and DJ-1 knock-out mice show different features. Transgenic mice containing Q300X parkin mutation have shown DA loss in the later stages of development accompanied with motor dysfunction (Lu *et al.,* 2006). PINK1 KO mice exhibit reduced striatal DA release and DJ-1 mutations lower resistance to oxidative stress (Dodson, 2007) but DJ-1 KO mice do not show PD phenotype, DA cell loss or nigral degeneration (Yamaguchi & Shen, 2007).

To counter the lack of DA loss in most genetically engineered models, recombinant adeno-associated viral (rAAV) or lentiviral vectors have been used in targeting the nigral DA neurons both in the rodent and the primate brain. Their long-term expression efficiency is very high in nigral DA neurons (Ulusoy *et al.,* 2008) and they show behavioural deficits (Kirik *et al.,* 2002). Such studies have shown formation of α-synuclein positive inclusions and dystrophic neurites as well as

phosphorylated α-synuclein at serine residue 129 (Fujiwara *et al.,* 2002). Similar experiments have reproduced toxicity using parkin associated endothelin-receptor like receptor (Pael-R) or another parkin target protein CDCrel-1 (Dong *et al.,* 2003; Kitao *et al.,* 2007). CDCrel-1 over-expression in rats through rAAV injection caused a progressive DAergic neurodegeneration.

1.1.3.3 Cell-models of Parkinson's disease:

The main advantages of cell-culture models are time-efficient experiments, quick screening of toxins, easy assessment of gene/protein expression, gene knock-down, transfection for over-expression proteins etc. Changes that occur due to different cell-types in brain can be mimicked through co-cultures of different cell-types like neurones and glial cell as observed in PD. Post-mitotic human dopaminergic neuronal cell lines can be ideal candidates for a PD model. Primary neuronal cultures from different transgenic mice can be readily immortalised by retroviral transduction to generate cell culture models to study PD-related proteins. A number of cell-lines have been extensively used to explore the neurotoxic potential of different toxins e.g. SH-SY5Y, MN9D, PC12, and NB41 cell lines as well as primary midbrain cultures (Onyango *et al.,* 2008) but protein expression can vary from cell-type to cell-type. A vast amount of data generated through cell studies has shown how PD related toxins affect different pathways. Such studies have been instrumental in explaining the role of protein aggregation, oxidative stress, the proteasome system and how toxins like MPP+ cause apoptotic cell death through caspase-3 activity, generate ROS, lead to LDH release and inhibit the electron transport chain (Orth and Tabrizi, 2003).

1.2 Biochemistry of Parkinson's disease:

ROS associated damage; proteasomal inhibition and mitochondrial dysfunction have been identified as major biochemical processes linked with dopaminergic cell-death in PD. Discovery of mutations in various dominant and recessive genes that cause abnormalities in the above mentioned processes has greatly helped the understanding of the biochemistry of PD. The heterogenous nature of PD suggests involvement of multiple genes rather than a single gene or mutation. Research into rare familial forms of PD has detected several gene mutations and chromosomal loci (Schapira, 2007; Belin & Westerlund, 2010) (fig 1.14). Their products, alpha-synuclein (SNCA), parkin (ubiquitin-conjugating enzyme; PARK2; UBCH7), PTEN induced kinase 1 (PINK1), DJ-1, ubiquitin C-terminal hydrolase L1 (UCHL1), and leucine-rich repeat kinase 2 (LRRK2/dardarin) (Moran *et al.,* 2007) have been extensively investigated and used in animal and cell-culture studies.

Fig 1.14: Genetic mutations linked with neurodegeneration in PD (Taken from Hardy *et al.,* 2006).

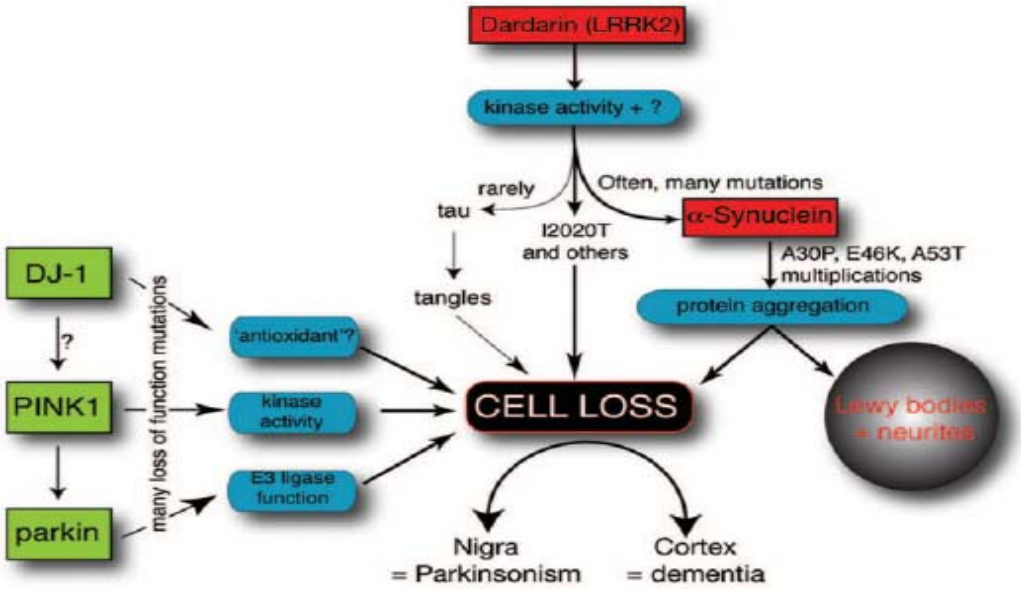

1.2.1: Genetic Mutations linked with Parkinson's disease:

1.2.1.1: α-synuclein:

α-synuclein, a natively unfolded protein, is the main constituent of Lewy bodies (fig 1.15). It is ubiquitously expressed in the brain. Its normal cellular functions are not well understood and studies suggest a variety of functions for α-synuclein. It may bind to transport vesicles (Murphy *et al.,* 2000) or vesicles with high phosphatidic acid content (Davidson *et al.,* 1998), inhibit phospholipase D2 (Jenco *et al.,* 1998), may negatively regulate dopaminergic neurotransmission (Abeliovich *et al* (2000), act as molecular chaperone or interact with chaperones (Ostrerova *et al.,* 1999) or cause deleterious effects through interaction with monoamines resulting in oxidative stress (Galvin, 2006).

Fig 1.15: α-Synuclein-positive Lewy body (red arrows) in the substantia nigra of idiopathic PD brain (Taken from Goedert, 2001).

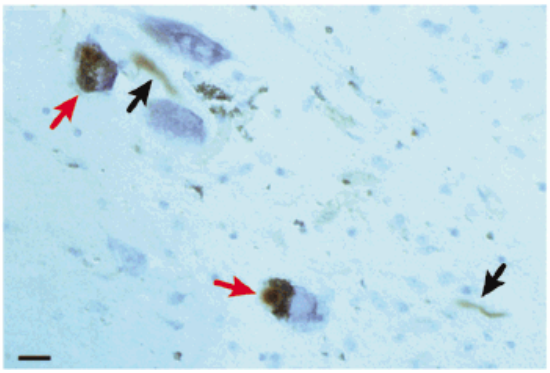

1.2.1.1.1 Mutations in α-synuclein:

The α-synuclein gene (*SNCA*) is located at chromosome 4q21 (Hofer *et al.,* 2005). Mutations in its structure include A53T point substitution (Polymeropoulos *et al.,* 1997), A30P missense mutation (Kruger *et al.,* 1998), E46K missense mutation (Zarranz *et al.,* 2004) and triplication of the wild-type gene (Singleton *et al.,* 2003). Miller et al (2004) have reported that triplication of α-synuclein results in almost double the amount of the protein in the blood. This has been linked with a reduction in the onset age of PD to as low as 30-40 years (Singleton *et al.,* 2003). Mutant proteins have different structural properties e.g. A53T mutant amasses at the plasma membrane, whereas A30P is largely found in the cytosol as it cannot bind strongly to the membrane (Willingham et al., 2003).

α-synuclein protein has a central hydrophobic region that promotes aggregation (Giasson *et al.,* 2001) whereas the C-terminal tail inhibits this (Park & Lansbury, 2003). A30P, E46K and A53T mutations are all identified in the imperfect KTKEGV repeat regions next to the hydrophobic region (fig 1.16). A53T and E46K are both considered to play a role in fibril formation leading to α-synuclein aggregation (Giasson *et al*., 1999; Wood *et al*., 1999) and it is this fibrillar form that is thought to be a major component of LBs (Crowther *et al*., 2000). All three mutations, A53T, E46K and A30P are involved in the formation of oligomeric forms of α-synuclein called protofibrils which may form pores and damage membranes (Volles & Lansbury, 2002). In a yeast model, α-synuclein over-expression and mutations of α-synuclein can cause endoplasmic reticulum (ER) stress by inhibiting vital proteins required in ER to golgi transport, thus causing ER stress (Chua & Tang, 2006).

Fig 1.16: α-synuclein protein motifs: The acidic part in the C-terminus decreases protein aggregation, whereas aggregation is promoted by the hydrophobic region near the KTKEGV repeats (Taken from Cookson, 2005).

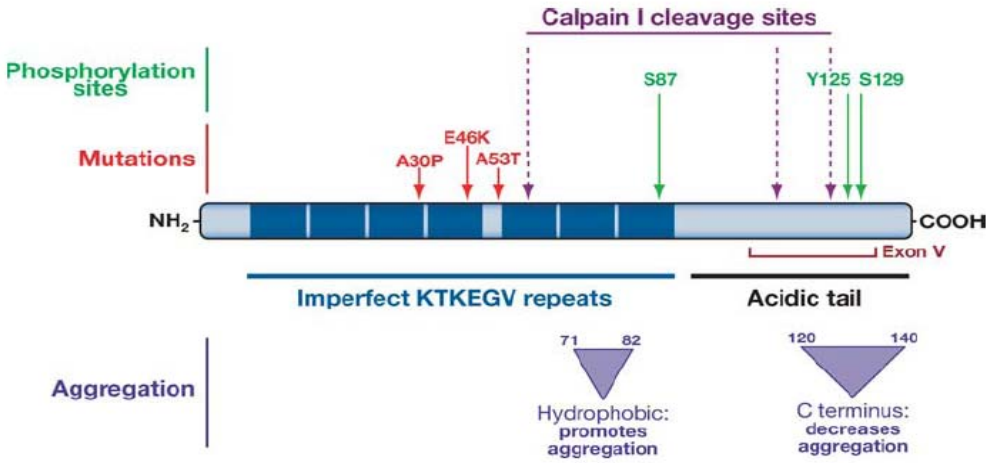

A53T and A30P mutations do not always produce the required nigral degeneration (i.e. nigral cell loss) and do not exhibit similar phenotypes even when their level of expression is the same. Interestingly, the wild-type protein also damages SN neurons and some studies have shown that the level of damage caused is equal to that caused by mutant α-synuclein (Xu *et al.,* 2002). Wild-type α-synuclein has a natural tendency to aggregate into oligomers and undergoes post-translational modifications which promotes aggregation. α-synuclein aggregates in all tissues but

symptoms only appear in certain neuronal cells (Miller *et al.,* 2004). This is because the expression level of α-synuclein is higher in the brain and the brain has a higher concentration of molecules that encourage aggregation (Uéda *et al*., 1993). In spite of extensive research, the precise function of α-synuclein and its over-expressed form and how exactly it causes selective dopaminergic neuronal death in PD is still unclear.

1.2.1.1.2 Transgenic models of α-synuclein:

α-synuclein is found in the presynaptic nerve terminal as well as in the cytoplasm. α-synuclein knockout mice have synaptic deficits, proposing a synaptic role for α-synuclein (Abeliovich *et al*., 2000). But knockout mice do not exhibit symptoms of PD suggesting that loss of protein function has no bearing on disease onset. This brings α-synuclein mutations into focus since when introduced into transgenic animals they do induce nigral degeneration in rats and primates (Lo Bianco *et al.,* 2002 & Kirik *et al.,* 2003). Song et al (2004) have shown that over-expression of α-synuclein in transgenic mice impairs mitochondrial function; causes oxidative stress and enhances MPTP toxicity. The latter could be due to the interaction of α-synuclein with the dopamine transporter, potentially increasing MPP+ uptake and causing greater injury.

1.2.1.2 Parkin:

The *PARKIN* gene is one of the largest genes in the human genome (1.53Mb) (Kitada *et al.,* 1998) and *PARKIN* mutations account for up to 10-20% of all early-onset parkinsonism (reviewed by Farrer, 2006). Mutations in *PARKIN* include exonic rearrangements, frameshift mutations, duplications, multiplications and point mutations. The latter being the most frequently occurring (Mata *et al.,* 2004) and mostly found in the RING-IBR-RING domain in the C-terminal (von Coelln *et al.,* 2004).

1.2.1.2 .1 Parkin function:

Several studies have identified various properties and functions of parkin. It encodes a ubiquitin E3 ligase that associates with the outer mitochondrial membrane (Darios *et al.,* 2003). Zhang et al (2000b) have shown that parkin promotes its own degradation via its own ubiquitination and can act in concert with GTPase septin

'CDCrel-1'. It ubiquitinates synphilin-1 (Chung *et al.,* 2001), dopamine transporter (Jiang *et al.,* 2004) and the cytoskeletal proteins α- and β-tubulin (Ren *et al.,* 2003).

A number of different parkin substrates have been identified, including, parkin associated endothelin-like receptor (Pael-R or GPR37) (Imai *et al.,* 2001), ataxin-3 (Tsai *et al.,* 2003), cyclin E (Staropoli *et al.,* 2003), o-glycosylated α-synuclein (Shimura *et al.,* 2004). Other than these, it interacts with DJ-1 (Moore *et al.,* 2005), BAG5, (Kalia *et al.,* 2004); E2 ubiquitin conjugating enzymes UbcH6/7/8 (Staropoli *et al.,* 2003), structural proteins CASK/LIN2 (Fallon *et al.,* 2002), actin filaments (Huynh *et al.,* 2000) and 26S proteasome subunit 'Rpn10' (Sakata *et al.,* 2003).

Some other parkin properties have come to notice recently, including its neuroprotective effect against mutant α-synuclein (Petrucelli *et al*., 2002), kinase induced excitotoxicity (Staropoli *et al.,* 2003), degradation of substrates localised in mitochondria, prevention of cytochrome c release and apoptosis (Darios *et al.,* 2003). It is not clear how these are connected with dopaminergic cell death in PD.

1.2.1.2.2 Mutations in *PARKIN*:

PARKIN encodes an E3-ligase, involved in the proteasomal protein degradation pathway (Farrer, 2006). It acts in concert with the ubiquitin conjugating enzyme UbcH7 (Shimura *et al.,* 2000). It is also known to play a vital role in the poly-ubiquitination of proteins by transferring ubiquitin from the 'ubiquitin conjugating E2 enzyme' to the substrates targeted for degradation. Mutations in the PARKIN gene can therefore reduce E3 activity. The R42P recessive mutation has been known to disrupt the interaction between the E3 ligase and the proteasome (Sakata *et al.,* 2003). Indeed mutations in the PARK2 gene locus of parkin are linked with autosomal-recessive juvenile parkinsonism (von Coelln *et al.,* 2004), where missense mutations are believed to impede protein degradation in vulnerable neurons, causing protein accumulation and eventual cell death. Yang et al (2003) have shown (using a drosophila model) that wild-type parkin protects against cell death caused by over-expression of Paelr1 (an E3 ligase substrate).

Ko et al (2005) have reported cell death in catecholaminergic neurons due to accumulation of another E3 substrate 'aminoacyl-tRNA synthetase cofactor p38' in

the ventral midbrain/hindbrain of young and old parkin null mice. This confirms the findings of analysis of brain tissue samples from idiopathic and AR-JP patients, which has also showed an increased level of p38. Knockout mice have not confirmed nigral cell loss or motor disabilities but have shown abnormalities in dopamine metabolism and glutamate neurotransmission (von Coelln *et al*., 2004). Autopsies have shown pure nigral degeneration in patients with parkin mutations but the presence of Lewy bodies is not noticed in all cases (Farrer *et al*., 2001).

1.2.1.3 DJ-1:

The *DJ-1* gene is linked with autosomal recessive parkinsonism (Bonifati *et al.,* 2003). Family based linkage studies have detected rare recessively inherited missense mutations and gene deletions (Lockhart *et al.,* 2004). DJ-1 is a highly conserved, ubiquitous and multifunctional protein dimer present in mitochondria, cytoplasm and extracellular space of mammalian cells (Herrera *et al.,* 2007). It is widely expressed in both glia and neurons (Bader *et al.,* 2005). Its known functions include co-regulation of tyrosine hydroxylase with its promoter, inhibition of α-synuclein aggregation (Zhou *et al.,* 2006), interaction with p54nrb, pyrimidine tract-binding protein-associated splicing factor and Topors/ p53BP3 causing changes in transcriptional activity (Shinbo *et al.,* 2005; Xu *et al.,* 2005), providing protection against mitochondrial complex-I inhibitors (Yokota *et al.,* 2003), acting as a ROS scavenger (Lockhart *et al.,* 2004) and a probable redox-regulated chaperone of α-synuclein (Zhou *et al.,* 2006). Its over-expression may protect against oxidative toxic injury, whereas mutations may result in it losing its ability to modulate gene expression under stress (Bonifati *et al.,* 2003).

A number of studies have suggested several ways of how DJ-1 may be associated with PD pathogenesis. Oxidation affects DJ-1 structure and function, resulting in reduced inhibition of α-synuclein fibrillation (Zhou *et al.,* 2006). It is also suggested that DJ-1 is an oxidative stress sensor; it accumulates as an acidic isoform after oxidative stress limiting cellular toxicity (Gosal *et al.,* 2006).

1.2.1.3.1 DJ-1 and Parkinson's disease:

Oxidised DJ-1 has been identified in post mortem PD brains (Choi *et al.,* 2006) but more research is necessary to show how it is linked with disease pathogenesis. Loss of DJ-1 leads to deficient antioxidant transcriptional responses through the loss of nuclear factor erythroid 2-related factor (Nrf2); which leads to a deficit in detoxifying enzyme [NAD(P)H quinone oxidoreductase 1] NQO1 (Clements *et al.,* 2006). DJ-1 stabilises the antioxidant transcription master Nrf2 and loss of DJ-1 may be related to PD aetiology.

1.2.1.3.2 Mutations in *DJ-1*:

Splice and frameshift mutations in *DJ-1* have been identified (Hague *et al.,* 2003) as well as deletion of the promoter region of the gene (Abou-Sleiman *et al.,* 2003). Both are considered to be linked with young-onset PD. DJ-1 is thought to function as a dimer whereas its mutant forms do not or in some cases (M26I mutation) not to the same extent as the wild type (Herrera *et al.,* 2007). L166P missense mutation causes a loss of function which has been associated with increased DJ-1 degradation which can lead to neurodegeneration (Zhou *et al.,* 2006).

1.2.1.4 UCHL1:

Ubiquitin C-terminal hydrolase-L1 (UCHL1) is an abundant neuron-specific protein (1-2% of total brain protein) (Lee & Liu, 2008). *UCHL1* gene (9.5kb) encodes ubiquitin C-terminal hydrolase, which hydrolyses peptide-ubiquitin bonds and converts ubiquitin chains to monomeric ubiquitin (Liu *et al*., 2002).

Genetic variability in *UCHL1* has been linked with PD through its reduced activity in the ubiquitin-proteasome pathway. UCHL1 has been identified in Lewy bodies and Alzheimer's neurofibrillary tangles (Lowe *et al.,* 1990). A missense mutation I93M has been identified in a German family with PD (Leroy *et al.,* 1998) but follow up studies have failed to identify this. Non-synonymous S18Y polymorphism in *UCHL1* has been linked with reduced or increased ligase activity but several issues concerning its role in PD remain inconclusive (Healy *et al.,* 2004). Liu et al (2002) have suggested that dual like ligase and hydrolase activities of UCHL1 may be involved in proteasomal degradation and lead to PD susceptibility.

1.2.1.5 PINK 1:

PTEN-induced kinase 1 (PINK1) is a nuclear-encoded kinase and after PARKIN mutations it is the most frequent mutation in parkinsonism (Hatano *et al.,* 2004). PINK1 is ubiquitously expressed in the human brain. It is localised in mitochondria with evidence of detection in the inner and outer-membranes (Valente *et al*. 2004a). About 10% of Lewy bodies identified in sporadic PD are PINK1 positive. This may be due to its poor solubility and tendency to aggregate but they have only been detected in brainstem LBs and not the cortical LBs (Gandhi *et al.,* 2006).

1.2.1.5.1 Mutations in *PINK1*:

Mutations in *PINK1* have been associated with mitochondrial dysfunction related to autosomal recessive familial PD. A number of missense and nonsense truncating mutations have been reported in the *PINK*1 gene and point mutations rather than deletions are most likely to be responsible for the disease phenotype (Valente *et al.,* 2004). Homozygous as well as single heterozygous mutations have been found in PD patients (reviewed by Wider & Wszolek, 2007). *PINK1* mutations are distributed throughout the gene and have different effects ranging from reduction in protein accumulation to decreased kinase activity (reviewed by Abeliovich & Beal, 2006).

PINK1 contains an N-terminal mitochondrial targeting, a serine/threonine-directed protein kinase domain (Zhou *et al*., 2008) with significant homology to the calcium-calmodulin protein kinases and a C-terminal domain that is involved in the regulation of autophosphorylation activity (Silvestri *et al*., 2005; Sim *et al*., 2006). This discovery suggests a possible link with cell-signalling processes.

1.2.1.5.2 Protective effect of PINK1:

PINK1 may also provide neuroprotection against oxidative stress and through a direct regulation of apoptosis (Valente *et al.,* 2004a). Wild-type PINK1 protects dopaminergic neurons against stress-induced mitochondrial dysfunction (Deng *et al.,* 2005) and apoptosis induced by proteasomal inhibitors (Valente *et al.,* 2004a). Over-expressed wild-type PINK1 lowers caspase cleavage and cytochrome c release. This was reported by Petit et al (2005) who suggested that PINK1 plays a part in

mitochondrial dependent cell-death pathways by preventing cytochrome c translocation to the cytosol and reducing caspase-9 and -7 activation. Indeed, the kinase activity of this protein is reduced by G309D missense mutation (Muqit *et al.,* 2006). It may regulate HtrA2 phosphorylation, modulating its proteolytic activity, which may protect against mitochondrial stress (Plun-Favreau *et al.,* 2007). *PINK1* loss of function has not been reported in mammalian in vivo studies. The majority of recent work suggesting a link with apoptosis and cell-signalling comes from *D. melanogaster* studies (Clark *et al.,* 2006; Park *et al.,* 2006).

1.2.1.6 LRRK2:

Leucine-rich repeat kinase 2 (*LRRK2*) is a large gene located on chromosome 12p11.2–q13.1 (144kb, consisting 7449 base pairs, 51 axons) (Mizuno *et al*, 2008; Lesage & Brice, 2009). LRRK2 protein contains different domains in its structure. Several functional domains are present in the carboxyl half of LRRK2, like 'ROC' domain (leucine rich repeat), COR (carboxy terminal of ROC) domain, ANK (ankyrin repeat domain), MAPKKK (mitogen activated protein kinase kinase kinase), putative tyrosine kinase catalytic domain and WD40 domain (Liu & Lee, 2008; Mizuno *et al.,* 2008). These domains may be involved in the regulation of different cellular processes such as neurite maintenance, neuronal survival, protein and dopamine interactions (Galter *et al.,* 2006).

1.2.1. 6.1 Mutations in *LRRK2*:

LRRK2 mutations have been linked with both sporadic and familial PD. 10% of all autosomal dominant familial and 3.6% of sporadic PD cases have *LRRK2* mutations (Belin, 2008; Lesage & Brice, 2009). Several *LRRK2* pathogenic mutations have been identified, including Y1699C, I2020T, R1441C/G/H, G2385R, of which the G2019S missense is the most common (fig 1.17). A high G2019S mutation frequency has been noted in 6% of hereditary and 1-2% of idiopathic PD cases. Its frequency varies, with high rates in Ashkenazi Jews and North African Arabs (Farrer, 2006). Other variants seem to be population specific. G2385R, a polymorphic mutation, is considered a PD risk factor in Asian populations (Di Fonzo *et al.,* 2006), R1441G mutation in Basque region of Spain (Simon-Sanchez *et al.,* 2006) and G2385R and R1628P in Chinese populations (Lesage *et al.,* 2009).

Fig 1.17: LRRK2 Gene with its functional domains and sequence changes (Taken from Lesage & Brice, 2009).

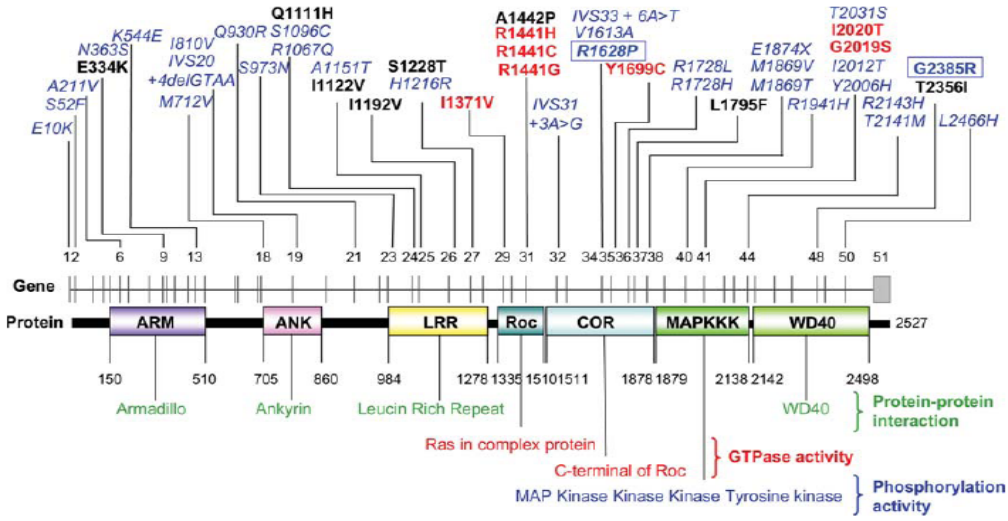

1.2.1.7 ATP13A2:

ATP13A2 is a predominantly neuronal P-type ATPase gene (Ramirez *et al.,* 2006) that codes for a lysosomal ATPase. It was mapped in a Chilean and Jordanian family with Kufor–Rakeb syndrome (KRS), a rare form of recessively inherited levodopa responsive juvenile onset parkinsonism with cognitive dysfunction and pyramidal degeneration (Lesage & Brice, 2009; Najim al-Din *et al.,* 1994). These families had compound heterozygous (c.1305 þ 5G .A/1019GfsX1021) and homozygous (552LfsX788) mutations which resulted in failure of proteasomal degradation of proteins and subsequent retention in endoplasmic reticulum instead of insertion in lysosomal membranes (Ramirez *et al.,* 2006). It is possible that failure of removal of α-synuclein aggregates due to failure of removal process caused by these mutations could contribute to PD development. Full function of ATP13A2 is not known and it is not clear how its loss of function causes lysosomal dysfunction.

Table 1.1: Summary of Genetic mutations in PD (Adapted from Belin & Westerlund, 2008; Farrer, 2006; Fahn & Sulzer, 2004; Haugarvoll *et al*., 2009; Satake *et al*., 2009; Strauss *et al*., 2005; Wider & Wszolek, 2007).

Gene	Locus	Mutations	Effects of Mutations
SNCA	PARK1 and PARK4 (4q21)	-Dominant Ala30Pro, Glu46Lys and Ala53Thr substitutions; genomic duplications and triplications -A53T and A30P may promote aggregation	-Missense mutations and genomic multiplications increase the cytoplasmic accumulation of α-synuclein monomer, promoting oligomerisation and toxicity.
PARKIN	PARK2 (6q25.2–q27)	-Recessive homozygous and compound -Heterozygous missense (>57) andexonic deletion/ duplication/triplication mutations -Over 70 mutations identified; most likely loss of function mutations	-Parkin is a part of UPS. Mutations can lead to protein build up due to impair in degradation process.
Unknown	PARK3 (2p13)	-	Autosomal dominant, Its putative function is unknown.
UCHL-1	PARK5 (4p14)	-Linkage for the Ile93Met substitution is equivocal -Late onset: Susceptibility to sporadic PD linked with a Ser18Tyr polymorphism	-Mutations in UCHL1 may prevent it from maintaining a pool of monoubiquitin for E3 ligase, hence disrupting the UPS.
PINK1	PARK 6 (1p35-p36)	Recessively inherited missense and exon-deletion mutations	-Mutations in DJ-1 and PINK1 impair the neuronal response to α-synuclein aggregation and also disrupt the mitochondrial function leading to ATP depletion.
DJ-1	PARK7 (1p36)	-Recessively inherited; homozygous missense (Leu166Pro) and deletion(delEx1–5) mutations, and compound heterozygotes	-Mutations in DJ-1 may alter its anti-oxidative properties.
LRRK2	PARK8 (12p12)	-Many dominant substitutions, notably Arg1441Cys/Gly/ His, Tyr1699Cys, Ile2012Thr, Gly2019Ser and Ile2020Thr	-LRRK, just like PINK1, encodes protein kinases. Mutations in the gene may disrupt cell signalling.
ATP13A2	PARK9 (1p36)	Homozygous and heterozygous ATP13A2 mutations, deletions (1-bp in exon 6) and splice site mutation recorded	Kufor-Rakeb syndrome, a rare recessively inherited levodopa responsive juvenile onset parkinsonism caused by a loss of function mutation of ATP13A2
Unknown	PARK10 (1p32)	-	Genetic variability in USP24 may be associated with PD
Unknown	PARK11 (2q36-q37)		No consistent evidence that variation in the GIGYF2 gene significantly contributes to PD
Unknown	PARK12 (Xq21-q25)	-	An X chromosome locus has been identified
OMI/HTRA2	PARK13 (2p12)	A polymorphism (A141S) and heterozygous mutation (G399S) identified in the HTRA2 gene	Both mutations cause defective activation of HTRA2 protease activity. Mutation causes mitochondrial

			swelling, reduced membrane potential and reduced neuroprotection
Unknown	PARK14 (18q11)	-	-
FBXO7	PARK15 (22q12-q13)	Autosomal recessive mutation in the FBXO7 gene	Recessive FBXO7 mutations cause early-onset parkinsonian-pyramidal syndrome
Unknown	PARK16 (1q32)	Linked with single-nucleotide polymorphisms and contains multiple independent association signals	-

1.3 Environmental factors and Parkinson's disease:

The role of environmental factors in PD development remains unclear. Several studies, exploring the relationship between PD risk and rural living, have reported a positive association and highlighted the involvement of agricultural factors. A number of other PD risk factors are interrelated with rural living, e.g. well-water drinking, farming, pesticide exposure, consumption of raw vegetables etc. Each of these has been investigated as an independent risk factor in the majority of the studies (Koller *et al.,* 1990).

1.3.1 Review of meta-analyses linking Parkinson's disease and exposure to pesticides:

1.3.1.1 Pesticide Exposure:

Meta-analysis carried out by Priyadarshi et al (2001) analysed 16 case-control studies and assessed demographic data including history of exposure to environmental factors, lifetime histories of places of residence, source of drinking water, and herbicide/pesticide exposure. They identified eleven studies with a positive association out of which statistically significant odds-ratio (OR) was reported for six studies. Three studies were negative and two reported no association. Only six studies provided information regarding duration of exposure/rural living, which ranged from 1 to >40 years. Cigarette smoking and caffeine/coffee use, considered to lower PD risk, were not considered in this metaanalysis. Evidence suggests a lower risk of PD in coffee drinkers and cigarette smokers (Hernan *et al.,* 2002). Indeed, a stronger inverse association between PD and cigarette smoking has been observed in workers handling pesticides regularly, compared with those who have never used pesticides (Galanaud *et al.,* 2005). None of the analysed studies however, specifically identified any particular agrochemical as being associated with increased risk of PD.

The same research group had earlier reported a consistent increase in PD development with pesticide exposure (Priyadarshi *et al.,* 2000). They used 19 out of 34 comparable case–control studies, opening the possibility of influencing the overall risk estimate due to the limited nature of the dataset which is a recurring problem. The BfR report commissioned by the European Union identified 62 studies to examine the link between PD and environmental factors, but found only 38 studies

compliant with their selection criteria, which were then included in their analysis. Remaining studies were excluded because they failed to include ORs or sufficient information to calculate the ORs (BfR, 2006). Priyadarshi *et al* (2000) did not find any dose-dependent relation or identify any specific categories of pesticides but the OR they calculated (1.94, 95% CI 1.49-2.53) was consistent with the findings of Lai et al (2002), who had earlier suggested that an increased pesticide exposure is strongly linked with rural living, farming and well water drinking rather than each of these risk factors directly causing PD. e.g. contamination of drinking water by pesticides, after the chemicals have leached into the soil (Metzler *et al.,* 1982).

In a critical review published by the 'Institute of Environment and Health' (IEH), a majority of the 38 case-control studies reviewed showed a significantly increased risk associated with pesticide exposure with excess risk ranging from 1.01 to 7.00. Even though some studies gave conflicting results, overall findings suggested a positive correlation between increased PD risk and pesticide exposure (IEH, 2005). Even some ecological studies have linked highest pesticide use with highest PD prevalence in heavily farmed areas (Dick, 2007) and mortality due to PD in some regions with higher pesticide use has been found to be greater than those with minimal pesticide use (Ritz & Yu, 2000).

1.3.1.2 Paraquat exposure:

Liou et al (1997) have reported the results of a case-control study in Taiwan, where paraquat is still widely used. They noticed a dose-dependent effect and found evidence of a strong correlation between PD incidence and the level of paraquat exposure. Individuals with more than 20 years paraquat exposure had a six times higher risk of developing PD. This trend is more commonly seen in studies focusing on occupational exposure where the long duration of pesticide, whether it is low or high dose is critical e.g. occupational exposure to paraquat was associated with parkinsonism in 57 cases in a British Columbia study (Dinis-Oliveira *et al.,* 2006).

Multiple exposures of paraquat and maneb, when administered together, have produced PD characteristics in mice; but no neurological changes were noted when administered separately (Thiruchelvam *et al.,* 2000a). Paraquat has been shown to

interact synergistically with maneb in mouse models, and reduce motor activity and damage nigral cell bodies (Thiruchelvam *et al.,* 2001a).

It has been suggested that the risk of PD significantly increases once the pesticide exposure has exceeded a threshold of greater than 10 or 20 years, as seen with paraquat (Liou *et al.,* 1997). According to Vanacore et al (2002), who evaluated PD risk in licensed pesticide users, PD risk is almost twice as high in these subjects (OR=1.85; 95% CI, 1.31–2.60) than in the general public. Another study found a high prevalence ratio for parkinsonism in a cohort of orchardists exposed to pesticides for more than 50 years (Engel *et al.,* 2001).

It is difficult to assess the effects of individual sub-groups like insecticides and herbicides because the majority of subjects can be exposed to herbicides as well as insecticides at the same time (up to 90% according to Gorell *et al.,* 1998). This along with the failure of recalling the specific class of chemical and its duration of exposure complicates the problem even more. Chronic low-level pesticide exposure is harder to detect and acute exposure produces delayed symptoms e.g. as seen in MPTP studies (Greenamyre *et al.,* 2003). Studies that have tried to categorise specific pesticide compounds have linked exposures to alkaline phosphates, organochlorines, carbamates, (Seidler *et al.,* 1996) and paraquat (Hertzman *et al.,* 1990) with increased PD risk.

1.3.1.3 Honolulu-Asia Aging Study:

The Honolulu-Asia Aging Study has also linked plantation work with PD risk, with longer pesticide exposure associated with increased risk (overall incidence 7.1/10,000 person-years, PD observed in 137 men). These results were not statistically significant (p=0.101) although based on prospective ascertainment of exposures. Most results were based on self-reported cases with no solid information of extent and duration of pesticide exposure (Abbott *et al.,* 2003). Factors such as coffee intake, cigarette smoking and polyunsaturated fat intake showed an inverse protective association with PD. Whereas carbohydrates increased the risk. A high PD risk (63.4/10,000 person-years) was noted in non-coffee drinkers exposed to pesticides (three times higher than coffee drinkers exposed to pesticides, 21.4/10,000 person-years). A similar relationship was observed in smokers (11.8/10000) against

non-smokers (27.4/10,000). Different cohorts are likely to be exposed to different sets of chemicals. This exposure misclassification may be the reason for the heterogeneity observed between different studies. Indeed, this heterogeneity comes from different study designs, selection of controls, differences in geography, ethnicity and genetic patterns (Nuti *et al.,* 2004).

1.3.1.4 Rural living and well water drinking:

Rajput et al (1986) have reported on cases of PD diagnosed in 19 patients who had spent the first 15 years of their lives in a rural community of about 169 people. When evaluating 'well-water studies only' Priyadarshi et al (2001) reported five studies with negative association, one with no association and eleven with positive association (combined OR of 1.26 (95% CI 0.96-1.64). Two studies were significant and five had statistically significant odds ratios. Furthermore, they identified five studies which assessed duration of well-water consumption and PD risk with the higher risk OR being 3.28 (95% CI, 0.93-11.51) after a minimum of 1 year exposure. Other risk values varied across the scale e.g. one study showed an OR of 0.95 (95% CI, 0.31-2.88) with an estimated 45 years exposure but another showed OR of 1.24 (95% CI, 0.77-2.0) with an estimated 10 years exposure. Wright & Keller-Byrne (2005) examined the 'well water use' link in a case control study and reported that PD risk increases (OR = 2.1; 95% CI: 0.7-6.4) if the subjects used well water during the first 20 years of their life. Hancock et al (2008) used generalised estimating equations to study the relationship between well-water consumption, pesticide usage and farming occupations/dwelling with PD. Data gathered from 319 cases and 296 relatives and other controls showed a positive association of broadly defined pesticide exposure with PD but showed no evidence of disease association with well-water consumption or working/living on a farm.

There is a relative inconsistency present among various studies. For example, Semchuk et al (1991) investigated the link between the development of idiopathic PD and exposure to environmental factors. They did not notice a significant increase in PD risk during the first 45 years of life. Jiménez-Jiménez et al (1992) reported in their study that PD cases drank more well-water than controls over a period of more than 30 years (OR 1.76, 95% CI 1.09–2.84) but they did not observe any link with

rural living and PD (OR 1.07, 95% CI 0.70–1.63). Stern et al (1991), in their case control study of young-onset and old onset PD, have reported an association with PD for cases who lived in rural areas for less than 10 years.

The ORs from studies investigating the 'PD link' with well-water use, farming and rural living are usually of the same order and direction but their magnitude of effect is different. Evidence for a positive association between farming, pesticide exposure, rural living and well water drinking outweighs that of any negative association. The duration of exposure of these factors varies considerably. There is no detailed database of specific pesticides (e.g., carbamates, organophosphates), duration of their usage, any dose-response relation, mode of usage (whether it is manually applied or sprayed from an aircraft) or determination of potential impacts from spray drift. Such data may help to calculate chemical doses used during normal occupational administration of the pesticides.

Evidence from case-control studies and case reports suggests that the duration of exposure is vital in disease development and particular classes of pesticides increase this risk. Exposure could be prolonged as well as acute. Positive results from studies with comprehensive exposure assessment, coupled with animal studies, support this association. Increasing toxicological and epidemiological data support positive PD association with insecticide/herbicide exposure and rural residency at the time of diagnosis but more data is required for each categorised herbicide, insecticide and fungicide to reliably confirm a causal relationship. Further evaluation of dose-response and understanding of relationship with other potentially confounding exposures is required. Most studies used idiopathic PD patients. It may be useful to consider the association between PD and subjects with familial forms of PD as it has been suggested that effects of pesticide/herbicide exposure may vary due to genetic heterogeneity among individuals.

Interpretability of studies is often hampered by the small study size and other methodological limitations. Recent well-designed prospective cohort studies are gaining insight into various risk-factors by gathering data on incident patients and person-years. Although recent findings are insufficient and some of the data equivocal, the current body of evidence suggests that exposure to pesticides and

other factors are closely linked and interrelated. PD risk does increase with rural-living and well water use, regardless of the age of disease onset (although the precise nature of this association varies between different studies) and validation of these results is seriously undermined by the lack of major significant associations. The weight of the evidence suggests a relatively consistent, though non-significant, relationship between pesticide exposure and increased PD risk. Replication of clinical and pathological signs in animal models is required to prove a causal link between PD and pesticide exposure.

1.4 Molecular pathways of cell death in Parkinson's disease

A number of different mechanisms have been implicated in the pathogenesis of PD. Their mode of action or trigger is different but their pathways can be inter-connected which eventually leads to neuronal death. Mitochondrial dysfunction, α-synuclein aggregation, protein degradation, oxidative stress, aberrant kinase signalling and neuroinflammation are triggers which commonly lead to cell death in PD. They act through pathways involving p53 activation, JNK/bcl-2 signalling and cell cycle activation/inhibition (Levy *et al.,* 2009).

1.4.1 Apoptosis:

Apoptosis is a gene-directed programmed cell death mechanism morphologically characterised by chromatin condensation, cell/cytoplasmic shrinkage, blebbing and formation of apoptotic bodies. Its main biochemical features include caspase activation (caspases 3, 6 and 7), DNA fragmentation (Ferraro and Cecconi, 2007), degradation of chromosomal DNA, cleavage of a specific subset of cellular polypeptides by caspases (8, 9 and 10), and expression of cell surface markers (Lazebnik *et al.,* 1994). Apoptosis is a wide ranging mechanism involving apoptosis-inducing or death receptors (*e.g.* Apo-1/Fas), apoptosis-initiating factors (AIFs), proteins released from damaged mitochondria, caspases and calpains (Jellinger, 2001). It can be triggered by a number of different stimuli including oxidative stress, irradiation, viruses, heat, hypoxia, toxins or the withdrawal of neurotrophic support (Jellinger, 2001).

1.4.1.1 Apoptosis and Parkinson's disease:

There are two main apoptotic pathways: the extrinsic (death receptor pathway involving FasL/FasR, TNF-*α*/TNFR1, Apo3L/DR3, Apo2L/ DR4 and Apo2L/DR5) and the intrinsic (non-receptor-mediated mitochondrial pathway). Cells expressing Fas or TNF receptors cause apoptosis via ligand binding and protein cross-linking. Both pathways converge on the same terminal. i.e. caspase-3 cleavage leading to DNA fragmentation, protein degradation, protein cross-linking, formation of apoptotic bodies, ligand expression and phagocytic uptake (reviewed by Elmore, 2007) (fig 1.18). Immunocytochemistry of PD post-mortem brain suggests two pre-mitochondrial apoptosis pathways are involved in nigral neuronal cell-death i.e. p53–GAPDH–BAX pathway and FAS or TNF–α receptor–FADD–caspase 8–BAX

pathway (Tatton *et al.,* 2003). Increase in signalling factors for apoptosis like Bax has been observed in PD. In their study, Hartmann et al (2001) reported that the percentage of Bax-positive melanised LB positive SNpc neurons was significantly higher than the overall percentage of Bax-positive neurons. These neurons were also immuno-positive for activated caspase-3.

Fig 1.18: Signalling cascade in apoptotic cell death. Receptor-mediated activation of caspase-8 leads to caspase-3 activation in the extrinsic apoptosis pathway. In intrinsic pathway, apoptosome and cytochrome c release from mitochondria leads to caspase-3 activation (Taken from Kermer, 2004).

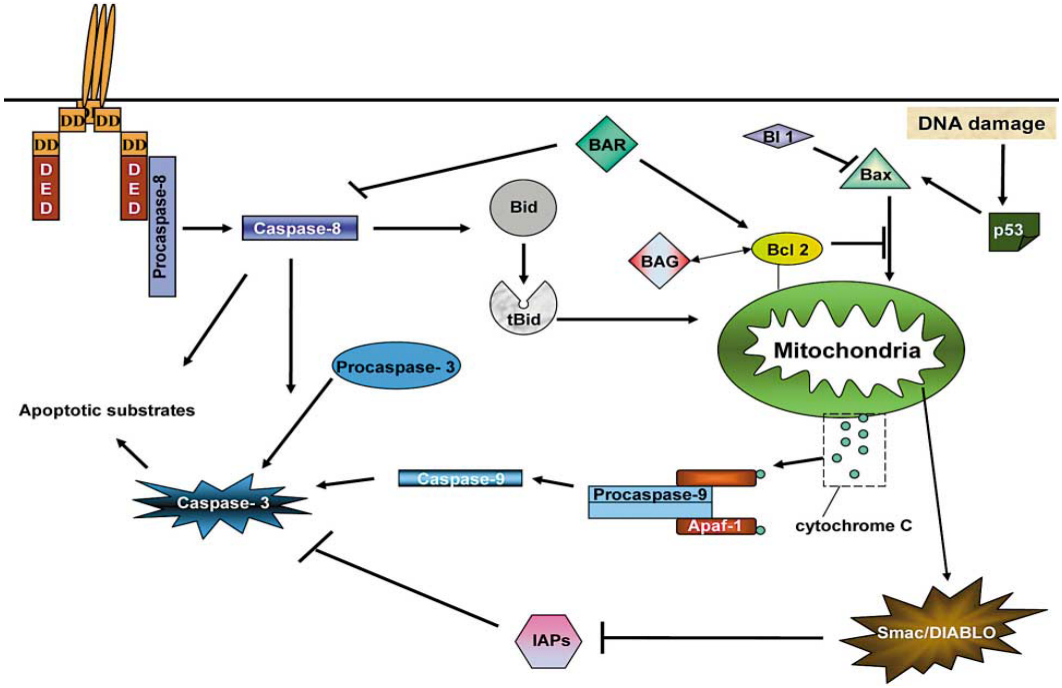

Evidence of apoptosis in PD autopsy material is conflicting. Some studies have shown apoptotic cells and DNA fragmentation in substantia nigra of PD patients (Mochizuki *et al.,* 1996) with a role of caspase-3 in neuronal cell-death in the SN (Hartmann *et al.,* 2000) but typical apoptotic features like nuclear condensation and pyknosis are not consistently seen. TUNEL labelling for DNA fragmentation has shown variable results (Tatton *et al.,* 2003). The slow rate of DA cell loss in the SN and rapid clearance of apoptotic cells makes it difficult to detect these markers. Hartmann et al (2000) have reported a significantly higher number of activated caspase-3-positive DA neurons in PD patients. They also suggested that caspase-3 activation is not due to apoptosis in PD but it actually precedes its

initiation as noted through its activation before chromatin condensation and final cell breakdown. Some studies have shown negative results with no changes in the expression of activated caspase-3, Fas or Bcl2 proteins in PD samples (Jellinger, 2000) whereas others have shown opposite results (Tatton, 2000; Hartmann *et al.,* 2001).

1.4.1.2 Experimental models and Apoptosis:

Experimental PD models using MPTP administration in mice has shown caspase-3 induction and DNA fragmentation with increased nigrostriatal activity of both c- Jun and c-Jun NH_2-terminal kinases fragmentation (Tatton, 2000; Hartmann *et al.,* 2000), and increased Bax expression (Eberhardt *et al.,* 2000). Inhibition of the JNK pathway leads to a reduction in dopaminergic cell loss in the SN (Saporito *et al.,* 2000). MPP+ initiates apoptosis via ROS production which disrupts the mitochondrial permeability pore leading to neuronal cell death (Tatton and Olanow, 1999). In the 6-OHDA animal model of PD, both necrotic and apoptotic (caspase involved) features are seen in SN neurons (Choi *et al.,* 1999).

Several animal or cell models as well as studies of PD post-mortem brains have shown the presence of activated caspases suggesting a possible role of caspases in the development of PD (Hartmann *et al*., 2000; Viswanath *et al*., 2001; Yamada *et al*., 2004). Experimental studies have shown an increase in caspase activity after treatment with high concentrations or over-expression of α-synuclein (Seo *et al*, 2002), whereas DJ-1 appears to inhibit caspase activation (Fan *et al*., 2008).Increased expression of A53T α-synuclein in differentiated PC12 cells can lead to higher levels of caspase-9 and -3 activities, mitochondrial cytochrome C release, endoplasmic reticulum stress and elevated caspase-12 activity (Smith *et al.,* 2005). Transgenic mice expressing A53T have shown nuclear condensation, eosinophilic Lewy body-like inclusions in cortical and spinal motor neurons. Subsets of neurons in the neocortex and brainstem were positive for cleaved caspase-3 and p53 (Martin *et al.,* 2006). Over expression of wild-type PINK1 can lead to apoptosis and can reduce levels of cleaved caspase-3, caspase-7, caspase-9 and PARP in staurosporine-induced apoptosis (Petit *et al.,* 2005). Similarly transient transfection of mutant LRRK2

shows apoptosis and can lead to neuronal death (Iaccarino *et al.,* 2007). Over expression of Parkin can delay mitochondrial swelling, subsequent cytochrome c release and caspase-3 activation. Parkin promotes substrate degradation and any loss of function due to mutation may lead to degeneration of nigral dopaminergic neurons in patients carrying parkin mutations (Darios *et al.,* 2003).

1.4.2 Autophagy:

Autophagy is a non-selective degradation system (unlike ubiquitination) that involves induction of proteins, organelles or cellular debris into multi-membrane vesicles called autophagosomes which are then fused with and degraded by lysosomes, particularly in times of cellular stress such as nutrient deprivation where energy producing substrates may be required by the cell. Autophagic bodies are then broken down and recycled to provide the cell with a source of cellular energy (fig1.19) (Elmore, 2007). Depending on the mode of delivery to the lysosomes, autophagy is divided into sub-categories including microautophagy (cytoplasm directly sequestered at the lysosomal surface), macroautophagy and chaperone-mediated autophagy (hsc70 complex binds to the lysosomal membrane receptor [lamp2a] and is then transported into lysosomes (Crotzer and Blum, 2005; Levine and Kroemer, 2008).

Autophagy was studied further as a separate mechanism once it was noted that cells can undergo programmed cell-death without displaying apoptotic features and without undergoing caspase-independent gene-activated cell death (Cohen, 1991). High number of autophagic vacuoles is thought to be responsible for neuronal cell death but an alternative theory suggests that autophagy removes abnormal proteins that could trigger apoptosis and hence protects neurons (Butler *et al.,* 2006).

Fig 1.19: Autophagic degradation of intracellular damaged and aberrant materials. Three main stages are involved: formation of the isolation membrane, elongation and completion of the mature autophagosome and fusion of the autophagosome with the lysosome (Taken from Vellai, 2009).

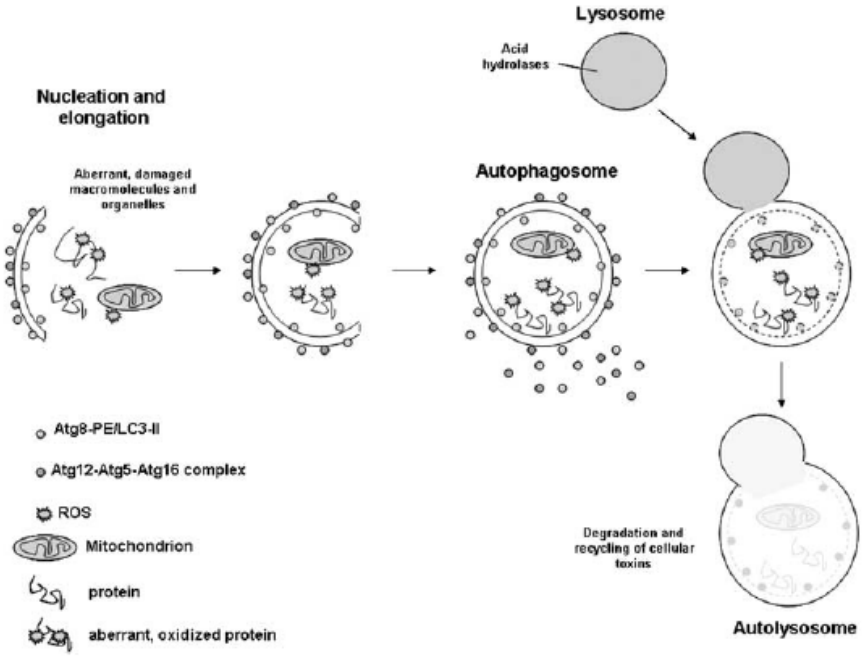

Autophagy can be induced through nutrient starvation, depletion of total amino acids, inhibition of mTOR (mammalian target of rapamycin) (Mizushima, 2007) or through small-molecule enhancers of the cytostatic effects of rapamycin (SMERs) (Sarkar *et al.,* 2007). A number of different factors can regulate autophagy including ROS, TNF-α induced increase in beclin-1 (Djavaheri-Mergny *et al*. 2006), free cytosolic calcium (Hoyer-Hansen *et al*. 2007), mTOR inhibition through adenosine monophosphate-activated protein kinase (AMPK) activation (Meley *et al*. 2006), kinases, phosphatases and guanosine triphosphatases (GTPases), TRAIL, BNIP3 and DRAM (Mizushima, 2007).

Autophagy is controlled by a number of different 'autophagy-specific genes' (*ATG*) (Kroemer and Jäättelä, 2005). 31 autophagy-related proteins have been identified in yeast out of which 18 (AP-Atg proteins) are involved in the formation of the autophagosome (Klionsky *et al*. 2003). Chemical inhibitors or gene knock-out can sensitise cells to autophagy. Knock-down of *ATG5*, *ATG10* or *ATG12* can prevent the formation of autophagic vacuoles. Experiments where *ATG5* or *ATG7* genes were suppressed led to the presence of polyubiquitinated proteins in the CNS

of mice. This can also increase susceptibility to apoptosis. Selective deletion of *ATG5* or *ATG7* genes in mouse models has shown a high number of ubiquitin-positive cytoplasmic bodies without neuronal loss in the SNpc (Hara *et al.,* 2006).

Indeed certain features of both autophagy and apoptotic processes propose a connection between these pathways (Piacentini *et al.,* 2003). Onset of autophagy can precede apoptosis and may also delay it but apoptotic signals may also trigger autophagy (Bauvy *et al.,* 2001). During caspase inhibition autophagy may cause neuronal cell death. Indeed, active autophagy has been noted in neurons when the pan-caspase inhibitor BAF is used. Autophagy markers such as autophagosome formation may appear before apoptotic markers but other data suggests that autophagy and apoptosis can overlap (Xue *et al.,* 1999). Cells can be prevented from undergoing apoptosis by autophagy by keeping substrate level high in cells either during nutrient depletion or during lack of growth factors (Boya *et al.,* 2005).

1.4.2.1 Autophagic-Lysosomal Pathways and Parkinson's disease:

Accumulation of autophagosomes and a high number of autophagic vacuoles has been reported in the brains of Alzheimer's and Parkinson's disease patients and in animal models of PD (Anglade *et al.,* 1997; Oztap and Topal, 2003). This may occur due to a failure of lysosomal clearance of autophagosomes or due to pathogenic deterioration which cannot maintain the cellular balance and which leads to neuronal death (Levine and Kroemer, 2008). Experimental data shows that MPTP can cause high levels of autophagic degeneration in mice (~35% of DA neurons in SNpc) (Oztap and Topal, 2003). Macroautophagy is linked to PD through an unknown mechanism that may include DJ-1, Parkin and PINK1 in assisting the uptake and removal of damaged mitochondria. For example, Parkin can associate with dysfunctional mitochondria and enhance their uptake by lysosomes (Narendra *et al.,* 2008) whereas DJ-1 may play a role in autophagic flux (Vasseur *et al.,* 2009).

Accumulation of wild-type α-synuclein is a common feature in PD and other than the ubiquitin-proteasome system; autophagy plays a part in α-synuclein removal (Webb *et al.,* 2003) further suggesting that any defect in this pathway may play a role in neurodegeneration in PD. Wild type α-synuclein is degraded through chaperone mediated autophagy and despite a high affinity for the CMA receptor, A53T mutant

α-synuclein is not translocated to the lysosomes and instead can block uptake of other CMA substrates resulting in slow overall protein degradation and possibly causing cellular stress and neurotoxicity (Cuervo *et al.,* 2004). Yang et al (2009) have proposed a mechanism where over-expression of either wild-type or mutant α-synuclein disrupts degradation of the neuronal survival factor myocyte enhancer factor 2D (MEF2D) through CMA. They suggest that MEF2D is regulated through autophagy and blocking this pathway through a PD linked protein compromises cell survival. In culture, α-synuclein accumulation increases when acidic compartments are neutralised. Treatment with lysosomal inhibitors leads to accumulation of Triton soluble and insoluble aggregates in a dose-dependent manner (Lee *et al.*, 2004).

Several features of age related neurodegenerative diseases like protein deposition, synaptic loss and neuronal cell-death have been linked with the inhibition of lysosomal enzymes leading to lysosomal dysfunction (Lee *et al.*, 2004). There is increasing evidence for an important role of lysosomes in PD aetiology. Defective lysosomal function can lead to α-synuclein accumulation without showing any changes in gene expression in mice (Meredith *et al.,* 2002) and mutation in *ATP13A2* leads to insufficient lysosomal protein removal. Kufor-Rakeb syndrome, a rare hereditary form of parkinsonism, develops due to mutations in *ATP13A2* (Ramirez *et al.,* 2006). Similarly, mutations in another PD linked gene lysosomal enzyme glucocerebrosidase (*GBA*) cause Gaucher's disease. Indeed, heterozygosity for a *GBA* mutation can predispose to PD and PD patients have a significantly higher chance of being a Gaucher's disease carrier than Alzheimer's patients (Aharon-Peretz *et al.,* 2004).

1.4.3 Endoplasmic reticulum (ER) Stress and PD:

The endoplasmic reticulum (ER) is the intracellular organelle where the correct folding and processing of newly formed membrane and secretory proteins takes place. Impairment of this function leads to the accumulation of unfolded proteins in the ER lumen leading to ER stress which can induce apoptosis (Kaufman, 1999). Evidence for the involvement of ER stress in PD comes from the studies of certain neurotoxins used to mimic PD features in cell culture and *in vivo* (Holtz *et al*., 2003; Ryu *et al*., 2002) and those involving a G-protein-coupled transmembrane protein called Pael receptor (Pael-R) which is ubiquitinated and degraded by Parkin

(Imai *et al*., 2001, Imai and Takahashi, 2004). Misfolded Pael-R and its aggregates have been found in Lewy bodies (Imai and Takahashi, 2004; Murakami *et al*., 2004). Parkin controlled ubiquitination and subsequent degradation of Pael-R protects dopaminergic neurons against various insults and therefore loss of function of *PARKIN* can lead to ER stress through increased protein aggregation (Imai and Takahashi, 2004). It has been suggested that neuronal cells over-expressing Parkin show resistance to ER stress (Imai *et al*., 2000).

Studies have shown up-regulation of ER chaperone expression (e.g. protein disulfide isomerase) in the brain of PD patients as well as evidence of accumulation in Lewy bodies (Conn *et al*., 2004). Chemicals such as 6-OHDA and MPP+ can trigger ER stress in dopaminergic neurons and induce a number of genes (Holtz and O'Malley, 2003; Ryu *et al*., 2002). Results from 6-OHDA, MPP+ and rotenone treatment show up-regulation of ubiquitin proteasome system transcription factor CHOP/Gadd153 and phosphorylation of ER stress kinases (inositol requirement [IRE] and PRKR-like endoplasmic reticulum kinase [PERK]) in treated cells (Holtz and O'Malley, 2003; Ryu *et al*., 2002).

Hypothesis:

Parkinson's disease is a major cause of morbidity with a complex aetiology possibly involving environmental exposure to neurotoxic pesticides. Prolonged exposure to low level neurotoxic pesticides and other environmental contaminants causes mitochondrial dysfunction which leads to raised levels of iron and consequently mtDNA mutation. This then leads to mitochondrial respiratory chain deficiency and neuronal cell death. We will test the hypothesis that 1) sub-lethal exposure to agrochemicals has an effect on proteins linked with PD and those involved in different cell death mechanisms, 2) toxin exposure causes mitochondrial dysfunction 3) and whether human central dopaminergic cell lines are more sensitive to agrochemicals than the human neuroblastoma cell line SH-SY5Y.

Aims and Project outline:

This project is divided into the following main objectives:

- The association of pesticide exposure with Parkinson's disease suggests a causative role and SH-SY5Y cells are routinely used to determine toxic potential of various chemicals in order to provide a better understanding of their mode of action. Keeping this scenario in mind, cytotoxicity screening of selected agrochemicals will be carried out using Alamar blue reduction assay and sub-cytotoxic doses will be administered over acute and chronic time periods to investigate protein expression using western blotting.

- Different pharmacological inhibitors will be used to determine the type of cell death mechanism or cell-signalling pathway involved. This will be done to determine if these signalling pathways are relevant to the mode of toxicity of selected chemicals.

- Low levels of agrochemicals will be administered in combination with application of siRNA to block the production of proteins linked with autophagosome formation to determine if it has any effect on cell viability after toxin treatment.

- Mitochondrial respiratory chain complexes will be measured in cells exposed to toxins because post-mortem biochemical studies (Hattori *et al*., 1991) coupled with the finding of a complex I defect in substantia nigra of PD patients (Schapira *et al*. 1990; Schapira 2006) suggest role of mitochondria in the pathogenesis of PD.

- TaqMan low density arrays will be used for RT-PCR to verify differential gene expression against appropriate housekeeping genes in toxin treated cells. This will be done to identify genes that are responsive to toxic insult and may serve as markers for protein aggregation, oxidative stress or other mechanisms associated with PD.

- Human dopaminergic cell line will be developed. This will involve use of embryonic brain samples, tissue extraction, neurosphere maintenance and growth followed by differentiation into cells exhibiting markers of dopaminergic neurones.

Chapter Two: Materials and Methods

2.1 Cell Culture:

2.1.1.1 Materials for Cell Culture:

The SH-SY5Y cell-line was purchased from the European Collection of Cell Cultures (Salisbury, UK). Dulbecco's modified Eagle's medium (DMEM), heat-inactivated fetal bovine serum (FBS), glutamine/penicillin/streptomycin solution, sodium pyruvate, non-essential amino acids (NEAA) were all purchased from Invitrogen Ltd (Paisley, UK). Other supplements required for culture maintenance and cell differentiation were purchased from Sigma Aldrich Chemical Co. (Poole, UK).

2.1.1.1 Cell culture Methods:

SH-SY5Y cells from passage number 18-30 were used for the whole project to allow consistency. They were maintained in a growth medium containing 90% DMEM, 10% FBS, 2 mm L-glutamine, 100 units/mL penicillin, 10 mg/mL streptomycin and 1% NEAA. Cells were subcultured to a fresh T75 flask when growth reached 80-90% confluence. Cells were incubated at 37^0C in a humidified atmosphere of 95% air/5% CO_2.

2.1.1.2 Differentiation of SH-SY5Y cells:

SH-SY5Y cells were plated out at the required density in growth medium. Typical cell-densities used were: 10-20,000 cells/well in 6 well-plates for experiments lasting 2 weeks; 100,000 cells/well in 6 well-plates for 1 week and 50,000-100,000 cells per T25 flask. Cells were incubated overnight to allow recovery. Growth media was removed and replaced with an equal volume of DMEM supplemented with 1% heat-inactivated FBS, 1% L-glutamine, 1% penicillin/streptomycin solution, 1% sodium pyruvate, 1% NEAA, 0.3mM dibutyryl cyclic AMP (dbcAMP) and 10mM Retinoic acid (RA) (Beck *et al*., 2006). Cells were re-incubated at 37^0C in a humidified atmosphere of 95% air/5% CO_2.

2.2.1 Cell Viability and Cytotoxicity Assessment:

For toxicity screening, SH-SY5Y cells were seeded at 100,000 cells per well in 24-well plates. An initial dose range of 1mM-0.00001mM was used for each chemical. Alamar Blue dye was added at 10% of total growth medium volume after

overnight exposure to agrochemicals or inhibitors and plates were incubated at 37 °C and 5% CO_2 for 4 hours after which triplicates of media were taken from each well and Alamar Blue reduction measured at emission wavelength of 530nm and excitation wavelength of 590nm.

2.1.2.1 Chemicals:

Table 2.1: Properties and agricultural uses of selected chemicals to be used.

Chemical	Category	Water Solubility	Main Uses	Cat-Number
2,4-D	Herbicide	900 mg/L (25 °C)	Broad leafed plants	Sigma 49083
2,4-D metabolite	-	-	-	Sigma 35811
2-imidazolidinethione	degradation product of ethylenebisdithiocarbamate (fungicide)	-	-	Sigma 45531
Chlorothalonil	Herbicide	0.6 mg/L @ 25°C	Wheat, potatoes, pulses	Sigma 36791
Cypermethrin	Insecticide	< 9 µg/L @ 20°C (99.5% pure)	Insect and arthropod pests in ornamental and agricultural crops	Sigma 3612
Diquat	Herbicide	700 g/l water @ 20°C	Broad leafed plants and grasses	Sigma 45422
Epoxiconazole	Fungicide	Limited solubility	Fruits, cereals	Sigma 36848
Fenpropimorph	Fungicide	7.3 mg/l (20°C, pH 4.4), 5.1 mg/l, 4.3 mg/l (20°C, pH 7), 3.5 mg/l (20°C, pH 9-11)	Cereals	Sigma 36772
Fluroxypyr	Herbicide	5.7 g/l, pH 5	Broad leaved weeds in cereals, maize, apple trees, olive trees and sorghum	Sigma 45758
Fluroxypyr methylheptyl ester	Herbicide	-	-	Sigma 36780
Isoproturon	Herbicide	70.2 mg/l	Wheat, winter barley	Sigma 36137
λ-cyhalothrin	Insecticide	extremely low water solubility	Insect and arthropod pests in ornamental and agricultural crops	Sigma 34325
Maneb	Fungicide	0.5 ug/ml		Sigma 45554

Data recorded from Extoxnet; Thomas & Wardman, 1986-1996; The Pesticide Manual, 1994; US EPA Fact sheets).

Table 2.2: Properties and agricultural uses of selected chemicals to be used.

Chemical	Category	Water Solubility	Main Uses	Cat-Number
Mancozeb	Fungicide	6 mg/L	Wheat, potatoes	Sigma 45553
Mecoprop-P	Herbicide	860 mg/l @ 20°C	Cereals, weeds	Sigma 36773
Mecoprop methyl ester	Herbicide	-	-	Sigma 36148
Metsulfuron methyl	Herbicide	270 mg/l @ 25°C, pH 4.6	Grass and broadleaf weeds	Sigma 46432
MPTP	-			Sigma M1021
MPP+	-			Sigma D048
Nabam	Fungicide	200000 g/L	Cotton, capsicums, onions and rice crops	Sigma 45593
Paraquat	Herbicide	700,000 mg/L @ 20°C		Sigma M2254
Pendimethalin	Herbicide	0.3 mg/L @ 20°C	Wheat, winter barley	Sigma 36191
Primicarb	Insecticide	-	Controls aphids on vegetable, cereal and orchard crops	Sigma 45627
Rotenone	Insecticide			Sigma R8875
Trifluralin	Herbicide	Limited solubility	Grasses and broadleaf weeds	Sigma 45700

(Data recorded from Extoxnet; Thomas & Wardman, 1986-1996; The Pesticide Manual, 1994; US EPA Fact sheets).

2.2.1.2 Trypan blue exclusion assay:

A small volume of cell suspension was diluted 1:1 with 0.5% trypan blue, thoroughly mixed and incubated at room temperature for 5 minutes. 50µl suspension was placed in a haemocytometer and cells counted under an inverted microscope. Percentage viable cells were counted as follows:

% viable cells = no. of viable cells/ Total number of cells x 100

2.3.1 Determination of cell viability in response to cell signalling/death inhibitors:

SH-SY5Y cells were incubated with Necrostatin-1 (Biomol), zVAD.fmk (Biomol), DEVD-CHO (Biomol), Ac-LEVD-CHO (Biomol), NAC (Sigma), Cyclosporin A (Sigma), Tunicamycin (Sigma), 3-Methyladenine (Sigma), Ammonium Chloride (Sigma), Tiron (Sigma), GW5074 (Biomol), H89 (Biomol), LY29002 (Biomol), PD98059 (Biomol), SQ22536 (Biomol), SP600125 (Biomol),

U0126 (Biomol) for 1h-3h prior to toxin administration. Agrochemical or toxin concentrations causing a 50-60% reduction in viability were used and cell viability assessed using Alamar Blue reduction assay.

2.4.1 Determination of reactive oxygen species generation:

To measure cellular reactive oxygen species (ROS), SH-SY5Y cells were loaded with H2DCFDA molecular probe (0.01mM, Invitrogen) and treated with hydrogen peroxide (0.5mM), diquat, paraquat, rotenone, maneb, mancozeb, mecoprop-p and MPP+ (dose range 0.001-1mM) for 24 hours. Plates were incubated at 37 °C and 5% CO_2 for 24 hours. After which triplicates were taken from each well and fluorescence measured at emission wavelength of 485nm and excitation wavelength of 520nm. Alternatively, after toxin treatment SH-SY5Y cells were extracted in a buffer containing 0.1M Tris pH 7.4, 1% triton X-100 and fluorescence of cell lysates was measured at 485nm emission/520nm excitation.

2.5.1 Analysis of mitochondrial membrane potential:

Changes in mitochondrial membrane potential ($\Delta\Psi_m$) were estimated using tetramethylrhodamine ethyl ester (TMRE) (Molecular Probes), a cationic dye that rapidly accumulates in energised mitochondria driven by the membrane potential. Damaged mitochondria cannot retain TMRE (Krohn *et al*., 1999). For estimation of $\Delta\Psi_m$, cells were incubated with 250 nM TMRE for 30-45 minutes at 37 °C and fluorescence was measured (excitation at 549 nm and emission at 574 nm). Protonophore carbonyl cyanide *p*-trifluoromethoxy-phenylhydrazone (FCCP; 0.1μM, Sigma) was used as a positive control. It was added 15 min prior to the end of the treatment. FCCP depolarises mitochondria by abolishing the proton gradient across the inner mitochondrial membrane (Gunter and Pfeiffer, 1990). The fluorescence for each treatment was expressed as percent fluorescence change compared with control.

2.6.1 Statistical analysis

Data representative of at least three independent experiments each of triplicate determination. Statistical analysis of the data was performed using *t*-test using Minitab Statistical software (Minitab Inc) followed by appropriate post hoc non-parametric testing. Error bars represented standard deviation (±SD). $*P < 0.05$ and $**P<0.01$ were considered statistically significant.

2.1 Protein Expression:

2.2.1 Acute and chronic toxin exposure:

SH-SY5Y cells were plated out at the required density as described before. Cells were exposed to sub-cytotoxic doses of selected toxins (diquat, epoxiconazole, fluroxypyr methylheptyl ester, maneb, mancozeb and mecoprop methyl ester for 24 hours (acute exposure) and up to 4 weeks (chronic exposure). Cell lysates were prepared using native lysis buffer (50mM TRIS pH 7.4 (HCl), 0.27M Sucrose, 1% Triton X-100, 1x protease/phosphatase inhibitor cocktail). Protein concentration was determined by Coomassie Plus Protein Assay Kit (Pierce, Rockford, IL) or Bradford assay (Pierce, Rockford, IL).

2.2.1.1 Western blotting:

Equal amounts of protein (i.e. 20µg), as determined by Coomassie Plus Protein Assay Kit (Pierce, Rockford, IL), were subjected to electrophoresis through 12% Bis-Tris gels (Invitrogen) at 120V for 20 minutes and 180 minutes for 1 hour. After electrophoresis, the separated proteins were transferred at 35V for 3 hours onto nitrocellulose membranes (Amersham Biosciences). Membranes were blocked for 1 hour with 5% non-fat dry milk in 1x TBS-Tween20 (0.05% v/v) and then probed overnight at 4°C with the relevant antibodies (table 2.2.1.2). Membranes were washed 3 times with TBS-T at room temperature for 10 min, followed by incubation with HRP conjugated secondary antibodies (Rabbit IgG ab6795 or Mouse IgG ab6728, Abcam) for 1 hour at room temperature. Membranes were thoroughly washed with TBS-T. An ECL detection kit (GE Healthcare) was used for protein band detection through a G:BOX Chemi XL camera (SYNGENE). ImageJ version 1.38x (NIH, USA) was used to quantify each protein band of the western blots.

2.2.1.2 Primary antibodies:

Table 2.3: Details of primar antibodies used.

Antibody	Details	Dilution
α-synuclein	Mouse IgG1, 610789, BD Biosciences	1:1000
ATG5	Rabbit polyclonal, 2630, Cell Signaling	1:1000
BECN1	Goat polyclonal, D-18: sc-10086, Santa Cruz	1:1000
Cytochrome c	Mouse monoclonal, (A-8) sc-13156, Santa Cruz	
Cleaved caspase-3	Rabbit monoclonal, Asp175, Cell Signaling	1:1000
Cleaved PARP-1	Human specific, Asp 214, Cell Signaling	1:1000
Dopamine β-hydroxylase	Rabbit polyclonal, DZ1020, Biomol	1:1000
GAD67	Rabbit polyclonal, ab52249, Abcam	1:1000
LAMP1	Mouse monoclonal, ab13523, Abcam	1:1000
LAMP2	Mouse monoclonal, ab13524, Abcam	1:1000
LC3B	Rabbit polyclonal, L7543, SIGMA	1:1500
Neurofilaments	Rabbit polyclonal antiserum cocktail, NA 1297, Enzo Life Sciences	1:500
p53	Mouse monoclonal IgG_{2b}, (DO-7): sc-47698, Santa Cruz	1:500
Phospho p53 serine 15	Rabbit polyclonal, 9284, Cell Signaling	1:1000
Phospho α-synuclein	Mouse monoclonal, sc-12767, Santa Cruz	1:1000
Poly-Ubiquitin	Mouse monoclonal (clone FK1), PW8805, Biomol	1:1500
RIP	Rabbit IgG, 3493, Cell Signalling	1:1000
Tyrosine hydroxylase	Purified mouse monoclonal IgG_1. Clone TH-2, mAb1423, R&D Systems.	1:1000

2.2.2 Immunofluorescence:

SH-SY5Y cells were seeded onto 2-well or 8-well chamber slides (BD Falcon, BD Biosciences) and incubated with different toxin doses for the required period of time. After which cells were fixed with 4% paraformaldehyde (Sigma) for 10 minutes and washed with PBS and permeabilised with 0.1% Triton-X-100 (Sigma) for 10 minutes. Cells were blocked in 1% BSA or 10% goat serum for 30 minutes. Cells were incubated overnight with primary antibodies at $4^{o}C$, washed with PBS and treated with Image-iT™ FX signal enhancer (Invitrogen) for 30 minutes at room temperature. Cells were washed with PBS and then incubated with secondary antibodies (conjugated with Alexa Fluor® 488 or 594) for 60 minutes with no light. Slides were washed with PBS and viewed under Zeiss Imager 21 microscope (Carl Zeiss Ltd).

2.3 *ATG5* knockdown:

2.3.1 ATG5 siRNA transfection and toxin treatment:

SH-SY5Y cells were plated at a cell density of 1 x 10^6 cells per well in 6 well plates. Human ATG5 siRNA (Dharmacon Accell SMARTpool siRNA A-004374-15, target sequence CUUCGAGAUGUGUGGUUU, final concentration 0.01mM) was applied to SH-ST5Y cells following the 'Thermo Scientific Dharmacon® Accell ™ siRNA Delivery protocol'. After 72 hour incubation with siRNA, cells were extracted in native lysis buffer and protein knockdown measured by western blotting. For toxin treatment, SH-SY5Y cells were plated and grown in 6 or 12 well plates. Different agrochemicals at required doses were added after 72 hour siRNA transfection and after overnight incubation cell-viability was measured using Alamar Blue reduction assay and cells extracted in native lysis buffer for protein analysis.

2.3.2 ATG5 shRNA lentiviral particles transduction and toxin treatment:

SH-SY5Y or HeLa cells were plated in 12 well-plates 24 hours prior to viral infection. 1ml complete optimum medium containing serum and antibiotics were added to cells and incubated overnight. Cells were infected with APG5 shRNA (h) Lentiviral Particles (Santa Cruz Biotechnology, Inc) and incubated at 37^0C (5% CO_2) for 72 hours. Cells were extracted in native lysis buffer and protein knockdown measured by western blotting.

2.3.3 Transfection of DJ-1, Parkin and wild-type α-synuclein plasmid DNA:

500ng plasmid DNA (pCDNA 3.1/Myc tagged DJ-1, Parkin and wild-type α-synuclein) (provided by Dr. Mark Cookson, Cell and Gene Expression Unit, Lab of Neuronal Genetics, Bethesda, USA) was diluted in 100µl 'Otpi-MEM® I Reduced Serum Medium' (Invitrogen) and thoroughly mixed. 1.25µl lipofectamine reagent LTX (Invitrogen) was added directly to DNA, thoroughly mixed and incubated at room temperature for 30 minutes. 100µl lipofectamine-DNA complex was added to each well and incubated at 37^oC for 48 hours after which cells were extracted in native lysis buffer and transfection efficiency measured by western blotting. For toxin treatment, transfected cells were incubated with selected agrochemical for 24 hours after which cell-viability was measured using Alamar Blue reduction assay.

2.3.4 Immunofluorescence analysis of lysosomal aggregation:

SH-SY5Y cells were seeded onto 2 or 8-well chamber slides (BD Falcon, BD Biosciences) and incubated with LysoTracker® Red DND-99 (Molecular Probes, Invitrogen) (0.001mM) for 30 minutes. Chemicals at required concentrations were added and incubated for 24 hours after which cells were fixed and viewed using a fluorescent microscope.

2.4 Mitochondrial assays:

2.4.1 Preparation of mitochondrial fraction from SH-SY5Y cells:

SH-SY5Y cell pellets were suspended in 1-2ml of ice-cold medium A (250mM sucrose, 2mM HEPES, 0.1mM EGTA, pH 7.4) and transferred to a 1-2ml capacity smooth-surfaced glass homogeniser. Cells were disrupted by 20 passes in the homogenizer with a tight-fitting power-driven Teflon plunger and homogenate were then centrifuged for 10 minutes at 600*g*av/ 4ºC. Mitochondria-rich supernatant was collected and cell debris pellet resuspended in 800µl medium A, homogenised and centrifuged as before. Two supernatants were pooled and centrifuged for 10 minutes at 11,000*g*av at 4ºC. The pellet (mitochondrial fraction) was suspended in 400µl medium A and stored in aliquots at -80^{o}C. All respiratory chain complex assays were performed in a final volume of 0.1ml using the Cary WinUV spectrophotometer. Pig heart mitochondrial fractions were used as internal control before each experiment to check normal function of assay.

2.4.2 Buffer preparation:

Stock buffers for complexes I and II contained 25mM potassium phosphate (Sigma) and 5mM magnesium chloride (Sigma) at pH 7.2. CI buffer (30ml) was supplemented with 2.5mg/ml BSA (Sigma), 2mM KCN (Sigma), 0.13mM NADH (Sigma), 2µg/ml antimycin A (Sigma) and 65µM ubiquinone$_1$ (Sigma). CII working buffer did not include BSA. Citrate synthase buffer contained 0.1mM Tris-HCl at pH 8.0.

2.4.3 Measurement of Complex I (NADH: ubiquinone oxidoreductase) Activity:

Immediately prior to each assay, mitochondrial fractions were first rapidly freeze-thawed in liquid nitrogen three times and diluted 5-fold using CI assay buffer. Complex I specific activity was measured by following the decrease in absorbance due to the oxidation of NADH at 340nm with 425nm as the reference wavelength (extinction coefficient for NADH 6.22/cm/mM, to account for the contribution of ubiquinone$_1$ to the absorbance at 340nm) (Watmough *et al*., 1989). 10µl 13mM NADH, 2.5µl 65mM ubiquinone$_1$ and 2µl 1mg/ml antimycin A were added to the assay medium (CI buffer). The absorbance change was measured for 10-50 seconds using Cary WinUV spectrophotometer. Mitochondrial proteins (10µl) were added to the cuvette and NADH: ubiquinone oxidoreductase activity was measured for 4-5 minutes. 2µl rotenone (1mg/ml) was added and activity measured for 3-4 minutes. Complex I activity was calculated as the rotenone-sensitive NADH: ubiquinone oxidoreductase activity using following formula:

Reaction:

$NADH + H^+ + Ubiquinone1 \rightarrow NAD^+ + Ubiquinone1.H_2$

$$\text{Complex I activity (µmols of NADH oxidised/min)} = \frac{\delta \text{ slope} \times \text{dilution factor} \times 1000}{6.22 \times 1000 \times \text{mitoch. volume}}$$

δ slope = slope 1 (absorbance/min) - slope 2 (absorbance/min)

2.4.4 Measurement of mitochondrial complex II (succinate: ubiquinone oxidoreductase) activity:

Complex II activity was measured by following the reduction of 2,6-dichlorophenol-indo-phenol (DCPIP) at 600nm (E_{600}=19.1/cm/mM) (Desnuelle *et al*., 1989). Mitochondrial proteins (20µl) were added to CII assay buffer and preincubated with 20µl 1M sodium succinate for 10 minutes at 30^{o}C. 2µl 1mg/ml antimycin A, 2µl rotenone and 10µl 5mM DCPIP were added after 10 minutes and baseline absorbance measured for 10-50 seconds. 2.5µl 65mM ubiquinone$_1$ was added to start the reaction and the enzyme catalysed DCPIP reduction was measured for 3-4 minutes. Complex II activity was measured as follows:

$$\text{Complex II activity (nmols of DCPIP reduc/min)} = \frac{\delta \text{ slope} \times \text{dilution factor} \times 1000}{19.1 \times 1000 \times \text{mitoch volume}}$$

2.4.5 Citrate synthase activity:

Citrate synthase specific activity was measured by following the rate of production of coenzyme A from oxaloacetate by measuring free sulfhydryl groups using the thiol reagent 5.5'-dithio-bis-(2-nitrobenzoic acid) (DTNB). DTNB reaction with sulfhydryl groups produces free 5-thio-2-nitrobenzoate anions (E_{412}=13.6/cm) which have a yellow colour and can be monitored at 412nm (Shepard and Garland, 1969).

Reactions:

Oxaolacetate + acetyl coenzyme A → citrate + CoenzymeA.SH (CoA.SH)
Citrate synthase
CoA.SH + DTNB → CoA.S-S-nitrobenzoate + 5-thio-2-nitrobenzoate anion

3µl 5mM acetyl-CoA, 10µl 10mM DTNB, 10µl of 10% Triton X-100 and 20µl mitochondrial protein were added in the assay medium and baseline absorbance measured for 10-50 seconds. 5µl 50mM oxaloacetate was added to reaction mixture to start the reaction. Reaction activity was measured as:

$$\textbf{Activity (nmols/min)} = \frac{\delta \text{ slope (Abs/min) x mitoch vol x dil. factor x 1000}}{13.6 \text{ x } 1000}$$

2.4.6 Immunofluorescence:

SH-SY5Y cells were seeded onto 2-well or 8-well chamber slides (BD Falcon, BD Biosciences) and incubated with MitoTracker® Red CMXRos (Molecular Probes, Invitrogen) (0.001mM) for 30 minutes. Chemicals at required concentrations were added and incubated for 24 hours. After which cells were fixed and observed using a fluorescent microscope.

Polymerase Chain Reaction:

2.5.1 RNA extraction:

RNA was isolated from SH-SY5Y using Ribopure RNA isolation kit (Ambion Inc) according to the manufacturer's instructions.

2.5.2 DNAse Treatment:

RNA sample (100µl) was split in 2 x 50µl aliquots. To each aliquot, 5µl 10x Turbo DNase buffer and 1µl Turbo DNase (TURBO DNA-free™, AM1907, Applied Biosystems) were added and mixed gently. Samples were incubated at 37^{o}C for 30 minutes. 5µl resuspended DNase Inactivation reagent was added to each sample and incubated at room temperature for 2 minutes with occasional mixing. Samples were spun at 10,000g for 90 seconds and supernatant transferred to fresh tubes and stored at -80^{o}C.

2.5.3 RNA concentration:

RNA concentration of above samples was measured using NanoDrop 2000.

2.5.4 Reverse transcription:

To a nuclease-free 200µl PCR tube, 1µl Oligo(dT)$_{12-18}$ primer (Invitrogen), total RNA (1µg) and 1µl 2.5mM dNTP mix (Invitrogen) were added and volume made up to 10µl with nuclease-free water. The mixture was heated in a thermal cycler at 65^{o}C for 5 minutes and then at 4^{o}C for 5 minutes to anneal the primer. A master mix of 4µl 5x First-strand buffer, 1µl 0.1M DTT, 1µl SuperRNase inhibitor (Ambion), 1µl Superscript III RT (Invitrogen) was prepared and the volume made up to 10µl and added to each RNA sample and heated at 50^{o}C for 2 hours to allow RNA reverse-transcription into cDNA. Samples were stored at -80^{o}C.

2.5.5 RT-PCR:

Semi-quantitative RT-PCR was performed using a Taqman® Custom Low Density Array (Applied Biosystems) containing 384 wells. Sample preparation involved a mixture of sample cDNA (200ng per well), 207µl nuclease free water,

and 225µl Taqman® Universal PCR Master Mix (Applied Biosystems) in a 1.5ml microcentrifuge tube. 100µl sample was loaded into each well of the card and the card was centrifuged at 1200g for 1 minute, stopped and centrifuged for a further minute at 1200g. The card was sealed and run on 7900HT Fast Real-Time PCR System (Applied Biosystems).

2.5.6 Statistical analysis:

Data were from or representative of at least three independent experiments, each of duplicate determination. The Student's t-test involving analysis of ΔcT values was used to identify genes having significant changes in expression levels. *GAPDH* was used as endogenous control gene and for data normalisation across samples. Normalisation of Ct values of each gene and determination of fold increase or decrease was measured by calculating the $2^{-\Delta\Delta Ct}$ value (Relative Quantification Method, Applied Biosystems 2008). Significant genes were selected with a cut-off of $p < 0.05$ and fold change >1.5.

2.6 Stem cell methods:

2.6.1 Propagation of human neural precursor stem cell:

Human neural precursor stem cell (hNPSC) lines were derived from two human embryos (CS18 and CS19) following ethical approval. Cells were grown as neurospheres according to previously described methods in proliferation medium: DMEM/F12 (Sigma D8062) supplemented with N-1 (1:100; sigma N6530), B27 (1:100; Gibco 17504-044), epidermal growth factor (EGF; 20ng/ml; R& D Systems 236-EG), basic fibroblast growth factor (FGF2; 20ng/ml; R& D Systems 4114-TC) and leukaemia inhibitor factor (LIF; 10ng/ml; Sigma L5283). Cells were incubated at 37˚C in a 5% CO_2, humidified incubator. Proliferation medium was replenished at 3-4 days intervals by replacing 60-70% of the medium with fresh medium. If neurospheres became larger than 100µm in diameter, they were triturated to avoid cells at the centre of the sphere becoming hypoxic. Single cell suspensions were obtained by extensive trituration of cultures once every 6-8 weeks. Viable cells were counted using a haemocytometer (C-Chip, Digital Bio DHC-N01) and replated under the same conditions. Cell-line designated 'N969' was derived from the

mesencaphalon of 6-8 week post conception human embryo (CS18) and used for this study.

2.6.2 Differentiation of hNPSC and toxin treatment:

N969 cells were plated at a density of 100,000 cells onto 2-well chamber slides (BD Falcon, BD Biosciences) or at 2500 cells/ml in 8 well chamber slides (BD Falcon) coated with either 0.25% gelatine or 0.1% poly-L-lysine and grown for 10 days, at which point neurospheres had attached onto the surface. Growth medium was replaced with differentiating medium containing DMEM/F12 supplemented with 1% FBS (Sigma F2442), N-1, B27 or N-2, brain derived neurotrophic factor (BDNF; 0.01μg/ml; R&D Systems 248-BD), glial derived neurotrophic factor (GDNF; 10ng/ml; R&D Systems 212-GD), interleukin-1α (IL-1α; 100pg/ml; R&D Systems 200-LA), interleukin-11 (IL-11; 1ng/ml; R&D Systems 218-IL) and LIF. Conversion of neurospheres into cells resembling neuronal morphology took 2-3 days. Cells were allowed to grow for at least 14 days after which they were fixed and used for immunocytochemical examination. Cytotoxicity testing was undertaken in 8-chamber slides and cells were exposed to given concentrations of chemical for 24 hours. Cytotoxicity was measured using Alamar Blue reduction assay and stained for cellular antigens using standard immunofluorescence.

2.6.3 Immunocytochemistry:

Storage solution was removed from the chamber slides and cells thoroughly washed in PBS. Cells were fixed in warm formaldehyde (3.7%, diluted in PBS), washed three times in PBS for 2 minutes and permeabilised for 5 minutes with 0.1% (v/V) triton X-100 in PBS at room temperature. After PBS wash (3 x 2 min), 4 drops (~200ul) of Image-iT™ FX signal enhancer (Alexa Flour SFX kit, Invitrogen) or sufficient volume to cover each coverslip were added. Slides were incubated for 30 minutes at room temperature and then thoroughly rinsed with PBS. To minimise background staining, cells were blocked with 1% BSA in TBS-T or 5% goat serum (Abcam Ab7481) for 30 minutes. Cells were washed thoroughly with PBS and incubated with primary antibodies overnight at 2-4˚C. The following day, cells were washed in PBS and incubated with secondary antibodies for 1 hr at room temperature or in dark. (Alexa Fluor 594-conjugated goat anti-mouse/goat anti-rabbit IgG,

2μg/mL; Invitrogen) or Alexa Fluor 488-conjugated goat anti-mouse/goat anti-rabbit IgG (2μg/mL; Invitrogen). Secondary antibodies were removed and slides rinsed with PBS. Where required, slides were counterstained with DAPI solution (1:50,000 in PBS) for 30 seconds followed by submersion in PBS for a further 30 seconds. Slides were then rinsed with distilled water. Differentiated cells were analysed for class III β-tubulin (Tuj1, early neuronal marker) and tyrosine hydroxylase (TH, dopaminergic neuronal marker).

2.7 General Statistics:

Minitab Statistical software or Microsoft Excel were used for statistical analysis. Data on all graphs were expressed as ±SD. All absorbance readings were performed in triplicates and repeated at least three times. AONVA (one-way) or unpaired *t*-tests were used for statistical analysis of groups or within groups. $*P < 0.05$ and $**P<0.01$ were considered statistically significant. For densitometric analysis of western blots, ImageJ version 1.38x (NIH, USA) was used to quantify each protein band. T-test was used to asses significance which was set at $*P < 0.05$ or $**P<0.01$.

Chapter Three: Cytotoxicity measurement of selected agrochemicals in SH-SY5Y cells

3.1.1 Introduction:

Around 450 active ingredients are currently available to be used as pesticides in the UK (IEH, 2005). For this study, pesticide usage survey report 202 (Garthwaite et al., 2004) was used. This report has clear summarised data on the number, extent and quantities of pesticides used in the UK. Chemicals selected for this study were chosen on the basis of their widespread application (as surveyed in 2004) such as chlormequat (2703 tonnes), isoproturon (2279 tonnes), chlorothalonil (1512 tonnes), pendimethlin (1187 tonnes), mancozeb (1045 tonnes), trifluralin (890 tonnes), mecoprop-p (505 tonnes), fenpropimorph (348 tonnes), epoxiconazole (247 tonnes), fluroxypyr (139 tonnes) and diquat (75 tonnes) as well as those which share structural similarity with other pesticides (paraquat, maneb) and chemicals which are active metabolites of other chemicals (2,4-D metabolite, mancozeb metabolite). Exposure to major chemicals derived from this list would represent those chemicals which an individual may come into contact with either through work or as a bystander through rural living.

SH-SY5Y is a neuronal-like catecholaminergic human neuroblastoma cell-line which has been cloned from SK-N-SH cell-line derived from malignant tumours of immature neurons. It maintains stem-cell characteristics, grows in monolayer, proliferates for long periods, expresses tyrosine hydroxylase and dopamine-β-hydroxylase activity (Ross *et al*., 1983), expresses the dopamine transporter and receptors and forms storage vesicles (Colapinto *et al*., 2006). It is a routinely used as an experimental model of neuronal apoptosis and a variety of chemicals can induce these cells to differentiate into different phenotypes (Presgraves *et al*., 2004). These properties make this cell-line a useful model for dopaminergic neurons and therefore it has been extensively used in cytotoxicity assays and protein analysis experiments.

The underlying mechanisms of Parkinson's disease remain partly unknown. Several hypotheses implicate different molecular pathways involving protein misfolding, oxidative stress, mitochondrial and ubiquitin-proteasome dysfunction, apoptosis, infectious agents and exposure to environmental toxins. More than 80,000 chemicals are commercially used and almost 2000 new ones are introduced annually (Congress of the United States Office of Technology Assessment, 1995). Few of

these, especially pesticides have been tested for their effects on development of neurological disorders.

3.1.1.1 Aims:

The aim of this study was to develop an *in vitro* model of dopaminergic neurones. Since SH-SY5Y cell-line shows a dopaminergic phenotype, it was used to screen commonly used selected agrochemicals through cell-viability assays. Once a basic cytotoxicity profile for SH-SY5Y cells was prepared, sub-cytotoxic doses for selected chemicals were used to investigate the effects of different cell-signalling/cell death inhibitors on cell-viability. Different cell-death inhibitors were used to determine the underlying mechanisms of toxicity of specific agrochemicals. Certain chemicals target mitochondria and lead to oxidative stress. Therefore, mitochondrial transmembrane potential and reactive oxygen species production was also measured.

3.1.2 Methods:

Refer to materials and methods (section 2.1).

3.1.3 Results:

3.1.3.1 Effect of Toxin treatment on cell viability and cytotoxicity:

SH-SY5Y cells were treated with different toxin concentrations (0.001, 0.01, 0.1, 1mM) for 24 hours. Alamar blue reduction assay, which provides an index of cell-viability as well as a measure of active mitochondrial functioning of the cell, was used to assess cytotoxicity. Inability of dying cells to reduce the blue dye to pink was used as a marker for cellular toxicity. Based on Alamar blue reduction data, chemicals were classed in three different groups. First category chemicals showed minor or no toxicity. These included 2,4-D, 2,4-D metabolite, 2-imidazolidinethione (mancozeb metabolite), cypermethrin, fenpropimorph, fluroxypyr, λ-cyhalothrin and mecoprop-P. SH-SY5Y cells showed no signs of toxicity after 24 hours (fig 3.1). Morphologically, cells appeared healthy. There was no evidence of dose response effect. Trypan blue cell counts showed no overall reduction in cell number in treated cells compared with untreated controls (trypan blue data not shown).

Second group included chemicals showing toxicity at the highest toxic dose used i.e. 1mM. These included chlorothalonil, isoproturon, MPTP, MPP+, nabam, paraquat, primicarb and trifluralin (fig 3.2). Significant toxicity was observed at higher doses but potency of each chemical varied. This was represented in viable cell counts. Isoproturon caused 90% cell death at 1mM, compared with chlorothalonil (80%), paraquat (60-70%), trifluralin (60-70%), nabam (40%), primicarb (20-40%), MPTP (20%) and MPP+ (20-30%).

Third category included chemicals showing toxicity below and including 0.1mM. Minimal level at which these chemicals elicited a significant loss of cell viability differed for each chemical. Diquat, epoxiconazole, mecoprop methyl ester, metsulfuron methyl and pendimethlin showed significant cell death from 1mM-0.1mM. whereas significant toxicity was observed at 0.01mM with fluroxypyr methylheptyl ester, maneb, mancozeb and rotenone (fig 3.3). Cell viability decreased in a concentration-dependent manner. In particular, 0.1mM and 1mM concentrations significantly decreased viability to 10% of control. Cell viability measured at different time points also showed a time dependent decrease. No toxic effects, in the form of reduction in cell-viability or structural damage, were observed in first 2

hours. A reduction of nearly 20% (of untreated control) was measured after 4 hours with maneb and mancozeb, followed by a drop in viability to 50% and down to 5-10% after 6 and 24 hours respectively. Cell counts determined by trypan blue exclusion showed similar proportional reduction in cell number for 0.1mM and 1mM (fig 3.4, 3.5, 3.6).

Fig 3.1: Effect of toxin treatment for 24 hours on viability in SH-SY5Y cells: Each graph is representative of three independent experiments. Viable cell counts are shown as percentage of untreated control. For each treatment group, the difference from control was tested for statistical significance using one-way analysis of variance and *p* values <0.05 were accepted as significant Error bars represent mean standard deviation (±SD).

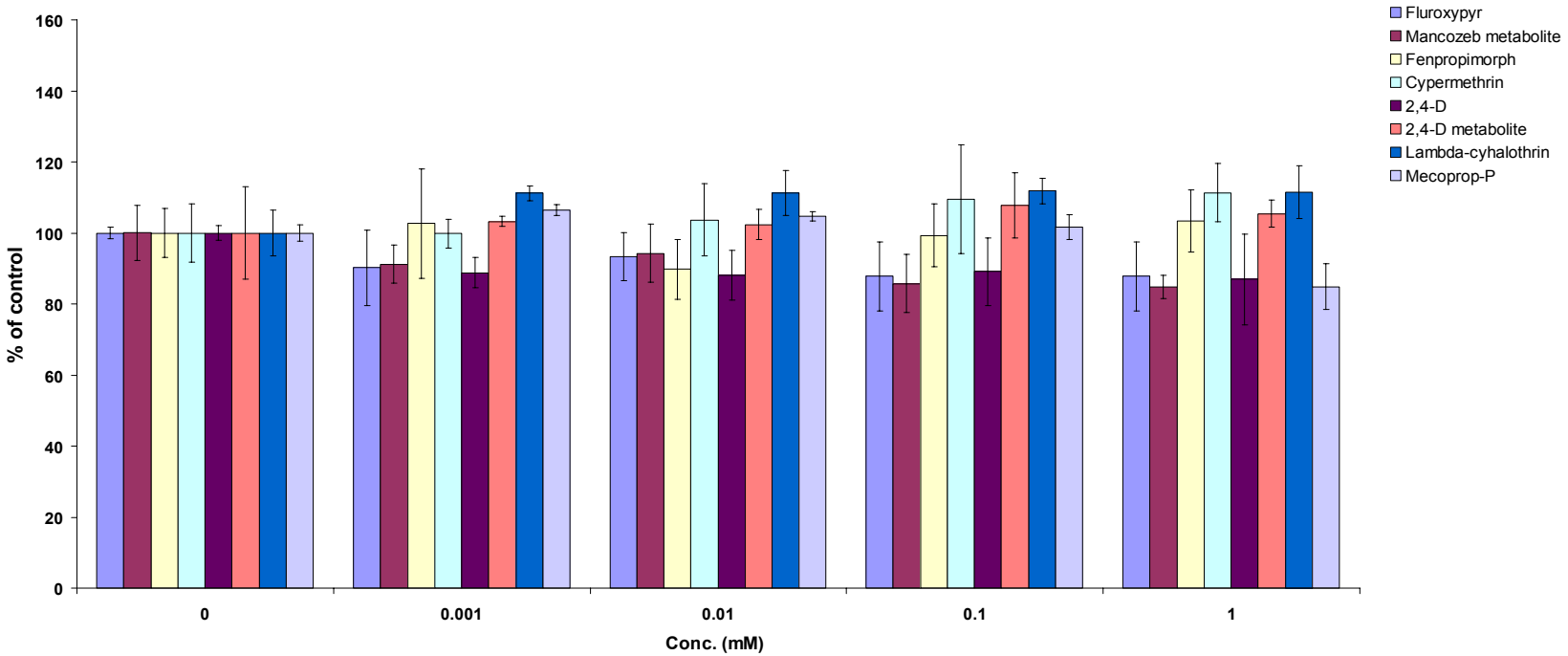

Fig 3.2: Effect of toxin treatment for 24 hours on viability in SH-SY5Y cells: Each graph is representative of three independent experiments. Viable cell counts are shown as percentage of untreated control. For each treatment group, the difference from control was tested for statistical significance using one-way analysis of variance and *p* values <0.05 were accepted as significant. Error bars represent mean standard deviation (±SD).

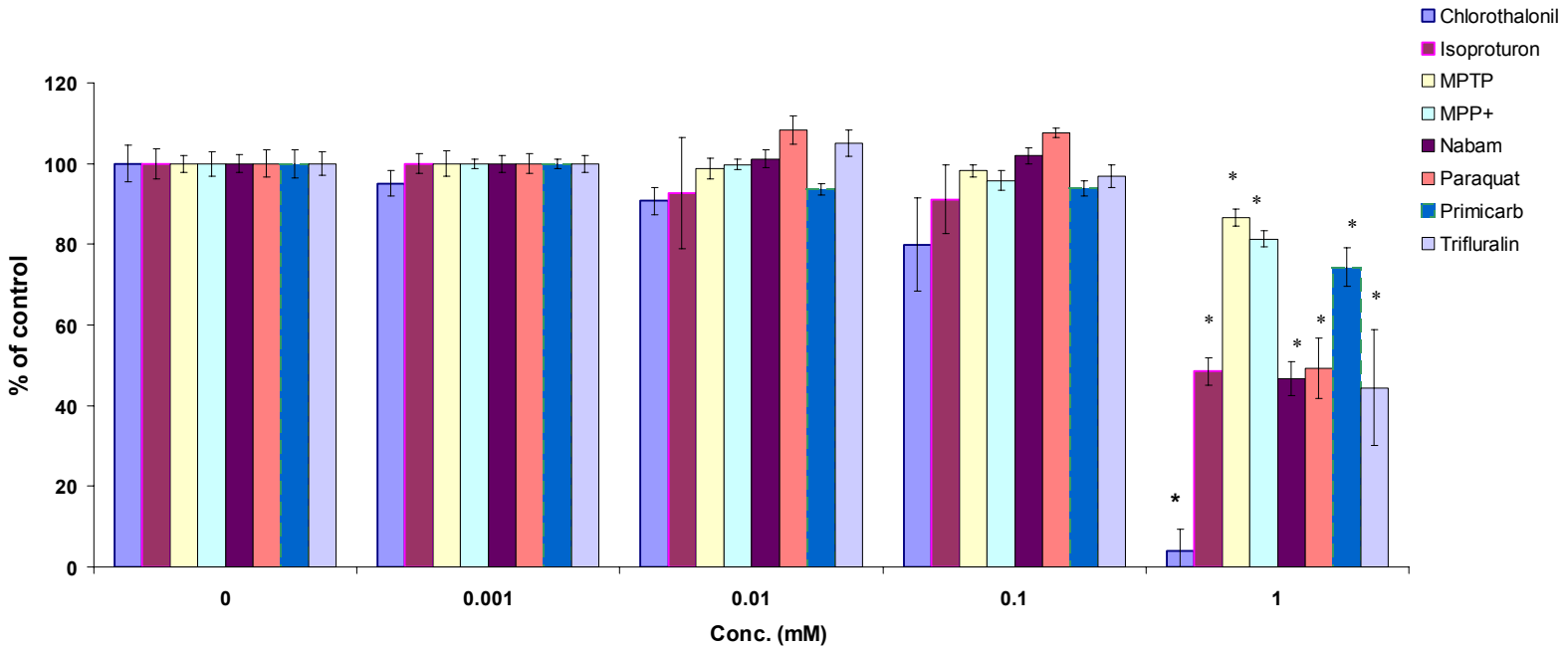

Fig 3.3: Effect of toxin treatment for 24 hours on viability in SH-SY5Y cells: Each graph is representative of three independent experiments. Viable cell counts are shown as percentage of untreated control. For each treatment group, the difference from control was tested for statistical significance using one-way analysis of variance and *p* values <0.05 were accepted as significant. Error bars represent mean standard deviation (±SD).

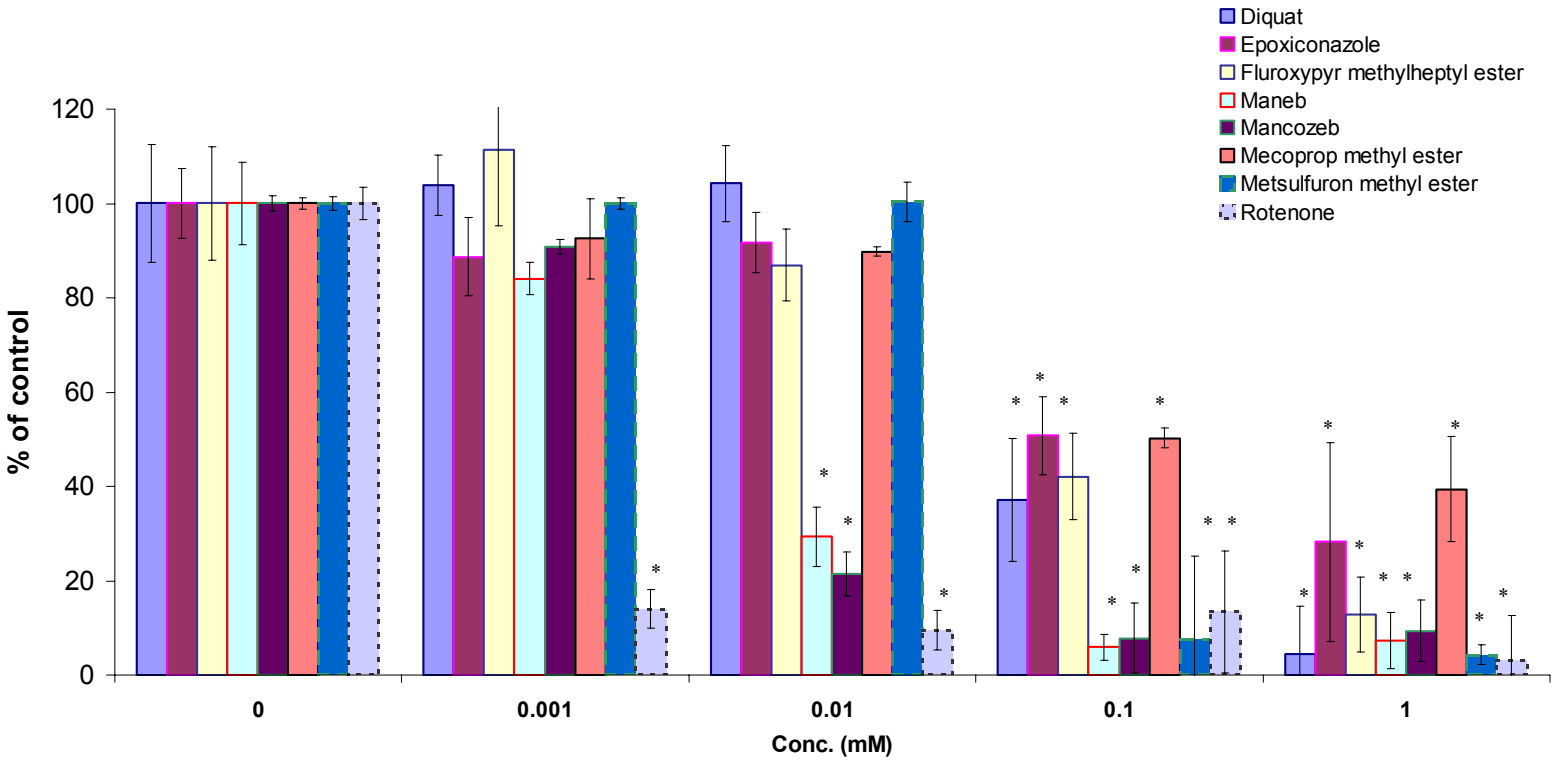

Fig 3.4: Trypan blue cell counts: Viable cell count from A) diquat, B) epoxiconazole and C) fluroxypyr methyl heptyl ester are shown as a percentage of cell viability (n=3, data expressed as 100% x viable count/ viable plus dead counts. * *p* values <0.05 or ** *p* values <0.01 were accepted as significant. Error bars represent mean standard deviation ±SD).

A:

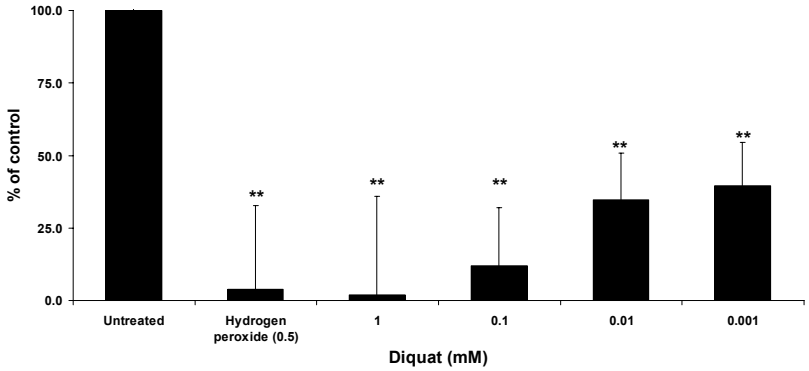

B:

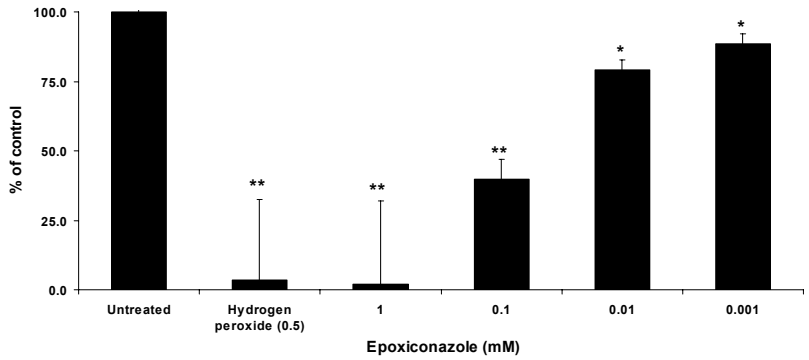

C:

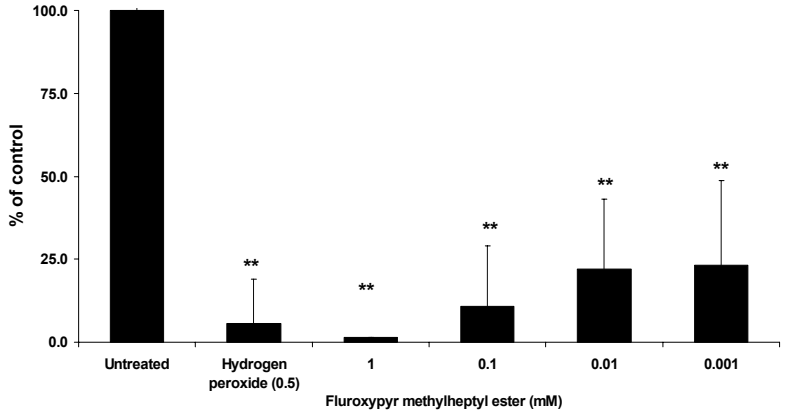

Fig 3.5: Trypan blue cell counts: Viable cell count from A) maneb, B) mancozeb, and C) MPP+ are shown as a percentage of cell viability (n=3, data expressed as 100% x viable count/ viable plus dead counts. * *p* values <0.05 or ** *p* values <0.01 were accepted as significant. Error bars represent mean standard deviation ±SD).

A:

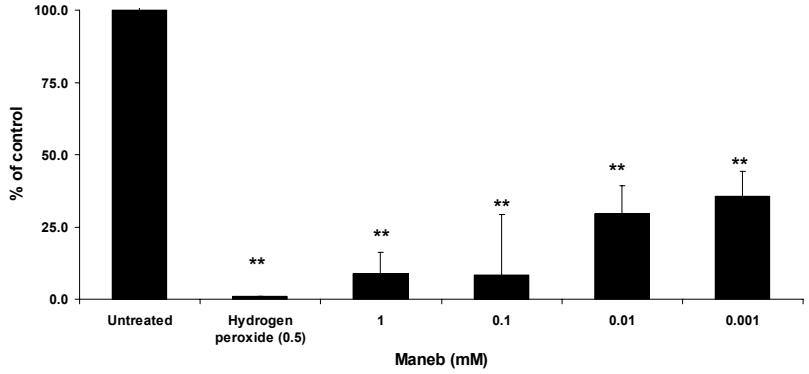

B:

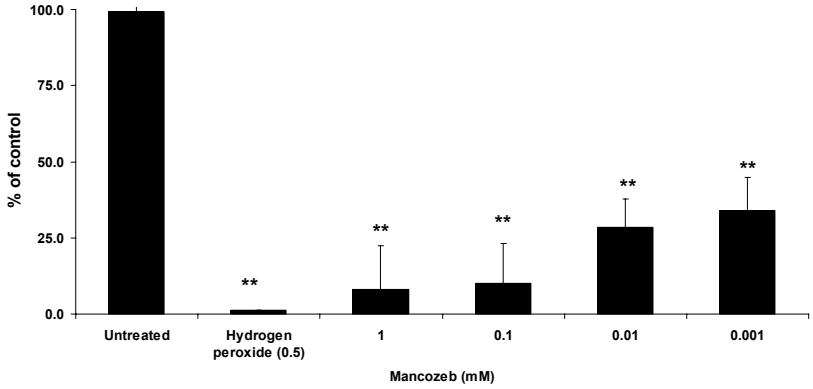

C:

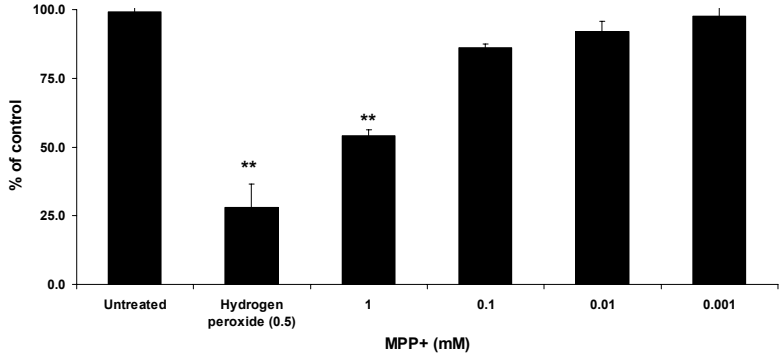

Fig 3.6: Trypan blue cell counts: Viable cell count from A) mecoprop methyl ester and B) rotenone are shown as a percentage of cell viability (n=3, data expressed as 100% x viable count/ viable plus dead counts. * *p* values <0.05 or ** *p* values <0.01 were accepted as significant. Error bars represent mean standard deviation ±SD).

A:

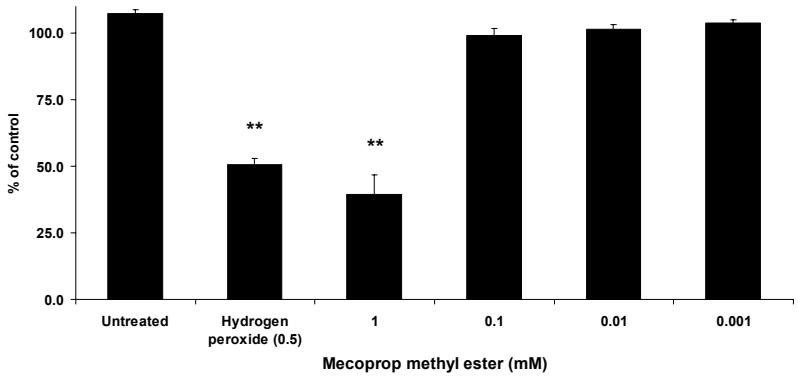

B:

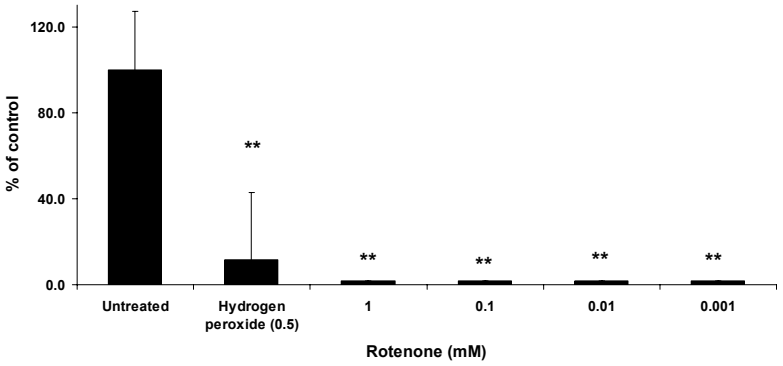

A summary of chemical toxicity is shown in table 3.1 with an estimation of percentage cell death as determined by data gathered from trypan test for each chemical. This study did not set out to calculate precise LD_{50} doses and an attempt to measure it was unsuccessful because set values like 0.001mM, 0.01mM, 0.1mM, 0.5mM and 1mM were used and these ranges were not expanded to determine the exact LD_{50} dose (see table 3.2).

Table 3.1: Summary of cytotoxicity of selected toxins to neuroblastoma SH-SY5Y cells (24 hour exposure) assessed using Alamar blue reduction assay.

Active substance	1mM		0.1mM		0.01mM	
	Toxic	Cell death*	Toxic	Cell death*	Toxic	Cell death*
Mancozeb	✓	90%	✓	90%	✓	60-70%
Maneb	✓	90%	✓	90%	✓	60-70%
Rotenone	-	30%	✓	30%	✓	30%
Diquat	✓	80-90%	✓	60%	×	-
Epoxiconazole	✓	80-90%	✓	40-50%	×	-
Fluroxypyr-ester	✓	90-95%	✓	80-90%	×	-
Mecoprop methyl ester	✓	40-50%	✓	30-40%	×	-
Pendimethlin	✓	60-70%	✓	50%	×	-
Zineb	✓	90-95%	✓	60-70%	×	-
Chlorothalonil	✓	80%	×	-	×	-
Metsulfuron-methyl	✓	90%	×	-	×	-
Isoproturon	✓	50%	×	-	×	-
MPTP	✓	20%	×	-	×	-
MPP+	✓	20-30%	×	-	×	-
Nabam	✓	40-50%	×	-	×	-
Paraquat	✓	60-70%	×	-	×	-
Primicarb	✓	20-40%	×	-	×	-
Trifluralin	✓	60-70%	×	-	×	-
2,4-D	×	-	×	-	×	-
2,4-D metabolite	×	-	×	-	×	-
2-imidazolidinethione (Mancozeb metabolite)	×	-	×	-	×	-
Chlormequat	×	-	×	-	×	-
Cypermethrin	×	-	×	-	×	-
Glyphosate	×	-	×	-	×	-
Mecoprop-P	×	-	×	-	×	-
Fenpropimorph	×	-	×	-	×	-
Fluroxypyr	×	-	×	-	×	-

* Percentage of untreated control

Table 3.2: Estimation of LD_{50} values of SH-SY5Y cells (24 hour exposure).

Active substance	LD_{50} Estimation
2,4-D	Exact LD_{50} dose not measured. Minor (non-significant) toxicity at 1mM
2,4-D metabolite	Exact LD_{50} dose not measured. Minor (non-significant) toxicity at 1mM
2-imidazolidinethione (Mancozeb metabolite)	Exact LD_{50} dose not measured. Minor (non-significant) toxicity at 1mM
Chlorothalonil	Exact LD_{50} dose not measured. It was estimated to be within the 0.1mM-1mM range.
Cypermethrin	No toxicity at 1mM
Diquat	LD_{50} dose estimated to be around 0.1mM
Epoxiconazole	LD_{50} dose estimated to be around 0.1mM
Fenpropimorph	No toxicity at 1mM
Fluroxypyr	Exact LD_{50} dose not measured. Minor (non-significant) toxicity at 1mM
Fluroxypyr-ester	LD_{50} dose estimated to be around 0.1mM
Isoproturon	LD_{50} dose estimated to be around 1mM
Λ-cyhalothrin	No toxicity at 1mM
Mancozeb	LD_{50} dose estimated to be around 0.01mM
Maneb	LD_{50} dose estimated to be around 0.01mM
Mecoprop-P	Exact LD_{50} dose not measured. Minor (non-significant) toxicity at 1mM
Mecoprop methyl ester	LD_{50} dose estimated to be around 0.1mM
Metsulfuron-methyl	Exact LD_{50} dose not measured. It was estimated to be within the 0.1mM-0.01 range
MPTP	Significant toxicity at 1mM but LD_{50} cannot be estimated from the chosen dose range
MPP+	Significant toxicity at 1mM but LD_{50} cannot be estimated from the chosen dose range
Nabam	LD_{50} dose estimated to be around 1mM
Paraquat	Exact LD_{50} dose not measured. It was estimated to be within the 0.1mM-1mM range
Pendimethlin	No toxicity at 1mM
Primicarb	Significant toxicity at 1mM but LD_{50} cannot be estimated from the chosen dose range
Rotenone	Exact LD_{50} dose not measured. It was estimated to be less than 0.001mM
Trifluralin	Exact LD_{50} dose not measured. It was estimated to be within the 0.1mM-1mM range

3.1.3.2 Contribution of the organic, manganese-metal and zinc-metal components of EBDC fungicides to neuronal toxicity:

It is estimated that 1.36 million kilograms of maneb and 3.76 million kilograms of mancozeb are annually applied in the USA (Zhou *et al*., 2004). Chronic maneb exposure has been linked with parkinsonism (Meco *et al*., 1994) and results from this study indicate maneb toxicity at doses as low as 0.01mM (60-70% reduction in viability vs. untreated control). Its major active component is manganese ethylene-bis-dithiocarbamate (Mn-EBDC) (fig 3.7). Identical results were seen with mancozeb exposure (which contains a mixture of Mn and Zn-EBDC). To identify the component contributing to toxicity, zineb (containing Zn-EBDC) was used to see if substituting zinc for manganese would reduce toxicity in SH-SY5Y cells. Indeed, it was less potent and showed significant reduction (* $p<0.05$) in toxicity (60-70% reduction in viability at 0.1mM vs. untreated control) (fig 3.8). Toxicity was less evident when the organic component Nabam (Na-EBDC) was used alone (40-45% reduction in viability at 1mM vs. untreated control) suggesting that manganese may be the principle component causing toxicity. These findings are consistent with recent reports showing significant toxicity with maneb and mancozeb in dopaminergic and GABAergic neurons accompanied with a decrease in TH positive neuritic processes, but not with nabam (Domico *et al*., 2006).

Fig 3.7: Chemical composition of dithiocarbamate fungicides: A) mancozeb, B) maneb, C) zineb and D) nabam.

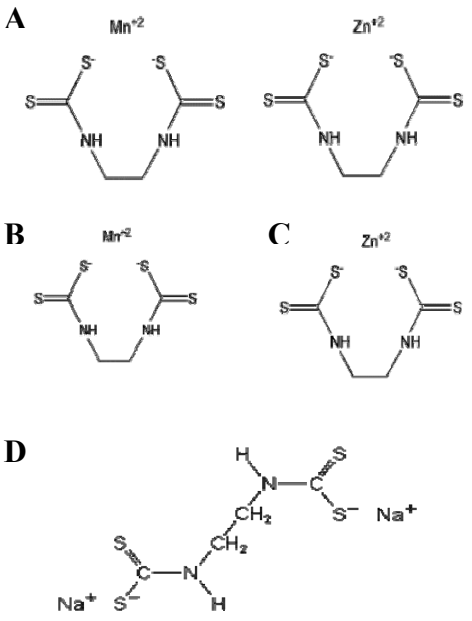

Fig 3.8: Dose–response effect of acute mancozeb, maneb, nabam and zineb on SH-SY5Y cell-viability: Each graph is representative of three independent experiments. Viable cell counts are shown as percentage of untreated control. For each treatment group, the difference from control was tested for statistical significance using one-way analysis of variance and *p* values <0.05 were accepted as significant. Error bars represent mean standard deviation ±SD).

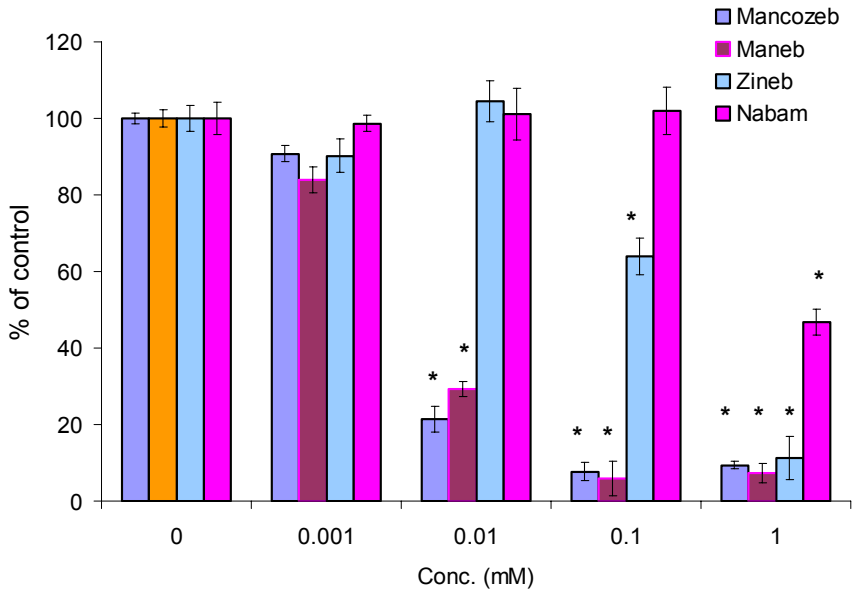

3.1.3.3 Differentiation of SH-SY5Y cells with 0.3mM dibutyryl cyclic AMP (dbcAMP) and 10mM Retinoic acid (RA):

Undifferentiated SH-SY5Y cell morphology shows short, rounded cell bodies and short processes (fig 3.9A). Morphological changes became noticeable after 2-3 days of incubation with growth medium containing 10mM RA and 0.3mM dbcAMP. By day 3, neurite-length was on average twice the size of undifferentiated cells (fig 3.9B). Structure transformation started with elongation of neurites, enhanced branching of neuronal processes and condensation of the cell body; in keeping with cell differentiation into a dopaminergic phenotype. By day 7, cells grew in small clusters with neurite length three to four times the length of undifferentiated cells (visual observation) (fig 3.9C, D) and appeared to have developed well-established cell-to-cell networks. Differentiated SH-SY5Y cells have been noticed to become growth inhibited as cells enter a late phase of neuronal differentiation (Pahlman *et al*., 1990); this was confirmed during these experiments, as the proliferation rate had significantly decreased by day 7.

Fig 3.9: Time-course of SH-SYSY cell morphology changes: A) Undifferentiated cells, (B) Day 5, (C-D) Day 7.

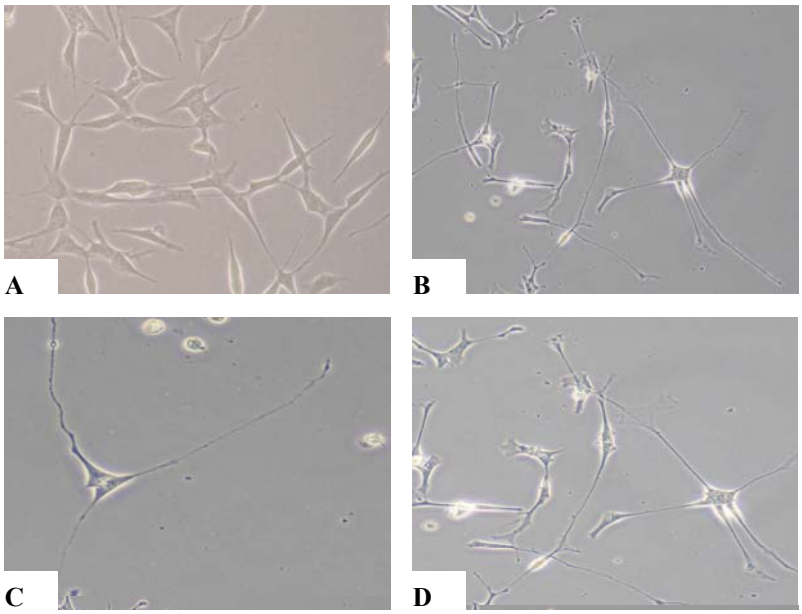

The neuronal phenotype of differentiated SH-SY5Y cells was confirmed by labelling with antibodies to the neuron specific beta-tubulin (Tuj1), low, medium and high molecular weight neurofilament proteins (NF-L, 68-70kDa; NF-M,150kDa; NF-H, 200-210kDa). The dopaminergic phenotype of differentiated SH-SY5Y cells was

confirmed by immunostaining with tyrosine hydroxylase (TH) and dopamine transporter (DAT). Images showed punctuate staining in the cell body and processes (fig 3.10).

Fig 3.10: Microscopic images of immunohistochemical staining of undifferentiated SH-SY5Y neural cells: A) Pan Neurofilaments staining (NF), B) Dopamine transporter (DAT), C) Tyrosine hydroxylase (TH), D) Neuronal Class III β-Tubulin (Tuj1). (Magnification = x10. Each image representative of 3 independent fields).

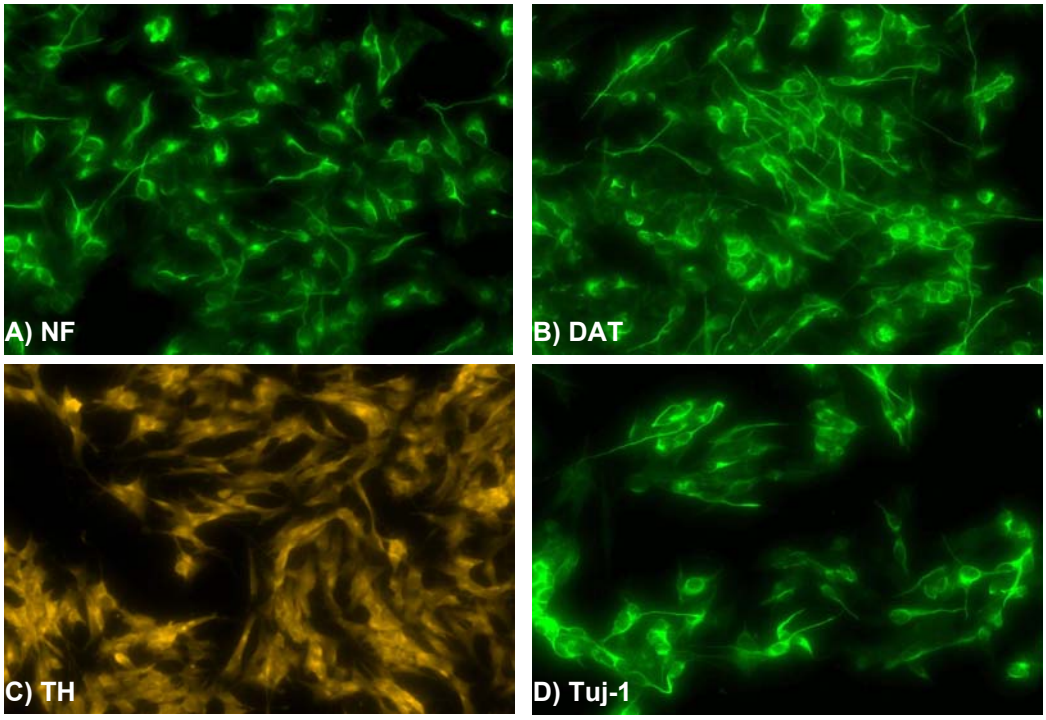

In order to investigate whether differentiated cells behave differently to toxic insults, differentiated SH-SY5Y cells were exposed to selected chemicals for 24 hours and then assayed for Alamar blue reduction. There was no overall reduction or increase in toxicity pattern when compared with undifferentiated cells, suggesting no extra sensitivity to these chemicals (fig 3.11, 3.12).

Fig 3.11: Toxin treatment of differentiated SH-SY5Y cells: Alamar blue reduction showed a dose dependent effect in A) diquat, B) maneb and C) mancozeb. n=3, * *p* values <0.05 or ** *p* values <0.01 were accepted as significant. Error bars represent mean standard deviation ±SD).

A:

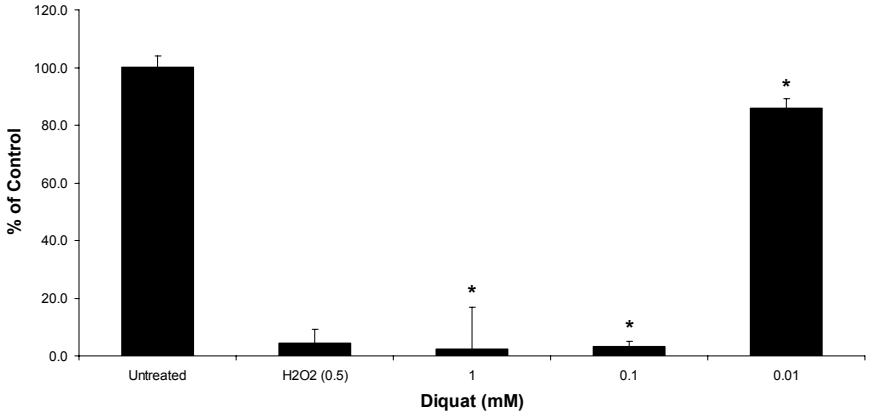

B:

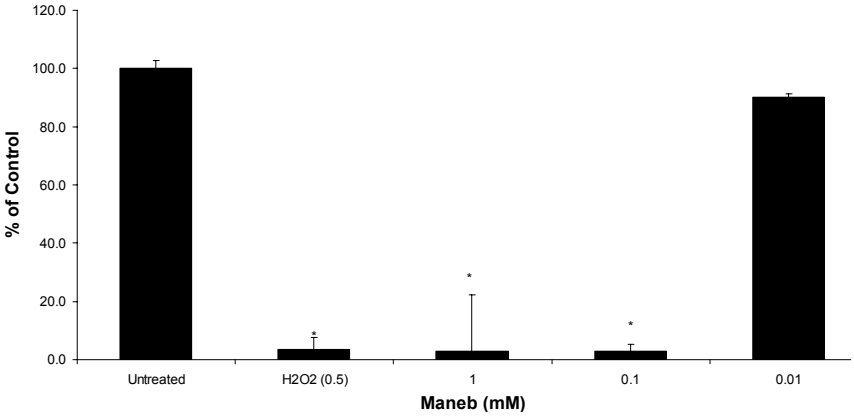

C:

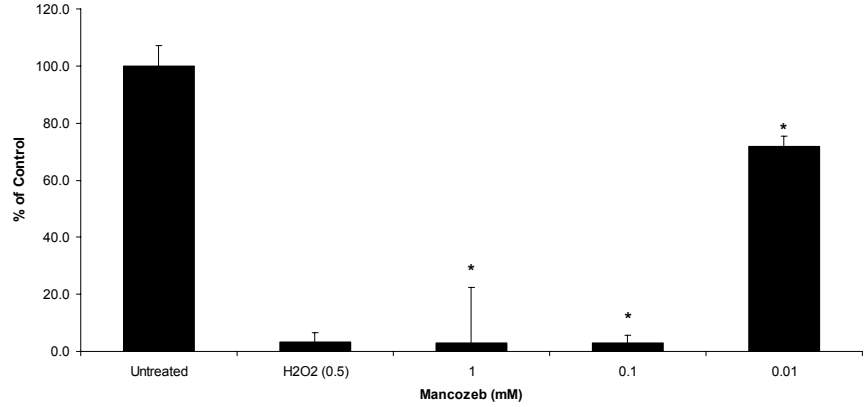

Fig 3.12: Toxin treatment of differentiated SH-SY5Y cells: Alamar blue reduction showed a dose dependent effect in A) epoxiconazole and B) fluroxypyr methyl heptyl ester. n=3, * *p* values <0.05 or ** *p* values <0.01 were accepted as significant. Error bars represent mean standard deviation ±SD).

A:

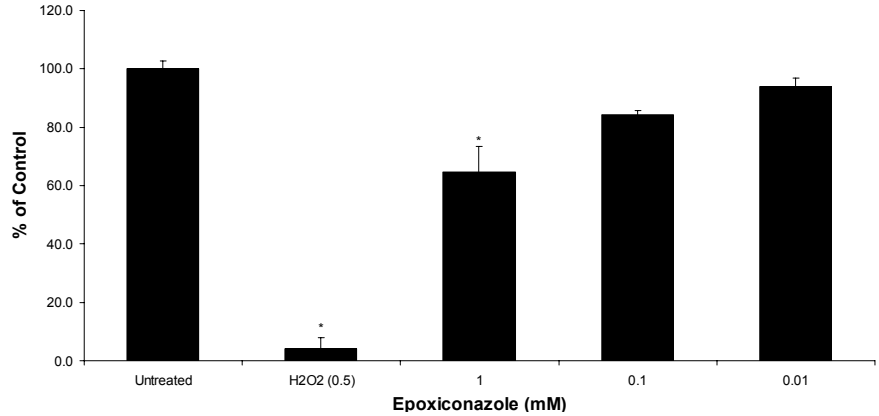

B:

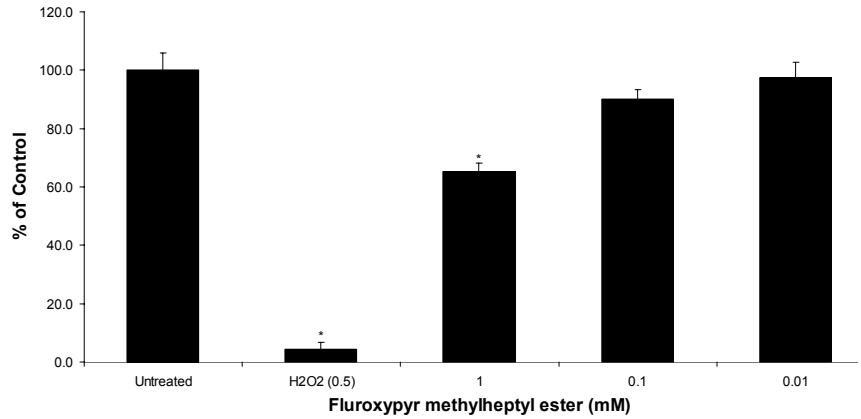

3.1.3.4 Effect of Dopamine Transporter inhibition on cell viability:

To determine if the cytotoxicity of toxins required mediation by dopamine transporter (DAT), SH-SY5Y cells were co-incubated with specific dopamine transporter inhibitors GBR12909 and N-[1-(Benzo[b]thien-2-yl-cyclohexyl)]piperidine hydrochloride (BTCP hydrochloride) for 1-2 hours before doses were added to give 50-60% toxicity. It has been suggested that differentiated cells show greater sensitivity than undifferentiated because DAT is highly expressed in differentiated cells. Therefore, both undifferentiated and differentiated SH-SY5Y cells were used. Western blotting analysis showed that SH-SY5Y cell-line expressed DAT and there was no significant difference in protein levels after 5 day differentiation (fig 3.13). It cannot be determined from these results that their enzyme activity also remains unchanged. Cell viability measured after 24 hours showed that these inhibitors did not protect cells against cytotoxicity or affected the degree or pattern of cell-death in undifferentiated (fig 3.14, 3.15) or differentiated cells (fig 3.16). Different concentrations of DAT inhibitors were used and all of these failed to show any reduction in cytotoxicity.

Fig 3.13: Western blot analyses of DAT in undifferentiated and differentiated SH-SY5Y cells. Overall expression of dopamine transporter (DAT), tyrosine hydroxylase (TH) and dopamine beta hydroxylase (DβH) did not change after 5 day differentiation with retinoic acid (Images representative of three independent experiments).

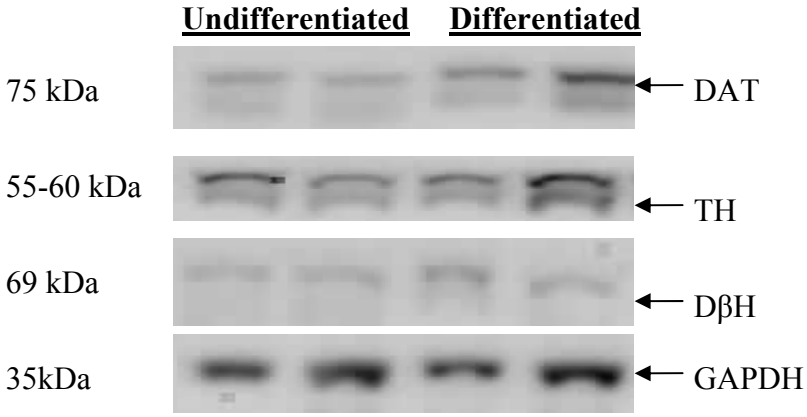

Fig 3.14: Effect of DAT inhibitor GBR 12909 cytotoxicity: Co-incubation with GBR12909 (A-C) failed to reduce toxicity in treated cells. Results from Alamar blue reduction assay. n=3, * *p* values <0.05 were accepted as significant. Error bars represent mean standard deviation ±SD).

A:

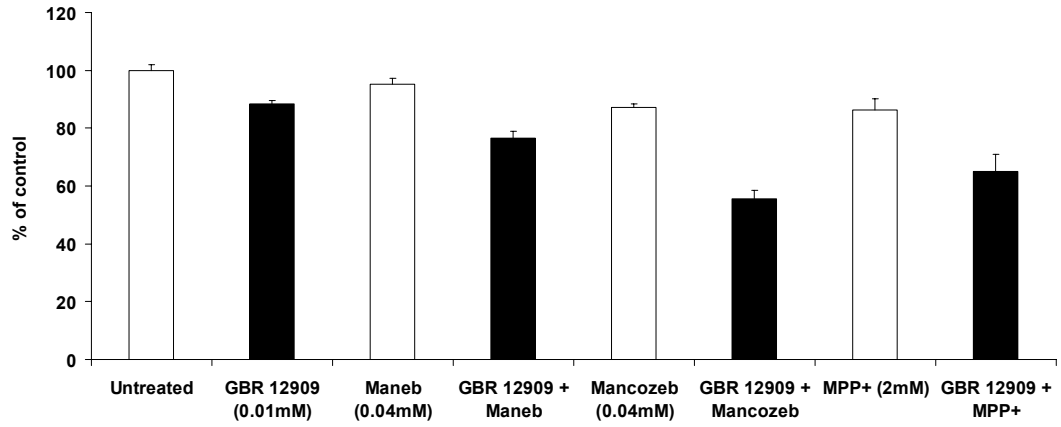

B:

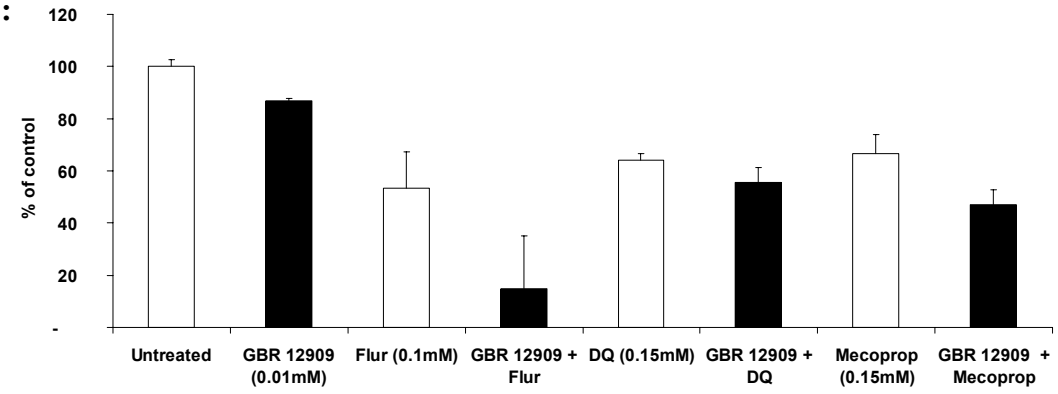

C:

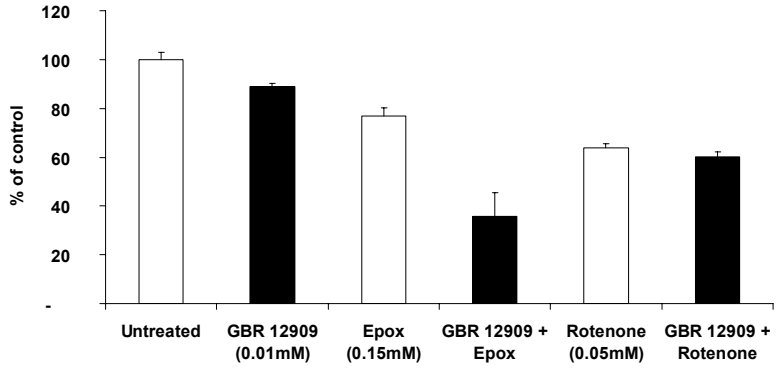

Fig 3.15: Effect of DAT inhibitor BTCP on cytotoxicity: Co-incubation with BTCP (A-C) failed to reduce toxicity in treated cells. Results from Alamar blue reduction assay. n=3, * *p* values <0.05 were accepted as significant. Error bars represent mean standard deviation ±SD).

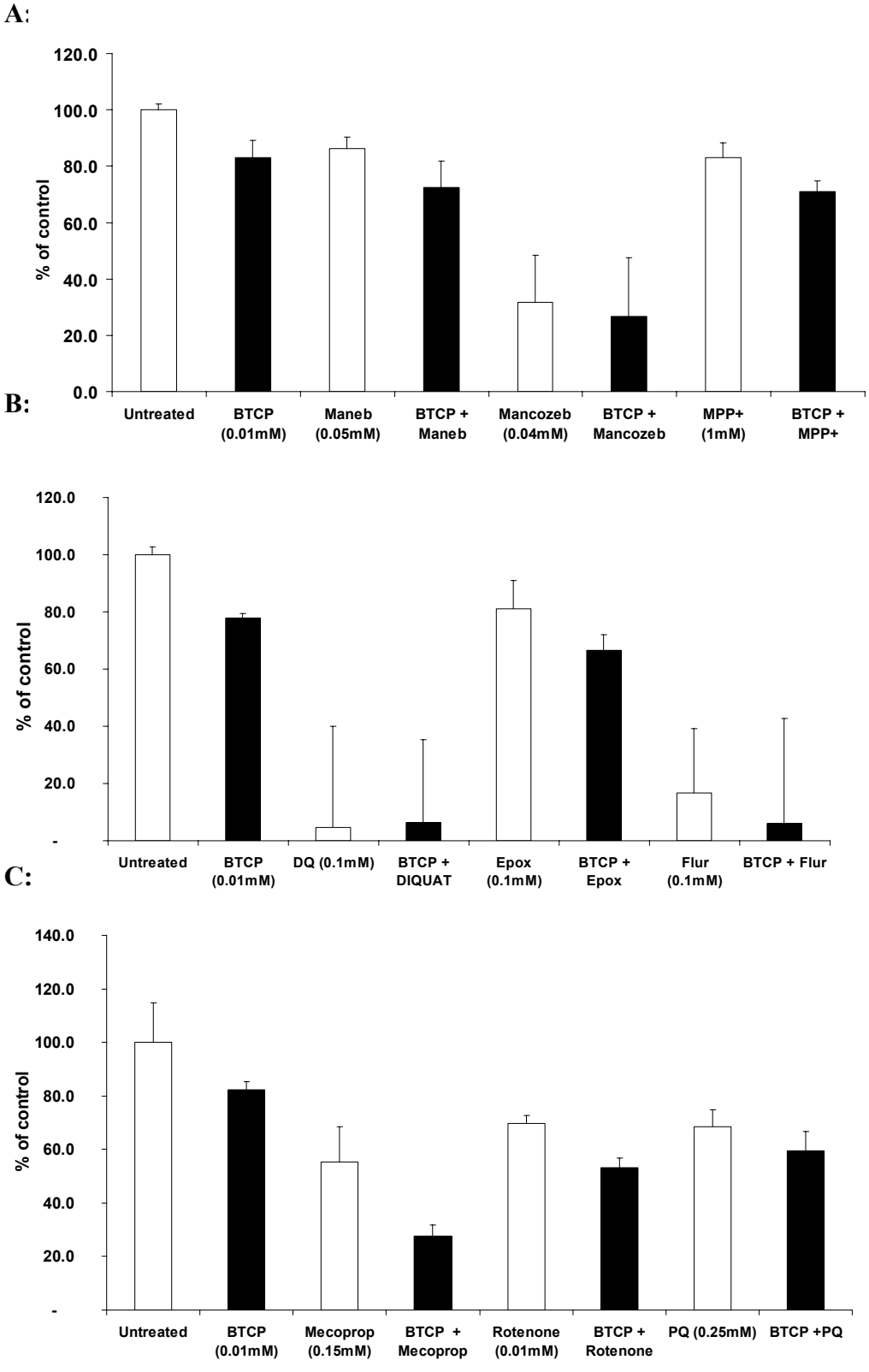

Fig 3.16: Effect of GBR 12909 on cytotoxicity in differentiated SH-SY5Y cells: Selected chemicals are shown below. Incubation of DAT inhibitor with diquat (0.05mM), MPP+ (1mM) and mancozeb (0.05mM) did not show any reduction in toxicity. n=3, * *p* values <0.05 were accepted as significant. Error bars represent mean standard deviation ±SD).

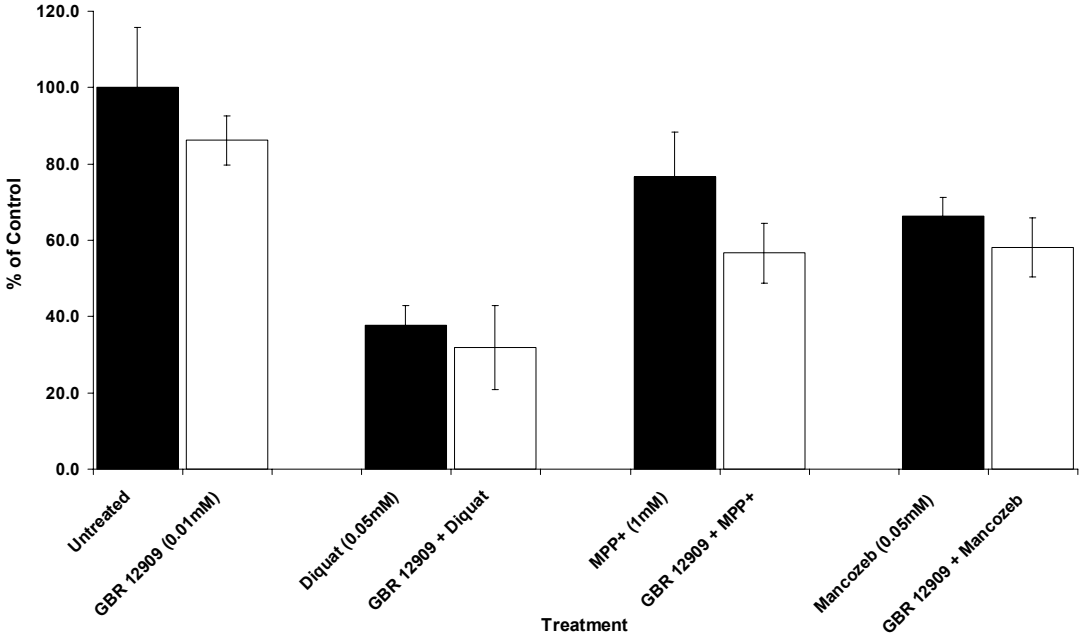

Previous studies have shown that MPP+ and dopamine share similar kinetics and DAT blockade by GBR 12909 can reduce their neurotoxicity (Presgraves *et al*., 2004). Co-incubation of different dopamine hydrochloride doses (0.5mM, 0.25mM and 0.1mM) with GBR 12909 (0.001mM) and BTCP (0.001mM) failed to show any reduction in toxicity (fig 3.17). Dopamine hydrochloride induced dose-dependent cytotoxicity. It was highly toxic at 2mM, 1mM and 0.5mM reducing cell number to less than 5% of untreated control. When SH-SY5Y cells were co-incubated with either GBR 12909 or BTCP, no significant change in toxicity was observed.

Fig 3.17: Effect on DAT inhibitors on dopamine hydrochloride induced toxicity: Co-incubation with A) GBR12909 (0.001mM) (B) BTCP (0.001mM) failed to reduce dopamine hydrochloride toxicity in SH-SY5Y cells. n=3, * *p* values <0.05 were accepted as significant. Error bars represent mean standard deviation ±SD).

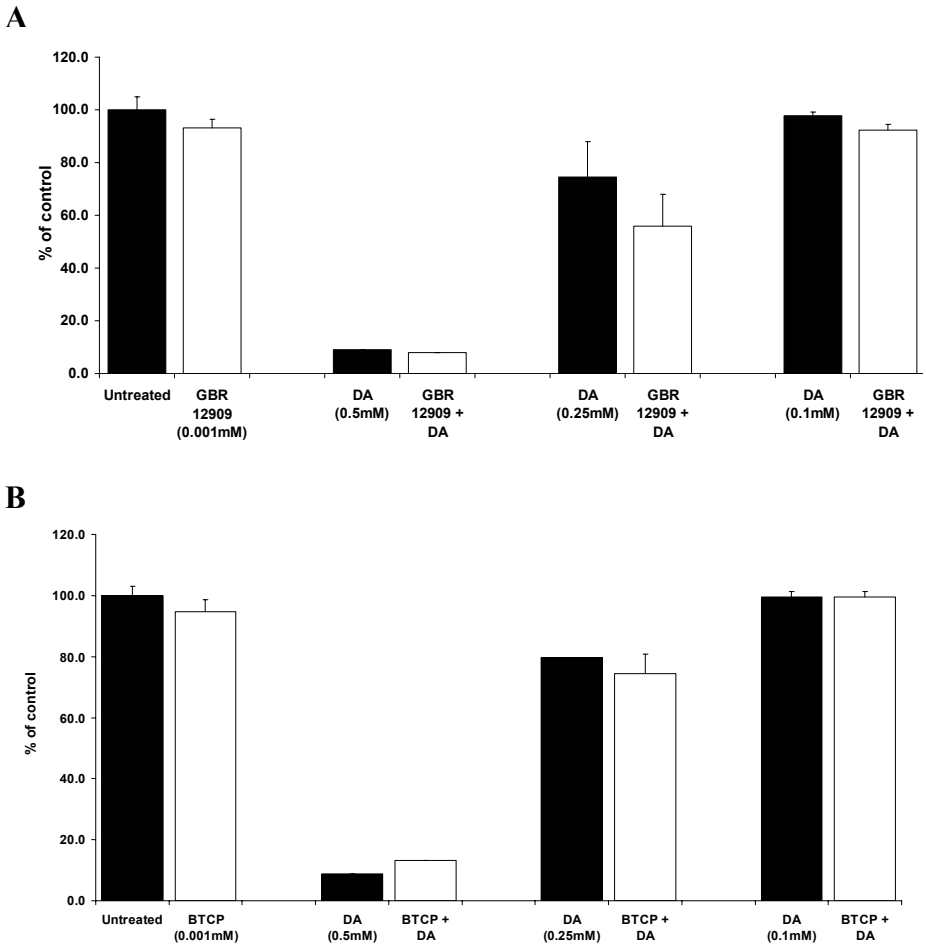

3.1.3.5 Effect of cell-death inhibitors on cytotoxicity:

During apoptosis, cytochrome c release from the mitochondria activates caspase-9, which leads to caspase-3 activation. Caspase-3 cleaves specific substrates required for downstream apoptosis signalling. SH-SY5Y cells were treated with toxins or vehicle (DMSO) in the presence or absence of the caspase-3 and 9 inhibitors (DEVD-CHO and Ac-LEVD-CHO respectively) and zVAD.fmk, a cell-permeable broad-spectrum caspase inhibitor that irreversibly binds to the catalytic site of caspase proteases and can inhibit apoptosis induction (Amstad *et al*., 2001). zVAD.fmk treatment showed a slight reduction in toxicity of diquat (0.1mM), epoxiconazole (0.1mM), fluroxypyr ester (0.1mM), maneb (0.04mM), mancozeb (0.04mM) and mecoprop methyl ester (0.2mM) which was not statistically significant (fig 3.18). Similarly, treatment with caspase-3 inhibitor (DEVD-CHO) and caspase-9 inhibitor (Ac-LEVD-CHO) also failed to affect toxicity (fig 3.19, 3.20).

Fig 3.18: Effect of zVAD.fmk on cell viability in toxin-induced cytotoxicity: Cells were pre-incubated with zVAD.fmk (0.1mM) for 1-2 hours before toxin addition. After 24 h incubation, cell viability was evaluated by Alamar blue reduction assay. Each experiment was performed in triplicate. Data expressed as mean±SD; (* *p* values <0.05 were accepted as significant).

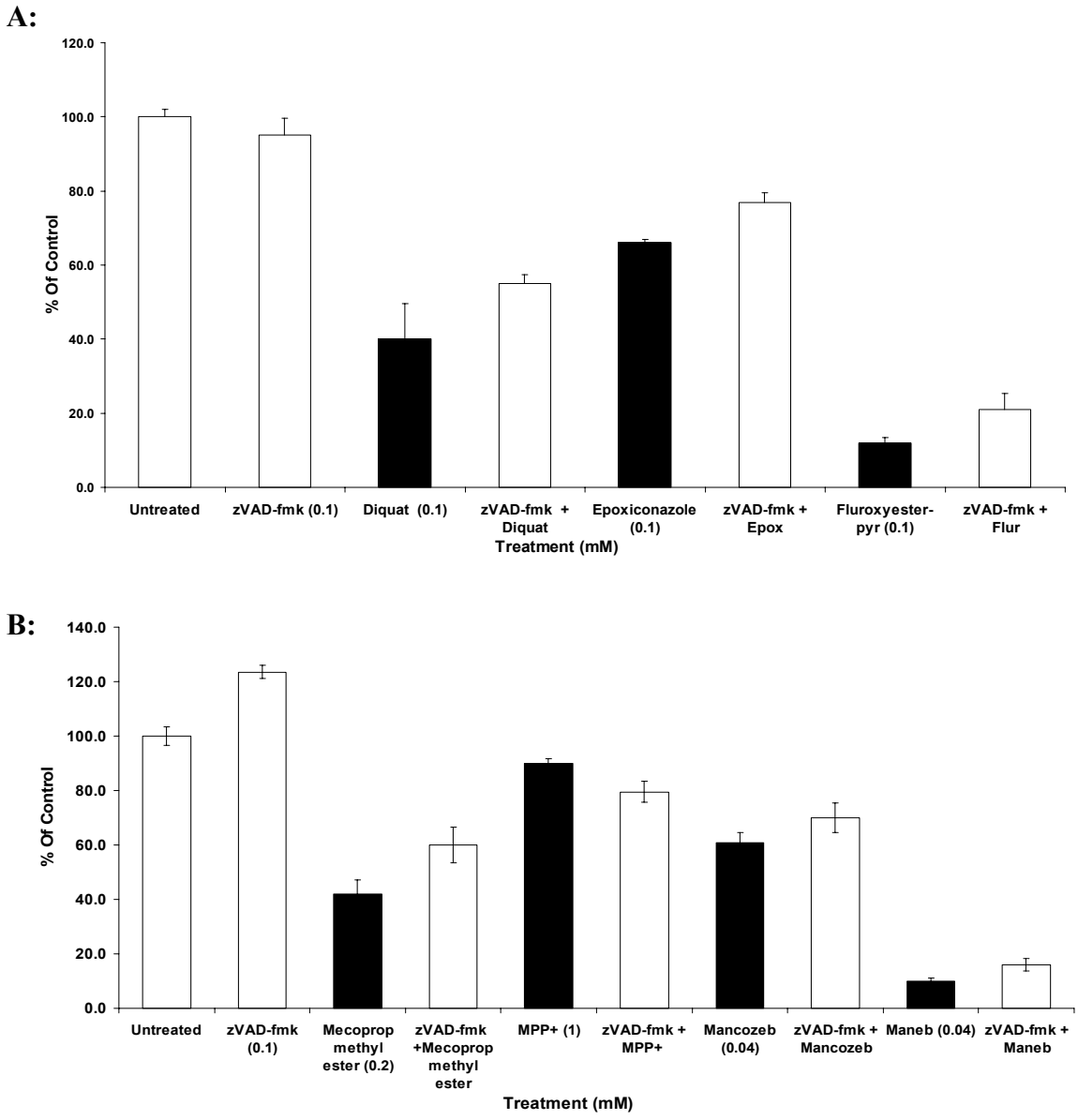

Fig 3.19: Effect of caspase-3 inhibitor on cell viability after toxin treatment: Cells were pre-incubated with (a-c) DEVD-CHO (0.001mM) for 1-2 hours before toxin addition. After 24 h incubation, cell viability was evaluated by Alamar blue reduction assay (n=3, data expressed as mean±SD; (* *p* values <0.05 were accepted as significant).

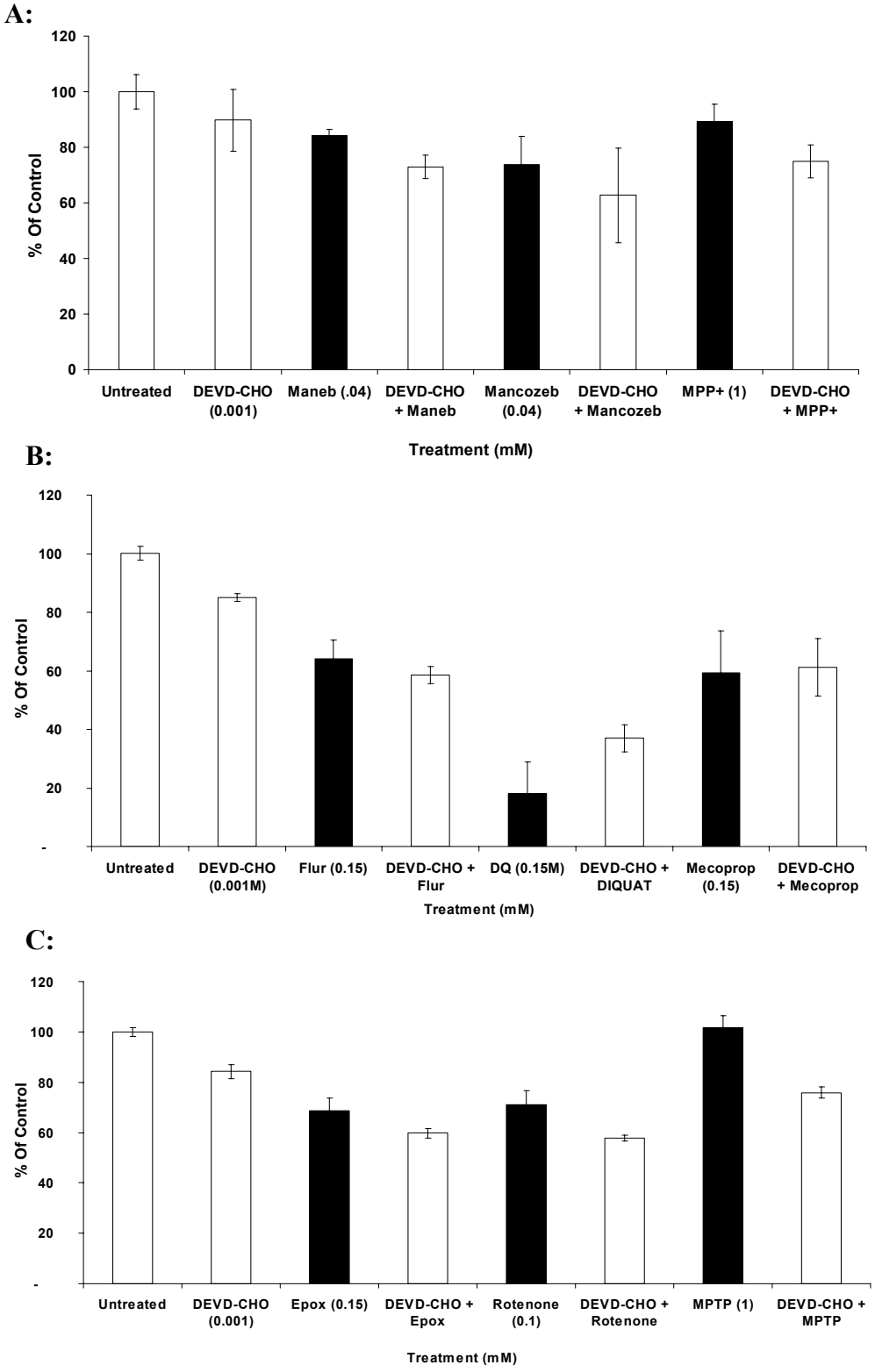

Fig 3.20: Effect of caspase-9 inhibitor on cell viability after toxin treatment: Cells were pre-incubated with (a-c) Ac-LEVD-CHO (0.001mM) for 1-2 hours before toxin addition. After 24 h incubation, cell viability was evaluated by Alamar blue reduction assay (n=3, data expressed as mean±SD; (* *p* values <0.05 were accepted as significant).

A:

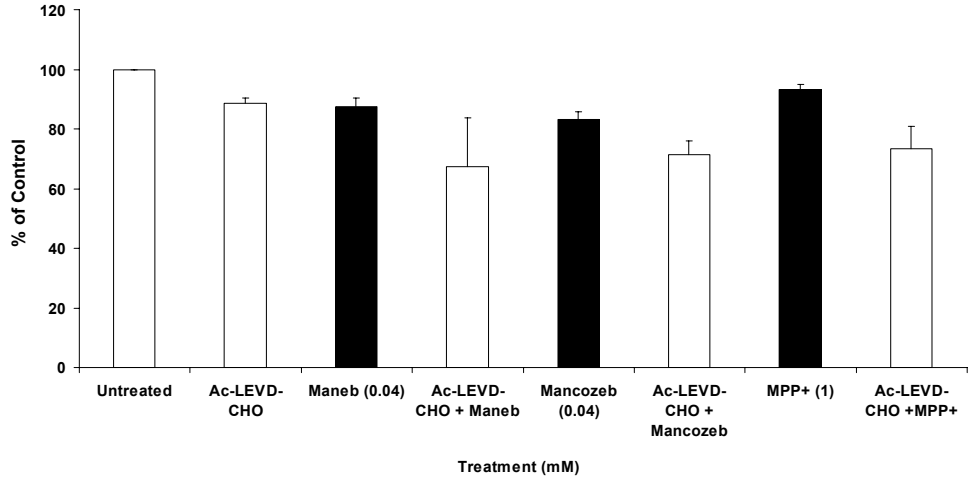

B:

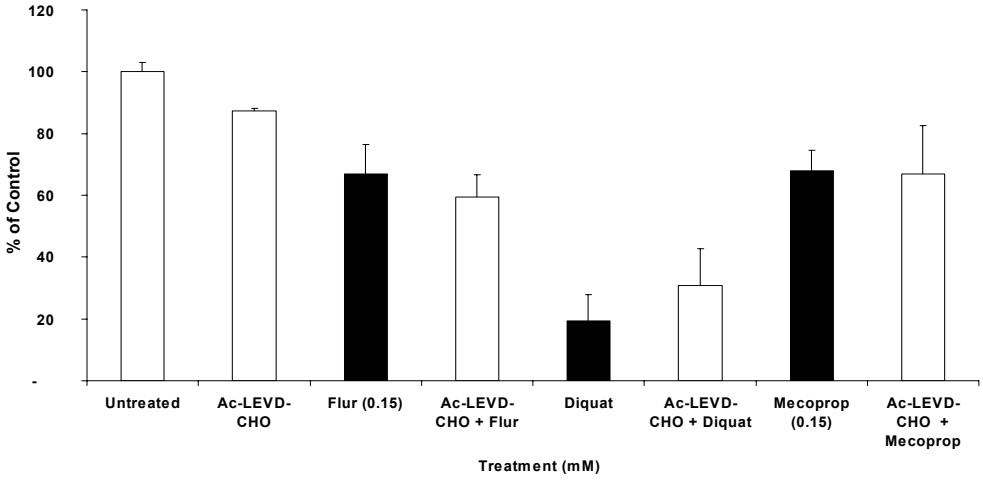

C:

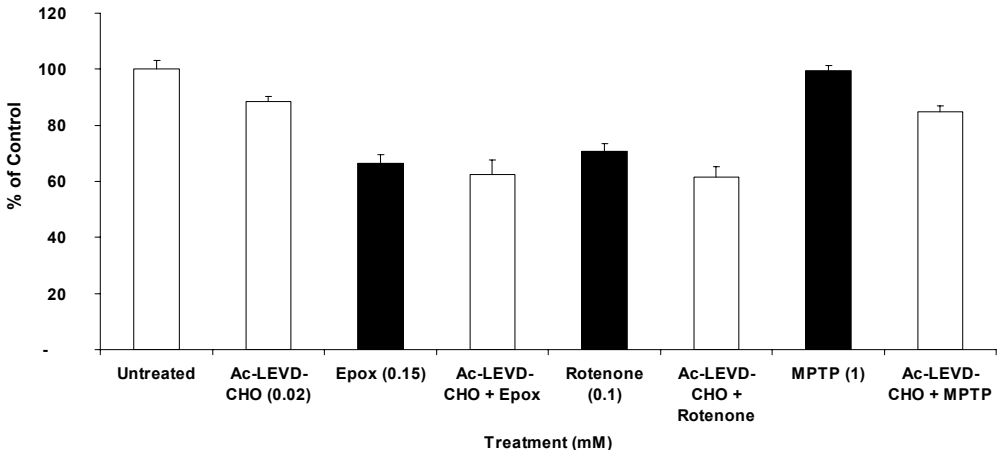

Previous studies have shown that caspase inhibition does not always protect against apoptosis and alternative cell-death mechanisms may be involved (McCarthy *et al*., 1997; Villa *et al*., 1998). Furthermore, autophagy may be responsible for cell-death caused by chemical insult which can be prevented by using autophagy inhibitors (Shimizu *et al*., 2004). To identify alternative cell-death pathways involved necrostatin-1 (Nec-1) a programmed necrosis inhibitor and 3-methyl adenine (3-MA) a macroautophagy inhibitor were used.

Pre-treatment with 3-MA (1.5mM, 2.5mM and 5mM) failed to prevent cell-death. Nec-1 (0.1mM) however showed significant increase in viability when treated with diquat (0.1mM), epoxiconazole (0.1mM), fluroxypyr-ester (0.1mM), maneb (0.04mM), mancozeb (0.04mM), MPP+ (1mM) and mecoprop methyl ester (0.2mM) (fig 3.21, 3.23). This was accompanied by an increase in cell number suggesting Nec-1 enhanced cell-proliferation or reduced endogenous cell death. Calculation of average increase/reduction in cell viability from three different experiments showed that necrostatin-1 caused 74.2% recovery in diquat (0.1mM), 35% in epoxiconazole (0.08mM), 70.5% in fluroxypyr methyl ester (0.1mM), 43.4% in maneb (0.025mM), 20.2% in MPP+ (1mM), 40.2% in mecoprop methyl ester (0.1mM) and 37.2% in mancozeb (0.04mM) treated cells.

Fig 3.21: Effect of Necrostatin-1 on cell viability in toxin-induced cytotoxicity: Cells were pre-incubated with necrostatin-1 (0.1mM) for 1-2 hours before toxin addition. After 24 h incubation, cell viability was evaluated by Alamar blue reduction assay. Each experiment was done in triplicate. Data expressed as mean±SD; (* *p* values <0.05 were accepted as significant).

A:

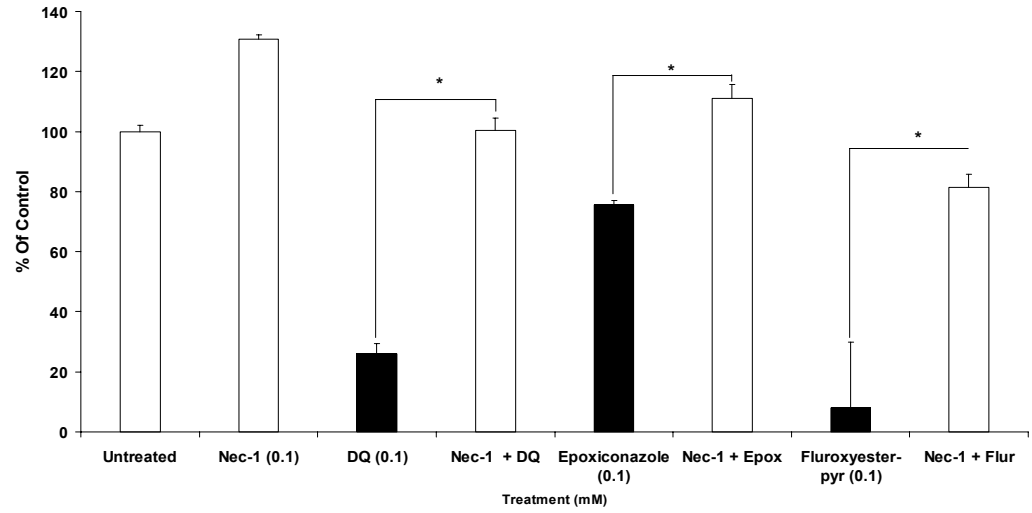

B:

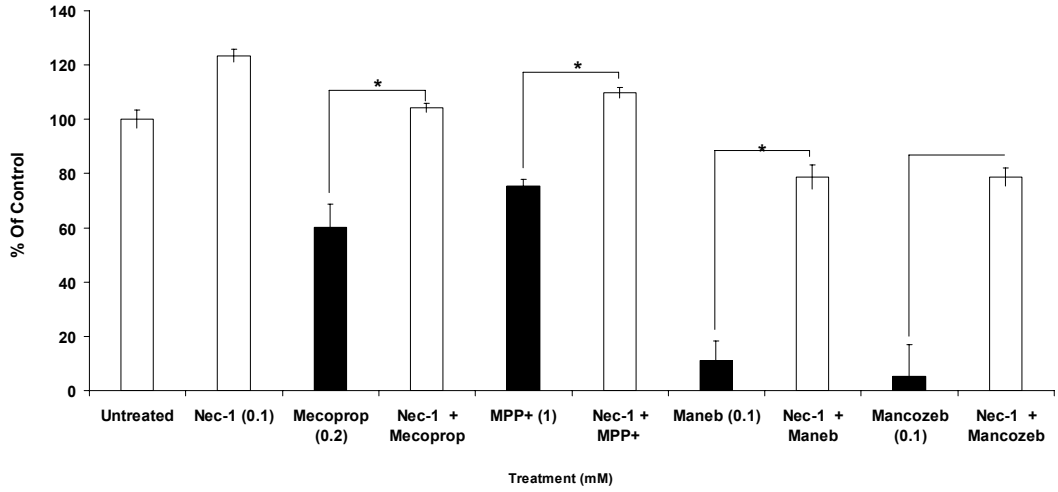

Staurosporine is an alkaloid widely used as a protein kinase C (PKC) inhibitor. It induces morphological changes typical of apoptosis, induces JNK1 activation (Chae *et al*., 2000) and inhibits cell-cycle (Abe *et al.,* 1991). Pre-incubation with Nec-1 (0.1mM) showed a significant prevention of cell death in staurosporine (0.001M) treated cells (greater than 80% difference) whereas zVAD.fmk (0.1mM) treatment showed no effect (fig 3.22).

Fig 3.22: Effect of necrostatin-1 and zVAD.fmk on cell viability in staurosporine treated cells: Cells were pre-incubated with necrostatin-1 (0.1mM) zVAD.fmk (0.1mM) for 1-2 hours before toxin addition. After 24 h incubation, cell viability was evaluated by Alamar blue reduction assay. Each experiment was done in triplicate. Data expressed as mean±SD; (* p values <0.05 and ** $p < 0.01$ were accepted as significant).

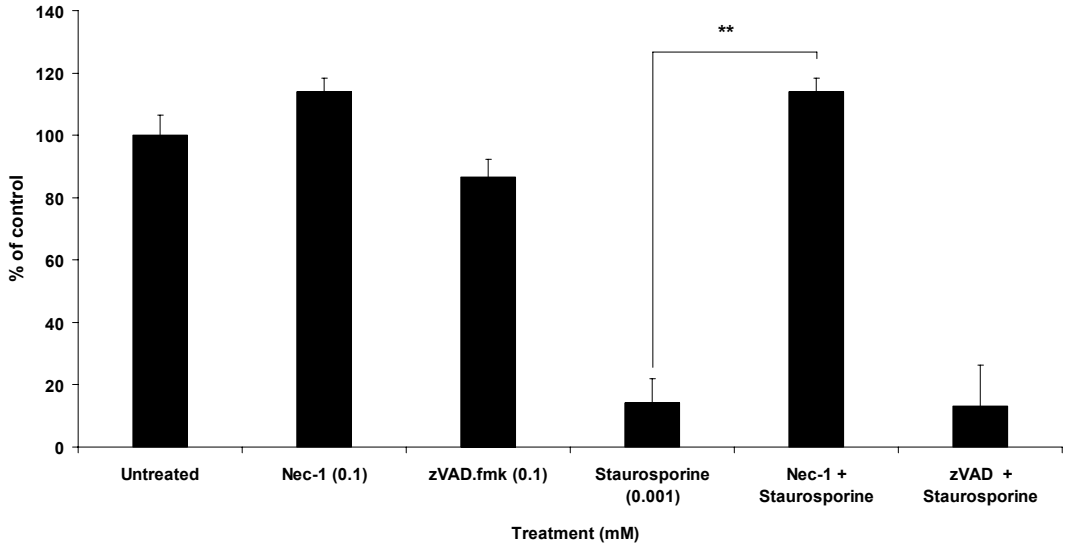

Fig 3.23: Visual presentation of Nec-1 treated cells after toxin treatment: A significantly higher number of DAPI stained cells after diquat (0.1mM), mancozeb (0.04mM) and MPP+ (1mM) treatment after 24 hours (Magnification = x40, each image is representative of three independent fields).

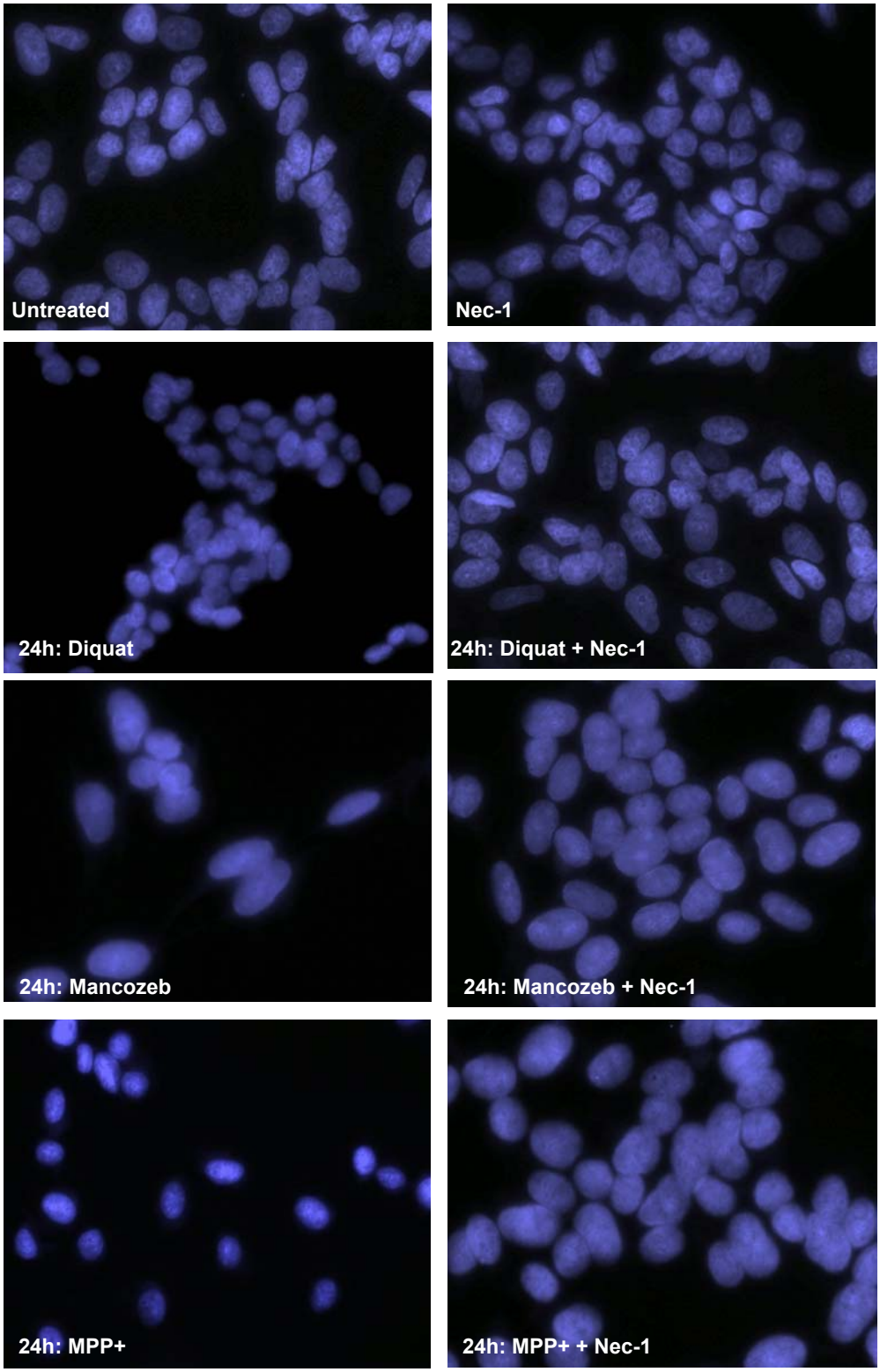

3.1.3.6 Effect of cell-signalling inhibitors on cytotoxicity:

In response to toxin insult, signalling pathways either alone or in conjunction with others, influence the final fate of the cell. A number of different signalling cascades can play a role in mediating cytotoxicity. To identify specific intracellular signalling pathways involved, a range of different cell-signalling inhibitors were used including H89 (protein kinase A inhibitor), U0126 (MEK inhibitor), PD-98059 (MEK inhibitor), LY294002 (PI3K inhibitor), GW5074 (ERK inhibitor), SQ22536 (adenylyl cyclase inhibitor), SP600125 (JNK 1, 2, and 3 inhibitor) and cycloheximide (protein biosynthesis inhibitor). Each experiment was repeated at least three times and average increase/reduction in cell viability calculated (shown below). Positive numbers indicate protection; negative numbers indicate exacerbation of toxicity. For positive results, difference from control was tested for statistical significance using t-test and p values <0.05 were accepted as significant (* indicates statistically significant). The extent of cell death was not significantly modified with different inhibitors (except SQ22536 after diquat treatment), most appeared to significantly potentiate toxicity (shown below) whereas other showed modest insignificant protection (tiron).

Table 3.3: Percentage increase/reduction in toxin treated cells after cell-signalling inhibition:

Inhibitor	Diquat	Maneb	Mancozeb	MPP+
Nec-1	+49.6*±17	+19.5*±18.7	+35.6*±4.5	+35.2*±0
zVAD.fmk	+5.7±7.8	+0.56±4.9	+4.1±8.7	-10.2*±0
NAC	+24.6*±5.2	+30*±8.6	53*±16.9	-25*±0
Cyclosporin A	+4.25±6.6	-14±7.7	-1±1	-11*±0
Tunicamycin	9.84*±16.0	-4.5±2.3	-5.08±1.3	-1.49±0
3-Methyladenine	1.12±12.3	-4.5±2.2	-5±2.3	-1.5±0
Ammonium Chloride	0.13±9.0	+3.35±.0.07	0.6±1.97	-6±0
Tiron	-14.4*±12.0	+4.26±0.6	+6.97±10.6	0
GW5074	-7±0	+1.1±1.1	-0.5±2.3	-9.6*±0
H89	+2.3±0	+1.1±02	+2.7±2.3	3.7±0
LY29002	-10*±0	-2.1±3.6	-3.9±4.4	-24.8*±0
PD98059	2.6±0	-29.0*±5.6	+4.5± 2.3	-22.9*±0
U0126	4.3±0	-12.4±4.4	-3.1±1.2	-33.4*±0
SQ22536	+17.1*±5.15	-10.4*±5.3	-8.9*±2.6	-18.9*±0
SP600125	-15.6*±3.18	-24*± 13.7	-11.53±4.04	-18.5*±6.3

Table 3.4: Percentage increase/reduction in toxin treated cells after cell-signalling inhibition:

Inhibitor	Mecoprop methyl ester	Epoxiconazole	FMH
Nec-1	+44.2*±0	30.6*±	+72*±1.25
zVAD.fmk	+8.2±5.3	+7.1±0.3	+6.15±4.45
NAC	-17*±2.3	-22±0	+2.5±0.7
Cyclosporin A	-6	-11±0	-2.3±1.8
Tunicamycin	-27.4*±1.3	-24±0	-12*±6.08
3-Methyladenine	-15*±2.5	--	-8±2.82
Ammonium Chloride	+3.7±0	--	+6.2
Tiron	-4.45±2.3	--	+6.5±10.5
GW5074		-2±0	-22.18*±0
H89	-8.4*±2.3	-9*±0	-20.2*±0
Ly29002	--	-32.35*±0	-13.06*±0
PD98059	--	-26.4*±0	-22.61*±0
U0126	-27.5*±3.6	-28.4*±0	-19.4*±0
SQ22536	-13.7*±1.1	--	+6.2*±0
SP600125	-34.125±5.6	--	-18.6±1.2

3.1.3.7 Measurement of reactive oxygen species (ROS) in toxin treated cells:

2',7'-dichlorofluorescein diacetate (DCFDA) detects a number of ROS species, including H_2O_2, superoxide anions and hydroxyl radical (Gomes *et al*., 2005). It diffuses through the cell membrane and is cleaved to 2',7'-dichlorofluorescein (DCF). DCF reacts with H_2O_2 to form the green fluorescent dye dichlorofluorescein. It is generally accepted that DCF fluorescence is proportional to H_2O_2 concentration. Dichlorofluorescein can either be measured at 485/520nm or viewed under a fluorescent microscope. Hydrogen peroxide (0.5mM) was used a positive control for these experiments. It caused a significant increase in fluorescence after 2 hours and measurements recorded after 3 and 4 hours showed an equally higher percentage of DCF fluorescence. After 24 hours, cell viability had reduced to less than 10% of untreated control and this was reflected in significantly lower fluorescence (fig 3.24). Rotenone can induce the production of superoxide and other ROS (Molina-Jimenez *et al.,* 2005). 24 hour incubation with different doses showed significantly higher DCF fluorescence with 0.001mM, 0.01mM and 0.05mM doses (fig 3.24). 0.1mM dose caused significant cell death and a very low number of cells were present in the cell lysates resulting in a low level of fluorescence. Diquat,

maneb and mancozeb, showed a similar trend with dose range (0.001mM-0.5mM) showing a significant increase in ROS production (fig 3.25). Paraquat is a potent pro-oxidant and generates ROS through cytochrome P-450-mediated redox cycling reaction (Suntres, 2002). Cytotoxicity experiments have shown that paraquat does not cause significant cell death at lower doses and indeed a similar pattern of ROS generation was observed with MPP+ and mecoprop-p where 0.001mM, 0.01mM and 0.5mM doses did not affect cell-viability nor induced any changes in DCF fluorescence. Only 1mM dose of these chemicals caused a significant change in fluorescence (fig 3.26).

Fig 3.24: Toxin induced ROS production in SH-SY5Y cells: A) Hydrogen peroxide (0.5mM) induced a time dependent increase in ROS production as determined by DCF-DA assay. A dose-dependent increase in ROS production was noted with rotenone (B) (n=3, results are mean ± SD, **p* values <0.05 or ***p*<0.01 were accepted as significant).

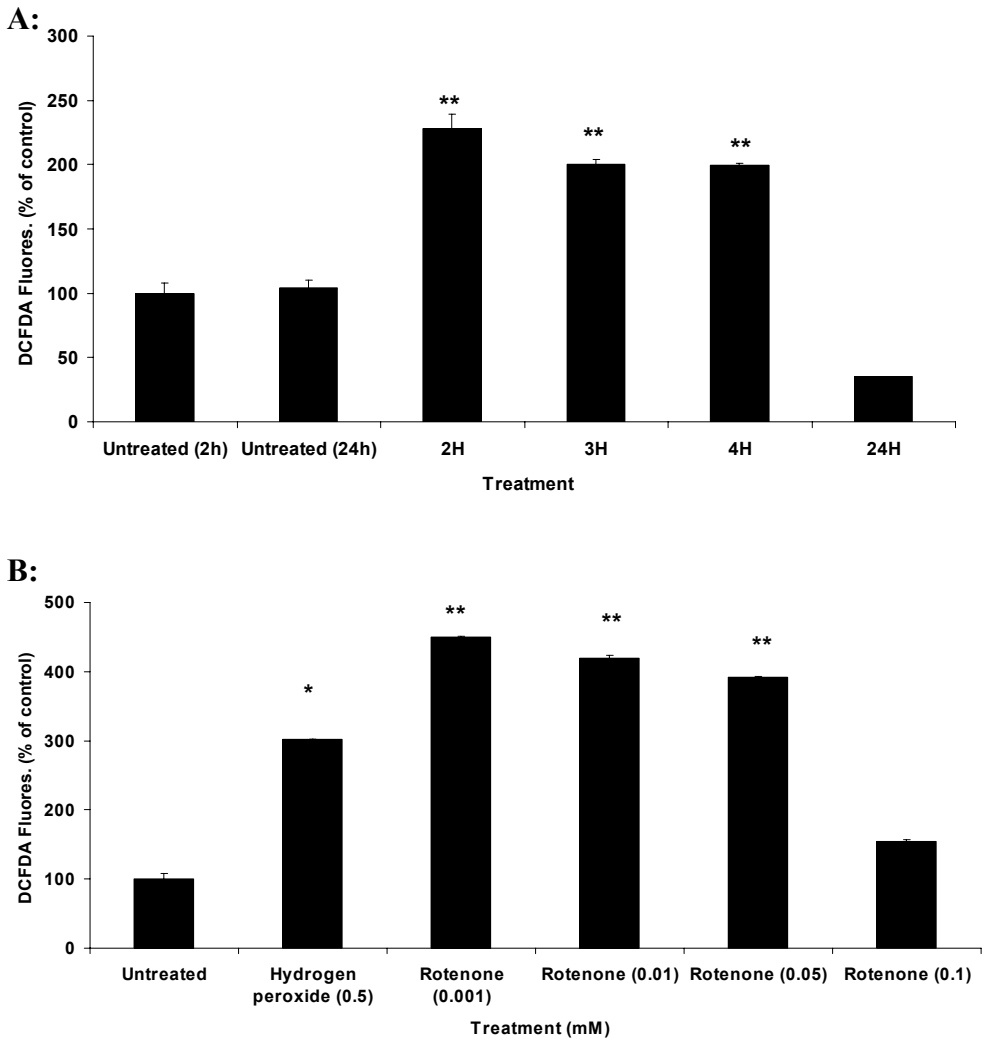

Fig 3.25: Toxin induced ROS production in SH-SY5Y cells: A dose-dependent increase in ROS production was noted with diquat (A), maneb (B) and mancozeb (C) (n=3, results are mean ± SD, **p* values <0.05 or ***p*<0.01 were accepted as significant).

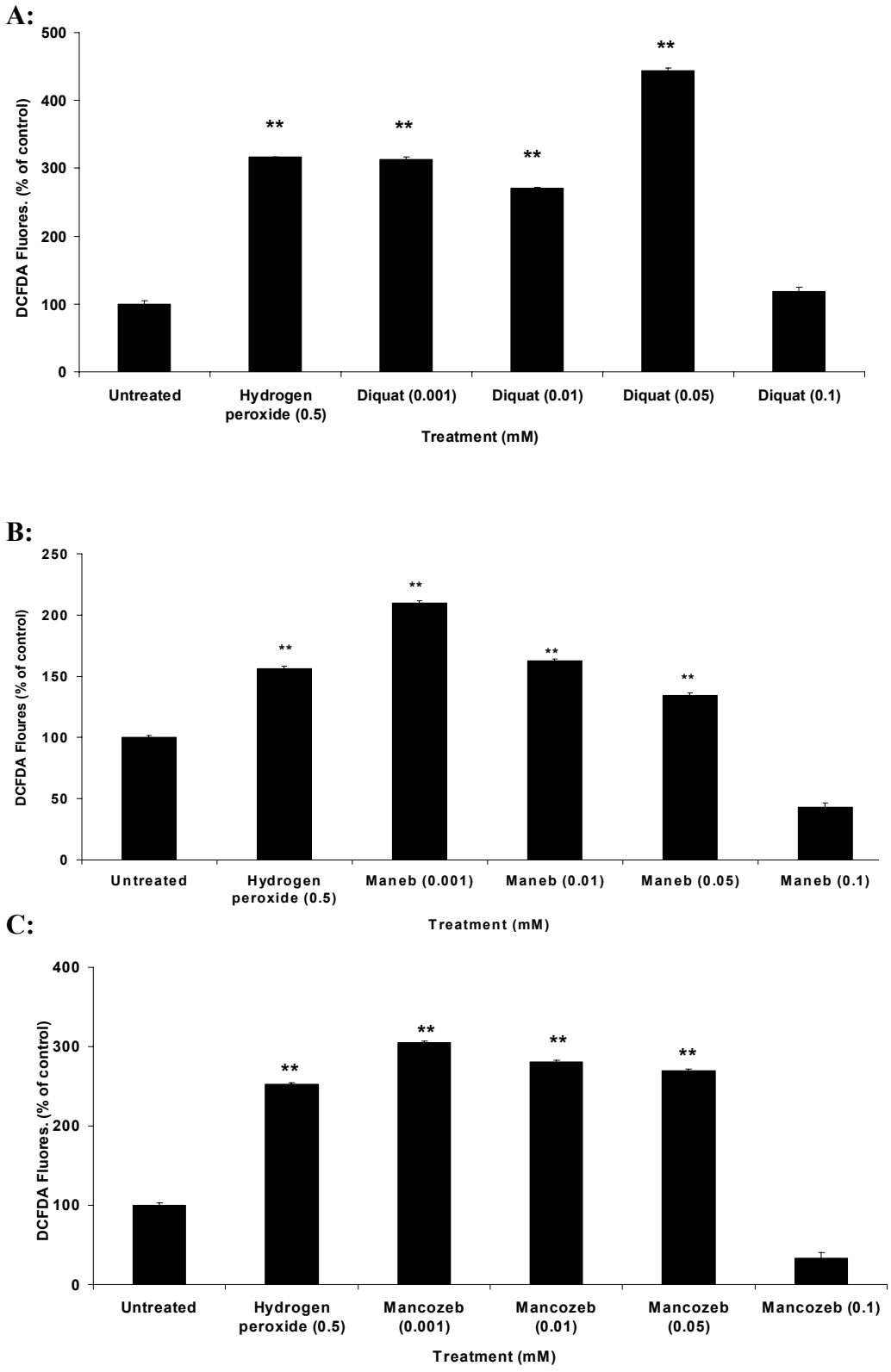

Fig 3.26: Toxin induced ROS production in SH-SY5Y cells: A dose-dependent increase in ROS production was noted with paraquat (A), mecoprop-p (B) and MPP+ (C) (n=3, results are mean ± SD, **p* values <0.05 or ***p*<0.01 were accepted as significant).

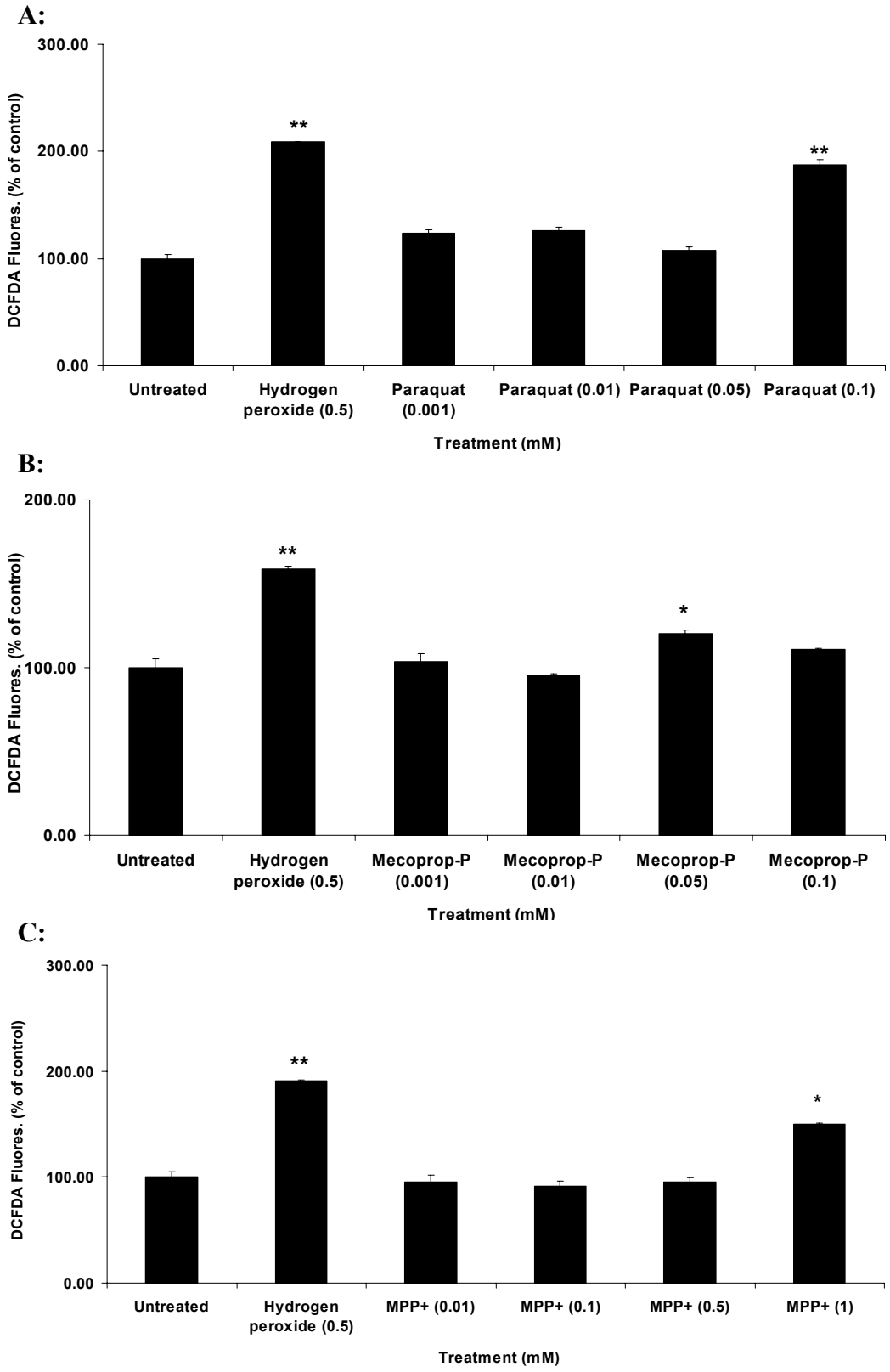

For visual confirmation of ROS production, cells were grown in chamber slides, incubated with the dye and treated with sub-cytotoxic doses of toxins for 6-8 hours. A large increase in the level of ROS was evident when cells were exposed to H_2O_2 in contrast to cells exposed to diquat (0.05mM) and mancozeb (0.04mM), paraquat (0.2mM) and rotenone (0.1mM). Paraquat and rotenone caused significant cell detachment and fluorescence was only visible from viable stressed cells (fig 3.27).

Fig 3.27: Visual determination of ROS level in SH-SY5Y cells following toxin insult: SH-SY5Y cells were plated out in chamber slides and treated with toxins for 8 hours. Untreated cells showed a low background whereas H_2O_2 (0.5mM), diquat (0.05mM) and mancozeb (0.04mM) showed higher fluorescence. Paraquat and rotenone caused significant reduction in cell-viability at 0.2mM and 0.5mM respectively but viable stressed cells showed clear increase in fluorescence. (Magnification = x10, each image is representative of three independent fields).

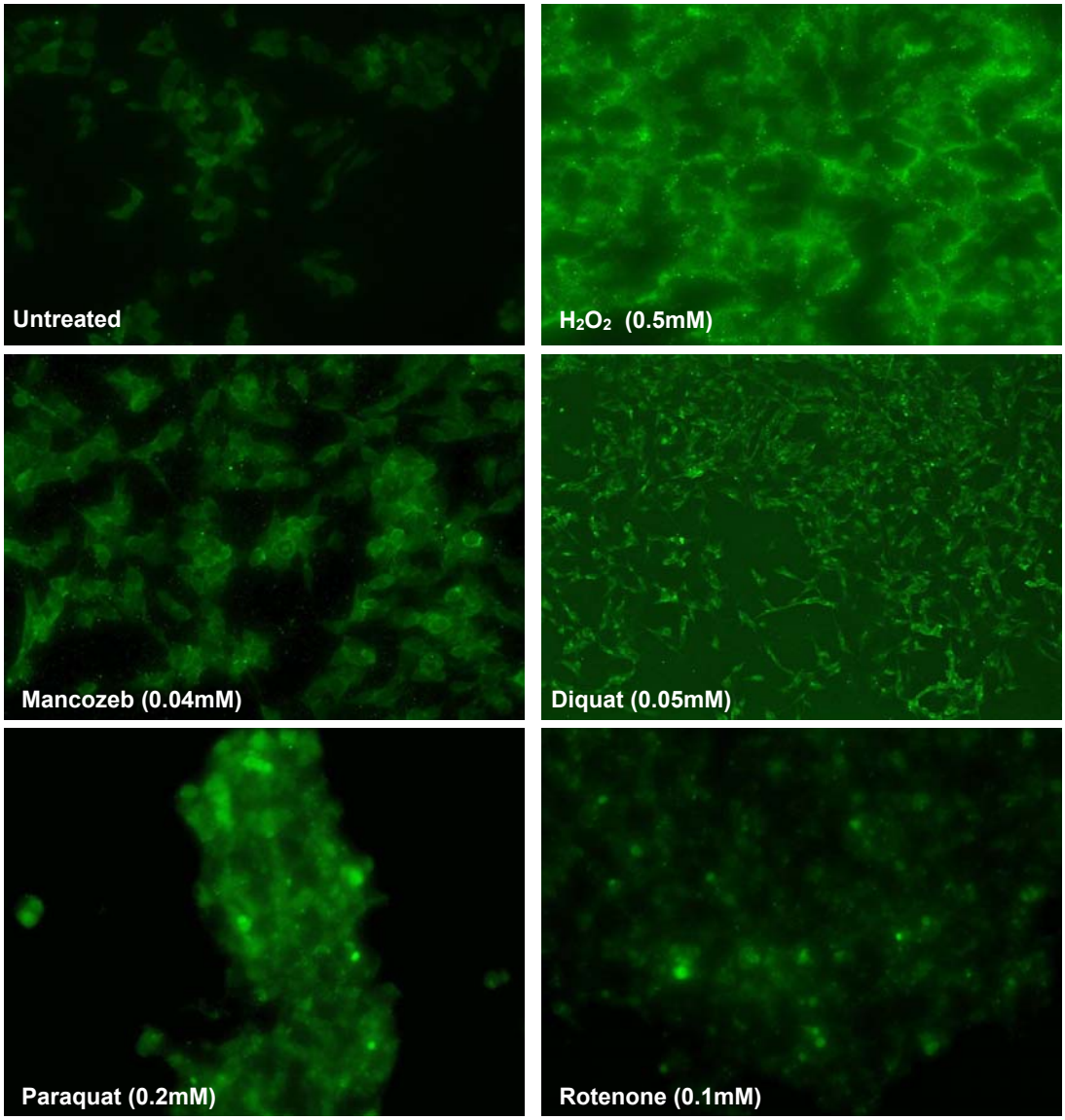

3.1.3.8 Effect of Antioxidants on toxin induced SH-SY5Y cell death:

Antioxidant molecules N-acetyl-L-cysteine (NAC), tiron, MnTBAP and MnTMPyP were tested for their ability to inhibit SH-SY5Y cell death. NAC is a free radical scavenger due to its thiol group and indirectly enhances the glutathione synthesis, which in turn reduces oxidative stress (Martinez *et al*., 1999). Co-incubation of NAC (5mM) caused a significant recovery in diquat (0.1mM) (+24.6±5), maneb (0.04mM) (+24.6±19.6) and mancozeb (0.04mM) (+48.6±14.1) treated cells. A minor statistically insignificant increase in viability was observed in fluroxypyr methyl ester (0.1mM). No NAC related recovery was recorded in epoxiconazole (0.08mM), MPP+ (1mM), or mecoprop methyl ester (0.1mM) treated cells. Tiron, (4,5-dihydroxy-1,3-benzene disulfonic acid) is an antioxidant and protects against ROS-induced cell death where it can act as a non-toxic chelator of intracellular iron to alleviate an acute metal overload. Tiron failed to reduce toxicity in diquat (0.1mM), MPP+ (1mM), mecoprop methyl ester (0.1mM) and mancozeb (0.04mM) treated cells and showed a marginal increase in viability (not statistically significant) in fluroxypyr methyl ester (0.1mM) and maneb (0.025mM) treated cells, however replication of assay failed to repeat this. When co-incubated with diquat (0.1mM), it significantly potentiated its toxicity. Both MnTBAP and MnTMPyP (SOD mimetics) act as antioxidants. Co-incubation with these chemicals showed no significant increase in cell viability.

3.1.3.9 Measurement of mitochondrial transmembrane potential:

Pathological conditions like ATP depletion, oxidative stress and Ca^{2+} can disrupt mitochondrial transmembrane potential ($\Delta\Psi_{m,}$ MTP; Škárka & Oštadál, 2002). It is conceivable that some of these toxins can decrease MTP, given that an increase in ROS generation has been observed. Experiments designed to measure MTP at different time points showed that diquat (0.15mM) significantly depolarised MTP in a time dependent manner (up to 50% of control after 4 hours) (fig 3.28). This is consistent with data gathered from Alamar blue reduction assay where a colour change implicating reduced mitochondrial activity can be observed within 6 hours of diquat treatment (reduction down to almost 50% after 6 hours). Chemicals known to affect MTP such as rotenone and MPP+ (Isenberg and Klaunig, 2000; Lee *et al*., 2005) when used at 0.0125mM and 1mM respectively, caused a significant gradual

reduction in TMRE fluorescence after 4 hours (fig 3.29). Carbonyl cyanide-(trifluoromethoxy) phenylhydrazone (FCCP) (0.05mM), a mitochondrial protonophore, was used as a positive control for each experiment where it successfully dissipated MTP. Similar results were seen with H_2O_2 (0.5mM). Other toxins including MPTP (1mM) (fig 3.29), paraquat (0.1mM), maneb (0.05mM), mancozeb (0.05mM) (fig 3.30), fluroxypyr methyl ester (0.1mM) and epoxiconazole (0.1mM) (fig 3.31) had no significant effect on MTP.

Fig 3.28: Toxin-induced changes of mitochondrial membrane potential ($\Delta\Psi_m$) in SH-SY5Y cells: TMRE fluorescence in cells exposed to H_2O_2 (0.5mM) and diquat (0.15mM) (A-B) for 24 hours. (n=3, data expressed as mean % of untreated control ± SD (* *P<0.05* accepted as significant*)*.

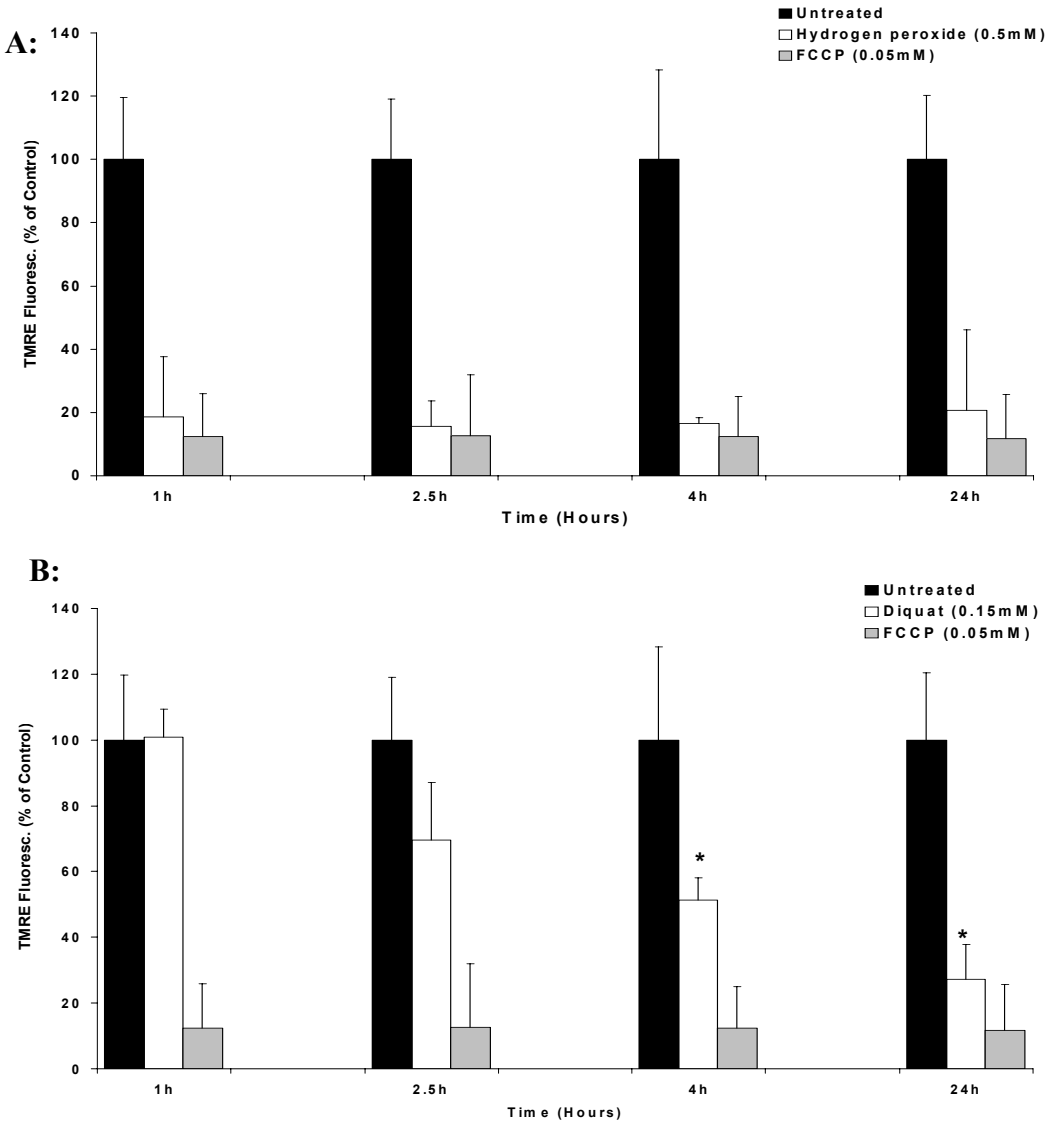

Fig 3.29: Toxin-induced changes of mitochondrial membrane potential ($\Delta\Psi_m$) in SH-SY5Y cells: TMRE (250nM) fluorescence in cells exposed to rotenone (0.0125mM), MPP+ (1mM) and MPTP (1mM) (A-C) for 24 hours. (n=3, data expressed as mean % of untreated control ± SD (* *P<0.05* accepted as significant*)*.

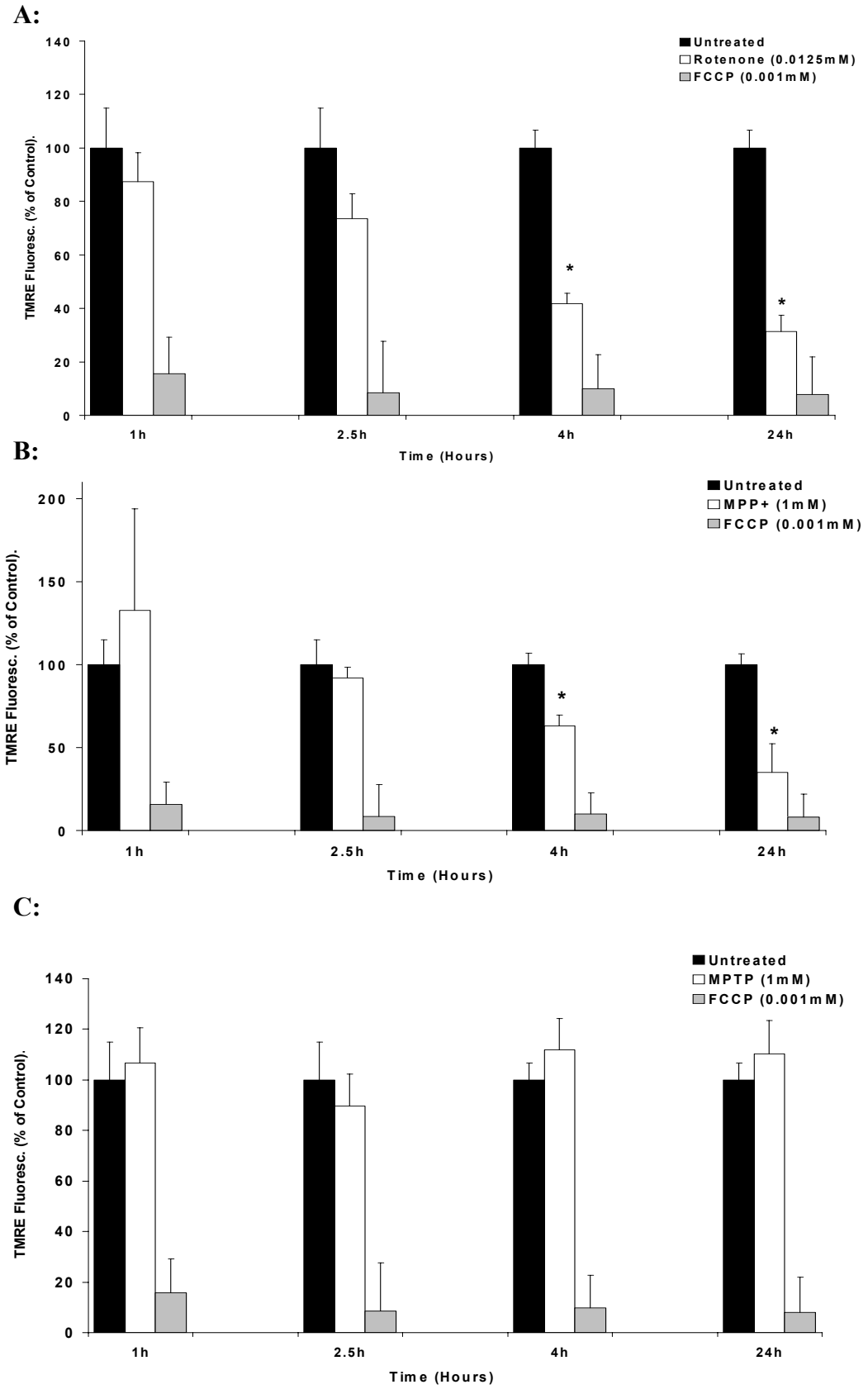

Fig 3.30: Toxin-induced changes of mitochondrial membrane potential ($\Delta\Psi_m$) in SH-SY5Y cells: TMRE fluorescence in cells exposed to paraquat (0.1mM), maneb (0.05mM) and mancozeb (0.05mM) (A-C) for 24 hours. (n=3, data expressed as mean % of untreated control ± SD (* *P<0.05* accepted as significant*)*.

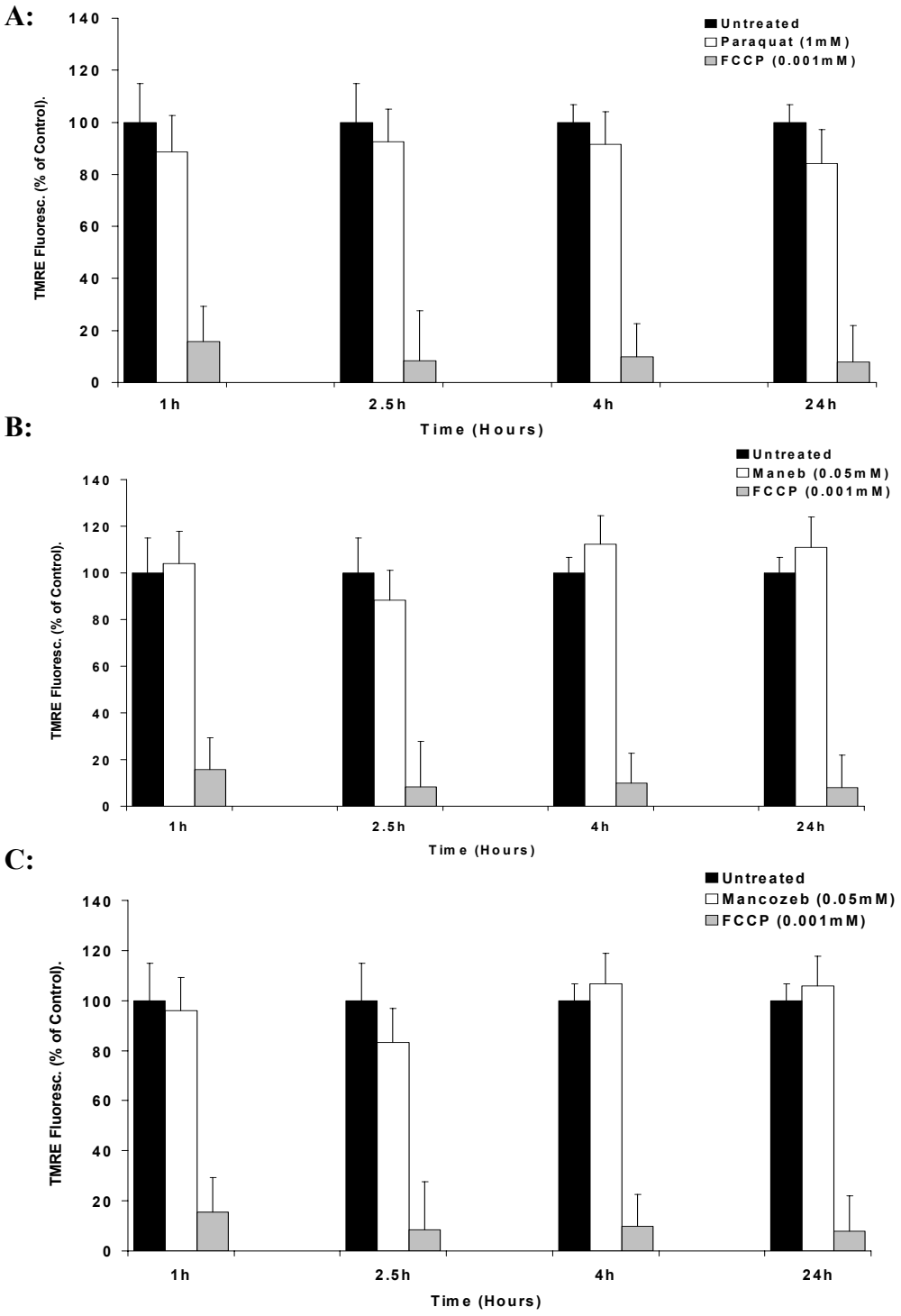

Fig 3.29: Toxin-induced changes of mitochondrial membrane potential ($\Delta\Psi_m$) in SH-SY5Y cells: TMRE (250nM) fluorescence in cells exposed to fluroxypyr methyl ester (0.1mM) and epoxiconazole (0.1mM) (A-B) for 24 hours. (n=3, data expressed as mean % of untreated control ± SD (* *P<0.05* accepted as significant*).*

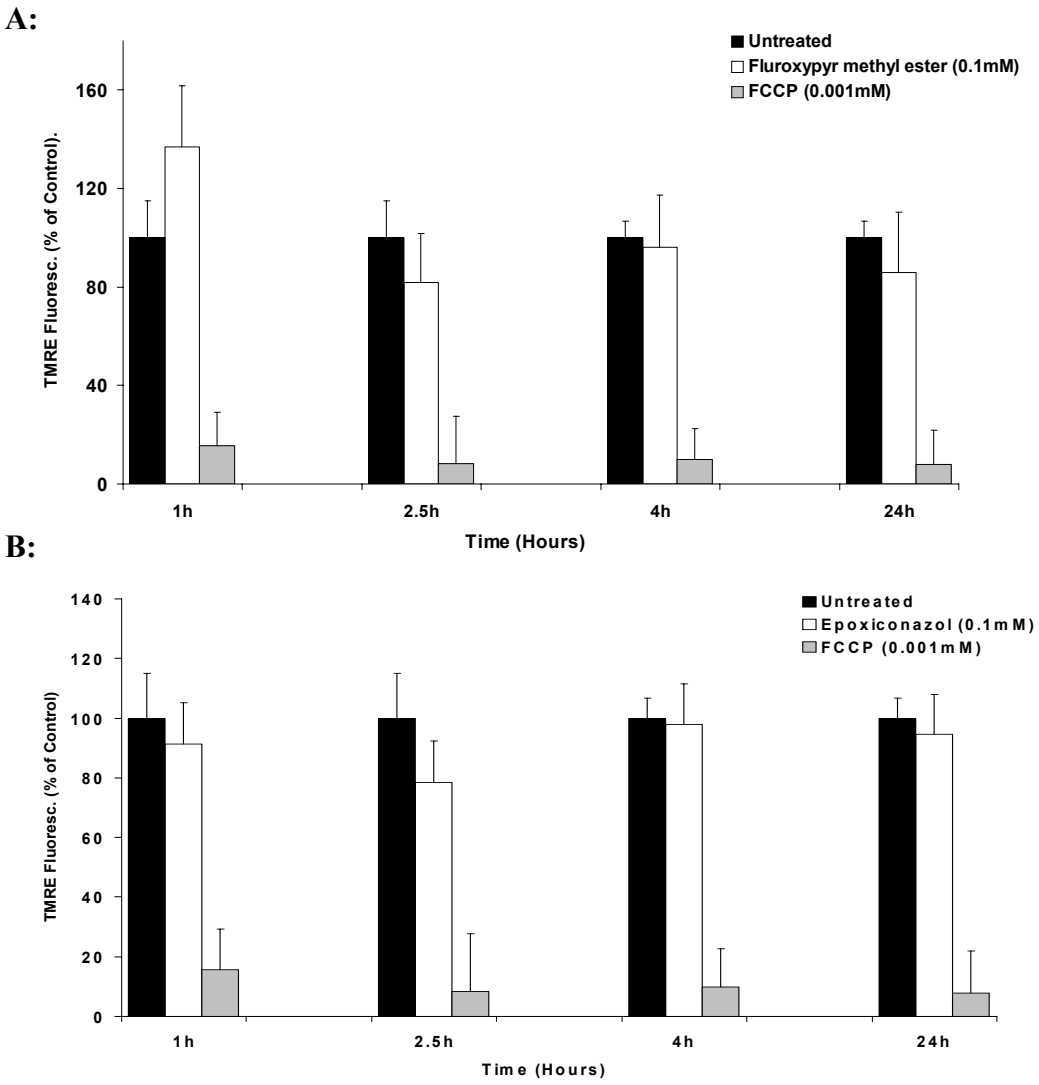

3.1.4 Discussion:

The first goal of this study was to determine the optimised conditions i.e. culture medium, cell-density and total dosage of toxins for evaluation of cytotoxicity in SH-SY5Y cells. Cell viability data, gathered from 24 hour exposure, showed a dose-dependent response. Most chemicals were of low toxicity using the SH-SY5Y system. However, significant toxicity was observed at concentrations as low as 0.01mM (Maneb, Mancozeb) and 0.1mM (diquat, epoxiconazole, fluroxypyr-ester, mecoprop-methyl ester and zineb). Chemicals known (MPTP or MPP+) or thought to be involved with PD (paraquat) showed modest toxicity. This investigation has allowed us to establish sub-cytotoxic concentrations for each chemical. These doses were used to examine toxin effects at the cellular level, their mode of action, involvement of cell-signalling and cell-death pathways (i.e. apoptosis, necrosis, necroptosis), mediation of intracellular signalling processes, loss of mitochondrial membrane potential, activation of caspases and if they have any possible role in PD.

Previous studies have shown that expression of dopamine D2 receptor (D2R), tyrosine hydroxylase (TH), dopamine transporter (DAT) and dopamine β-hydroxylase (DβH) can be higher in differentiated cells. Such change in protein expression was not observed in cells differentiated for 7 days (see fig 3.13). It was noticed that once induced to differentiate; cell number increased in a linear manner for the first 4-5 days and then reached a plateau. After 7 days cell division rate decreased and cells had more rounded cell bodies and neuritic extensions emanating from cells were almost double that of undifferentiated cells. It has been reported that differentiated cells show much stronger resistance against drug treatment than undifferentiated SH-SY5Y cells (Presgraves *et al*., 2004). Considering dopaminergic neurons are fully differentiated in adult humans, these toxins might be less toxic in differentiated SH-SY5Y cells than in undifferentiated SH-SY5Y cells but results from this study showed no significant difference in toxicity in differentiated or undifferentiated SH-SY5Y cells (see fig 3.11, 3.12).

Previous studies have shown that DAT and DA receptors are expressed in SH-SY5Y cells (Presgraves *et al*., 2004) and DAT facilitates dopamine uptake into the presynaptic neurons (Lee *et al*., 2000). Experiments aiming to block this transport

pathway to reduce the loss of cell-viability failed to show that inhibition of dopamine transporter alleviates toxicity of these chemicals (see fig 3.14, 3.15). This included MPP+ and dopamine which are selectively uptaken by DAT (Gainetdinov *et al*., 1997; Javitch *et al*., 1985). Immunohistochemical staining and western blotting has shown DAT expression in these cells (fig 3.10, 3.13). Lower DAT expression could be one reason why its inhibition cannot prevent toxicity and toxicity could be mediated through non-DAT mechanisms. For instance, previous studies have suggested that a neutral amino acid transporter, most likely the system L carrier (LAT-1) may specifically transport paraquat into the brain (Shimizu *et al*., 2001) and pre-treatment of mice with a LAT-1 substrate (L-valine) prevented the dopaminergic toxicity of paraquat (McCormack and Di Monte, 2003).

Pharmacological inhibition of apoptosis showed a marginal but insignificant reduction in toxicity for most chemicals (see fig 3.18, 3.19, 3.20) whereas a macroautophagy inhibitor had no effect at all. An overlap between these two processes has been proposed (Zakeri *et al*., 1995) and 3-methyladenine (3-MA) has been used to block drug-induced apoptosis and autophagy (Kundu & Thompson, 2005). In primary dopaminergic neurons or cell lines, caspase inhibitors have shown protection against MPP+ toxicity but such effects could be temporary and can switch from apoptosis to necrosis (Choi *et al*., 1999). Indeed toxicity caused by staurosporine, an apoptosis initiator under certain conditions, can be blocked by caspase-independent inhibition (Zhang *et al*., 2004). Staurosporine can activate Bax and act through the mitochondrial caspase-dependent apoptotic pathway. The caspase-dependent apoptotic pathway is activated soon after staurosporine exposure and leads to the release of cytochrome c and Smac/DIABLO from mitochondria and cleavage of poly (ADP-ribose) polymerase (Zhang *et al*., 2004). Previous studies have shown that this pathway can be inhibited by broad caspase inhibitors. Results from this study failed to show this. However, involvement of caspase-independent mechanisms associated with staurosporine suggests that multiple mechanisms may be involved. Reduced staurosporine induced cytotoxicity by Nec-1 therefore suggests protection through non-apoptotic mechanism. Indeed, previous studies have shown that apoptotic stimuli such as CD95-L or TNF cause necrotic cell-death (Edinger and Thompson, 2004; Festjens *et al*., 2006). Alternatively, morphological changes associated with apoptosis may occur during caspase-independent cell death

(Lockshin and Zakeri, 2004a) suggesting some kind of inter-connection. Furthermore, caspase-3 and 9 inhibitors failed to reduce toxicity suggesting involvement of non-mitochondrial directed pathway since caspase-3 is a downstream target of caspase-9 which is involved in the mitochondria-initiated pathway of apoptotic cell death.

Involvement of non-apoptotic mechanisms sheds light on necrostatins which act through a regulated cellular necrosis mechanism different from apoptosis. Activity of RIP1 kinase, a death-domain-containing kinase, is needed for necroptosis activation (Holler *et al*., 2000) and Nec-1 is an allosteric inhibitor of RIP1 kinase (Degterev *et al*., 2008). RIP1 is required for the initiation of necrotic cell death and is proposed to have a role in caspase-independent necrotic cell death (Lin *et al*., 2004). RIP1 is part of a signalling complex comprised of TNF-R1-associated death domain protein (TRADD), small GTPase Rac1 and Nox1 (NADPH oxidase). RIP1 recruits Nox1 to the signalling complex when necrosis is initiated. RIP1 deficient cells do not form this complex (Kim *et al*., 2007). NADPH oxidase enzymes actively play a role in the production of ROS (Lambeth, 2004). RIP interacts with TNF receptor-associated factor 2 (TRAF2) which can recruit IKK (IkB kinase). Presence of RIP is required for the activation of IKKs (Devin *et al*., 2000). Down-stream effects of these interactions lead to the activation of MAP kinase and NF-kB pathways (Chen and Goeddel, 2002; Wajant *et al*., 2003). In this study, most toxins responded to Nec-1 suggesting the unique nature of Nec-1 activity and regulation of necroptosis. Although the mechanism(s) underlying the protective action of Nec-1 is currently unknown, it is likely that it directly interacts with cellular events leading to cell death after oxidative stress.

A range of different cell-signalling inhibitors were used to evaluate the contribution of adenylate cyclase, protein kinase C, phosphatidylinositol- 3 kinase (PI3K), mitogen-activated protein kinase (MAPK) and c-Jun N-terminal kinases (JNK) to the toxin induced cell-death. Inhibitors like GW5074, LY29002, PD98059, SQ22536, SP600125 and U0126 further potentiated toxicity. A number of signal transduction pathways converge on MEK/ERK. Therefore, to determine whether toxins interacted with the MEK/ERK signalling pathway, we tested the involvement of signalling kinases Ras and Raf by using specific inhibitors for these kinases

(GW5074 for Raf inhibition and PD98059/U0126 for MEK Inhibition). Inhibition of these pathways did not reduce toxicity and in some cases made it significantly worse (e.g. PD98059 potentiated epoxiconazole, FMH, maneb and MPP+ toxicity; GW5074 increased toxicity of diquat, epoxiconazole, FMH, MPP+ and mancozeb; U0126 increased toxicity of epoxiconazole, FMH, maneb, mancozeb, MPP+ and mecoprop methyl ester). Using two inhibitors of MEK activity show that MEK activity is not required for toxin-potentiated cell-death but may be involved in protective mechanisms.

Tunicamycin has been used to study pathways involved in the endoplasmic reticulum stress-induced cell death in SH-SY5Y cells (Oda *et al*., 2008). ER triggers cell apoptosis when cell comes under stress leading to excessive protein misfolding (Patil and Walter, 2001). Results from this study show that tunicamycin pre-treatment causes significant reduction in diquat treated cells but it potentiates toxicity for all other chemicals. Some chemicals cause apoptosis or necrosis by rupturing lysosomes in a time and dose-dependent way (Li *et al*., 2003). It is suggested lysosomal rupture may set off a cascade of events activating pro-apoptotic proteins, releasing cytochrome c and inducing oxidative stress. These factors can rupture lysosomes, damage mitochondria and activate caspase (Roberg 2001; Roberg *et al*., 1999). Treatment with ammonium chloride can raise lysosomal pH and can prevent chemical uptake by proton trapping. When pre-treated with ammonium chloride and treated with selected chemicals, a slight reduction in toxicity was noticed (not significant).

The role of oxidative stress in toxin-induced cell death was evaluated by the use of different antioxidants including N-acetyl-L-cysteine (NAC), tiron, MnTBAP and MnTMPyP. Antioxidant NAC prevented the loss of cell viability caused by diquat, maneb and mancozeb and caused marginal increase in viability in fluroxypyr ester treated cells. NAC enhances glutathione synthesis and if glutathione metabolism is compromised hydrogen peroxide is converted to toxic hydroxyl radicals (Niesink *et al*., 1996). Indeed, glutathione depletion potentiates MPTP and MPP+ toxicity in nigral dopaminergic neurones (Wullner *et al*., 1996). SOD mimetics MnTBAP and MnTMPyP on the other hand, prevent the formation of the more toxic peroxynitrite together with nitric oxide by detoxifying superoxide. SOD

can alleviate chemical induced toxicity and over-expression of SOD in transgenic mice provides resistance to MPTP toxicity (Przedborski *et al*., 1992). This study suggests that these selected agrochemicals act by increasing oxidative stress as anti-oxidant NAC prevented toxin-mediated cell-death. Mitochondrial dysfunction also plays a part as observed through dissipation of mitochondrial transmembrane potential and Alamar blue reduction. It remains to be determined if mitochondrial dysfunction and oxidative stress interact in a pathologically reinforcing cycle or if one is a result or cause of the other. Neurotoxic effects by different toxins are mediated partly through intracellular events. Determination of free radical species that are generated by these toxins delineating the cell-signalling pathways responsible for DA cell death would be significant aspects in future studies.

Oxidative damage has been identified as contributing to dopaminergic cell death in MPTP model and PD. Increases in markers of oxidative stress have been noted in PD substantia nigra and other brain regions (Jenner, 1998). Mitochondrial damage and oxidative stress are inter-related. Impairment of oxidative phosphorylation in mitochondria contributes to the production of oxygen radicals. Toxins such as MPP+ and rotenone contribute to oxidative stress and various radical-scavenging agents such as dihydrolipoic acid and nicotinamide can counter MPP+ toxicity in cell culture or of MPTP *in vivo* (Seaton *et al*., 1997). ROS generation is involved in the mechanism of toxicity of various chemicals and these experiments have successfully shown a rapid increase in ROS production which is proportional to the cell-viability data gathered from Alamar blue reduction assays. These results when taken with the measurement of mitochondrial transmembrane potential suggest that ROS generation occurs before complete mitochondrial dissipation. It has been suggested that the opening of mitochondrial transition pore (MTP) is one of the initiating events in cellular apoptosis (Zamzami *et al*., 1996) and the immunosuppressant cyclosporin A (CSA) can inhibit this opening through binding to mitochondrial matrix cyclophilin (Zoratti and Szabo, 1995) therefore interfering with apoptosis and the reducing the mitochondrial permeability dissipation that precedes apoptosis. Pre-treatment of SH-SY5Y cells did not show any protective effect and in fact potentiated the toxicity. This effect has been observed by Fall et al (1998) who noticed that CSA potentiated MPP+ induced apoptosis. Hydrogen peroxide, rotenone, diquat and MPP+ results from both experiments showed a directly

proportional relationship between ROS generation and disruption of the MTP whereas a lack of dissipation of MTP is seen with maneb, mancozeb, epoxiconazole and fluroxypyr methyl ester at shorter exposure. Mitochondrial dysfunction has been linked with cytochrome c release which in turn leads to the activation of caspase-3 and caspase-9, which are associated with neuronal apoptosis during brain development and in delayed neuronal cell-death after brain injury in the developing and adult brains (Krajewski *et al*., 1999). Lack of change in MTP and failure to block cell death by caspase inhibitors suggests a mode of death not involving mitochondrial pathway.

Diquat

Among tested compounds, diquat (a potent redox cycler and ROS generator) was most responsive to different inhibitors. Nec-1, NAC, tunicamycin and SQ22536 significantly prevented the loss of cell-viability. These patterns could be due to necroptosis inhibition, abolition of ROS generation capacity or early scavenging of ROS. Given that ROS-mediated oxidative damage is a prominent feature of dopaminergic pathogenesis (Cohen, 1986); current data suggest that diquat may induce oxidative stress in dopaminergic neurons through the production of ROS. Intracellularly, diquat undergoes redox cycling, producing superoxide anions. This reaction takes place in the presence of NADPH and cytochrome P450 reductase and the resultant highly unstable diquat radical transfers an electron to molecular oxygen to form a superoxide anion radical (Saeed *et al*., 2001). This continuous oxidation and reduction of diquat results in superoxide anion radicals reacting with each other and producing molecular oxygen and hydrogen peroxide. This reaction may be facilitated by superoxide dismutase or may occur spontaneously (Jones & Vale, 2000). Under normal circumstances, glutathione peroxidase and catalase detoxify hydrogen peroxide, but if these are compromised or overwhelmed then they may lead to the formation of highly reactive hydroxyl radical which can attack the lipid chains of biological membranes causing lipid peroxidation and cell death (Niesink *et al*., 1996). NADPH depletion may also play a role in toxicity, as hydrogen peroxide detoxification and redox cycling are NADPH dependent (Saeed *et al*., 2001).

SQ22536 (adenylyl cyclase inhibitor) prevented the loss of cell viability caused by diquat. Since SQ22536 is used as an inhibitor of the cAMP pathway and

successfully used in studies to inhibit increases in cAMP (Gao and Raj, 2001), it may provide useful insight into cAMP-dependent signalling, which has been linked with the control of cellular cascades in mammalian cells. It is involved not just with adenylyl cyclase but with other signalling pathway components including G proteins and protein kinase A (Fabbri and Capuzzo, 2010). There is evidence that Parkinson's disease course also affects the DA-dependent cAMP system (Cash *et al*., 1987) and an imbalance in cAMP may play a part in changes of levodopa/dopamine signal transduction. This may have an effect on PD pathology as dysregulation of DA receptors has been linked with levodopa-induced dyskinesias in experimental PD models (Giorgi *et al*., 2008).

Mancozeb/Maneb

Dithiocarbamates (DTCs) have been linked with several extrapyramidal syndromes (Meco *et al*., 1994) and a variety of neurobehavioral abnormalities (hind limb paralysis, convulsions, ataxia, hemiparesis) (Vaccari *et al*., 1999), affecting both glutamate and DA systems (Barlow *et al*., 2005). DTCs are believed to exert their toxicity through dopamine catalysation and oxidative stress caused after metal chelation (Drechsel & Patel, 2008). Details about maneb's mode of neurotoxicity are though unclear. It can inhibit glutamate transport, interfere with DA uptake and release (Vaccari *et al*., 1998) and potently inhibit complex III of the electron transport chain (activity reduced to 20% of controls) in a dose dependent manner in rats. 1 hour maneb exposure can also cause a 50% reduction in ATP levels suggesting a possible inhibition of energy metabolism and mitochondrial respiration (Domico *et al*., 2006). Like MPP+, maneb causes striatal dopamine influx (Zhang *et al*., 2003). Similarly, mancozeb affects energy metabolism and inhibits ATP at exposure times that precede toxicity. Both are toxic to *in vitro* DAergic and GABAergic cell populations, act as inhibitory uncouplers, uncouple and inhibit respiration at low doses, completely inhibit respiration at high doses (30mM) and cause a dose-dependent reduction in TH-positive cell number along with decrease in neurite length (Domico *et al*., 2006).

Several *in vivo* and *in vitro* studies have documented toxic effects caused by mancozeb. Baligar and Kaliwal (2004) investigated the effects of mancozeb treatment on ovarian follicular development and found organ-specific biochemical

changes and disruption of oestrous cycle. Shukla et al (2004) evaluated the mutagenic potential of mancozeb and noticed a dose-dependent rise in revertant number. While investigating genotoxic and pro-apoptotic effects of mancozeb in isolated peripheral blood mononucleated cells and cultured fibroblasts of rats, Calviello et al (2006) observed dose-dependent strand breaks and increased ROS production. Pre-treatment with an antioxidant reduced formation of DNA adducts and ROS production. Mills *e*t al (2005) reported a statistically significant increase in leukaemia in workers exposed to agricultural mancozeb.

Results from this study are consistent with previous studies investigating the toxic potential of organic and metal components of mancozeb and maneb. EBDC fungicides share a common backbone and only the addition of a metal ion gives it a characteristic identity (Domico *et al*., 2006). Mancozeb contains manganese and zinc ions and it is slightly more toxic than maneb suggesting that the organic moiety and the ionic components produce its toxic effects. Zineb's structure is identical to maneb except it has a zinc ion instead of manganese but it is significantly less toxic than maneb causing 40% cell death at 0.1mM compared with 90% caused by maneb with same dose. Nabam, containing the organic backbone is only toxic at 1mM dose and caused no cell death at 0.1mM. This suggests that manganese component of mancozeb acts as 'cytotoxicity inducing portion' of the chemical. Vaccari et al (1999) have shown that mancozeb inhibits glutamate uptake more potently than zinc containing ethylene bis-dithiocarbamate zineb. The true extent of the involvement of either component cannot be determined from these data. For instance it is not clear if the metal ions are detached from the organic backbone to cause toxicity or they remain attached. This may be worth investigating as manganese itself is a neurotoxin, causing oxidative stress which leads to cell death in glial and neuronal cell-lines (Dukhande *et al*., 2006) and can contribute to an extrapyramidal syndrome that shows some PD features (Calne, 1994). High level manganese exposure may lead to manganism with features similar to PD but it mainly damages the pallidum and striatum rather than SN as seen in PD (Dobson *et al*., 2004; Levy and Nassetta, 2003). Although the molecular and cellular mechanisms of manganese toxicity are not clear, it is suggested that it exerts its effects through ROS generation (either direct or indirect) (Ali *et al*., 1995), disrupts iron and Ca^{+2} homeostasis (Gavin *et al*., 1990; Zheng and Zhao, 2001), causes direct oxidation of biological molecules like

dopamine (Archibald and Tyree, 1987), accumulates in mitochondria and generates ROS through disruption of oxidative phosphorylation (Gunter *et al*., 2006). Results from this study suggest that maneb and mancozeb lead to the formation of ROS without primarily targeting mitochondria and do not exhibit signs of causing cell death through apoptosis as noted through caspase-inhibition.

Epoxiconazole

Epoxiconazole, a triazole fungicide widely used in different fruit crops and cereals (Grote *et al*., 2008), has a very high rate of absorption, metabolism and excretion. Its single low dose has a plasma half life of 5 hours compared with 30 hours for its single high dose. Its metabolites, about 30 of which have been identified, can be detected in bile, urine and faeces, whereas epoxiconazole itself has only been detected in faeces when used at a high single dose. Epoxiconazole caused 40-50% reduction in cytotoxicity at 0.1mM but showed no evidence of mitochondrial transmembrane potential dissipation. Caspase inhibition with zVAD.fmk caused marginal but insignificant reduction in toxicity but pre-incubation with cell-signalling inhibitors like GW5074, LY29002 and SQ22536 failed to significantly attenuate or potentiate its toxicity. Nec-1 treatment as with other toxins successfully inhibited cell death and cell-viability measured after 24 hours was at the same level as untreated cells suggesting that epoxiconazole causes programmed necrosis possibly by glutathione depletion.

Epoxiconazole inhibits ergosterol biosynthesis and disrupts fungal cell membrane synthesis but shows no mutagenic potential. Acute and subchronic studies have shown no evidence of significant neurotoxicity (EPA, 2006). Studies investigating endocrine disrupting activities of epoxiconazole in rats have suggested that epoxiconazole exerted its effect by disrupting enzymes involved in steroid hormone synthesis (Taxvig *et al*., 2007). They noticed elevation in progesterone and 17a-hydroxyprogesterone levels suggesting that this class of fungicides may target lyase function of CYP17. Indeed, *in vitro* studies in cultured human, rat and pig cells have shown that epoxiconazole inhibited aromatase and 17-hydroxylase activity, thus inhibiting androstenedione to estrogen conversion and cortisol production,

respectively. Testosterone imbalance can be induced in rats after epoxiconazole dosage (Goetz *et al*., 2007).

Fluroxypyr methylheptyl ester:

Fluroxypyr methylheptyl ester (FPMH), a pyridinecarboxylic acid herbicide, is manufactured from fluroxypyr methyl ester (FPM) (Hewitt *et al*., 2000). It is highly lipophilic and once inside the target crop, it is non-enzymatically hydrolysed into fluroxypyr (Lehmann *et al.,* 1993). Lehmann et al (1991) have shown that fluroxypyr is degraded in soil. They observed a reduction of 60% of applied chemical after 60 days and only its metabolite methoxypyridine remained after 366 days. Methoxypyridine was not uptaken by the plants and showed no adverse effects in the soil. Hewitt et al (2000) have shown complete metabolism of both FPM and FPMH when passed through human and rat skin *in vitro*. Other in vivo studies have reported FP in faeces and urine after intravenous FPMH administration. FPMH caused 80-90% reduction in cytotoxicity at 0.1mM but showed no evidence of mitochondrial transmembrane potential dissipation. Like epoxiconazole, caspase inhibition with zVAD.fmk caused marginal but insignificant reduction in toxicity but pre-incubation with cell-signalling inhibitors like GW5074, LY29002 and SQ22536 did not attenuate or potentiate its toxicity. Nec-1 treatment as with other toxins successfully inhibited cell-death. Evidence of FPMH toxicity is limited as shown by Carney et al (1995) who assessed the maternal and developmental toxicity potential of FPMH in rats and found no evidence of developmental toxicity at 100-300mg/kg/day dose, though higher doses in foetuses showed skeletal variations.

In summary, results from this study suggest that these agrochemicals (except diquat) lead to the formation of ROS without primarily targeting mitochondria and do not exhibit signs of cell death through apoptosis as noted through caspase-inhibition. Prevention of cell death with Nec-1 suggests involvement of necroptosis through non-caspase related mechanism but shows features of both necrosis and apoptosis primarily involving the Fas/TNFα receptors and activation of RIP1. Diquat successfully responded to Nec-1 and zVAD.fmk (statistically insignificant), generated ROS and caused a reduction in mitochondrial transmembrane permeability suggesting its acts through mitochondria and involves both necrosis and apoptosis.

Chapter Four: Intracellular protein expression in toxin treated SH-SY5Y cells

4.1.1 Introduction:

Understanding the molecular mechanisms of cell-death continues to be an important area of investigation in PD pathology. Extensive evidence indicates that apoptosis is associated with neurodegenerative diseases such as Alzheimer's disease, Parkinson's disease and Huntington's disease (Honig & Rosenberg, 2000; Mattson, 2006). Biomarkers of apoptosis such as p53 up-regulation, p53 and Bax activation (de la Monte *et al*., 1998; Tatton, 2000), caspase 3 and 9 activation (Andersen, 2001) and DNA fragmentation (Mochizuki *et al*., 1997; Tatton *et al*., 1998) have been reported in dopaminergic neurons of PD patients but the overall mechanisms causing dopaminergic cell-death are poorly understood.

Although several PD features in animal and cell culture models have been reproduced by using PD linked toxins such as rotenone, paraquat and MPTP. Their molecular mechanisms of action are well known e.g. paraquat does not act through DAT or inhibit complex I (Richardson *et al*., 2005) and activates caspase-3 whereas rotenone and MPP+ do not activate caspase-3 (Ramachandiran *et al*., 2007). Rotenone induces cell-death through caspase-independent pathway in undifferentiated cells but through caspase-dependent pathway in differentiated cells (Li *et al*., 2005). Paraquat can cause oxidative stress in dopaminergic neurons of mice (McCormack *et al*., 2005) through mitochondria-linked apoptosis, p53 induction (Ueda *et al*., 2002) and by causing an increase in p53 levels (Takeyama *et al*., 2004).

4.1.1.1 Aims:

The level of protein expression and therefore the mode of cell-death depends on the nature of neurotoxic insult. The aim of this study was to investigate changes in the levels of protein expression and distribution after acute and chronic toxin treatment in SH-SY5Y cells. In order to investigate the mechanism underlying agrochemical-induced toxicity, protein expression of PARP-1, caspase-3, cytochrome c, RIP, p53, α-synuclein, DJ-1 and tyrosine hydroxylase amongst others was examined. Immunocytochemical techniques were used to view changes in

nuclear structure and distribution of PARP-1, RIP, α-synuclein, DJ-1, tyrosine hydroxylase and neurofilaments.

4.1.2 Methods:

Refer to materials and methods (section 2.2).

4.1.3 Results:

4.1.3.1 Changes in protein expression after acute toxin exposure:

4.1.3.1.1 PARP-1, Cytochrome c:

Certain features of neurones including their longevity, post-mitotic phenotype, structure and synapses make them vulnerable to toxic insult. Since neurones have a limited regenerative capacity, they are at increased risk to toxicants which gradually accumulate in the cells. Neurons are frequently larger than other cells and depend on synapses for information transfer between neighbouring cells therefore agents interfering with protein or organelle transport or synaptic function can lead to neuronal apoptosis (Gibson, 1999).

A range of different apoptotic markers can be detected after toxin treatment. Their absence, presence or cleavage hints towards the mode of cell-death. For example, poly (ADP-ribose) polymerase (PARP-1, 116 kDa) is a nuclear enzyme involved in DNA repair in response to cellular stress (Satoh and Lindahl, 1992). ICE-like caspases (Interleukin 1b-converting enzyme) especially caspase-3 cleave PARP-1 (Lazebnik *et al*., 1994) which occurs between Asp214 and Gly215 in humans forming a carboxy-terminal catalytic domain (89 kDa) and amino-terminal DNA binding domain (24 kDa) (Nicholson *et al*., 1995). By using an antibody which recognised the 89 kDa cleaved fragment and not the full-length or other isoforms, toxic treatment with maneb (at 0.01mM, 0.1mM and 0.001mM) and mancozeb (at 0.001mM, and 0.1mM) showed PARP-1 cleavage (fig 4.1, 4.3 A-C. 4.4 A-C). Nuclear condensation, chromatin condensation, DNA cleavage and nuclear fragmentation are commonly observed during apoptosis (Buja *et al*., 1993). Nuclear chromatin was uniformly dispersed throughout control cells whereas hyper-intense chromatin staining of treated cells was suggestive of apoptotic features. A higher number of condensed inter-nuclear fragments were visualised after 24 hour H_2O_2

(0.1mM), rotenone (0.05mM), mancozeb (0.05mM), maneb (0.05mM) and diquat (0.05mM) treatment (fig 4.2). A relatively lower number of condensed inter-nuclear fragments were visualised after fluroxypyr methyl ester (0.05mM) and epoxiconazole (0.05mM) (data not shown).

Fig 4.1: Visual presentation of cleaved PARP-1 in toxin treated cells: A significantly higher number of cleaved-PARP-1 positive cells (green) were visualised after 24 hour diquat (0.05mM), rotenone (0.05mM), mancozeb (0.05mM), maneb (0.05mM) and MPP+ (1mM) treatment (Each image representative of 3 different fields. Magnification is x40 for untreated, diquat and maneb treated cells, x10 for rotenone, mancozeb and MPP+).

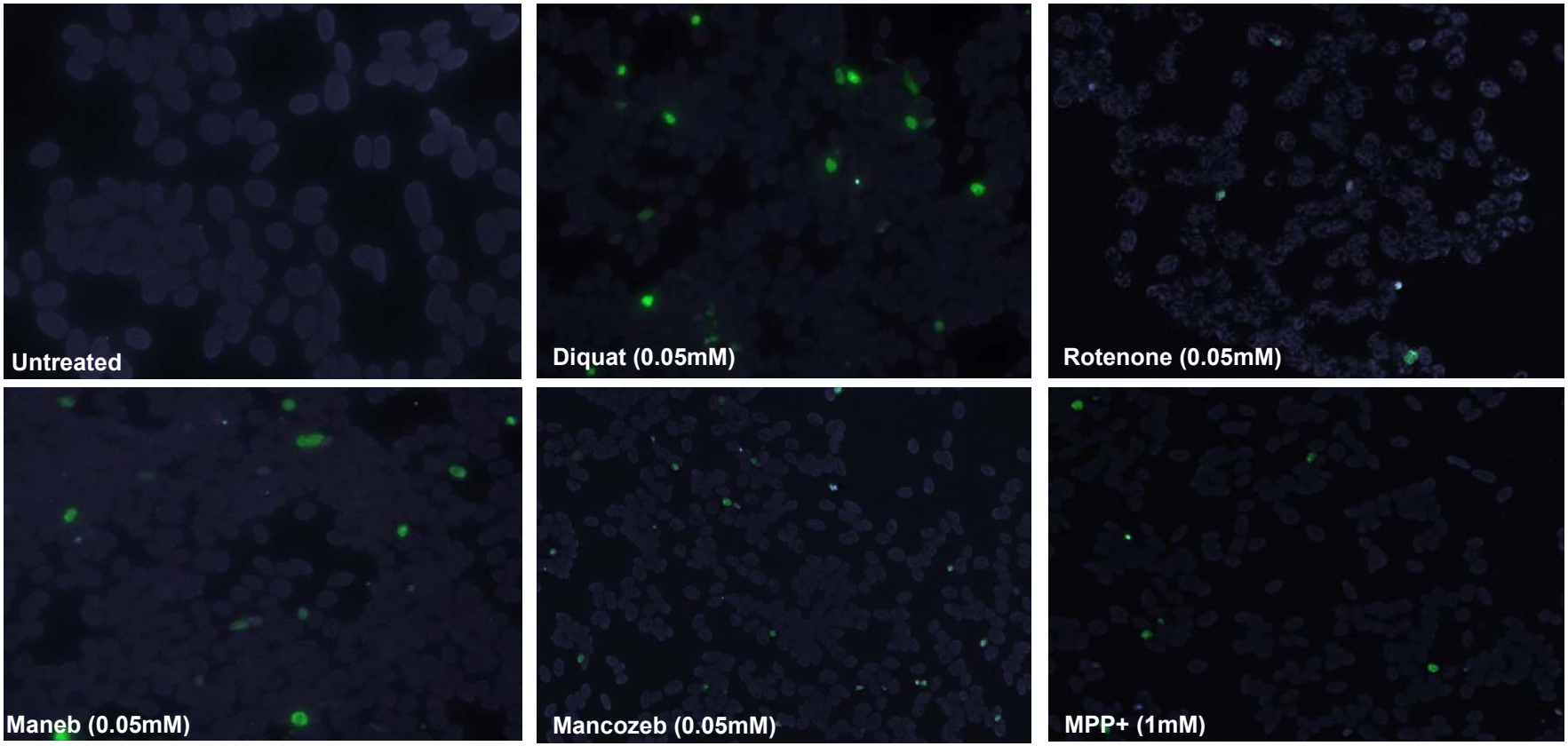

Fig 4.2: Changes in nuclear morphology after toxin treatment: A significantly higher number of condensed inter-nuclear fragments were visualised using DAPI staining after 24 hour treatment with H_2O_2 (0.1mM), rotenone (0.05mM), mancozeb (0.05mM), maneb (0.05mM) and diquat (0.05mM). (Each image representative of 3 different fields, Magnification = x 60).

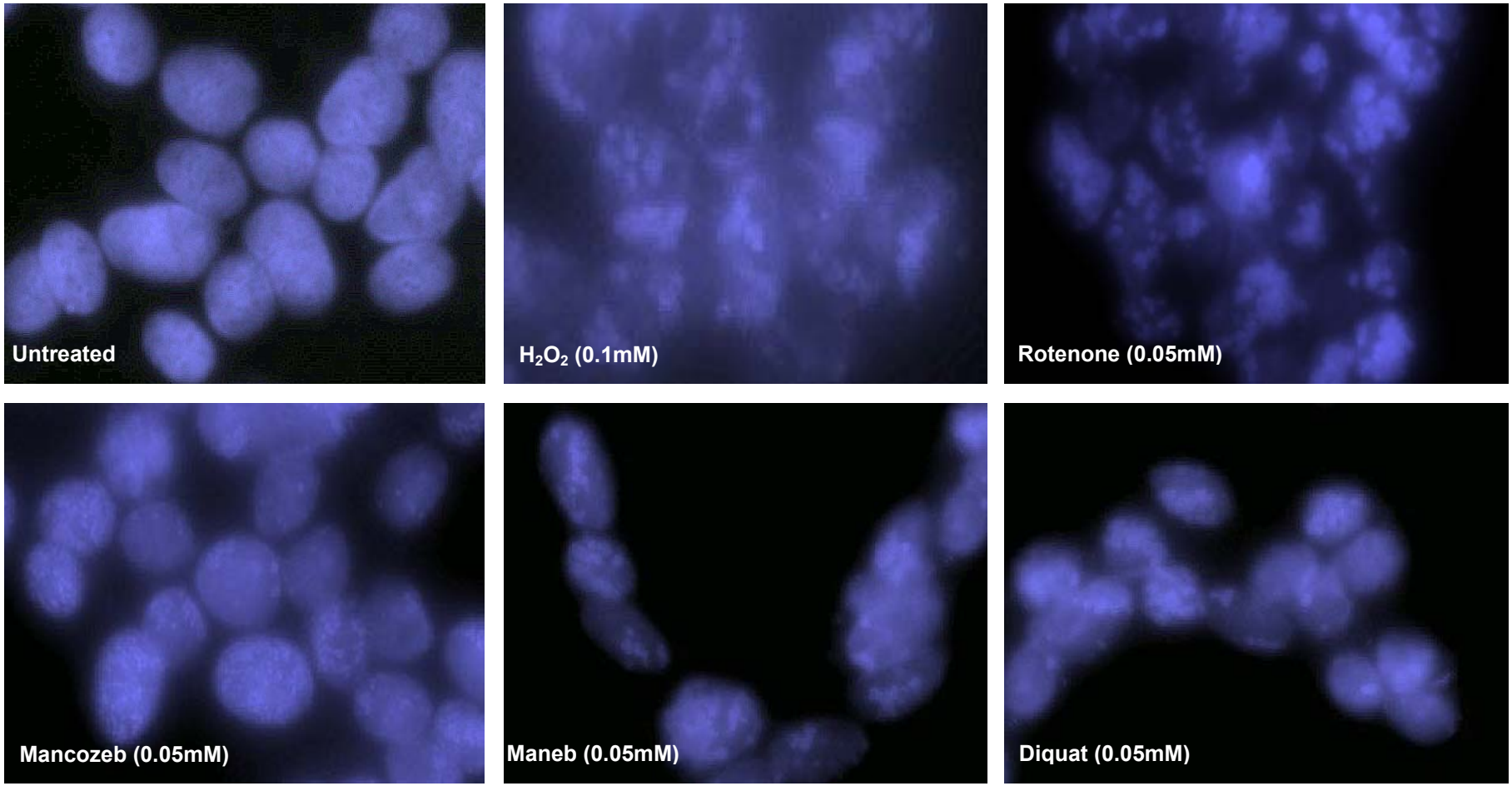

Previous studies have shown that rotenone induces PARP-1 cleavage during apoptotic cell-death in SH-SY5Y cells (Nakamura *et al*., 2004). 24 hour rotenone treatment at 0.001mM, 0.01mM and 0.1mM showed PARP-1 cleavage and densitometric analysis showed that the band intensities were similar to the hydrogen peroxide control (fig 4.4 D-F). MPP+ treatment showed no evidence of caspase-3 cleavage but caused PARP-1 cleavage at 1mM, consistent with the cytotoxicity data which showed significant MPP+ toxicity at this dose (fig 4.5 A-B).

Similarly maneb and mancozeb induced a significant increase in the levels of cytochrome c which is a highly conserved protein normally localised to the mitochondrial intermembrane but translocates from the mitochondrial membrane to the cytosol during apoptosis, where it is required for caspase-3 activation (Gonzales *et al*., 1990). Cytochrome c release from the mitochondria is thought to trigger an apoptotic cascade (Kluck *et al*., 1997). A significant increase in cytochrome c levels was observed with maneb (0.001mM, 0.01mM, 0.1mM) (fig 4.3 A, C) mancozeb (0.001mM and 0.1mM) (fig 4.4 A, C) and rotenone (0.01mM) (fig 4.4 D, F) compared with untreated controls and hydrogen peroxide (*$p<0.05$). No such change was observed after MPP+ or diquat treatment (fig 4.5).

Fig 4.3: Effect of toxin treatment on the expression of apoptotic markers: Expression of cleaved-PARP-1 and cytochrome c by Western blot analysis after 24 hour maneb treatment (A-C) (Values are presented as mean±SD, n=3, *p<0.05 accepted as significant).

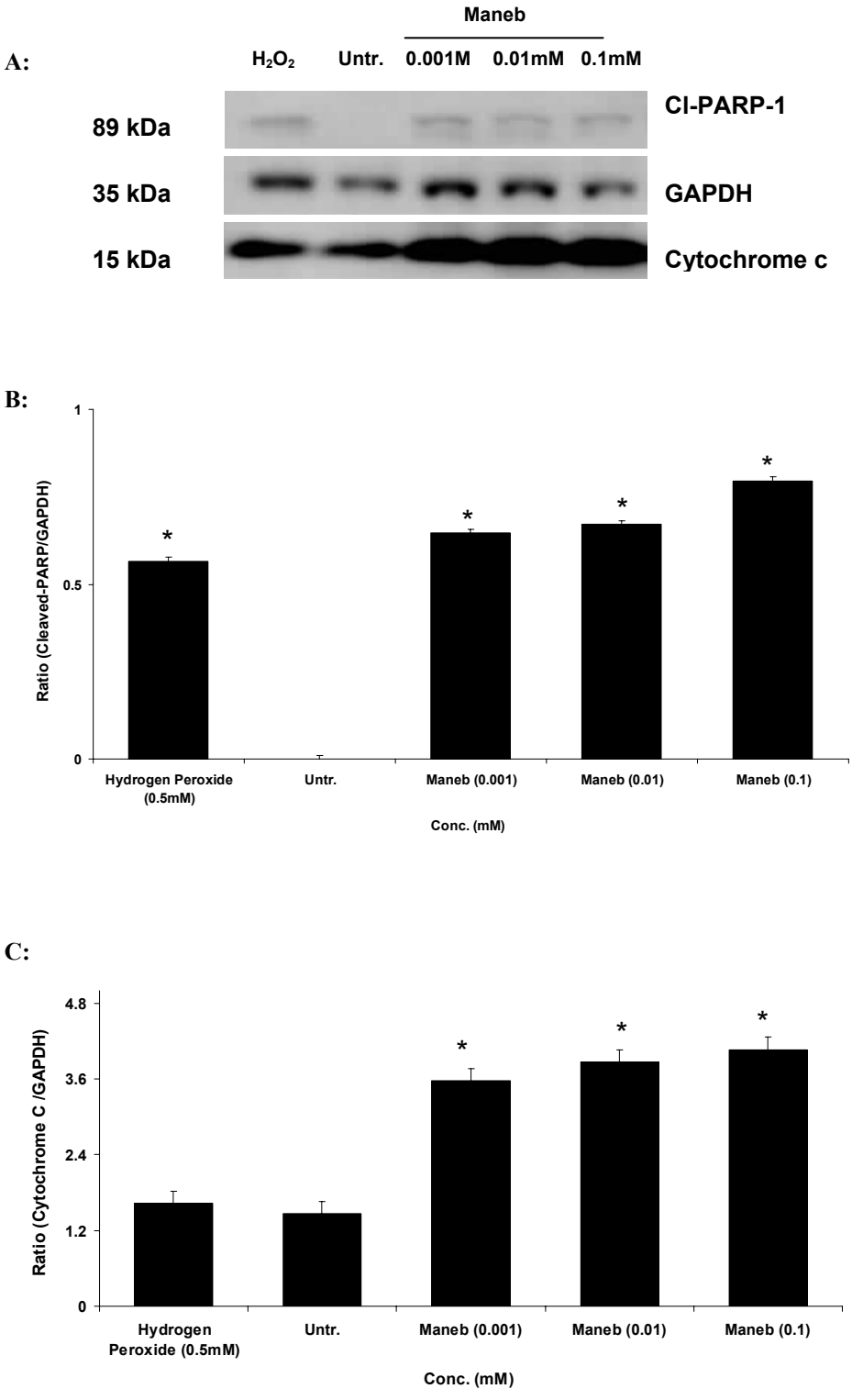

Fig 4.4: Effect of toxin treatment on the expression of apoptotic markers: Expression of cleaved-PARP-1 and cytochrome c by Western blot analysis after 24 hour mancozeb (A-C) and rotenone (D-F) treatment (Values are presented as mean±SD, n=3, *p<0.05 accepted as significant).

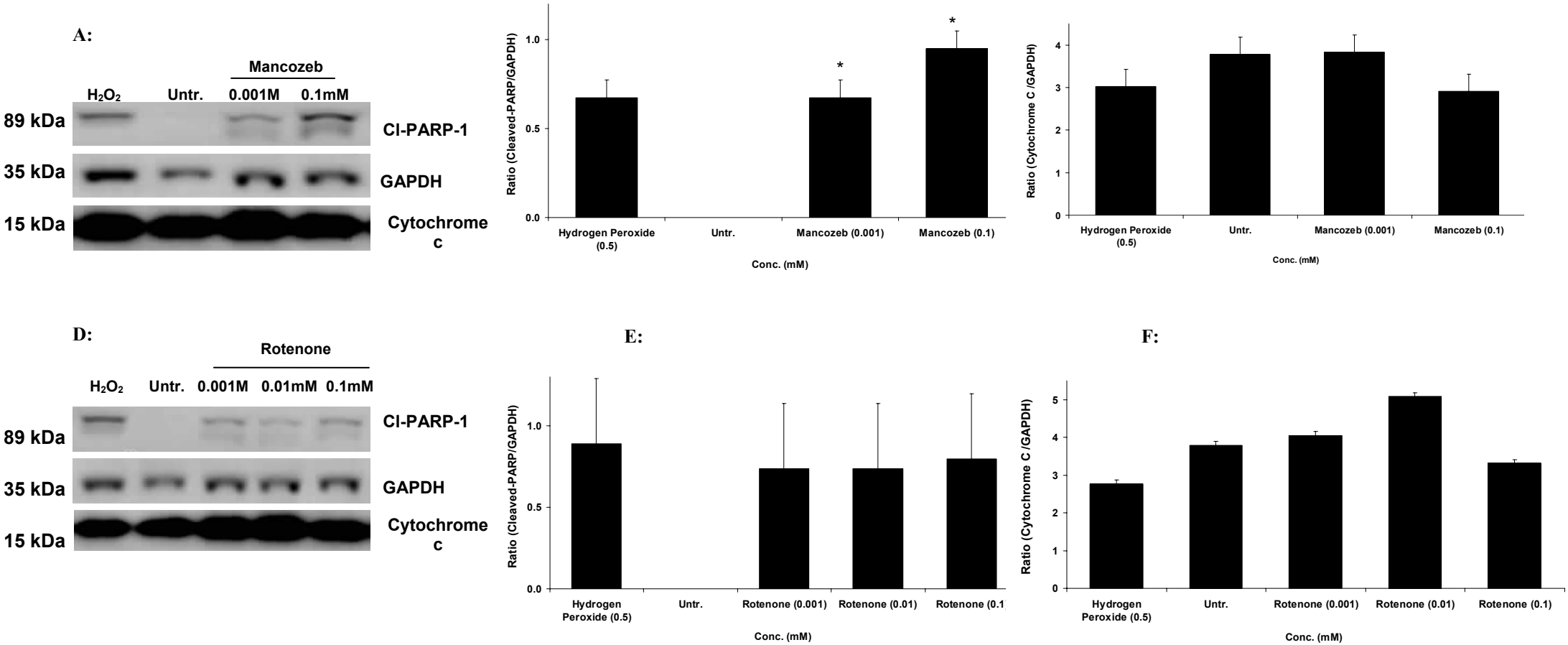

Fig 4.5: Effect of toxin treatment on the expression of apoptotic markers: Expression of cleaved-PARP-1 and cytochrome c by Western blot analysis after 24 hour MPP+ (A, B) and diquat (C) treatment (Values are presented as mean±SD, n=3, *p<0.05 accepted as significant).

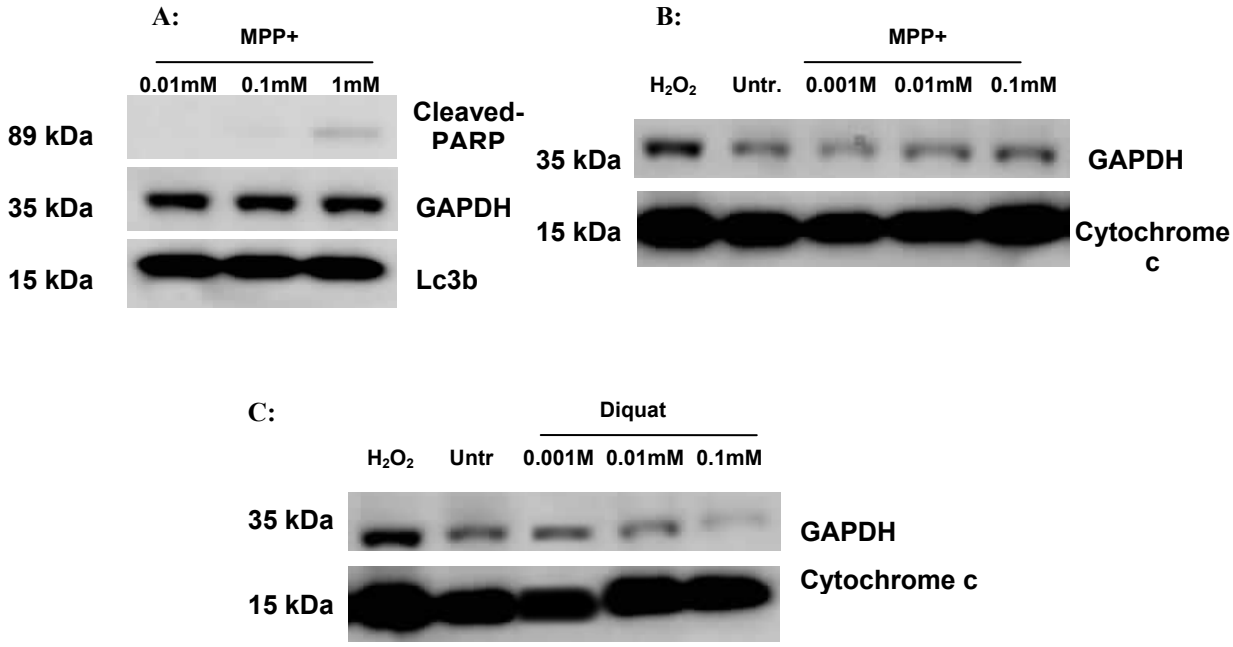

Treatment with different doses of diquat showed a significant increase in cleaved-PARP-1 and LC3 (16kDa) expression at 0.1mM (fig 4.6) after 24 hours. To determine the time-course of PARP-1 cleavage, SH-SY5Y cells were treated with 0.1mM diquat and protein expression quantified at different time points. Results showed significant increase in protein levels after 24 hour exposure followed by a decrease which complements the data gathered from cytotoxicity screening suggesting maximum toxicity at 24 hours after which cell-number tails off due to high toxicity.

Fig 4.6: Effect of diquat treatment on PARP-1 expression: A) Expression of cleaved PARP-1 by Western blot analysis after A): 24 hour 0.001mM, 0.01mM and 0.1mM and (B) 48 hour treatment at 0.1mM. (Values are presented as mean ± SD, n=3, *p<0.05).

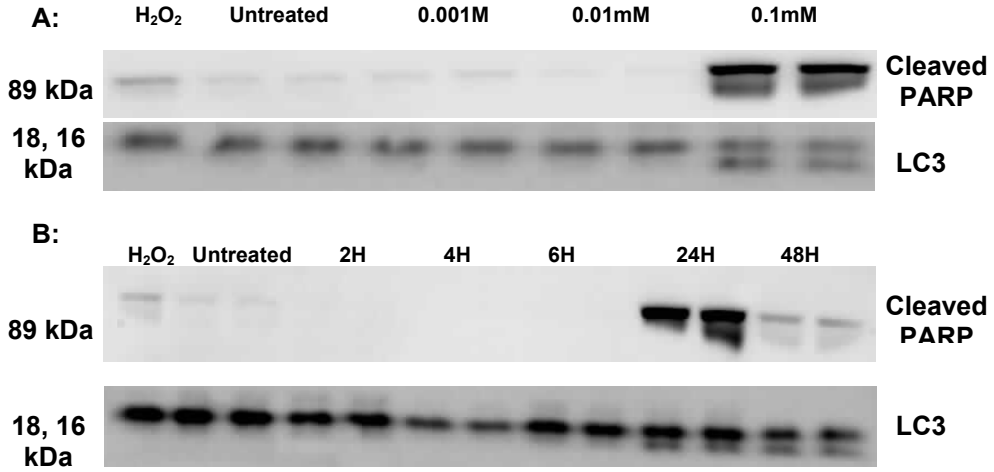

Given that a slight reduction in toxicity of diquat (0.1mM) was noted with zVAD.fmk in previous experiments (see chapter 3, fig 3.18). SH-SY5Y cells were pre-incubated with caspase-3, -9 inhibitors, NAC and tunicamycin to investigate whether these could have an effect on PARP-1 cleavage. Results showed no change in cleaved PARP-1 expression after 24hrs with caspase-3, and -9 inhibitors. NAC exacerbated PARP-1-cleavage at 0.1mM, whereas tunicamycin which enhances PARP cleavage and TRAIL-induced apoptosis (Jiang *et al*., 2007; Shiraishi *et al*., 2005) and can be toxic itself caused PARP-1 cleavage at a lower 0.01mM dose (fig 4.7).

Fig 4.7: Effect of diquat treatment on PARP-1 expression: Expression of cleaved PARP-1 (89 kDa) after 24 hour treatment with diquat co-incubated with caspase-3 inhibitor, caspase-9 inhibitor, NAC and tunicamycin (n=3).

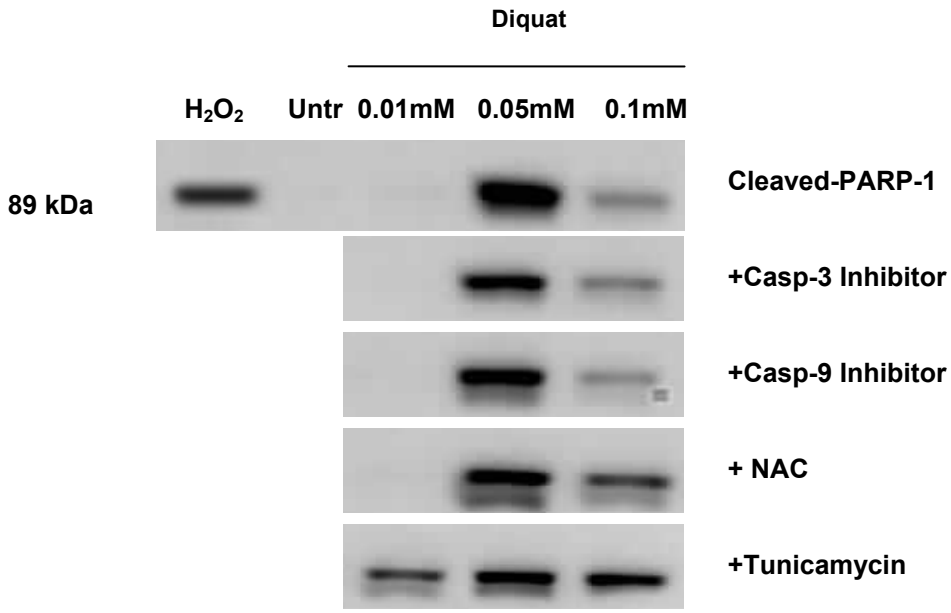

For chronic exposure lasting 4 weeks, SH-SY5Y cells were grown in medium supplemented with rotenone (5nM), MPP+ (0.01mM), diquat (0.001mM), maneb (0.001mM), mancozeb (0.001mM) and epoxiconazole (0.01mM). Etoposide (0.5mM) was used as a positive control. Lower chronic doses of agrochemical failed to show any evidence of PARP-1 cleavage (fig 4.8).

Fig 4.8: Effect of chronic toxin treatment on the cleaved-PARP-1 expression: Expression of cleaved-PARP-1 after 4 week exposure of (A) rotenone (5nM), (B) MPP+ (0.01mM), (C) diquat (0.001mM), (D) maneb (0.001mM), (E) mancozeb (0.001mM) and (F) epoxiconazole (0.01mM) (n=3).

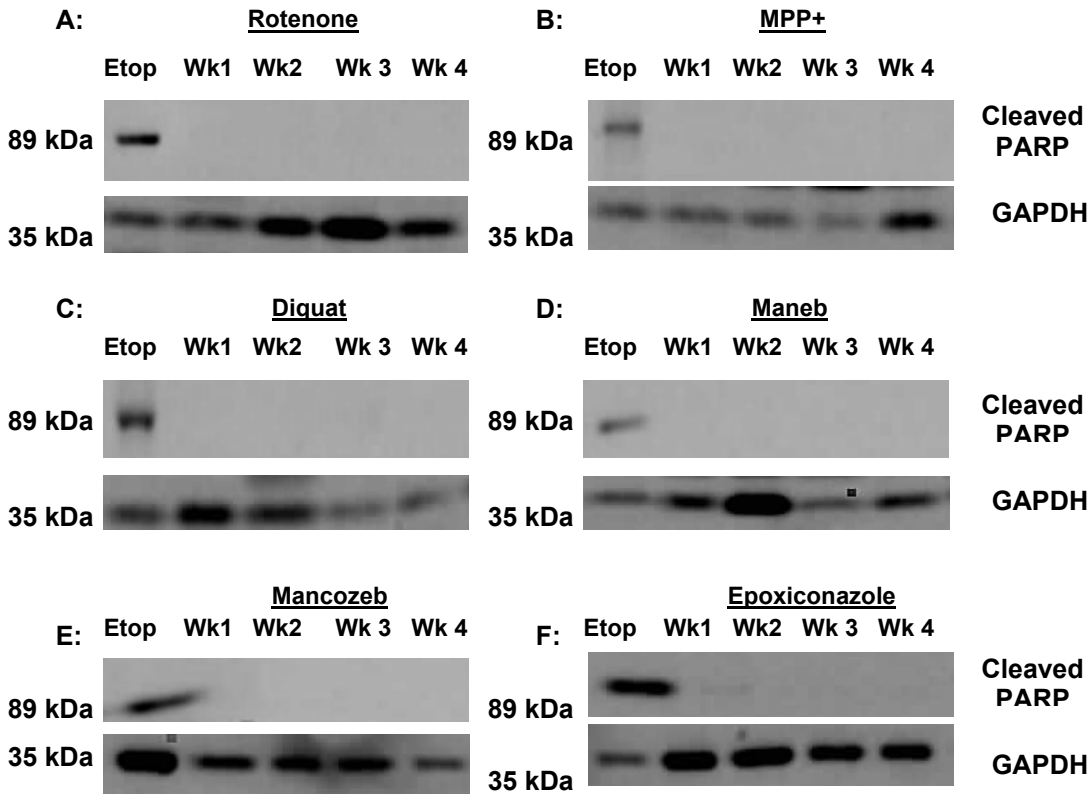

4.1.3.1.2 Caspase-3:

A role of caspases in apoptotic cell death in PD has come to light in studies using human PD brain samples. Increased levels of caspase-1 and -3 activities have been detected in PD substantia nigra compared with healthy controls (Mogi *et al*., 2000). Similarly, induction of apoptosis in cultured cerebellar granule neurons has shown an up-regulation of caspase-3 (Ni *et al*., 1997). Caspase-3 plays a role in proteolytic cleavage of PARP-1. Its cleavage is required for its activation. Western blots failed to detect endogenous levels of the large fragment (17/19 kDa) of

activated caspase-3 which results from cleavage adjacent to Asp175 (data not shown).

4.1.3.1.3 p53:

Free radical generation has an effect in causing DNA damage and affecting a DNA-damage response in cells. Protein levels of p53 can be elevated through accumulation of DNA strand breaks which can also activate p53-mediated signalling pathways (Morrison RS and Kinoshita, 2000). This has prompted research into the role of p53 in regulating neuronal cell death. Protein expression in SH-SY5Y cells after 24 hour toxin treatment showed significant change in the level of total p53 protein (*p<0.05) after mancozeb (0.075mM) and maneb (0.01mM, 0.1mM) (fig 4.9). Similarly, 0.05mM diquat caused a significant increase in p53 levels.

To determine the time-course of p53 expression, SH-SY5Y cells were treated with 0.05mM diquat and protein expression quantified at different time points. Results showed significant increase in protein level only 24 hour exposure followed by a significant decrease suggesting maximum p53 expression when cell is under most stress, an effect which was similar to that of PARP-1 expression. MPP+ (0.01mM-1mM), epoxiconazole (0.001mM-0.5mM) and fluroxypyr-ester (0.001mM-0.5mM) had no effect on p53 levels (data not shown). However, significantly higher levels were noted after rotenone treatment at 0.001mM and 0.01mM but not at 0.1mM (fig 4.9 E-F).

Fig 4.9: Toxin induced changes in p53 levels: SH-SY5Y cells were treated with different toxins i.e. A-B) mancozeb, C-D) maneb and E-F) rotenone for 24 hours after which cell extracts were probed for p53 (n=3, mean ± SD, *p<0.05).

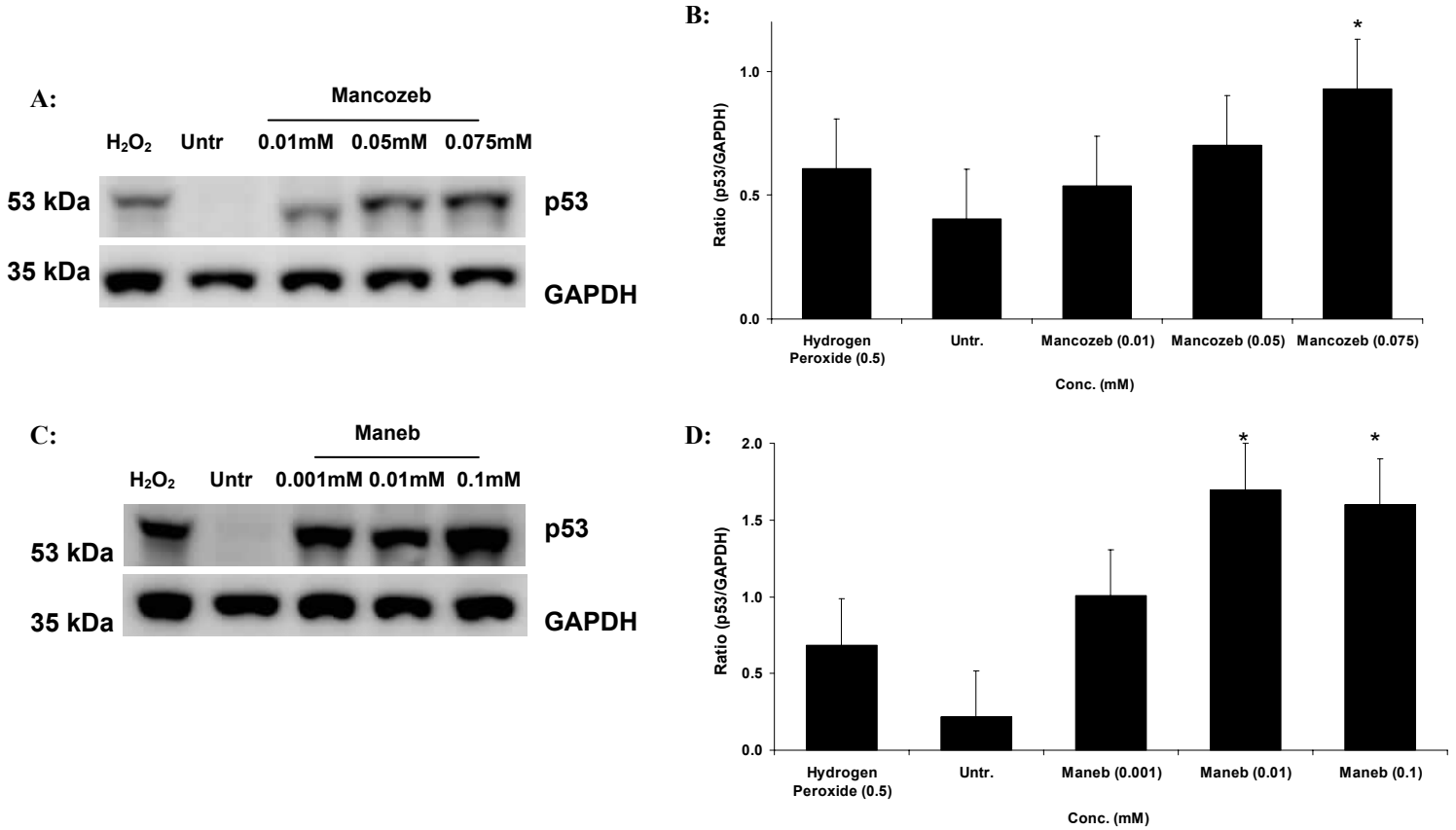

E:

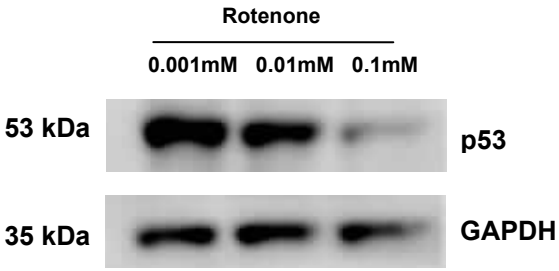
Rotenone
0.001mM 0.01mM 0.1mM
53 kDa
p53
35 kDa
GAPDH

F:

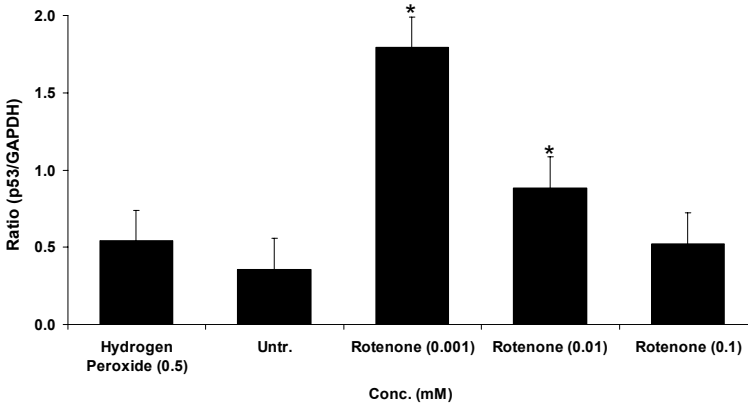
Ratio (p53/GAPDH)
2.0
1.5
1.0
0.5
0.0
*
*
Hydrogen Peroxide (0.5)
Untr.
Rotenone (0.001)
Rotenone (0.01)
Rotenone (0.1)
Conc. (mM)

Treatment with different doses of diquat showed a significant increase in p53 expression at 0.05mM (fig 4.10 A, B). To determine the time-course of its expression, SH-SY5Y cells were treated with 0.05mM diquat and protein levels quantified at different time points. Results showed time-dependent significant increase in protein levels only 24 hour exposure (fig 4.10 C, D).

Fig 4.10: Effect of diquat treatment on p53 expression: Western blot analysis showing p53 expression after 24 hour treatment with 0.01mM, 0.05mM and 0.1mM. C-D show p53 levels at different time points after 0.05mM treatment (n=3, mean ± SD, *p<0.05).

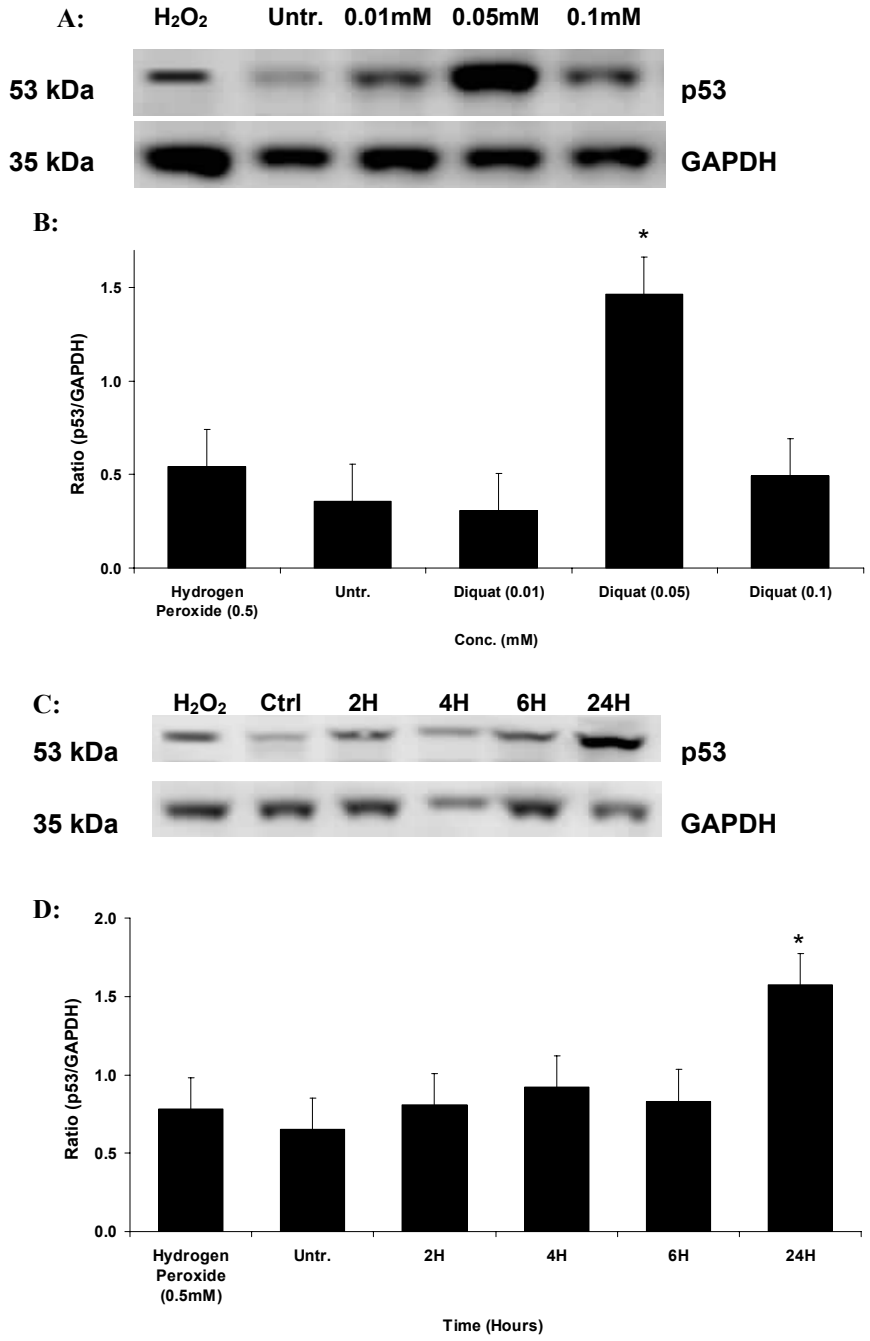

To investigate whether caspase inhibition or the use of antioxidants affects protein levels of total p53, SH-SY5Y cells were pre-incubated with caspase-3, -9 inhibitors, NAC and tunicamycin but results failed to show any change in p53 protein expression (fig 4.11).

Fig 4.11: Effect of diquat treatment on p53 expression: Expression of p53 in SH-SY5Y cells preincubated with capase-3 inhibitor, caspase-9 inhibitor, NAC and tunicamycin after diquat treatment. (n=3, mean±SD, *p<0.05).

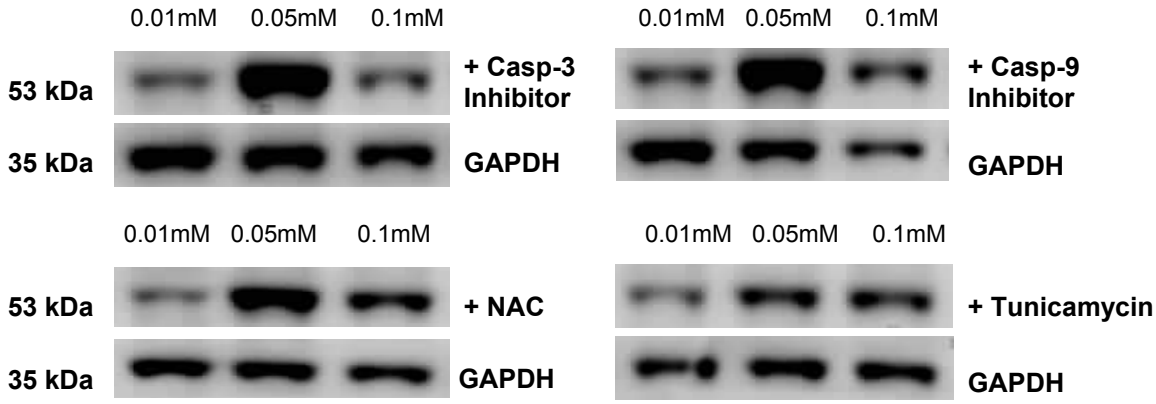

4.1.3.1.4 RIP:

Use of Nec-1 in previous experiments caused a significant reduction in cell-death. Over-expression of RIP can induce both NF-κB activation and apoptosis (Hsu *et al*., 1996). Therefore, to investigate if Nec-1 affects protein expression, the endogenous levels of total and cleaved RIP protein were measured after toxin treatment.

Results showed a significant change in the levels of full length RIP in mancozeb (0.01mM and 0.1mM) (fig 4.12 A-B), maneb (0.001mM-0.1mM), rotenone (0.001mM-0.1mM) and MPP+ (0.001mM-1mM) treated cells (fig 4.13, densitometric analysis not shown) compared with untreated cells. Diquat (0.01mM-0.075mM) showed no change in protein levels. There was no difference in cleaved RIP (~35-45kDa) in untreated and treated cells (data shown for mancozeb, fig 4.12 C). Fig 4.13 C, D and E show reduction in cleaved RIP band (~35-45kDa) at 0.05mM and 0.075mM after diquat treatment, at 0.1mM after rotenone treatment and at 0.001mM and 1mM after MPP+ treatment, however replication of these experiments failed to repeat this effect. RIP expression in cells pre-incubated with Nec-1 failed to show any significant change in RIP levels (densitometric data not shown).

Fig 4.12: Toxin induced changes in RIP levels: SH-SY5Y cells (±Nec-1) were treated with a-c) mancozeb, d) maneb, e) diquat, f) rotenone and g) MPP+ for 24 hours after which cell extracts were probed for RIP (n=3, mean ± SD, *p<0.05).

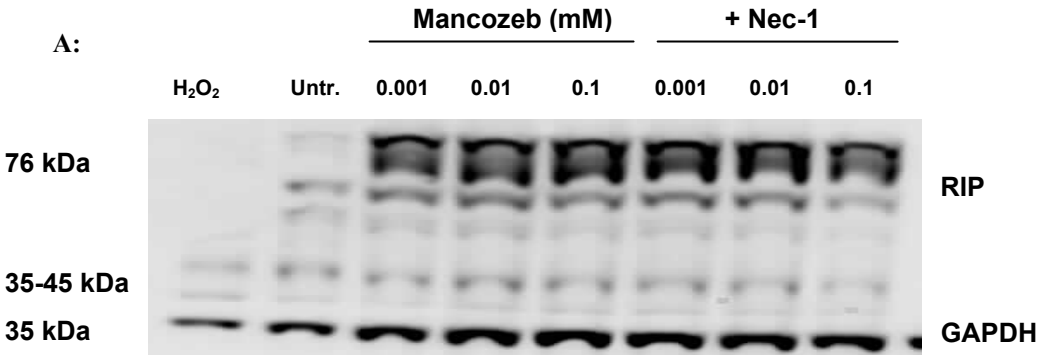

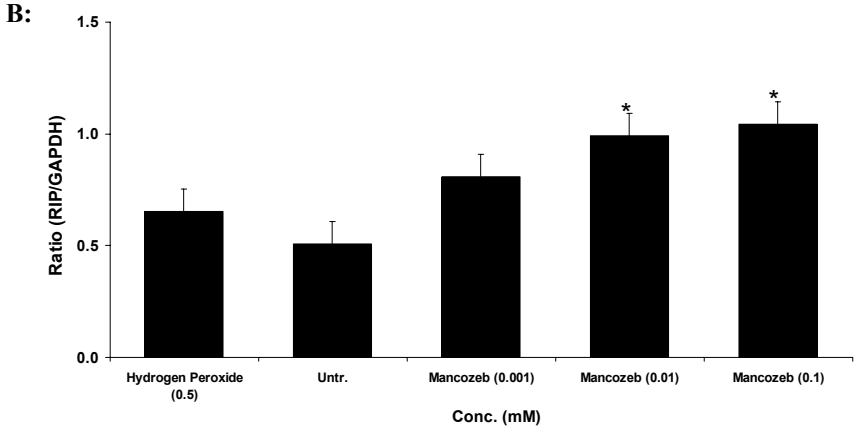

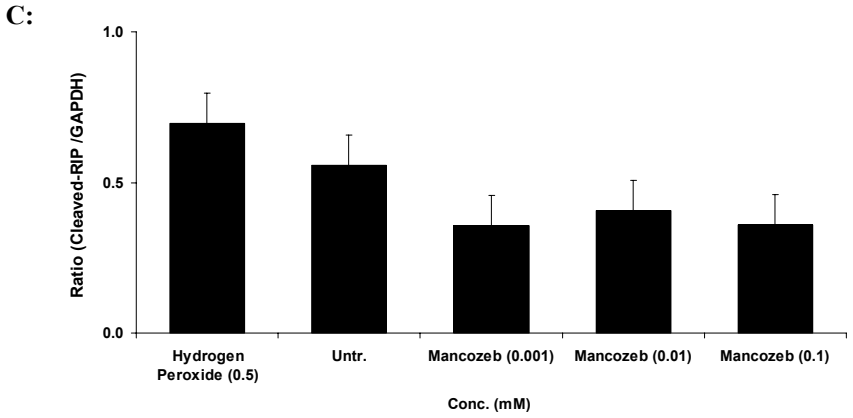

Fig 4.13: Toxin induced changes in RIP levels: SH-SY5Y cells (±Nec-1) were treated with A) maneb, B) diquat, C) rotenone and D) MPP+ for 24 hours after which cell extracts were probed for RIP (n=3, mean ± SD, *p<0.05).

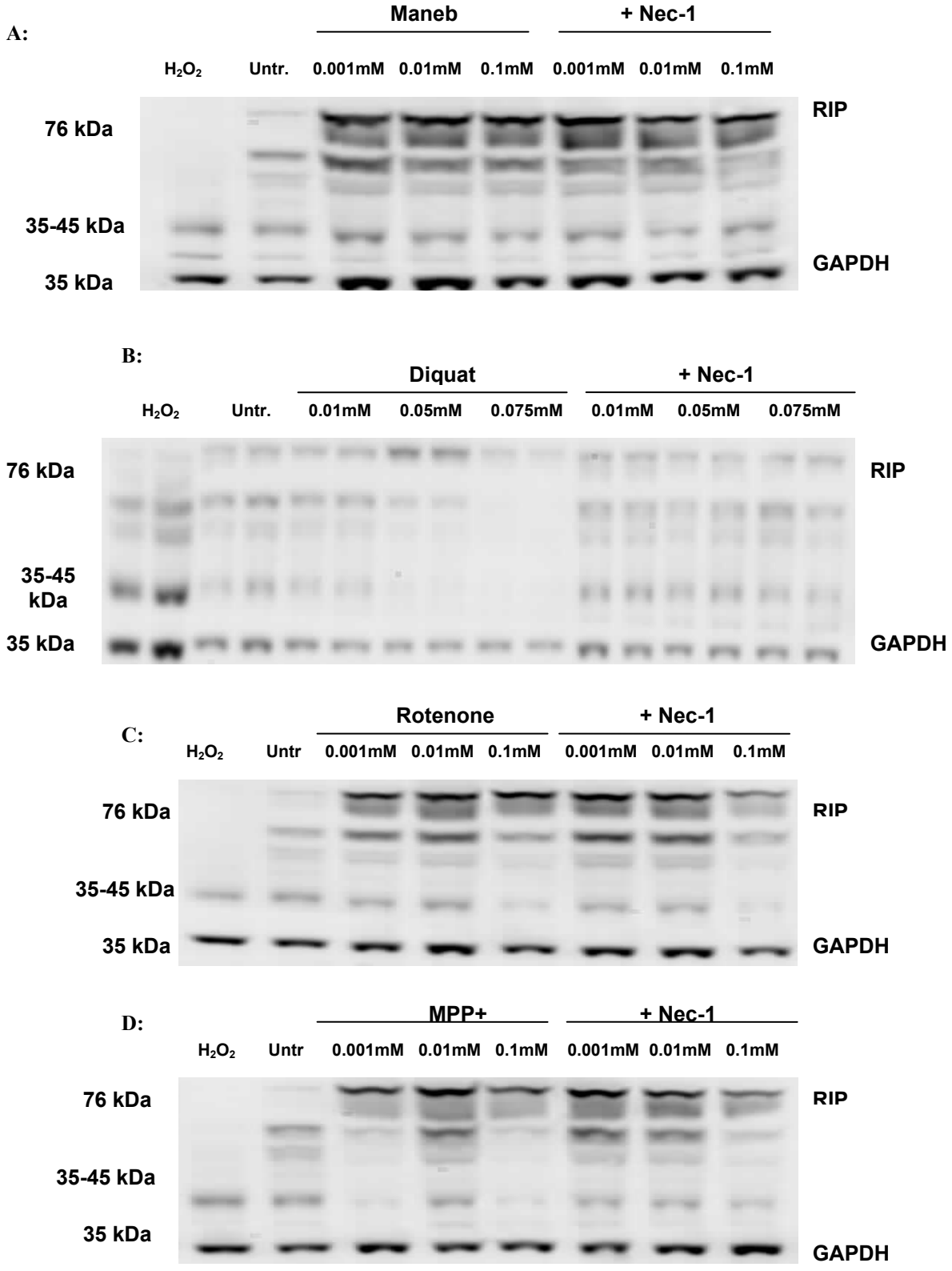

Immunostaining of RIP clearly showed extra-nuclear distribution of RIP in SH-SY5Y cells. No significant change in its localisation was observed between untreated cells and those exposed to diquat (0.05mM), rotenone (0.05mM), mancozeb 0.05mM), maneb (0.05mM) and MPP+ (1mM) (fig 4.14).

Fig 4.14: Visual presentation of RIP in toxin treated cells: Cellular distribution of RIP in untreated and toxin treated SH-SY5Y cells (Magnification = x40, each image is representative of three independent fields).

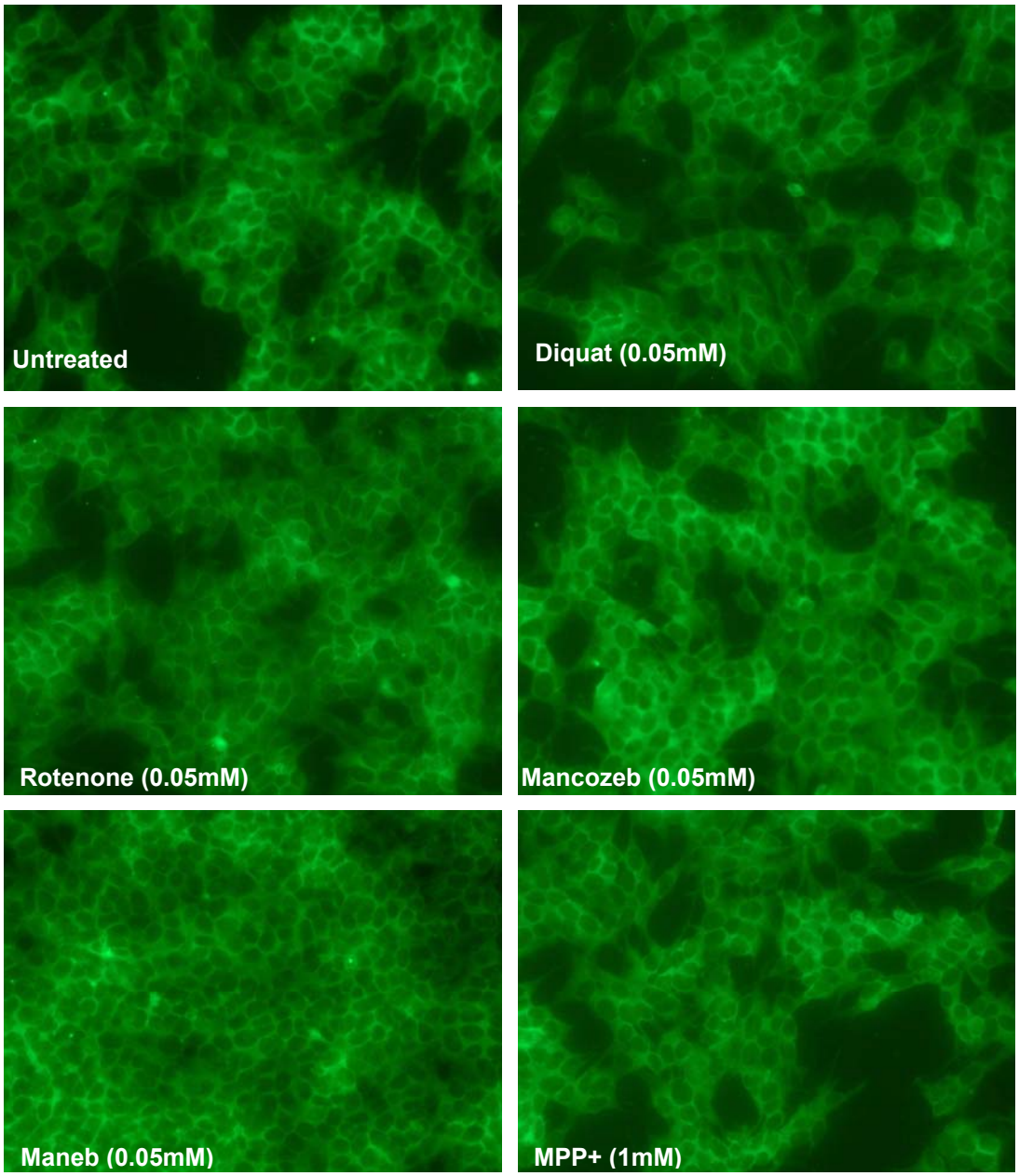

Similar experiments where SH-SY5Y cells were preincubated with Nec-1, treated with different chemicals and then probed for p53, phosho p53, LAMP1, LAMP2 and LC3 failed to show any significant difference in protein levels compared with untreated cells (data not shown).

4.1.3.1.5 α-synuclein:

To determine whether α-synuclein may be involved in the deleterious cascade of events induced by toxin treatment, α-synuclein protein expression levels (wild-type and α-synuclein phosphorylated at Ser129) were assessed after 24 hour treatment. α-synuclein can undergo several post-translational modifications with serine 129 phosphorylation being the most important. Up to 90% of α-synuclein in Lewy bodies have this modification and it is linked with aggregate formation in cell models (Fujiwara *et al*., 2002; Smith *et al*., 2005). Immunoblots showed a single 19kDa wild-type band and heavy bands between 40-55kDa with anti-α-synuclein and anti-phosphorylated α-synuclein antibodies respectively. Results showed a marginal but insignificant change in the level of α-synuclein (both wild-type and phosphorylated) after rotenone treatment (fig 4.15 A-C). Treatment with MPP+ (fig 4.15 D-F) had no effect on their expression. Similarly treatment with maneb, mancozeb and diquat showed no change in protein levels (fig 4.16 A-C).

Immunohistochemical analysis from previous studies have shown that rotenone treatment increases the amount of cellular α-synuclein in apoptotic cells (Watabe and Nakaki, 2004) and chronic treatment with 50nM rotenone can form neuritic swellings morphologically resembling the α-synuclein immunoreactive Lewy neurites seen in PD brain samples (Borland *et al*., 2008). As shown above, acute toxin exposure failed to change α-synuclein levels. Therefore, cells were grown in medium containing lower doses of different toxins i.e. rotenone (5nM), maneb (0.001mM), diquat (0.001mM), mancozeb (0.001mM) and epoxiconazole (0.001mM) for 4 weeks but analysis of their protein expression through western blotting and immunocytochemistry showed no significant change in protein levels (fig 4.17, 4.18).

Fig 4.15: Expression of α-synuclein in toxin treated cells: SH-SY5Y cells were treated with different toxins i.e. A-C) rotenone and D-F) MPP+ for 24 hours after which cell extracts were probed for α-synuclein and phosphorylated α-synuclein (n=3, mean±SD, *p<0.05).

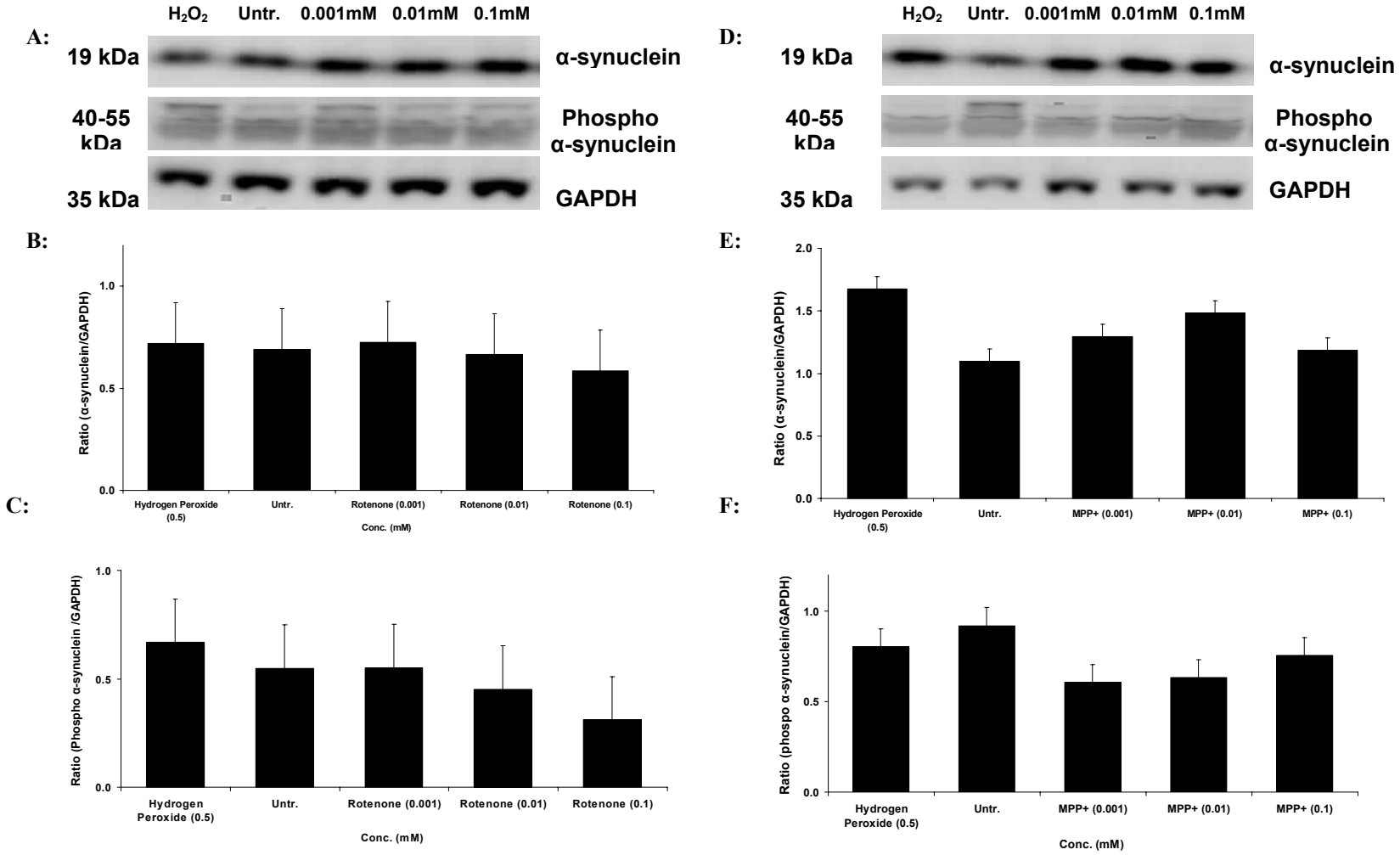

Fig 4.16: Expression of α-synuclein in toxin treated cells: SH-SY5Y cells were treated with different toxins i.e. a) maneb, b) mancozeb and c) diquat for 24 hours after which cell extracts were probed for α-synuclein and phosphorylated α-synuclein (n=3, mean±SD, *p<0.05).

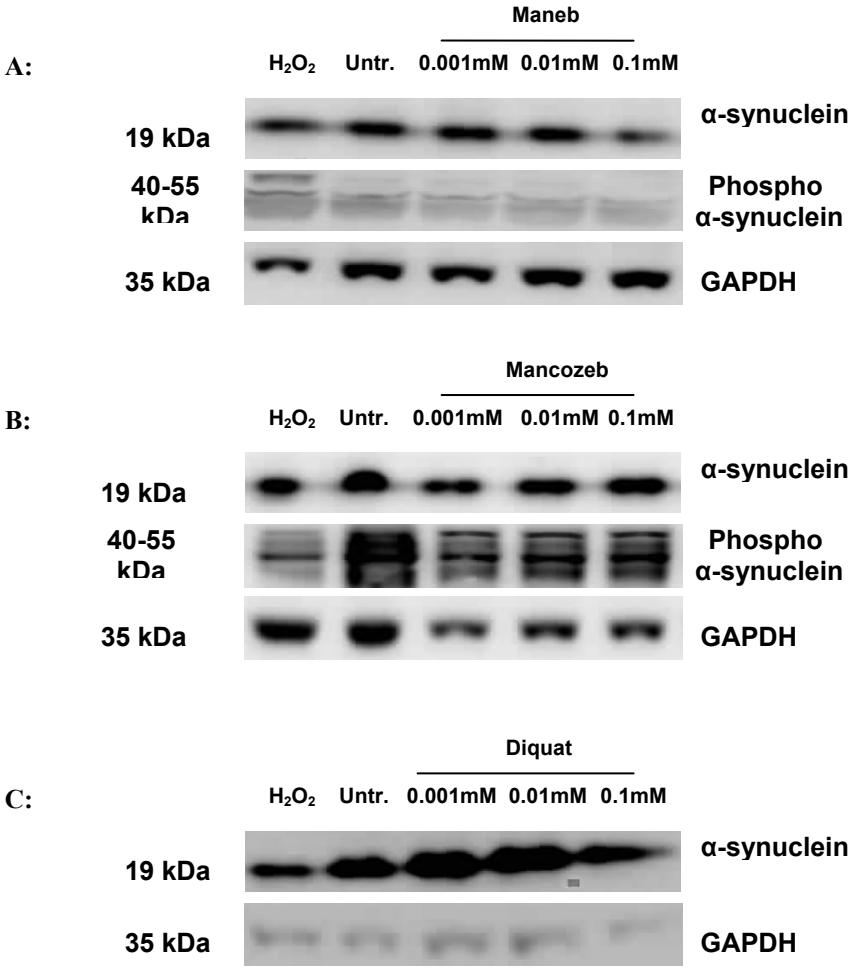

Fig 4.17: Visual presentation of α-synuclein in toxin treated cells: Cellular distribution of α-synuclein in untreated and toxin treated SH-SY5Y cells after 4 weeks exposure (Magnification = x40, each image is representative of three independent fields).

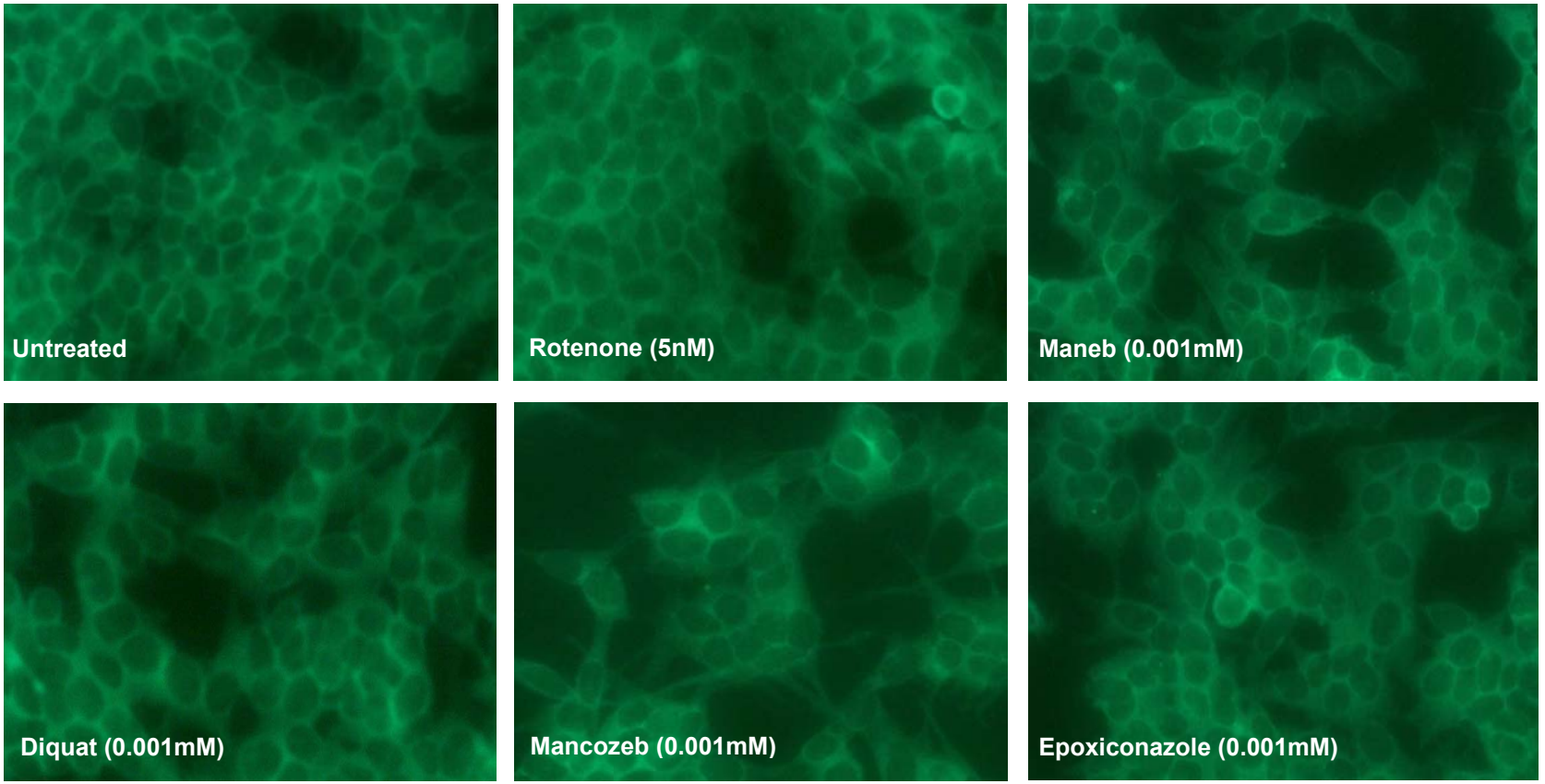

Fig 4.18: Chronic toxin induced changes in α-synuclein levels: SH-SY5Y cells were grown in medium containing rotenone, MPP+, maneb, mancozeb and diquat for 4 weeks after which cell extracts were probed for α-synuclein (19 kDa) (n=3).

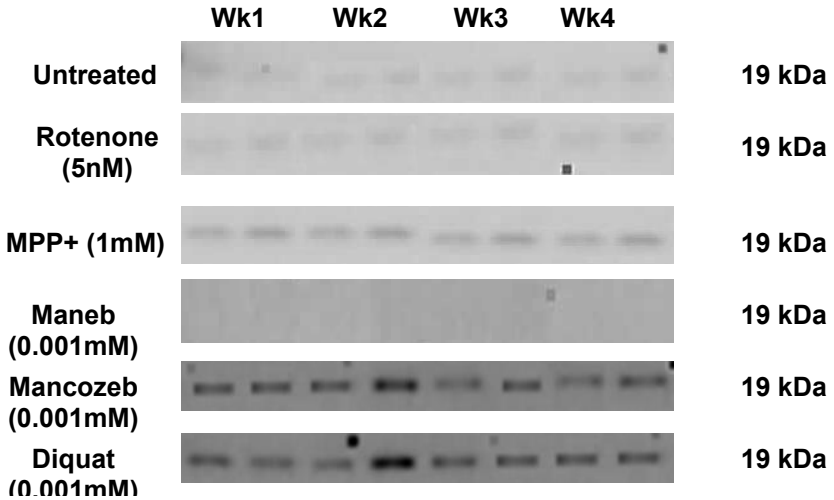

4.1.3.1.6 DJ-1:

DJ-1 plays a role in anti-oxidative stress, inhibition of α-synuclein aggregation and transcriptional regulation. Therefore, its loss of function sensitises cells to oxidative stress and increased accumulation of insoluble α-synuclein which may cause onset of PD (Inden *et al*., 2006; Shendelman *et al*., 2004). Oxidative stress can induce oxidation and increased expression of DJ-1 (Kinumi *et al*., 2004; Taira *et al*., 2004). DJ-1 mutants derived from PD patients have shown reduced activities against oxidative stress (Takahashi-Niki *et al*., 2004). Similarly, abnormally oxidised DJ-1 has been noticed in sporadic PD patients (Bandopadhyay *et al*., 2004).

Effect of DJ-1 over-expression on toxin treatment is discussed in chapter 4. However, protein expression in SH-SY5Y cells after toxin exposure failed to show any changes in protein levels (fig 4.19). Densitometric analysis of DJ-1 bands normalised against GAPDH showed that protein levels neither increased nor decreased after 24 hour exposure (data not shown). Analysis of oxidised DJ-1 was not performed. These findings were backed up by visual observation of DJ-1 where SH-SY5Y cell exposure to toxins did not markedly alter DJ-1 distribution. There was no significant change in the staining pattern. DJ-1 immunoreactivity was observed in all cell bodies and highly branched and thinner processes (fig 4.20).

Fig 4.19: Toxin induced changes in DJ-1 levels: SH-SY5Y cells were treated with different toxins i.e. a) maneb, b) mancozeb, c) rotenone, d) MPP+ and e) diquat for 24 hours after which cell extracts were probed for DJ-1 (n=3, mean±SD, *p<0.05)

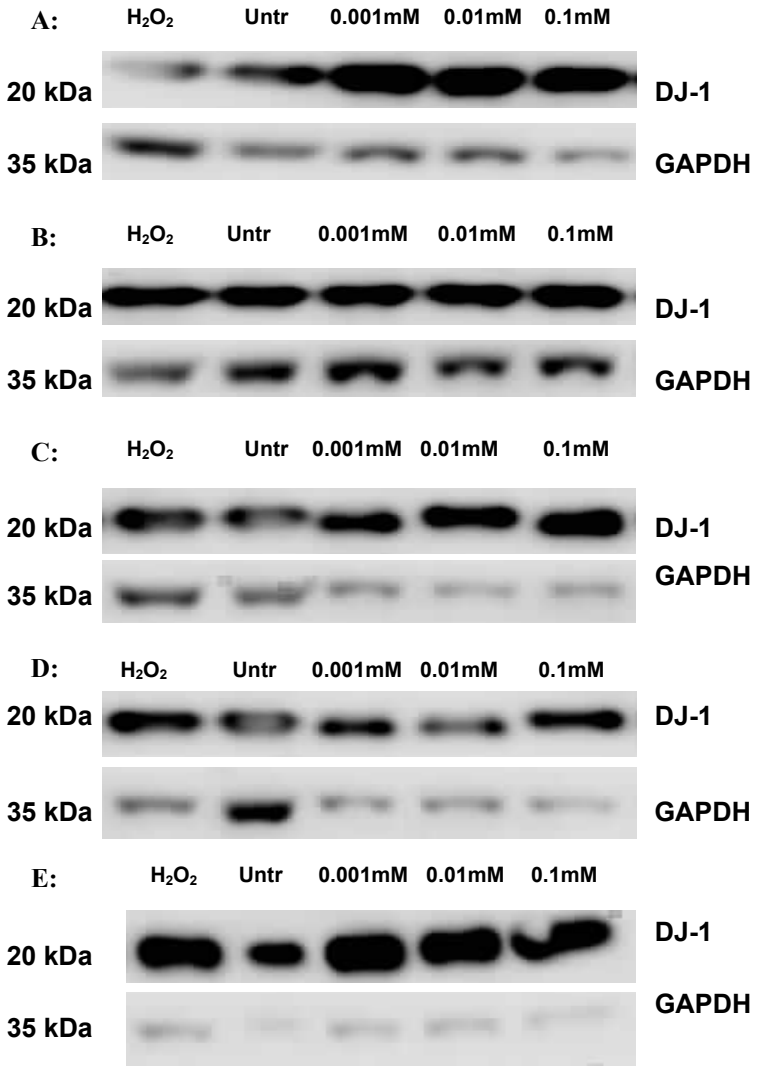

Fig 4.20: DJ-1 immunoreactivity following treatment with different toxins: Cellular distribution of DJ-1 in untreated and toxin treated SH-SY5Y cells after 4 weeks exposure (Magnification = x40, each image is representative of three independent fields).

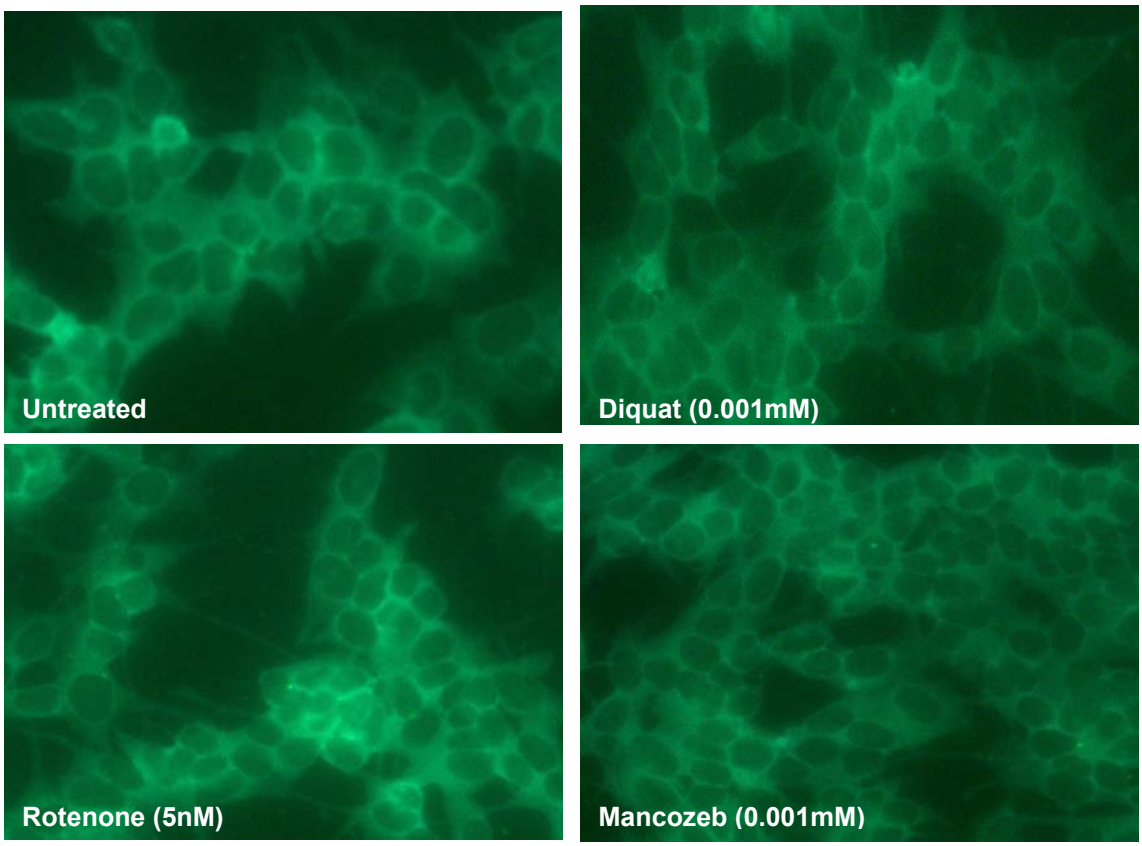

4.1.3.1.7 Tyrosine hydroxylase (TH):

Studies have shown that SH-SY5Y cells express tyrosine hydroxylase, the rate-limiting enzyme in dopamine synthesis. SH-SY5Y cells are capable of producing and transporting dopamine making it an ideal *in vitro* system to examine the effects of toxin treatment on dopaminergic markers such as TH (Presgraves *et al*., 2004).

Cells treated with rotenone, diquat, MPP+, maneb and mancozeb for 24 hours showed no change in TH levels, as measured through western blotting (fig 4.21). Similarly, chronic 4 week exposure had no effect on TH levels (data not shown). To examine morphology and TH immunocytochemistry in chronically treated cells, anti-mouse TH antibody was used. Examples of TH immunoreactivity in untreated and treated cells are shown in fig 4.22. All cells, treated and untreated showed smooth cytosolic localisation of tyrosine hydroxylase evenly distributed with no evidence of aggregation.

Fig 4.21: Effect of 24-h toxin treatment on TH expression in SH-SY5Y cells: Western blot detection of TH expression (62 kDa) against GAPDH (35kDa) in A) rotenone, B) MPP+, C) maneb, D) mancozeb and E) diquat treated cells (n=3).

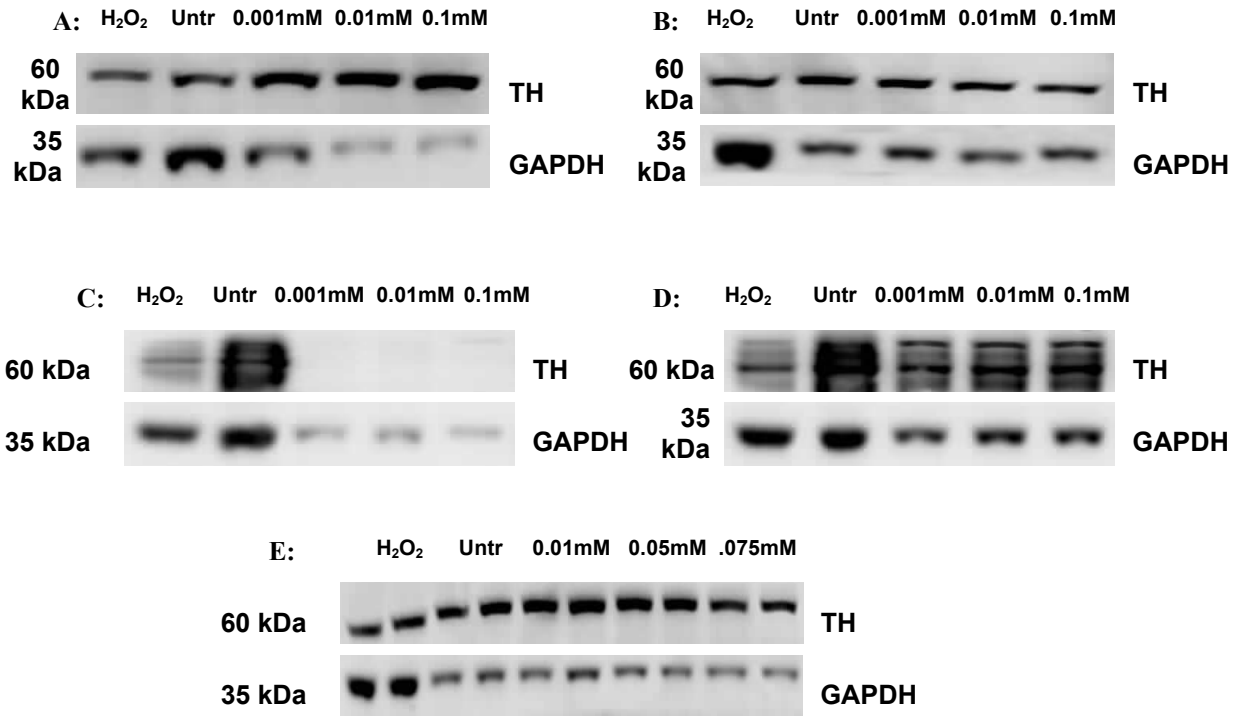

Fig 4.22: SH-SY5Y cell morphology and tyrosine hydroxylase immunoreactivity following treatment with different toxins: Cellular distribution of tyrosine hydroxylase in untreated and toxin treated SH-SY5Y cells after 4 weeks exposure (Magnification = x40, each image is representative of three independent fields).

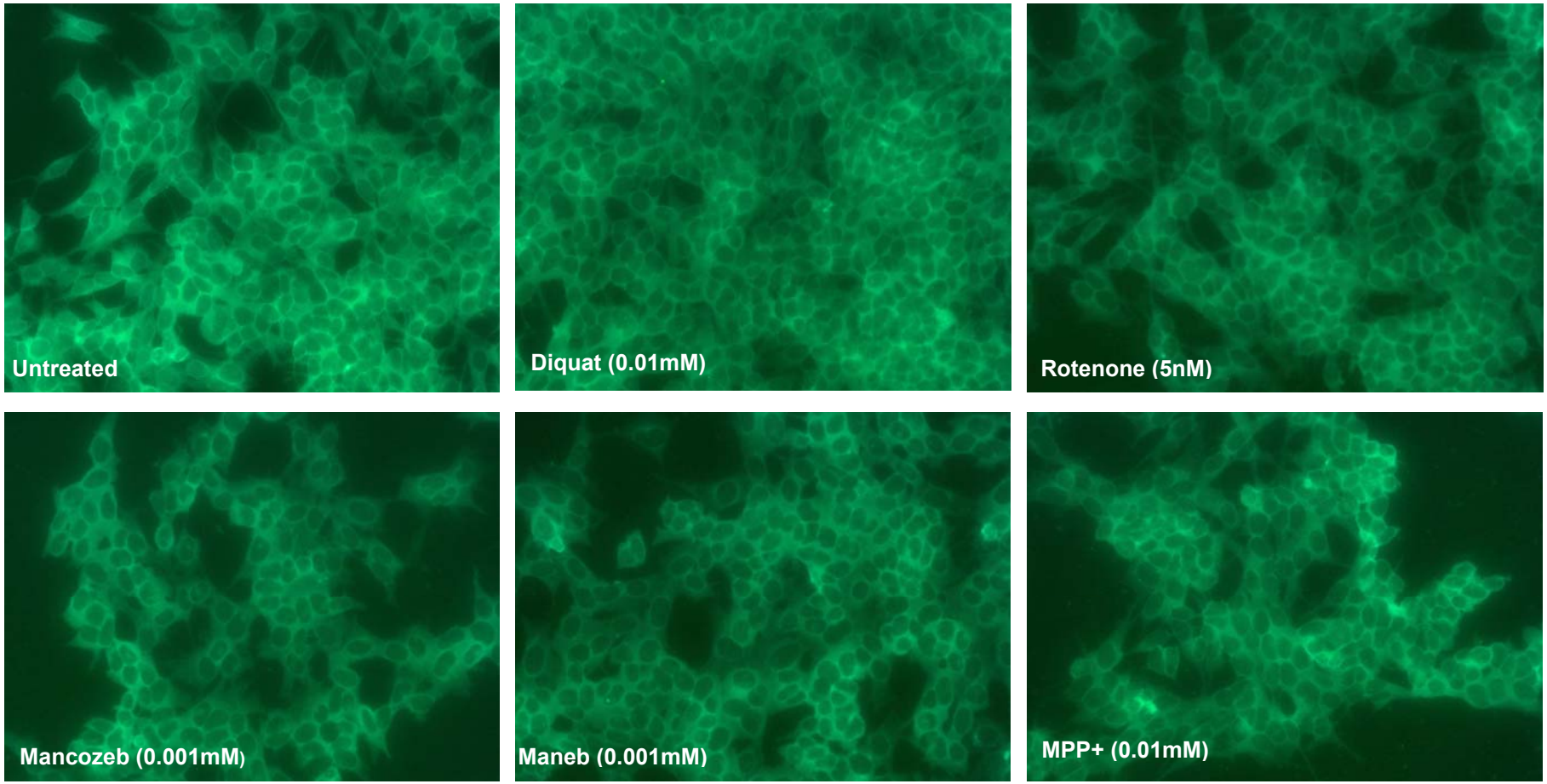

4.1.3.1.8 Neurofilaments:

Neurons degenerate during ageing and neurodegenerative disorders contain neurons with disrupted cytoskeleton as observed in dopaminergic neurons in PD and hippocampal neurons in Alzheimer's disease (Mattson and Magnus, 2006). Cytoskeleton containing microtubules, intermediate filaments and microfilaments help to maintain neuronal morphology with long neurofilament-rich axons and dendrites. Previous studies have shown that sub-cytotoxic concentrations of MPTP can induce neurotoxic changes in neuronal cells by inhibiting axon outgrowth at exposure times lower than those causing highly significant cell-death (De Girolamo *et al*., 2000).

In order to investigate if agrochemical mediated damage can disrupt cytoskeletal structure; a pan-neurofilament antibody was used for immunocytochemical staining of SH-SY5Y cells. Distinct morphological features of dopaminergic phenotype including neurites and enhanced branching of neuronal processes were observed in untreated cells. Treated cells however showed disrupted cytoskeletal integrity with maximum immunoreactivity in the cell-body (fig 4.23). Overall, the proportion of neurite staining was very low in treated cells. This relates with the visual observation that stressed cells under high toxicity have a morphological transformation from long neuronal structure to spherical shape. This could explain minimal neurite staining. Future studies using antibodies specific for microtubules, intermediate filaments and microfilaments can provide a better understanding of the structure more susceptible to toxicity.

Fig 4.23: Representative images showing neurofilament staining after toxin treatment: Representative immunofluorescence images of SH-SY5Y cells treated with diquat (0.05mM), rotenone (0.05mM), maneb (0.05mM), MPP+ (1mM) and mancozeb (0.05mM) for 24 hours. Green staining = pan-neurofilament staining (Magnification = x60, each image is representative of three independent fields).

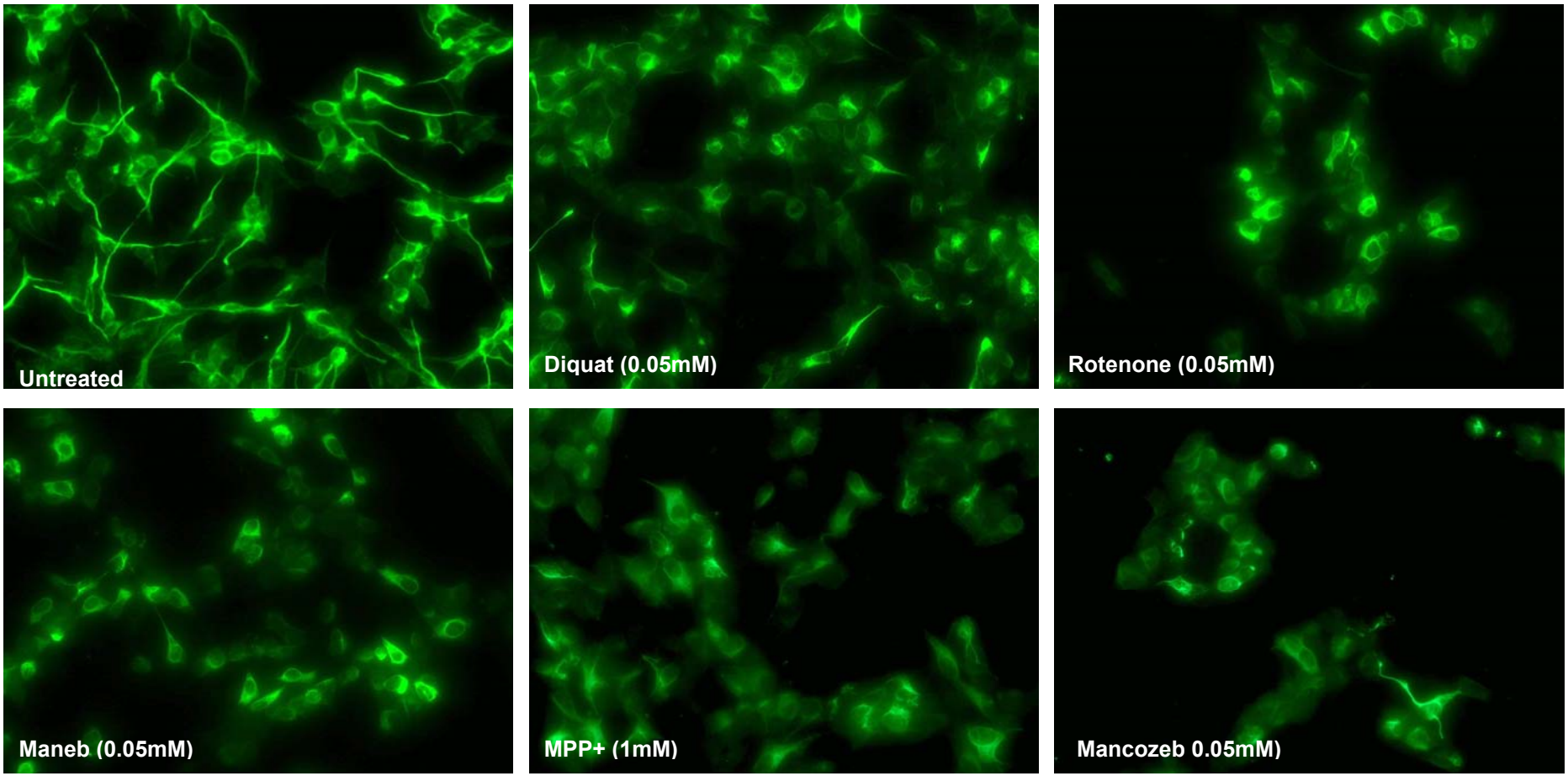

4.1.4 Discussion:

In general, induction of PARP-1 was seen as a late event in agrochemical treated cells and treatment seems to cause caspase independent cell death processes involving RIP. Experimental data from different studies points towards the involvement of apoptotic processes in toxin-induced *in vitro* cell-death but specific mechanisms are not extensively described. In order to differentiate apoptosis from other forms of cell-death, cleavage of PARP-1, cytochrome c and cleaved caspase-3 levels were measured following exposure to a range of different doses of selected agrochemicals. A dual role for PD-inducing agents including rotenone has been put forward which suggests that other than causing oxidative stress they may be involved in apoptotic pathways. Rotenone can dephosphorylate the BAD protein in SH-SY5Y cells which blocks Bcl-2 which has role in preventing Fas cell-death receptor mediated apoptosis (Watabe and Nakaki, 2004).

In response to internal and external stimuli, cells protect their genomic information through DNA repair and DNA damage signalling pathways. PARPs are vital for repair of single- and double-strand breaks and control the integrity of the chromosomal ends (Beneke and Burkle, 2007). Genotoxic exposure results in PARP-1 over-activation (Berger *et al*., 1983) which leads to a reduction in cellular NAD+ levels and greater ATP consumption which can push cells towards necrotic cell death. However, caspase-independent apoptosis can be induced by PARP-1 activity leading to AIF dependent apoptosis involving high-molecular weight DNA fragmentation (Cregan *et al*., 2004). Cleavage of PARP-1 and PARP-2 occurs in classical apoptosis to preserve energy by preventing PARP-1 activation and thus NAD+ consumption (Beneke and Burkle, 2007). To confirm the apoptotic changes caused by selected chemicals on SH-SY5Y cells, PARP cleavage was used as an index of apoptosis. Results showed a dose-dependent increase in cleaved PARP-1 (89kDa) fragment. PARP cleavage became apparent in cells incubated with mancozeb, maneb and diquat for 24 h at concentrations of 0.01mM-0.1mM and was more obvious at 0.1mM (fig 4.3-4.6). It was highly expressed after 24 hours (data shown for diquat, fig 4.6), a time-point where toxicity was at its maximum. The absence of any effect of caspase inhibitors on this process for most agrochemicals with the exception of diquat, may suggest caspase independent induction of PARP-1.

The release of cytochrome c from the inner mitochondrial membrane provides a crucial checkpoint on apoptosis via the Bcl-2 gene family (reviewed by Gross *et al*., 1999). Activation of Bax (a Bcl-2 subfamily member) induces permeabilisation of outer mitochondrial membrane resulting in cytochrome c release leading to initiation of apoptosis (Ventimiglia *et al*., 2001). Results from this study showed a significant increase in overall cellular cytochrome c levels after maneb, mancozeb and rotenone treatment. The loss of mitochondrial transmembrane potential causes cytochrome c release into the cytosol and initiates a cascade involving caspase activation (Kluck *et al*., 1997) but there is no evidence of the dissipation of mitochondrial transmembrane potential accompanied by cytochrome *c* release in PD patients. The activated caspase 3 cleaves its substrates including PARP, which is a substrate of multiple caspases (Ventimiglia *et al*, 2001). Elevated activities of caspase-1 and -3 have been detected in the substantia nigra of post-mortem PD brain (Mogi *et al*., 2000). Other studies have suggested a link between the numbers of caspase-3 immunoreactive neurons in midbrain of control brains and the amount of loss of these neurons in PD brain (Hartmann *et al*., 2000). Previous studies using caspase inhibitors to determine the role of toxins like rotenone in apoptosis have shown significant attenuation of apoptosis (Newhouse *et al*., 2004). Same authors used caspase-3 inhibitor to inhibit PARP cleavage in SH-SY5Y cells and observed a reduction in number of apoptotic cells. This is in contrast with results from this study which failed to detect any change in total (data not shown) or cleaved caspase-3 levels suggesting a presence of a caspase-independent mechanism.

Observation of changes in cell/nuclear morphology, enzymatic activity and ATP concentration helps in assessing the mode of cell-death (Fawthrop *et al.,* 1991). Both morphological and biochemical methods for evaluating cell death were utilised in this study because different characters ascribed to either necrosis or apoptosis can be induced by different toxins. Nuclear condensation has been observed in dopaminergic neurons of PD patients (Anglade *et al*., 1997) and gross nuclear changes observed after toxin treatment in this study suggested involvement of either apoptosis or necrosis as fluorescence staining clearly showed nuclear condensation and partition into fragments visible as discrete clusters of nuclear material (fig 4.2). These alterations in nuclear morphology were visible after maneb, mancozeb, diquat,

rotenone and epoxiconazole treatment. Similar nuclear changes have been reported by Newhouse et al (2004) who observed condensed cell-bodies and fragmented and condensed nuclei into discrete dense chromatin clumps after rotenone treatment.

Several acute injuries can cause p53 activation. Neuronal stimulation by excitatory amino acids or receptor agonists can lead to accumulation of p53. p53 expression can be induced in neurons with neurotoxins like kainic acid (Sakhi *et al*., 1996). Studies using transgenic p53 knock-out mice have shown protection against MPTP toxicity (Trimmer *et al*., 1996). p53 regulates expression of select target genes and thus promotes apoptosis. It can either repress transcription or act as a site-specific transactivator (Asker *et al*., 1999). Results investigating the effects of selected chemicals on p53 expression showed a dose-dependent increase in active p53 levels. It was highly expressed in cells treated with mancozeb, maneb and rotenone at concentrations between 0.01mM-0.1mM (fig 4.9).The amount of p53 increased in a time-dependent manner. After a 24-hour treatment, it reached a plateau, and no further increase was observed (data shown for diquat, fig 4.10). There is a shortage of studies supporting the hypothesis that diquat may produce apoptosis in SH-SY5Y cells but studies using the structurally similar chemical paraquat suggest that it acts through a mechanism involving p53 and mitochondria (Yang and Tiffany-Castiglioni, 2008). Other studies have shown evidence of paraquat induced apoptosis in rat primary neurons (Kim *et al*., 2004b) and increased p53 levels in human lung epithelial-cells (Takeyama *et al*., 2004). It has been reported that p53 may promote cell death by regulating the expression of enzymes involved in controlling the redox state of cells (Polyak *et al*., 1997). In order to check if p53-induced changes arise from changes in free radical metabolism and altered mitochondrial function, cells were pre-incubated with NAC and tunicamycin before diquat treatment. But analysis of results showed no change in p53 expression level (fig 4.11). Studies examining the relationship between p53 and caspase activation have shown that caspases may be a component of the p53-induced cell death pathway and during genotoxic stress, p53 is needed for caspase activation (Cregan *et al*., 1999). These findings propose the presence of a common pathway involving p53, caspase activation, mitochondrial dysfunction and cytochrome c release (Morrison and Kinoshita, 2000). Results from this study have shown that pre-incubation with capase-3 and -9 inhibitors has no bearing on p53 expression levels (fig 4.11)

suggesting that caspase activation can thus be regulated by both p53-dependent and independent pathways.

Similarly, there was no change in the levels of phospo-Chk1 and phospo-Chk2 (data not shown), the cell-cycle check-points which are activated after DNA single strand breaks/bulky lesions and DNA double strand breaks, respectively (Reinhardt and Yaffe, 2009). Chk1 and CHk-2 mediated phosphorylation inhibits Cdc25 which is a positive regulator of cell cycle progression. Genotoxic stress causes phosphorylation of Chk-1 at Ser317 and Ser345 (Zhao *et al*., 2001) whereas DNA damage causes Chk-2 phosphorylation at Thr68 (Lee and Chung, 2001). Data from this study failed to detect changes in the levels of Chk1 (phosphorylated at serine 345) or endogenous levels of Chk2 when phosphorylated at threonine 68 (data not shown).

Other than apoptosis, necrosis may also occur in diseases like PD and Alzheimer's disease (Kitanaka and Kuchnio, 1999) but the involvement of RIP which is a serine-threonine kinase involved in NF-κB activation remains undetermined (Kelliher *et al*., 1998). RIP has been implicated in caspase-independent pathways and undergoes cleavage by caspase-8 forming two fragments, one smaller fragment and the other containing the entire kinase domain. Inhibition of the TNF-induced and NF-κB pathways is a result of RIP cleavage which also increases TNF-R1-associated death domain (TRADD) and FADD interactions, enhancing cell-death along the way (reviewed by Bárcia *et al*., 2003). FLICE-inhibitory protein (FLIP) mediates the recruitment and/or stabilisation of RIP (Kataoka *et al*., 2000) and blocks apoptosis by competing with caspase 8 (Thome *et al*., 1997). Therefore any imbalance in caspase 8, FLIP and RIP may regulate the levels of uncleaved RIP (Bárcia *et al*., 2003). To confirm RIP expression and cleavage, untreated and toxin treated SH-SY5Y cells were lysed for Western blot analysis. Results showed RIP expression (total, ~74kDa and cleaved 42kDa) in both control and treated cells. Densitometric analysis showed a dose-dependent increase in total RIP fragment in mancozeb treated cells but not in cleaved fragments. No change was observed after treatment with other chemicals.

Over expression of free α-synuclein can cause cytotoxicity in neuronal cell types like sympathetic neurons, dopaminergic neurons and human neuroblastoma cells (Li *et al*., 2009). It has been suggested that mutant and post-translationally modified α-synuclein may have a role in the degeneration of SN dopaminergic neurons in PD. Oxidatively damaged wild-type α-synuclein can mimic certain features of mutant α-synuclein (Hashimoto *et al*., 1999). Therefore, to gain better understanding about the relationship between α-synuclein and SH-SY5Y cells, the expression and distribution of α-synuclein was investigated. No significant changes in α-synuclein protein levels (both wild-type and phosphorylated) were detected after acute or chronic toxin exposure. A marginal but insignificant change in the level of α-synuclein was noticed after rotenone treatment but replication of these results failed. There was no evidence of α -synuclein up-regulation, which has been noticed after MPTP-induced apoptotic death in SNpc dopaminergic neurons (Vila *et al*, 2000). There is shortage of studies exploring the effects of pesticides like maneb and mancozeb on α-synuclein expression. However, studies using manganese (a component of both maneb and mancozeb) have shown induction of α-synuclein expression (Giltler *et al*., 2009) which can promote apoptosis in SH-SY5Y cells. α-synuclein is initially produced in the cell-body but as it is a synaptic-associated protein, it is rapidly transported to the nerve terminals (Withers *et al*., 1997). α-synuclein immunostaining was distributed diffusely with greater immunoreactivity in the cytoplasm which extended to neuronal processes. α-synuclein has a significant propensity to aggregate and PD-linked mutations or post-translational modifications caused by oxidative stress can enhance such aggregation (Conway *et al*., 1998; El-Agnaf *et al*., 1998). Chronic toxin treatment lasting 4 weeks failed to alter the levels of α-synuclein-positive staining. Most of α-synuclein-positive neurons had a healthy morphological appearance with no evidence of aggregation in the cell bodies.

In vivo PD animal studies show that DJ-1 has a neuroprotective effect in disease process (Inden *et al*., 2006) but the mechanism and signalling pathways that are central to its function have not been fully identified as it is implicated in a number of different biological processes ranging from being involved in the oxidative stress response, ROS quenching (Mitsumoto and Nakagawa, 2001), transcription modulation (Niki *et al*., 2003), functioning as a regulatory subunit of an RNA-binding protein (Hod *et al*., 1999) and having a possible role as a molecular

chaperone preventing α-synuclein aggregation (Shendelman *et al*., 2004). Previous studies show that DJ-1 can play a part in suppressing ROS-mediated neuronal apoptosis pathway after 6-OHDA exposure (Inden *et al*., 2006) but results from this study showed no change in DJ-1 protein levels after toxin exposure and its cellular localisation after chronic treatment remained unaltered (fig 4.19, 4.20).

A reduction in DA levels has been observed in Parkinson's disease (PD) patients. This makes tyrosine hydroxylase, the rate-limiting enzyme in dopamine synthesis, a critical player in dopamine control. As well as acting as a dopaminergic cell-marker it plays a role in regulating the production of dopamine, which if over-produced can elevate the levels of ROS leading to degeneration of dopaminergic neurons (Miyazaki and Asanuma, 2008). To detect the TH protein following toxin treatment, a similar procedure was used. SH-SY5Y cells transfected with human tyrosine hydroxylase isoform 1 have proven to be more resistant to cell death induced by hydrogen peroxide and 6-OHDA. This may suggest an increased antioxidant activity if its levels are increased in the cell (Franco *et al*., 2010). Results from western blotting showed no change in TH levels after 24 hour treatment. Similarly, no morphological changes were observed in chronically treated cells. These cells exhibited distinct neuronal morphological features including increased neurite length and enhanced branching of neuronal processes, in keeping with their dopaminergic phenotype.

Neurofilaments (NFs) are part of the cytoskeleton and provide stability and help maintain neuronal structure. Newly formed unphosphorylated NFs are transported to the axons, a process which causes their phosphorylation (Nixon *et al*., 1987). Any change in NF structure disrupts axonal transport, conduction speed or cause degeneration (Pant and Veeranna., 1995; Schlaepfer *et al*., 1987). Such effects have been observed after traumatic brain injury which results in reduced NF immunoreactivity and/or loss of neuronal cytoskeletal proteins (Posmantur *et al*., 1994; Saatman *et al*., 1998). Neuronal cytoskeletal alterations are visible in many neurodegenerative disorders. Accumulation of phosphorylated neurofilaments in the perikarya has been observed in Alzheimer's disease (Cork *et al*., 1986) and Parkinson's disease (Forno *et al*., 1986). In order to investigate if acute toxin treatment alters NF architecture and adversely affects survival of SH-SY5Y cells, a pan-neurofilament antibody which reacted with NF-low, NF-medium and NF-high

molecular weight sub-unit was used. Antibody predominantly stained the cytoplasm and cell-processes (fig 4.23). Overall NF immunoreactivity was lower in treated cells which mostly showed staining around the nucleus in the cell-body with very minimal staining in neurites. Neurofilament subunits have been detected in Lewy bodies (Galvin *et al*., 1999) but results from this study showed no evidence of aggregated bodies in cells.

In summary, results from this study suggest that agrochemical treatment causes cell death through caspase independent mechanisms which also involve RIP. Induction of cell-death marker such as PARP-1 occurred independent of caspase involvement as observed through absence of any effect of caspase inhibitors and can be a late event in agrochemical treated cells. Examination of nuclear morphology after maneb, mancozeb, diquat, rotenone and epoxiconazole treatment showed nuclear condensation and therefore suggests involvement of either apoptosis or necrosis. Levels of proteins associated with PD such as α-synuclein and DJ-1 remained unchanged after agrochemical treatment. Although a change in neurofilament staining was observed after acute toxin treatment, SH-SY5Y cells labelled with tyrosine hydroxylase, DJ-1 and α-synuclein showed normal staining after 4 week exposure, cells appeared in healthy condition suggesting that long term low dose exposure does not affect cell-structure or function.

Chapter Five: Toxin treatment and Autophagy

5.1.1 Introduction:

Autophagy is a cellular protective mechanism which degrades organelles and molecules and produces energy and amino acids for protein synthesis (Bresden *et al*., 2006). It involves degradation of biological macromolecules through different mechanism such as i) microautophagy which directly fuses small amounts of cytosol or specific proteins with the lysosomes, ii) macroautophagy (generally referred to as autophagy) which involves vesicle formation which results in subsequent degradation of proteins and entire organelles by lysosomes and iii) chaperone-mediated autophagy (CMA) which involves direct import of target proteins across the lysosomal membrane (Wang and Levine, 2010). A number of different signalling pathways involving tyrosine kinase receptors, casein kinase II (Holen *et al*., 1993), MAP kinases (Häussinger *et al*., 1999) and calcium (Gordon *et al*., 1993) control autophagy. Nutrient starvation, depletion of total amino acids and inhibition of the mammalian target of rapamycin (mTOR) are among several stimuli which can induce macroautophagy. Autophagy is active at a low level and is markedly up-regulated by starvation and nutrient or growth factor deprivation. Once nutrients are withdrawn, mTOR is inactivated which in turn activates the ATG complex. The autophagic process involves the formation of an isolation membrane from a pre-autophagosomal structure which encloses and sequesters different cytoplasmic materials such as endoplasmic reticulum, ribosomes, mitochondria, membrane lipids and proteins to form an autophagosome. The fusion of the autophagosome with a lysosome leads to the formation of an autolysosome which degrades the sequestered material to generate energy (Levine and Yuan, 2005). Nutrient deprivation triggers a response in starvation-induced autophagy and upstream signals like VPS34 (a class III PI3K) complexed with Atg6 (beclin-1) regulate bulk phase starvation (Tassa *et al*., 2003). Genetic screening of *Saccharomyces cerevisiae* and other fungi has led to the discovery of nearly 17 *ATG* (autophagy-related) genes which are actively involved in this catabolic process (Klionsky *et al*., 2003; Reggiori and Klionsky, 2002). The discovery of their homologues in eukaryotic organisms has provided information on the function of their gene products such as the conjugation of Atg5/Atg12 proteins which plays a part in autophagy initiation, and Atg8 (ubiquitin-like protein) which is involved in the formation of the autophagosome membrane (Zhu *et al*., 2007).

Autophagic pathways are implicated in neurodegenerative diseases like Parkinson's disease (Cheung, 2009), Huntington's disease (Qin *et al*., 2008) and Alzheimer's disease (Nixon *et al*., 2003). Autophagolysosomal alterations such as up-regulation of lysosomal enzymes and granulovacuolar degeneration have been observed in Alzheimer's disease (Stadelmann *et al*., 1999) and studies of PD/Lewy body disease cases reveal increased nigral autophagic vacuoles (AV) (Anglade *et al*., 1997). Indeed, analysis of PD brain shows deregulation of autophagy (Levy *et al*., 2009). The first evidence in support of autophagy in PD came from the macroautophagic and chaperone-mediated autophagic degradation of α-synuclein (Webb *et al*., 2003; Cuervo *et al*., 2004). Inhibition of chaperone-mediated autophagy (CMA) forms detergent-insoluble and high molecular-weight species of α-synuclein (Vogiatzi *et al*., 2008). The pathogenic A53T and A30P α-synuclein mutants act as uptake blockers and bind to CMA receptor (LAMP2A) on the lysosomal membrane and inhibit their own degradation and that of other cytosolic proteins destined for CMA which may further contribute to cellular stress (Cuervo *et al*., 2004). Kabuta et al (2008) have demonstrated that UCH-L1 physically interacts with LAMP-2A and other components of the CMA pathway including Hsc70 and Hsp90. The mutant UCH-L1 containing I93M mutation showed enhanced affinity for LAMP-2A and Hsc70 and induced a CMA inhibition-associated increase in the level of α-synuclein.

Neurodegeneration can be caused by the knock down of *ATG* genes or molecules required for the induction and execution of macroautophagy (Komatsu *et al*., 2006; Hara *et al*., 2006). Loss of autophagy in the CNS or the suppression of basal autophagy in neural cells fail to clear protein aggregates and cytoplasmic inclusions which causes cell-death. This is evident in animal models where *ATG7* conditionally null mice show ubiquitin-positive aggregates and damaged mitochondria (Komatsu *et al.,* 2005). Similarly, beclin-1 null mice deficient in autophagy die early in embryogenesis (Yue *et al*., 2003).

5.1.1.1 Aims:

Limited data are available showing how chemical exposure is linked with autophagy but some studies have shown that an autophagic response can be generated using MPP+ exposure in primary dopaminergic neurons and SH-SY5Y cells (Zhu *et al*., 2007). The autophagy gene *ATG5* is a critical protein needed at the stage of autophagosome-precursor synthesis. Previous studies have shown that its deletion in yeast or mammalian cells/mice effectively blocks autophagy (Kametaka *et al.,* 1996; Kuma *et al.,* 2004). Similarly, its down-regulation in HeLa cells can reduce cell death and vacuole formation induced by IFN-γ (Pyo *et al.,* 2005). Therefore, the aim of this study was to investigate the effect of the selected chemicals on SH-SY5Y cells after siRNA knockdown of *ATG5*, expression of lysosomal aggregation after acute 24 hour toxin exposure and cell-viability of toxin treated SH-SY5Y cells after transfection of plasmid DNA.

5.1.2 Methods:

Refer to materials and methods (section 2.3).

5.1.3. Results:

5.1.3.1 ATG5 siRNA transfection/Lentiviral Particles Transduction:

Previous studies indicate that autophagy can be abolished by complete knockout of *ATG5* and formation of autophagic vacuoles can be reduced through lower Atg protein expression (Hosokawa *et al*., 2006). Autophagy proteins play a vital role in stress-induced cell-death and ATG gene knock down can regulate autophagy to a certain extent. *ATG5* siRNA knockdown using 'Dharmacon® Accell ™ delivery protocol' significantly reduced Atg5 protein expression to 40% of untransfected control (fig 5.1a, b) and completely blocked LC3-II expression (fig 5.1c). Lentiviral transduction was not successful and knockdown of RAD51 protein (used as a positive control for siRNA knockdown) in SH-SY5Y and HeLa cells failed to alter its expression (fig 5.1d). Therefore, Dharmacon® protocol was preferred as a method of choice.

Fig 5.1: ATG5 knockdown efficiency in SH-SY5Y cells: A-B) ATG5 protein levels were measured using western blotting and ATG5/GAPDH ratio showed a decrease of ~40% in ATG5 levels in siRNA transfected cells after 72 hours. C) LC3 (16kDa) bands were only visible in H_2O_2 (0.5mM) treated cells (positive control). D) Lentiviral transduction for RAD51 in SH-SY5Y and HeLa cells was unsuccessful.

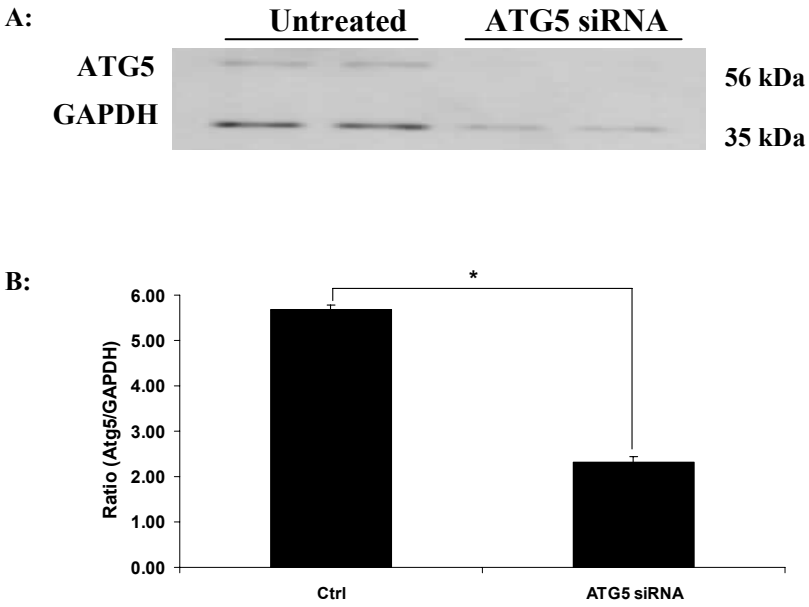

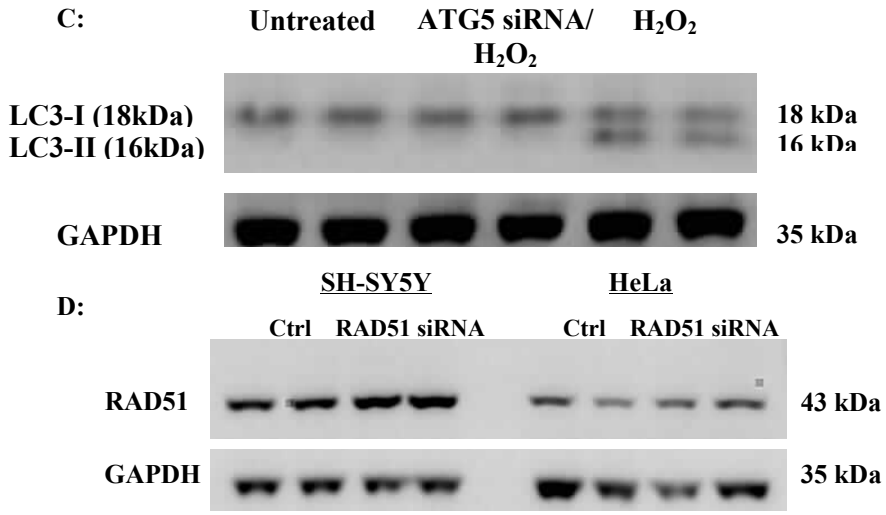

A significant decrease *(*p<0.05)* in Alamar Blue reduction was noticed in siRNA transfected cells (74.4%±2.5 of untreated controls) after 24 hours (fig 5.2a) but western blotting showed no decrease in Atg5 protein level at this stage (fig 5.2b). After 48 hours cell-viability of siRNA treated cells was still significantly lower than controls (67.2%±3.2 of controls) but a significant reduction in protein levels was evident, showing that at least 48 hours are required for knockdown to take effect. At the 72 hour time point, there was no further decrease in Alamar Blue reduction (75%±2.2 of controls) but further significant reduction in Atg5 levels.

Fig 5.2: Alamar Blue reducing capacity of ATG5 KO SH-SY5Y cells: A) Percentage Alamar Blue reduction in mock vs. siRNA treated cells calculated at 24, 48 and 72 hours after transfection. B) Cells were extracted in native lysis buffer and ATG5/GAPDH protein ratios measured after western blotting.

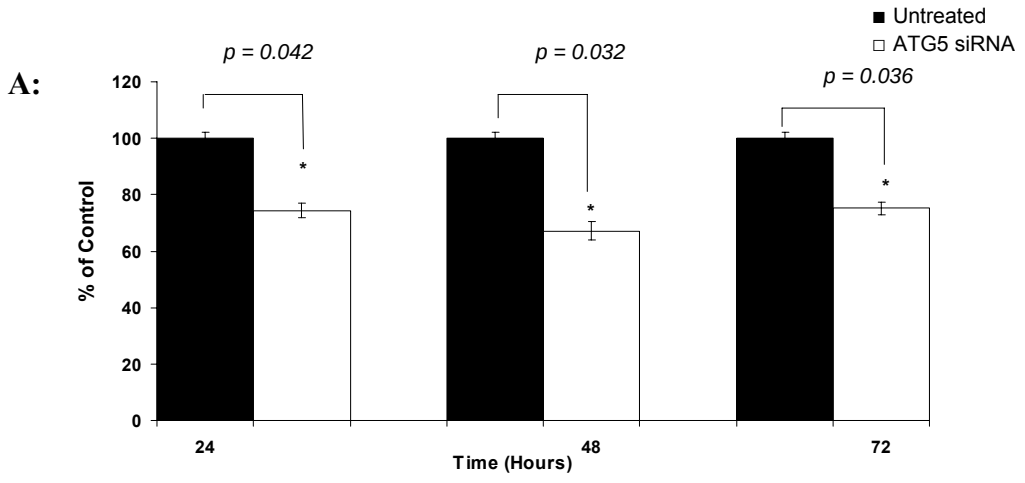

B:

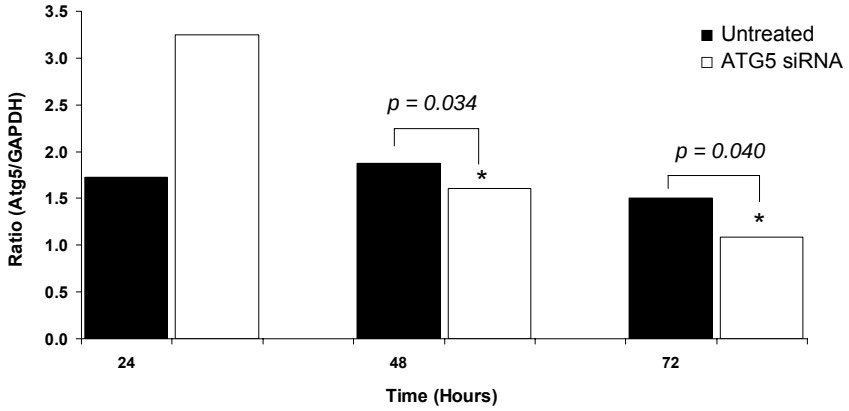

5.1.3.2 ATG5 knockdown and toxin treatment:

In order to investigate if toxin treatment has an effect on Atg5 protein levels, selected chemicals were added to SH-SY5Y cells 72 hours after siRNA transfection. Cell viability was measured after 24 hours (96hrs total) and overall results indicated no significant increase or reduction *(*$p<0.05$*)* in cell-viability or Atg5 levels in cells treated with diquat, rotenone, MPP+, epoxiconazole, maneb and mancozeb. Alamar Blue reduction assay showed that *ATG5* siRNA knockdown was unable to attenuate the toxicity by selected chemicals (fig 5.4, 5.5). Successful *ATG5* knockdown was not achieved in all experiments and this remained a recurring problem. In experiments where *ATG5* was successfully knocked down (fig 5.3) protein levels remained unchanged after toxin treatment (data shown for diquat (0.1mM) and rotenone (0.05mM).

Fig 5.3: *ATG5* knockdown and toxin treatment: A-D: Cell extracts from siRNA (72 hours) and toxin treated cells (diquat at 0.1mM and rotenone at 0.05mM) for 24 hours were probed for ATG5 knockdown. Densitometric analyses of untreated and ATG5 knockdown bands were calculated using ImageJ 1.38x software and data are shown as arbitrary units (mean±SD; $n=3$;*$P<0.05$).

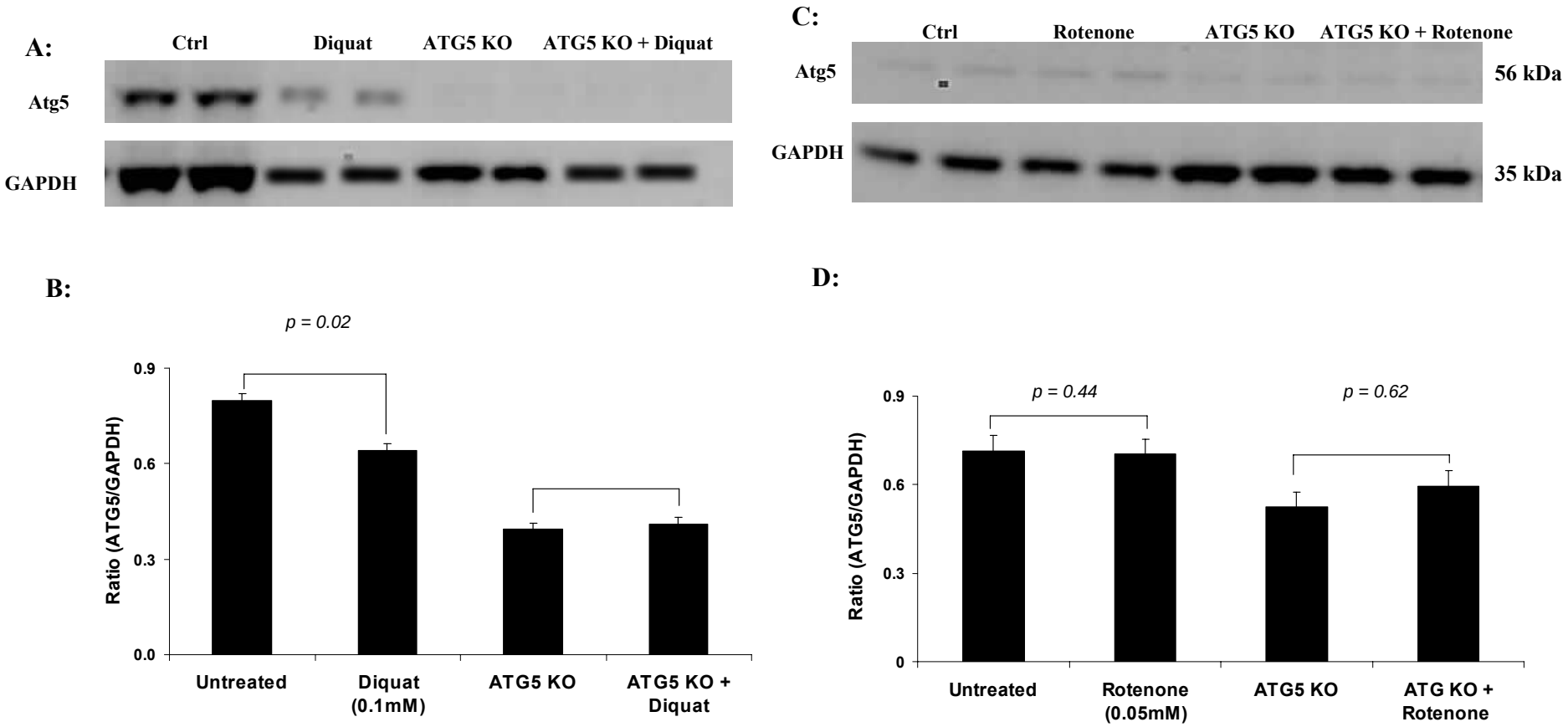

Fig 5.4: ATG5 siRNA treatment and cell-viability in toxin treated cells: Alamar Blue reduction assay showed that ATG5 siRNA knockdown was unable to attenuate toxicity by A) diquat, B) rotenone and C) MPP+ (n = 3, ±SD, *p<0.05).

A:

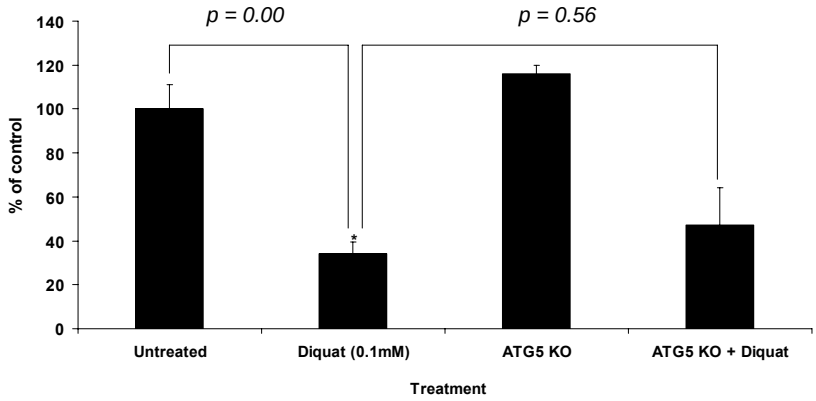

B:

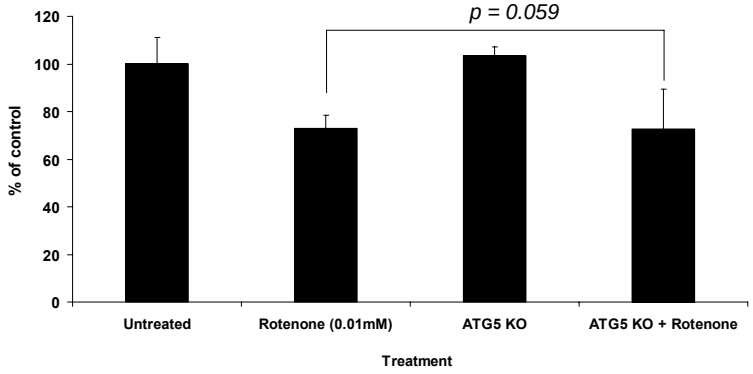

C:

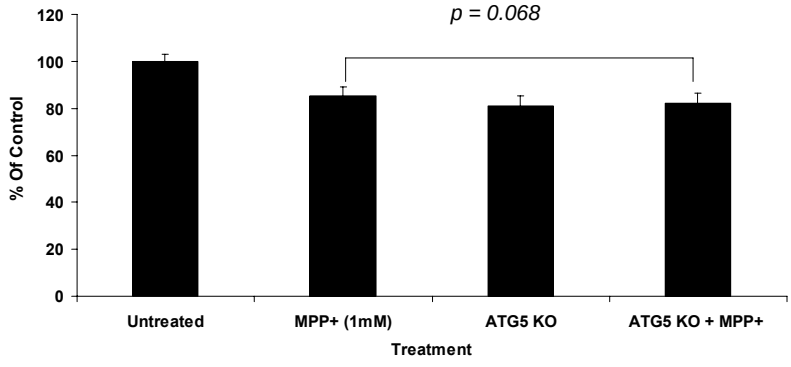

Fig 5.5: ATG5 siRNA treatment and cell-viability in toxin treated cells: Alamar Blue reduction assay showed that ATG5 siRNA knockdown was unable to attenuate toxicity by A) epoxiconazole, B) maneb and C) mancozeb (n = 3, ±SD, *p<0.05).

A:

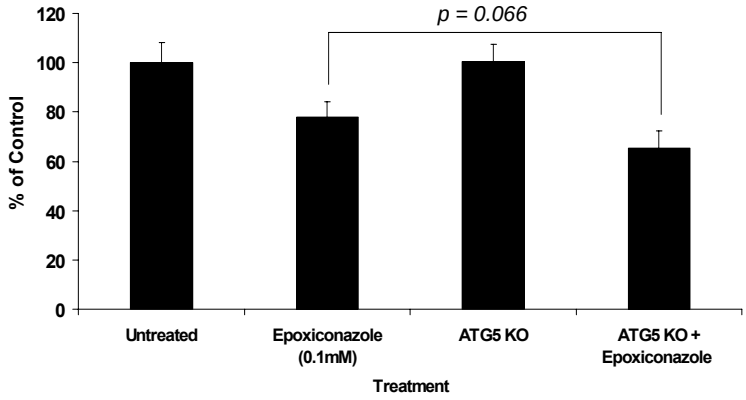

B:

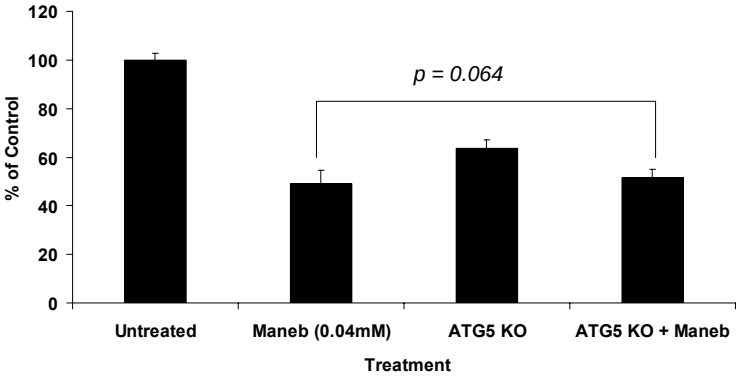

C:

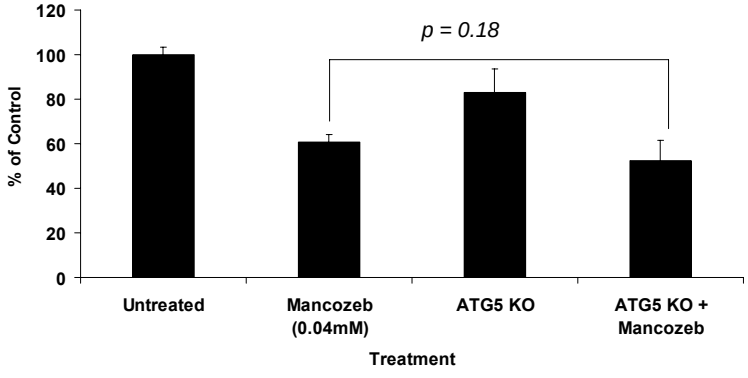

5.1.3.3 Changes in protein expression after acute toxin exposure:

Protein expression using western blotting of SH-SY5Y cells after 24 hour toxin treatment showed no significant change in the level of Atg5 protein or LC3 level (data not shown, $*P<0.05$) (fig 5.6 A-E) except diquat which showed a highly expressed LC3 (16kDa) band at 0.1mM dose (fig5.6C).

Fig 5.6: Toxin induced changes in Atg5 levels: SH-SY5Y cells were treated with different toxins i.e. A) maneb, B) mancozeb, C) diquat, D) MPP+ and E) rotenone for 24 hours after which cell extracts were probed for Atg5 protein (Each image is representative of 3 experiments).

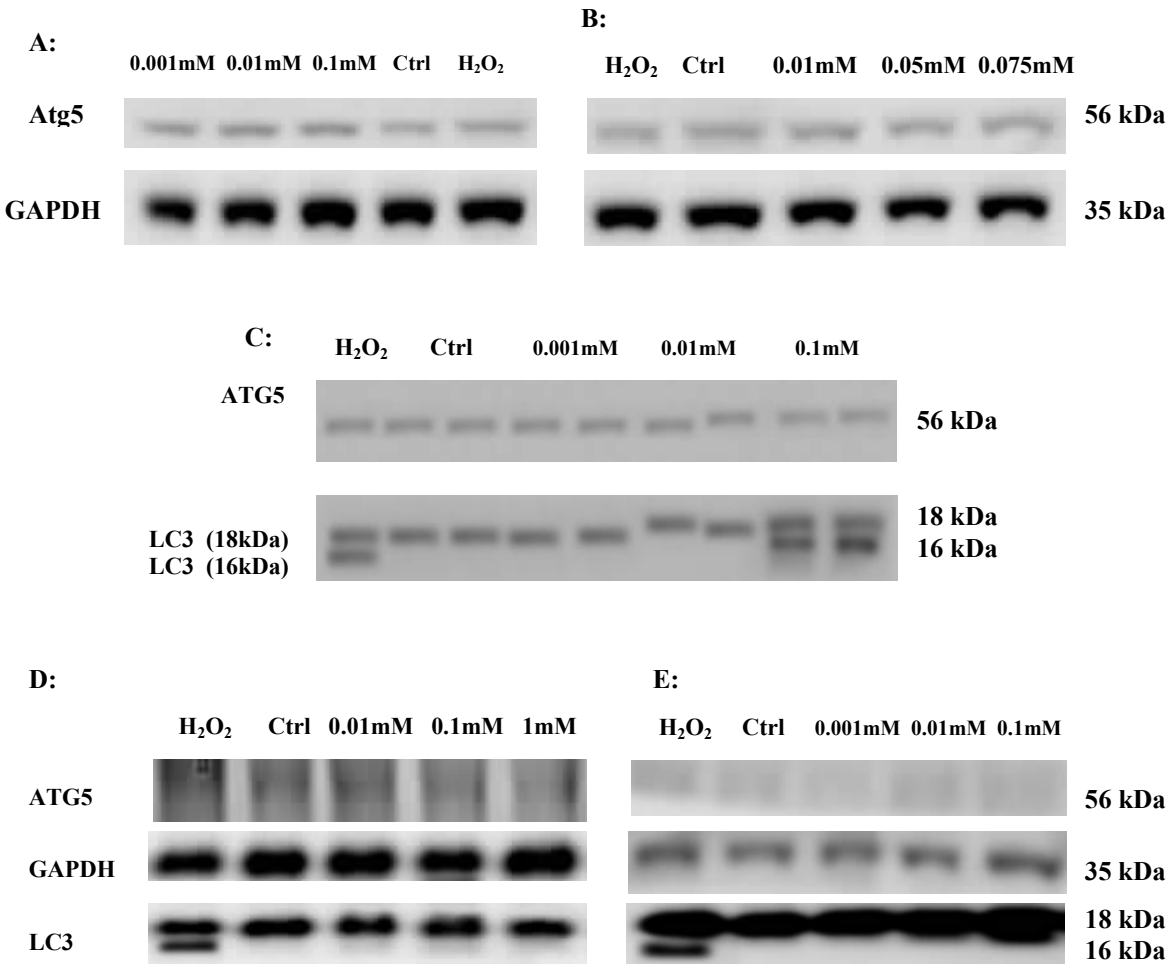

Similarly, beclin-1 levels were measured after 24 hour toxin exposure and results showed a significant increase (*P<0.05) in beclin-1 levels with maneb 0.001mM, 0.01mM (fig 5.7 A-B) and reduction with mancozeb at 0.01mM (fig 5.8 C-D). A dose and time related increase in beclin-1 was observed with diquat treatment. 0.1mM dose showed a significantly increased beclin-1 band (fig 5.9 A-B). Beclin-1 expression in SH-SY5Y cells treated with 0.1mM diquat and examined at different time points showed a significant increase ($p<0.05$) after 4 hours (fig 5.9 C-D). Different doses of MPP+ (0.01mM-1mM) (fig 5.8A) and rotenone (0.001mM-0.1mM) (fig 5.8 B) did not have any effect on beclin-1 levels.

Fig 5.7: Toxin induced changes in beclin-1 levels: SH-SY5Y cells were treated with different doses of maneb (A, B) for 24 hours after which cell extracts were probed for beclin-1 protein (* = $p < 0.05$ compared with untreated control).

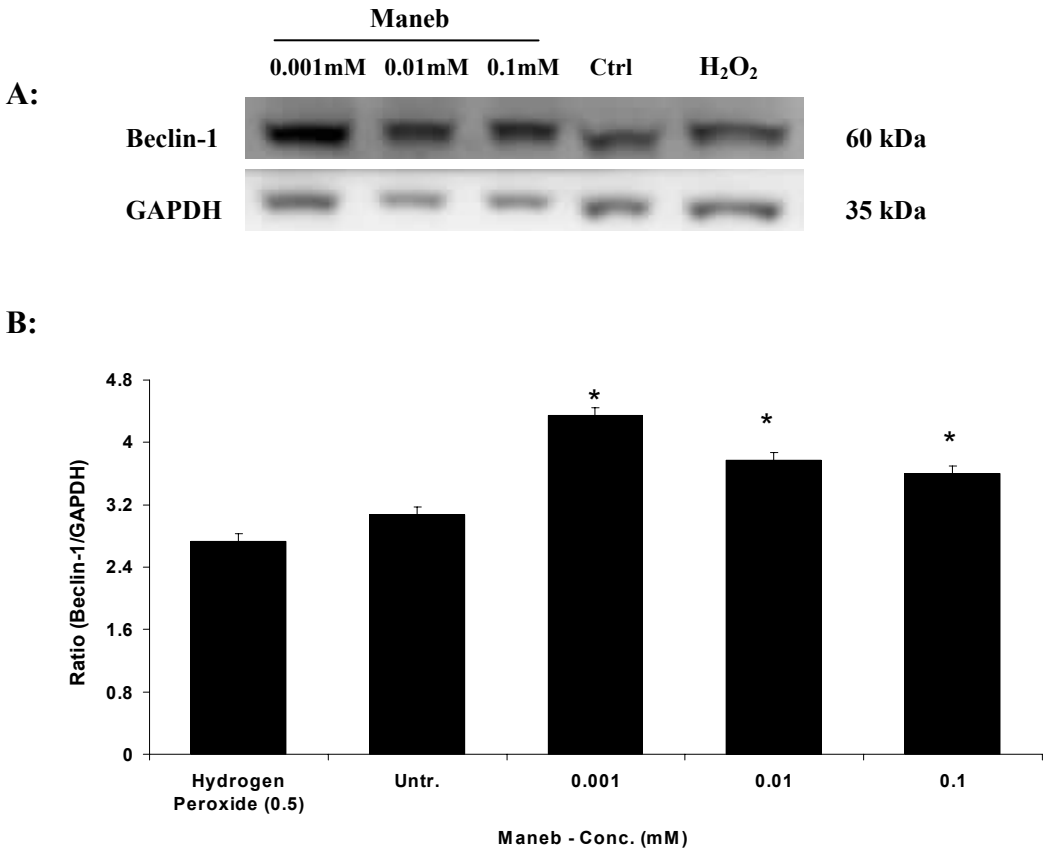

Fig 5.8: Toxin induced changes in beclin-1 levels: SH-SY5Y cells were treated with different doses of MPP+ (A), rotenone (B) and mancozeb (C, D) for 24 hours after which cell extracts were probed for beclin-1 protein (* = $p < 0.05$ compared with untreated control).

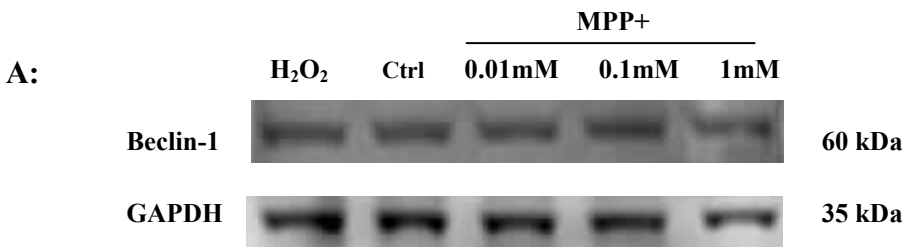

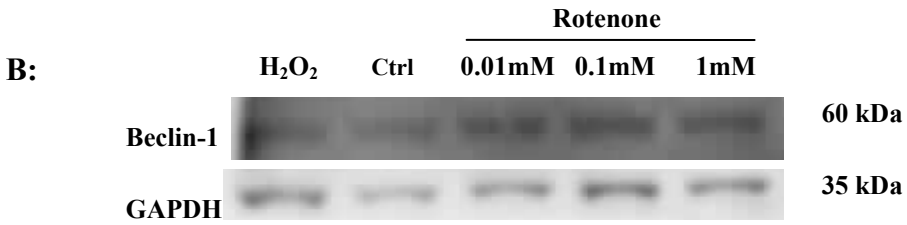

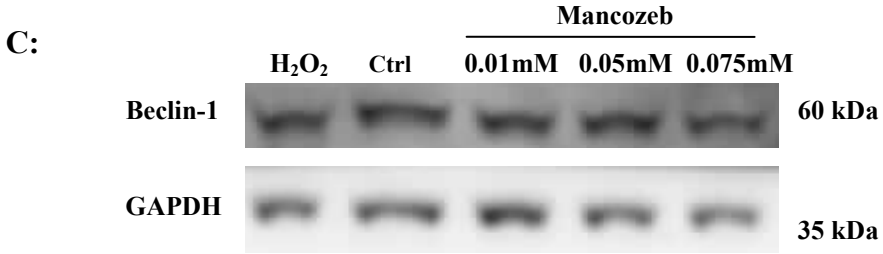

D:

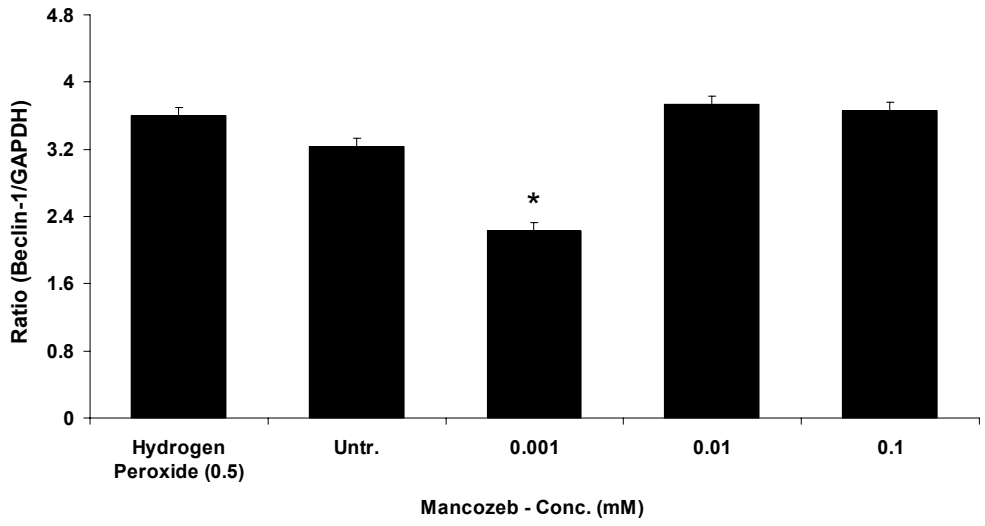

Fig 5.9: Toxin induced changes in beclin-1 levels: SH-SY5Y cells were treated with diquat (A-D) for 24 hours after which cell extracts were probed for beclin-1 protein (* = $p < 0.05$ compared with untreated control).

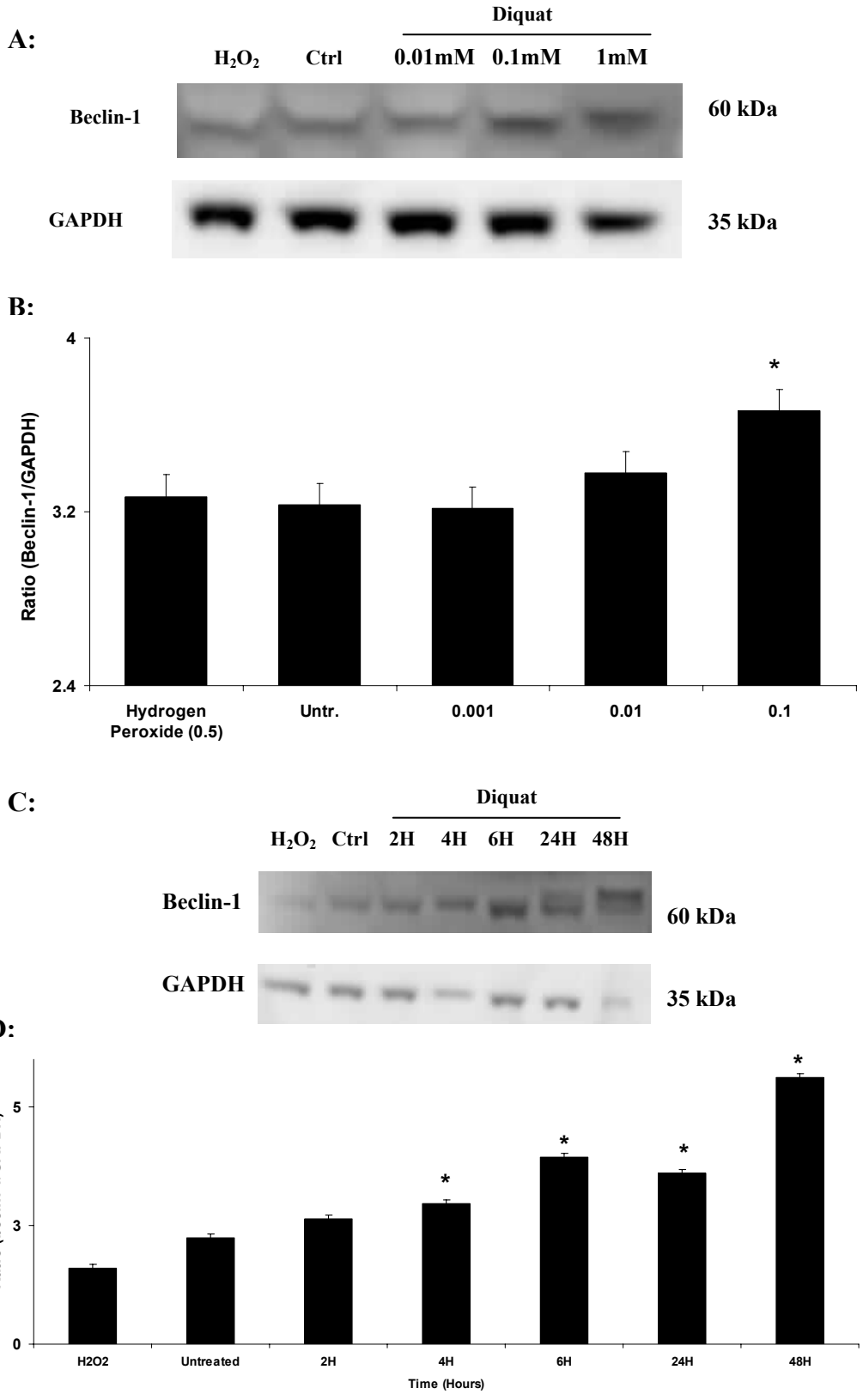

Lysosome-associated membrane proteins-1 and -2 (LAMP1, LAMP2) are lysosome specific transmembrane proteins required for autophagolysosome formation (González-Polo *et al*., 2005). It has been suggested that down-regulation of LAMP1/2 can increase sensitivity to lysosome mediated cell death (Fehrenbacher *et al*., 2008). LAMP1 levels were measured after 24 hour toxin exposure and results showed a significant increase ($p<0.05$) in LAMP1 levels after maneb (0.001mM, 0.01mM and 0.1mM) (fig 5.10 A-B) and mancozeb (0.01mM, 0.05mM and 0.075mM) treatment (fig 5.11 A-B). No such effect was observed after diquat (0.001mM, 0.01mM and 0.1mM) (fig 5.11 C), MPP+ (0.01mM, 0.1mM and 1mM) (fig 5.11 D) and rotenone treatment (0.001mM, 0.01mM and 0.1mM) (fig 5.12).

Fig 5.10: Toxin induced changes in LAMP-1 levels: SH-SY5Y cells were treated with different doses of maneb (A-B) for 24 hours after which cell extracts were probed for LAMP-1 protein (* = $p < 0.05$ compared with untreated control).
.

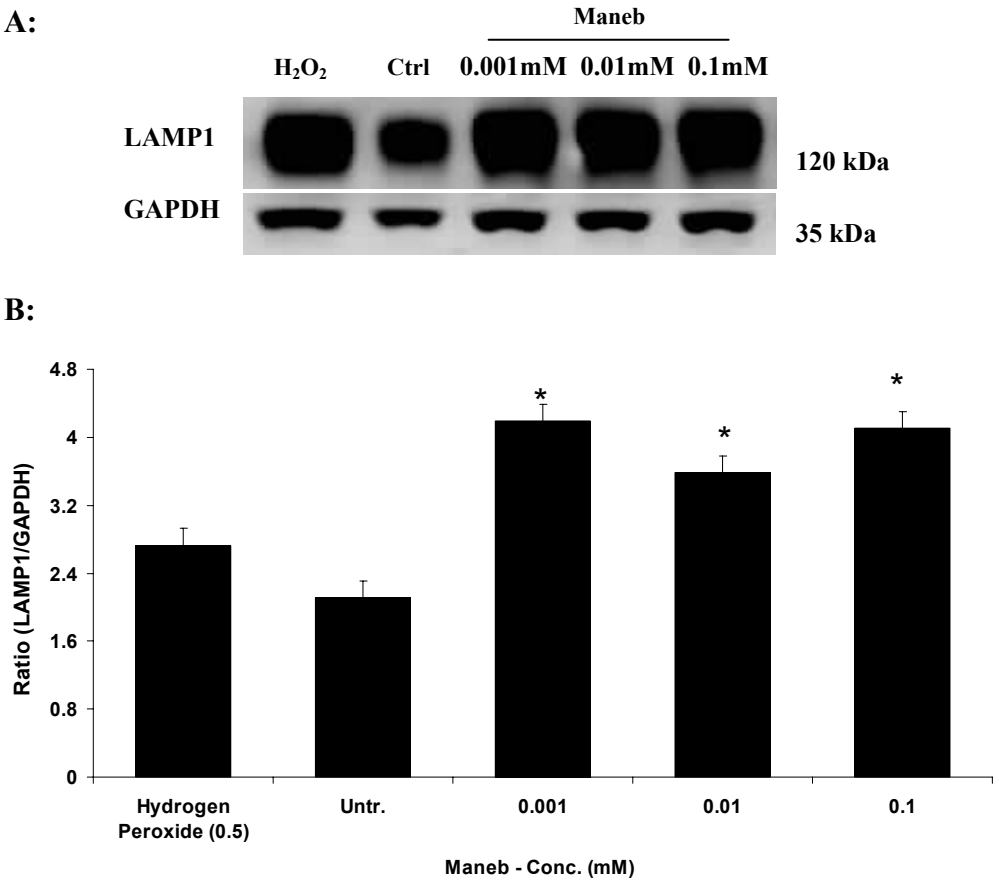

Fig 5.11: Toxin induced changes in LAMP-1 levels: SH-SY5Y cells were treated with different doses of mancozeb (A-B), diquat (C) and MPP+ (D) for 24 hours after which cell extracts were probed for LAMP-1 protein (* = $p < 0.05$ compared with untreated control).

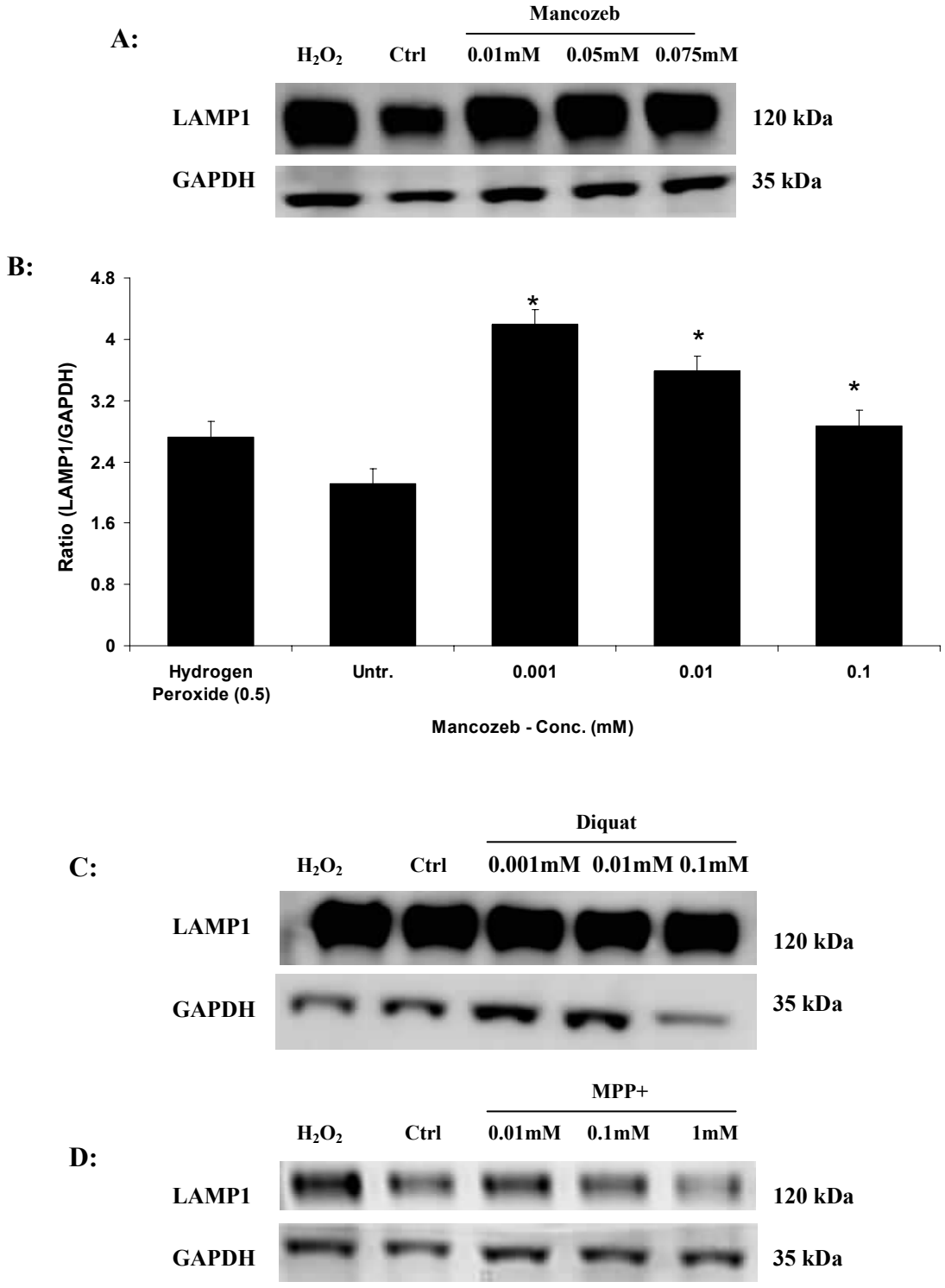

Fig 5.12: Toxin induced changes in LAMP-1 levels: SH-SY5Y cells were treated with different doses of rotenone for 24 hours after which cell extracts were probed for LAMP-1 protein (* = $p < 0.05$ compared with untreated control).

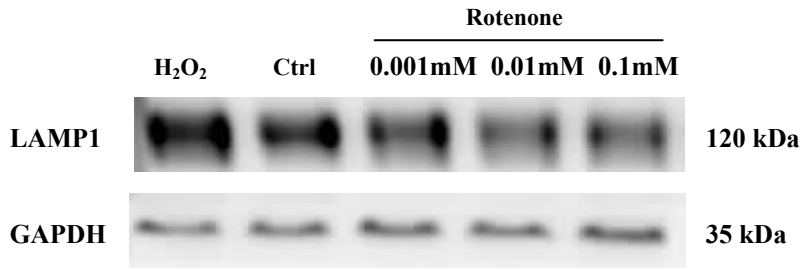

LAMP2 levels measured after 24 hour toxin exposure showed a significant increase ($p<0.05$) after high dose maneb (0.1mM) (fig 5.13 A-B) and mancozeb (0.075mM) treatment (fig 5.14 A-B). No such effect was observed after diquat (0.001mM, 0.01mM and 0.1mM) (fig 5.14 C), MPP+ (0.01mM, 0.1mM and 1mM) (fig 5.14 D) and rotenone treatment (0.001mM, 0.01mM and 0.1mM) (fig 5.15).

Fig 5.13: Toxin induced changes in LAMP-2 levels: SH-SY5Y cells were treated with different doses of maneb (A-B) for 24 hours after which cell extracts were probed for LAMP-2 protein (* = $p < 0.05$ compared with untreated control).

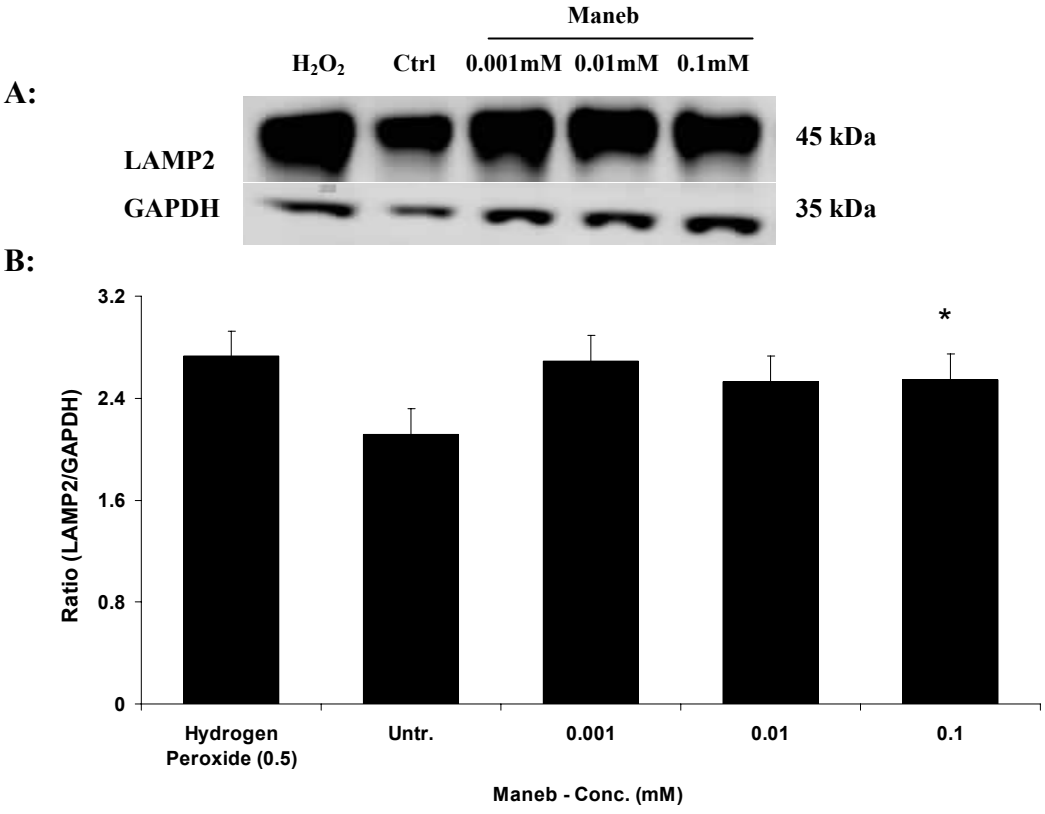

Fig 5.14: Toxin induced changes in LAMP-2 levels: SH-SY5Y cells were treated with different doses of mancozeb (A-B), diquat (C) and MPP+ (D) for 24 hours after which cell extracts were probed for LAMP-2 protein (* = $p < 0.05$ compared with untreated control).

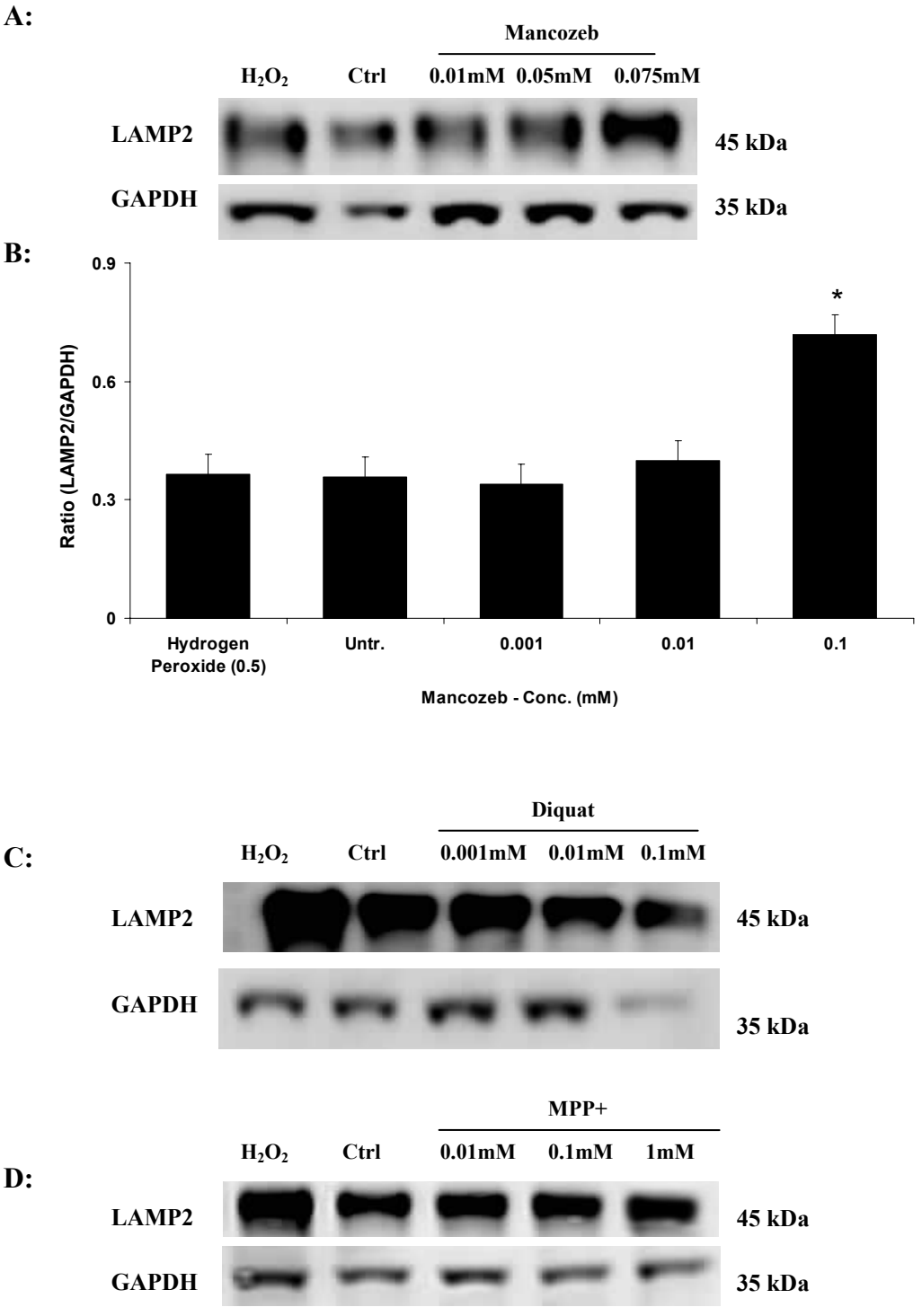

Fig 5.15: Toxin induced changes in LAMP-2 levels: SH-SY5Y cells were treated with different doses of rotenone for 24 hours after which cell extracts were probed for LAMP-2 protein (* = $p < 0.05$ compared with untreated control).

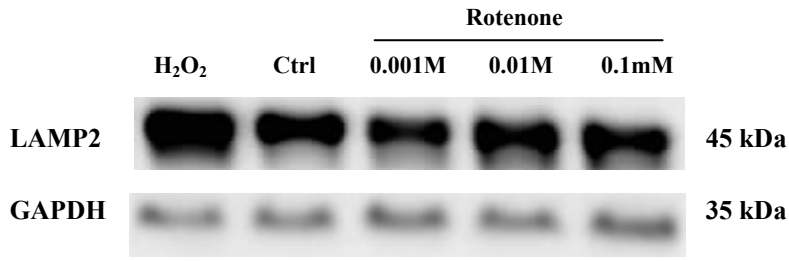

5.1.3.4 Toxin exposure and lysosomal aggregation:

Lysosomes play an important part in the clearance of autophagosomes and if this mechanism fails, the activation of autophagy can result in build up of debris which may cause cellular toxicity. This scenario may occur naturally with aging as well as in PD and other neurodegenerative disorders (Levine and Kroemer, 2008). To investigate the distribution of lysosomal aggregates after toxin treatment, SH-SY5Y cells were incubated with LysoTracker® red DND-99 a fluorescent acidotropic dye used to label acidic organelles (LysoTracker® and LysoSensor™ Probes, Invitrogen). 24 hour treatment including exposure to H_20_2 (0.1mM), diquat (0.1mM), maneb (0.05mM), mancozeb (0.05mM), rotenone (0.05mM) and MPP+ (0.05mM) (fig 5.16 A, B) appeared to show a higher number of circular cytoplasmic aggregates whereas paraquat (0.1mM) exhibited a relatively low number of such aggregates. Media-treated control cells showed a uniform distribution of fluorescent bodies in the cytoplasm whereas the toxin-treated cells exhibited abundant aggregates distributed throughout the cell body. Aggregate formation was dose and time dependent as cells exposed to diquat and maneb for 24 hours showed a relatively smaller number of stained bodies when treated with 0.001mM but the number of these increased when treated at 0.1mM (fig 5.17). Cells visualised at 4 and 6 hours after diquat (0.1mM) and rotenone (0.05mM) treatment did not show significantly higher number of aggregates when compared with cells treated for 24 hours (fig 5.18).

Fig 5.16A: Localisation of lysosomal aggregates after toxin treatment: Treatment with diquat (0.1mM), maneb (0.05mM) and rotenone (0.05mM) for 24hrs resulted in the formation of lysosomal aggregates which were stained with LysoTracker® red DND-99 and viewed under fluorescent microscope (magnification = x40; each image is representative of three independent fields. Selected cells magnified to show aggregation pattern).

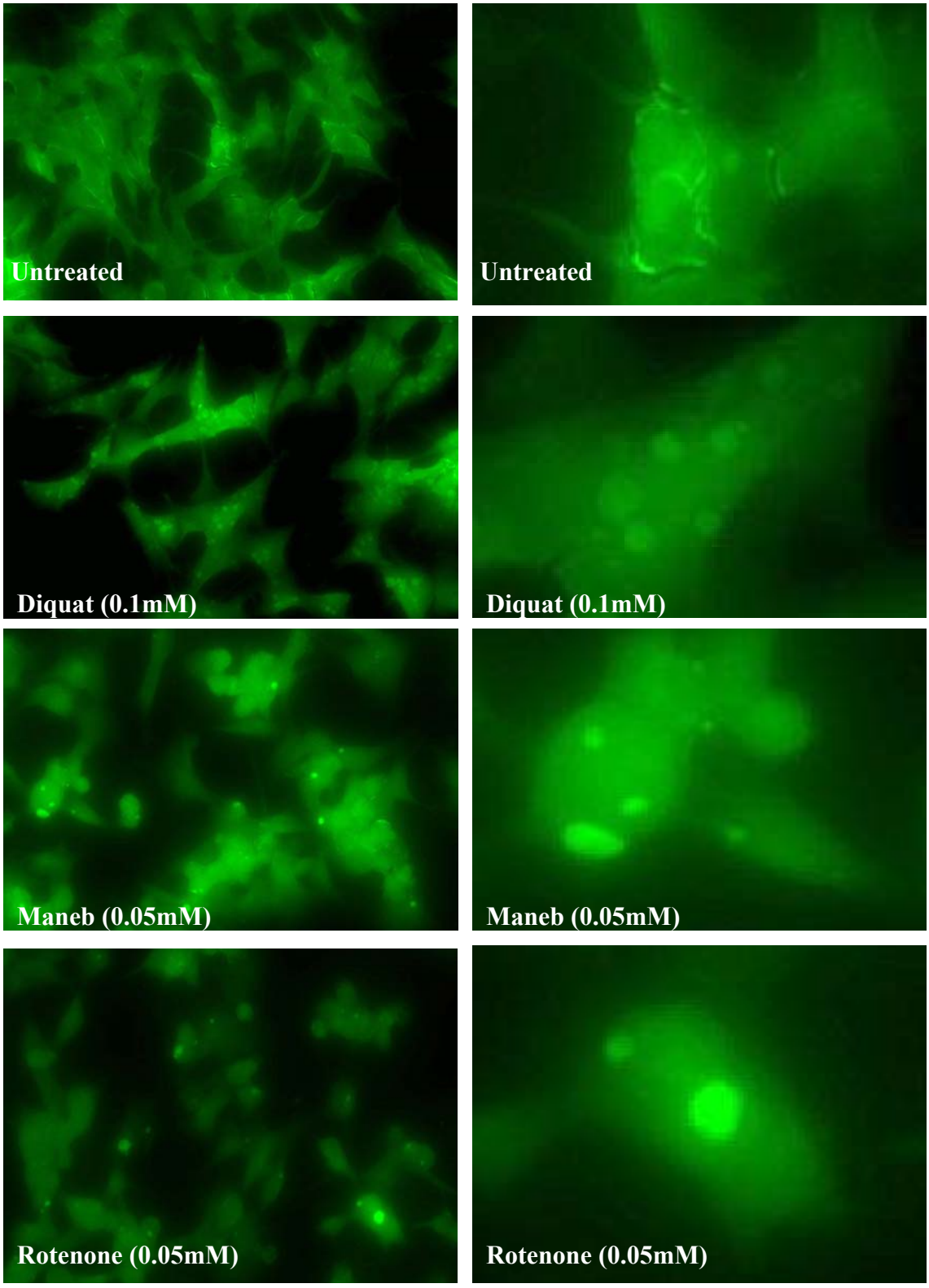

Fig 5.16B: Localisation of lysosomal aggregates after toxin treatment: Treatment with hydrogen peroxide (0.1mM), paraquat (0.1mM), mancozeb (0.05mM) and MPP+ (0.5mM) for 24hrs. LysoTracker® red DND-99 staining viewed under fluorescent microscope (magnification = x40; each image is representative of three independent fields. Selected cells magnified to show aggregation pattern).

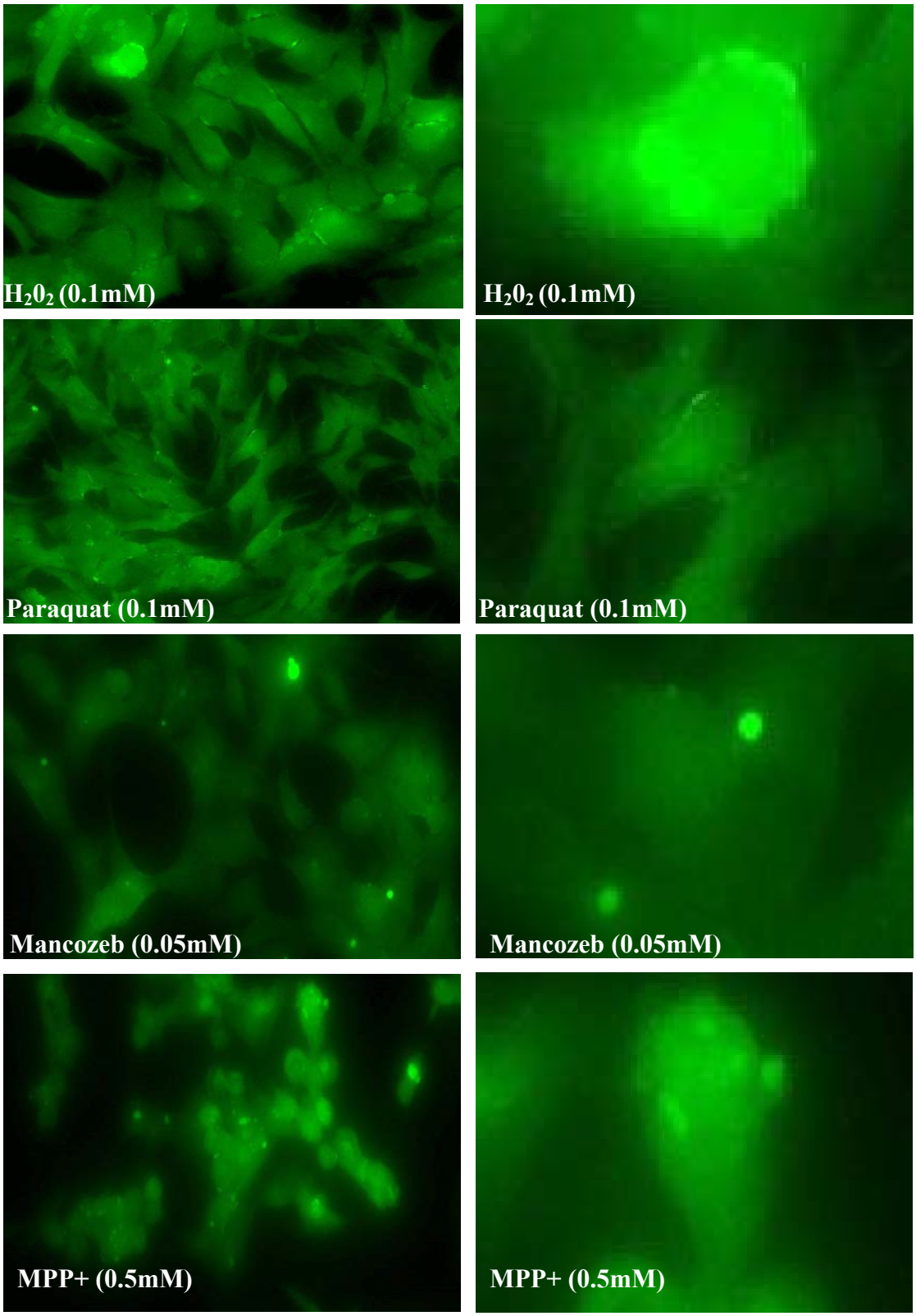

Fig 5.17: Dose dependent increase in lysosomal aggregates after toxin treatment: Large lysosomal aggregates were observed after SH-SY5Y cells treatment with diquat and maneb at 0.1mM after 24 hours, compared with 0.001mM treatment (magnification = x60; each image is representative of three independent fields. Selected cells magnified to show aggregation pattern).

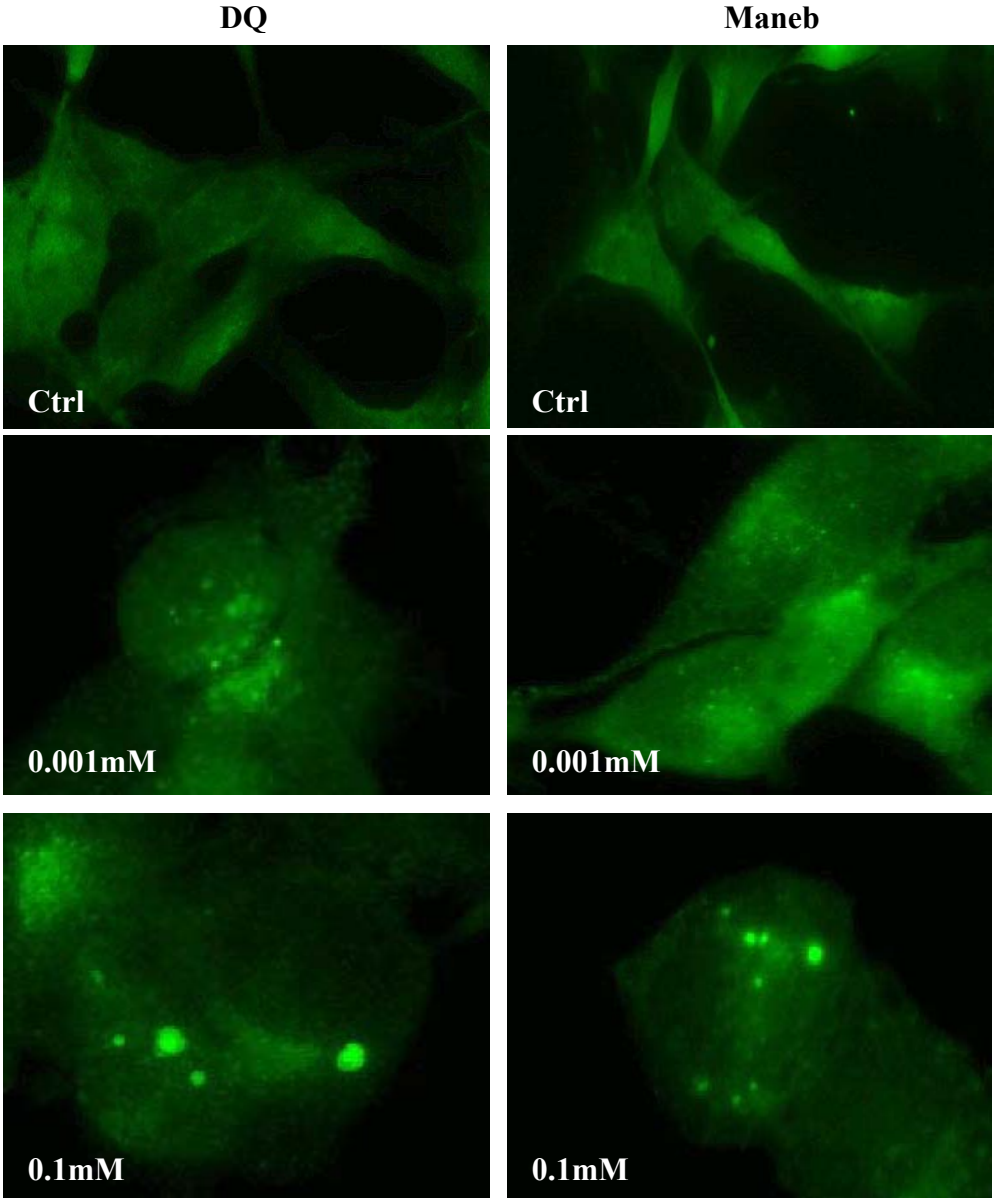

Fig 5.18: Time dependent increase in lysosomal aggregates after toxin treatment: High numbers of large lysosomal aggregates were observed after SH-SY5Y treatment with diquat and rotenone at 0.1mM and 0.05mM respectively after 24 hours, compared with shorter exposure lasting 4 and 6 hours (magnification = x40, each image is representative of three independent fields).

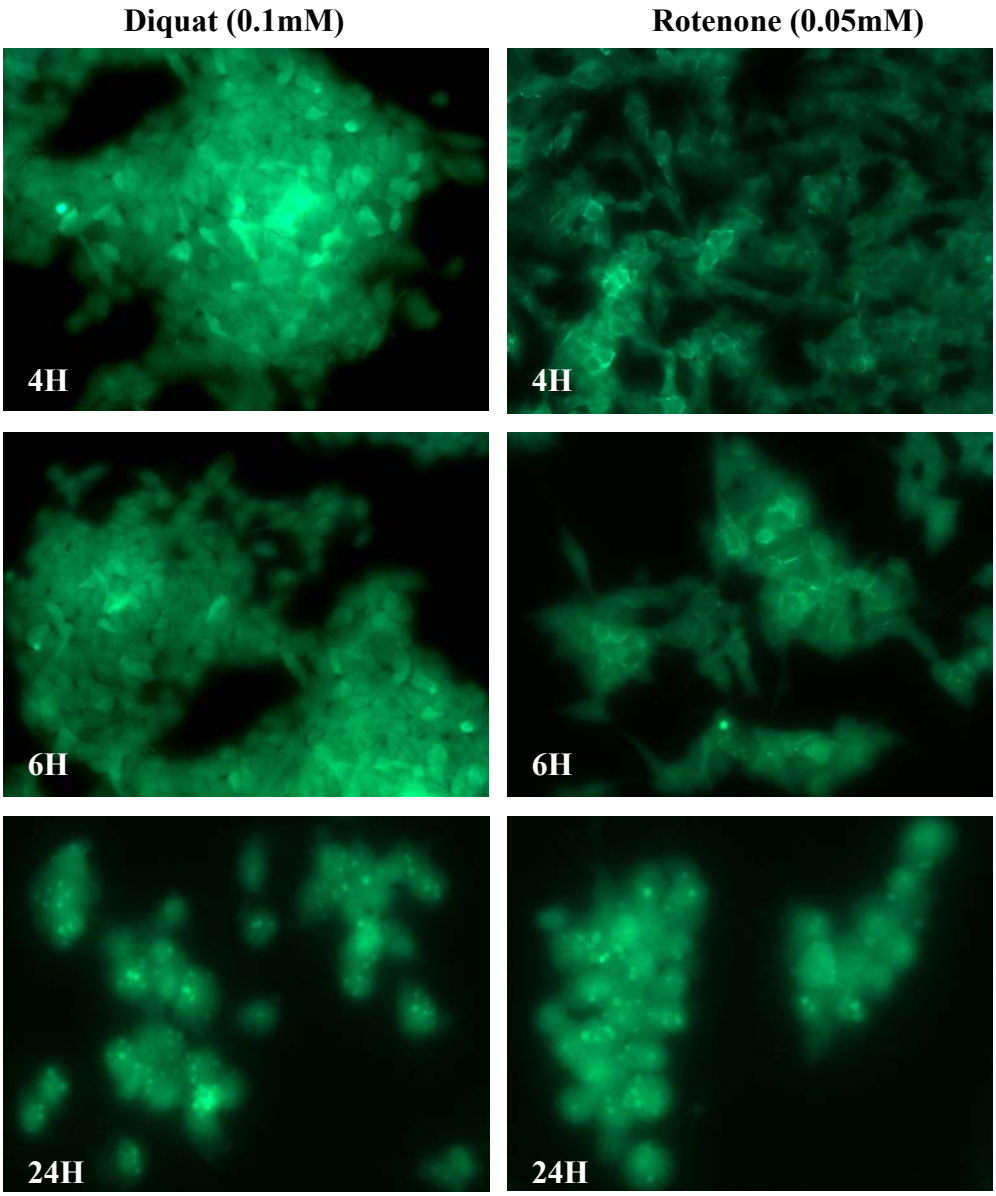

5.1.3.5 Transfection of DJ-1, Parkin and wild-type α-synuclein plasmid DNA:

To study the physiological function of DJ-1, Parkin and wild-type α-synuclein in cells, these proteins were over-expressed using plasmid DNA transfection. Results showed successful transfection of DJ-1 through c-myc tagged antibody (fig 5.19A) but failed to show Parkin or α-synuclein in transfected cells. Therefore, DJ-1 transfected cells were used for toxin treatment. Cell viability measured after 24 hours toxin treatment indicated no significant increase or reduction *(*p<0.05*) in cell-viability in transfected and non-transfected cells treated with epoxiconazole (0.15mM), rotenone (0.01mM), mancozeb (0.04mM), maneb (0.04mM) B) diquat (0.15mM), mecoprop methyl ester (0.15mM), fluroxypyr ester (0.1mM) and MPP+ (2mM) (fig 5.19 B, C).

Fig 5.19: DJ-1 Transfection and cell-viability in toxin treated cells: A) SH-SY5Y cells were transfected with c-myc tagged DJ-1 plasmid DNA for 48 hours and then treated with B) epoxiconazole (0.15mM), rotenone (0.01mM), mancozeb (0.04mM), maneb (0.04mM) C) diquat (0.15mM), mecoprop methyl ester (0.15mM), fluroxypyr ester (0.1mM) and MPP+ (2mM) for 24 hours. (n = 3, ±SD, *p<0.05).

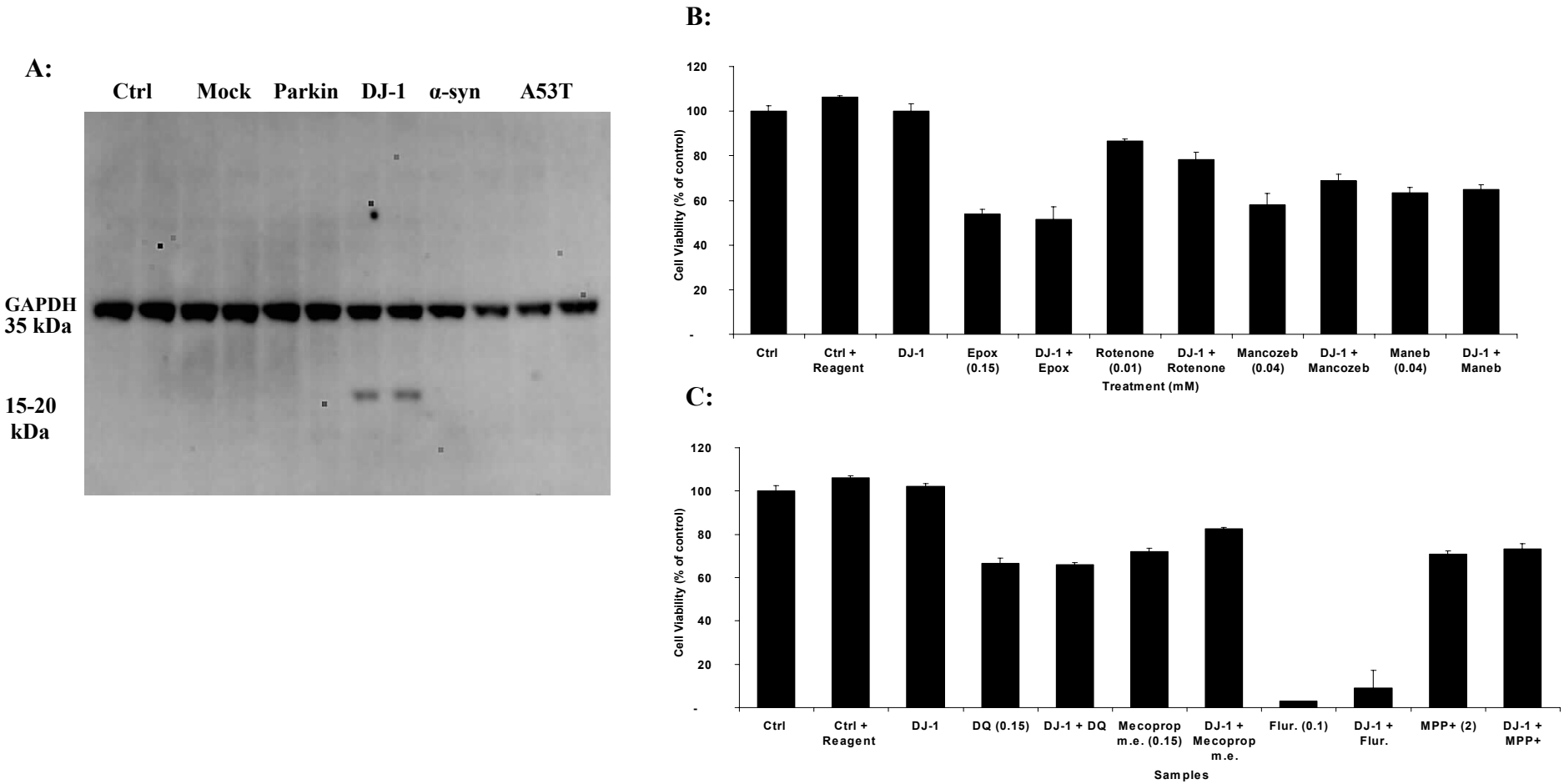

5.1.4 Discussion:

Previous studies have suggested that melanised neurones in PD brain show evidence of autophagic degeneration (Anglade *et al*., 1997). In this study the induction of autophagy was evaluated by detecting changes in the levels of Atg5 protein, beclin-1, a Bcl-2-interacting protein and LC3, an autophagosomal membrane form of microtubule-associated protein 1 light chain 3. Suppression of Atg5 or Atg7 genes has been linked with neurodegeneration in mice accompanied with an accumulation of polyubiquitinated proteins (Hara *et al*., 2006). These studies demonstrated a functional involvement of autophagy in neurodegeneration by showing motor deficits and progressive accumulation of ubiquitin-containing aggregates (Hara *et al*., 2006; Komatsu *et al*., 2006). Additionally, α-synuclein degradation also depends on macroautophagy and CMA (Webb *et al*., 2003). Previous studies have shown that RNAi knockdown of genes linked with autophagy confers protection from cell death. Zhu *et al* (2007) have shown that RNAi knockdown of *ATG5, ATG7* or *LC3* protects against cell death. Similarly, siRNA targeting *LC3* prevented neurite shortening in differentiated SH-SY5Y cells (Plowey *et al*., 2008) whereas *ATG5* and beclin-1 knockdown protected 661W cells from hydrogen peroxide induced injury (Kunchithapautham and Rohrer, 2007). Inhibition of specific Atg proteins linked with autophagy regulation can change the morphological appearance of cell-death to necrosis. In the current study successful *ATG5* knockdown occurred in SH-SY5Y cells 72 hours after transfection. Alamar Blue reduction assay showed that *ATG5* knockdown had no effect on the toxicity of selected chemicals as there was no significant change ($p<0.05$) in the viability of toxin treated and siRNA transfected cells exposed to toxins (fig 5.4, 5.5). When Atg5 levels were visualised using western blotting and band intensities measured, no significant change was noticed (fig 5.3). SH-SY5Y cells treated with different doses of agrochemicals following 72hrs siRNA treatment for 24 hours also failed to show any change in Atg5 levels (fig 5.6) suggesting that knockdown was not consistent.

Levels of beclin-1, which can stimulate autophagy when over-expressed in mammalian cells (Liang *et al*., 1999), were significantly higher in maneb, mancozeb and diquat treated cells (see fig 5.8) but showed no change in MPP+ and rotenone treated cells. Indeed, constitutive activation of beclin-1 in mice can activate

autophagy causing cerebellar Purkinje cell-death (Yue *et al*., 2002) but shows reduced aggregate formation when it is over-expressed (Pickford *et al*., 2008). It is possible therefore that mancozeb, maneb and diquat cause induction of autophagy which is mediated in part by beclin-1 induction. Beclin-1 has more complicated functions as Atg5 and -7 knockout mice survive until birth (Kuma *et al*. 2004), whereas beclin-1 knockout mice die at about embryonic day 7.5 (Yue *et al*. 2003). Bcl-2, an anti-apoptotic protein (Liang *et al*., 1998) that inhibits starvation-induced autophagy by binding to beclin-1, blocks beclin-1 mediated autophagy in mammalian, yeast and *in vivo* models. Bcl-2 mutants which cannot bind to beclin-1 do not inhibit autophagy (Luo S and Rubinsztein, 2007). Starvation reduces Bcl-2–beclin-1 interaction and frees beclin-1 to activate autophagy. Inexplicably, endoplasmic reticulum-targeted Bcl-2 but not mitochondria-targeted Bcl-2 inhibits autophagy (Pattingre *et al*., 2005). Class III phosphoinositide (PI-3) kinase activity has been linked with the regulation and control of macroautophagy. In *Saccharomyces cerevisiae* class III PI-3 kinase activity required for autophagosome-vesicle nucleation resides in a complex containing Atg6 (orthologous to mammalian beclin-1) (Petiot *et al*., 2000). Additionally, Petiot and colleagues have shown that inhibition of PI3K by 3-MA and lower doses of wortmanin blocks macroautophagic sequestration and protein degradation. 3-MA however had no effect on cell viability when exposed to the current series of chemicals (see Chapter 3), which possibly suggests that beclin-1 up-regulation is related to CMA, rather than macroautophagy. Other ways in which beclin-1 may affect autophagy include UVRAG (UV irradiation resistance-associated gene) (Liang *et al*., 2006) and Ambra1 (a WD-40 domain-containing protein) (Maria Fimia *et al*., 2007). UVRAG is part of class III PI-3 complex and is involved in positive regulation of autophagy whereas Ambra1 is a beclin-1 interacting protein primarily expressed in neural tissues and positively regulates beclin-1-dependent autophagy (Mizushima, 2007). Given the up-regulation of beclin-1 following maneb, mancozeb and diquat exposure, it would be of interest to determine the effects of beclin-1 reduction following chemical exposure.

LAMP-1 and LAMP-2 are highly glycosylated lysosomal membrane proteins which play an important role in chaperone-mediated autophagy (Kiffin *et al*., 2007). Their down-regulation has been linked with increased sensitivity to lysosomal cell death (Fehrenbacher *et al*., 2008). Results from this study showed a significant

increase in LAMP1 and LAMP2 levels in response to maneb and mancozeb treatment. Indeed, increase in the levels of LAMP-2A and CMA has been observed during oxidative stress (Kiffin *et al*., 2004). LAMP2 has more specific tasks and can substitute some of the normal functions of LAMP-1 although in this study LAMP1 is similarly elevated. Absence of LAMP1 has been linked with an altered distribution of lysosomes, accumulation of autophagic structures and LC3-positive autophagic compartments (Satfig *et al*., 2008) and its depletion prevents the co-localisation of lysosomal and autophagosomal markers (Eskelinen *et al*., 2002). LAMP1 knockout mice are fertile and viable whereas LAMP2-deficient mice show accumulation of autophagic vacuoles and cause embryonic lethality (González-Polo *et al*., 2005). The current study would indicate that CMA may be involved with diquat, maneb and mancozeb toxicity.

An increasing number of studies have shown that neuronal aggregation of misfolded proteins in different brain regions can play a vital role in the development of neurodegenerative diseases including PD (Pan *et al*., 2009). Mechanisms including the ubiquitin-proteasome system (UPS) and autophagy lysosome pathway (ALP) play an important role in the clearance of misfolded proteins and aggregates (Klionsky and Emr, 2000) where their dysfunction may increase the accumulation of aggregated/misfolded proteins. In the case of PD, oxidative damage leading to cell-death may occur if damaged mitochondria are not disposed of through autophagy (Germain and Slack, 2010). Virtually all eukaryotic cells have the capacity to sequester organelles and cytosol into autophagosomes so that they can be degraded through the lysosomal vacuolar system (Dunn, 1994). If this process is taken to completion it may cause cell-death (Xue *et al*., 1999). Enzyme deficiency in lysosomes leads to neurodegeneration in lysosome storage disorder accompanied with abnormal accumulation of toxic materials in the cells (Fukuda *et al*., 2006). Immunostaining analysis using LysoTracker® red showed a diffuse distribution of lysosomes in untreated cells whereas treatment with diquat, paraquat, maneb, mancozeb, MPP+ and rotenone exhibited a prominent and enlarged lysosomal punctate pattern of fluorescence in the cytoplasm of cells (see fig 5.16 A, B). Dyes like LysoTracker Red are fluorescent lipophilic weak bases which are accumulated in acidic organelles after becoming membrane-impermeant in their protonated form (Larsen and Sulzer, 2002). In this study lysosomal accumulation occurred after

chemical treatment, which indicates that damage organelles or proteins may be removed by lysosome mediated CMA.

Neuronal culture systems have been used in similar studies to investigate autophagy in neurones. Hollenbeck (1993) investigated the effect of nerve growth factor on sympathetic ganglia. Using fluorescent dextran TR-Dx marker they observed an exclusively punctate cytoplasmic staining consistent with lysosomal compartments. Electron microscopy revealed the presence of double membranes in most of these organelles which was characteristic of autophagic vacuoles (AVs). Similarly, Cubells et al (1994) exposed cultured dopaminergic ventral midbrain neurons to methamphetamine and noticed vacuole formation in axons and cell bodies. Inhibition of autophagy results in a decreased import of nutrients through the plasma membrane (Lum *et al*, 2005) and it may be possible that the rate of degradation of non-essential or misfolded protein is increased to provide energy for the cell resulting in a higher number of aggregates. Similar results have been reported in other studies with MPP+ treatment which caused an increase in size and average number of autophagic vacuoles (Zhu *et al*., 2007). The current results, particularly for maneb, mancozeb and diquat, would indicate that chemical treatment leads to ATP and energy depletion, direct damage to cell components (see chapter 3), with induction of autophagy.

Previous studies have shown that Parkin plays a role in protection from neurotoxicity induced by unfolded protein stresses (Imai *et al*., 2000). In experiments, where Parkin was over-expressed in human kidney-derived 293(T) and SH-SY5Y cells, presence of polyubiquitin proteins was noticed using western blotting. Similar results were observed with α-synuclein over-expression in 293T cells (Imai *et al*., 2000). Loss-of-function of Parkin and DJ-1 can involve processes leading to neuronal cell death in PD (see Chapter 1). Based on these observations, it was anticipated that the up-regulation of these proteins might protect cells from toxicity. As Parkin and DJ-1 dysfunction can lead to neuronal cell death, experiments were designed to over-express their levels in SH-SY5Y and then measure cell-viability in response to toxin treatment. DJ-1 is a cytosolic redox-dependent chaperone capable of preventing protein aggregation (Shendelman *et al*., 2004) and therefore its over-expression in cell-system could provide a protective effect.

Although DJ-1 plasmid DNA was successfully transfected, transfected cells were not significantly more resistant to non-transfected cells following toxin treatment.

In the current study it is unclear whether the accumulation of autophagic lysosomal vacuoles in response to chemical treatment represents up-regulation or blockage of autophagy as neither 3-MA (chapter 3) nor *ATG5* knockdown reduces toxicity (although ATG5 knockdown was not consistent). The up-regulation of beclin-1 and LAMP1/2 would suggest that there is up-regulation of autophagy in response to chemical treatment, possibly as a response to the formation of oxidised proteins, in the form of CMA. Since neurodegeneration can be caused by neural tissue-specific knockout of autophagy genes, it is possible that up-regulation of autophagic activity may play a vital role in disease pathogenesis. In the current context, autophagy may be an attempt to remove damaged proteins, though the extensive cell death seen following chemical treatment may indicate that this is not an effective when chemical dose is high.

Chapter Six: Toxin Treatment and Mitochondrial Dysfunction

6.1.1 Introduction:

Evidence from numerous studies has linked mitochondrial dysfunction with the development of Parkinson's disease. Discovery of a mild deficiency in complex I activity in the substantia nigra of PD patients (Schapira *et al*., 1989; Mann *et al*., 1994) followed by similar deficiencies in the frontal cortex (Parker *et al*., 2008), platelets (Blandini *et al*., 1998) lymphocytes (Barroso *et al*., 1993) and to a lesser extent in muscle tissue (Penn *et al*., 1995) showed that impairment of the respiratory chain can be a part of PD pathology. Substantia nigra appears more vulnerable to impairments of complex I activity than other brain regions and complex I activity in the PD substantia nigra can be reduced up to 30-40% (Dawson and Dawson, 2003). This can be due to complex I misassembly or insufficient production of certain subunits (Keeney *et al*., 2006). Use of cybrid cell-lines containing mtDNA from PD patients and normal nuclear genomes show a complex I deficit, formation of LB like inclusions and a higher sensitivity to MPP+ (Trimmer *et al*., 2004). Mitochondria are central to the actions of several neurotoxins and mitochondrial dysfunction caused by neurotoxicants leads to selective degeneration of dopaminergic neurons (Kanthasamy *et al*., 1994). Indeed, selective complex I inhibitors like MPP+ and rotenone cause features similar to those seen in PD and PD models (Schmidt *et al*., 2006). While there are differences in cell death mechanisms elicited by these chemicals, mitochondrial oxidative stress and mitochondrial autophagy have emerged as common factors.

6.1.1.1 Aims:

As the mitochondrial electron transport chain is a known source of reactive oxygen species and generation and inhibition of mitochondrial complexes increases free radical production (Fiskum *et al*., 2003), this study was designed to investigate whether acute or chronic exposure to different toxins has an inhibitory effect on the mitochondrial complex I and II activity. Further, if there is any change in distribution or structure of mitochondria in response to these chemicals which may provide evidence of mitochondrial dysfunction.

6.1.2 Methods:

Refer to materials and methods (section 2.4).

6.1.3 Results:

6.1.3.1 Acute toxin exposure and complex I-II activity:

Protocol and facilities required for this study were kindly provided by Prof. Robert Taylor and Dr. Langping He, NHS Mitochondrial Diagnostic Service. This protocol is used to measure the activity of mitochondrial respiratory chain deficiencies in patient muscle biopsy or fibroblast for the diagnosis of mitochondrial disease. This study used isolated SH-SY5Y cell mitochondria instead of pig heart mitochondria for which this method was optimised. Therefore, the protocol was altered using SH-SY5Y cells and complex I-II activity from untreated SH-SY5Y cells (±SD) and ratios are shown in table below.

Table 6.1: Standard Assay measurements: Complex I (CI; µmols of NADH oxidised/min), complex II (CII; µmols of DCPIP reduc/min) and citrate synthase (CS) activity in pig heart mitochondria (internal control) and untreated mitochondrial extracts from SH-SY5Y cells (n=5).

	Pig Heart mitochondria (1:20) (µM)	**SH-SY5Y cell mitochondria (1:5) (nM)**
CI	6.98±1.67	128.52±0.14
CII	10.2±1.32	178.01±2.62
CI/CII	0.68±1.23	0.73±0.01
CS	23.08±2.55	355.9±8.2
CI/CS	0.1-0.2	0.37±0.008
CII/CS	0.1-0.35	0.51±0.01

Rotenone (0.005mM) was used to completely inhibit complex I activity which was measured as the rotenone-sensitive NADH: ubiquinone oxidoreductase activity. Comparison of treatment with (fig 6.1b) and without rotenone (fig 6.1a) clearly showed that after a 5 minute time point when rotenone is added to the reaction mixture, the decrease in absorbance due to the oxidation of NADH is stopped. Bearing in mind how quickly rotenone acts, different toxins were added to the reaction mixture and CI activity measured immediately to check if they are as potent as rotenone in inhibiting complex I.

Graphical presentation of results are shown in fig 6.1. Overall results showed that diquat (0.04mM; also see fig 6.3, 6.4), paraquat (0.04mM, 1mM), MPP+ (0.04mM), MPTP (0.1mM), mancozeb (0.001mM, 0.1mM, 1mM), maneb (0.001mM, 0.1mM, 1mM), epoxiconazole (0.1mM) and fluroxypyr methyl ester (0.1mM) had no immediate inhibitory effect on complex I activity (data not shown).

Fig 6.1: Inhibition of NADH: quinone reductase (complex I) activity: Complex I activity (µmols of NADH oxidised/min, Red line) in (A) Untreated (DMSO; without rotenone addition), (B) Rotenone(0.005mM), (C) Diquat (0.04m), (D) paraquat (0.04mM), (E) MPP+ (0.04mM), (F) MPTP (0.1mM), (G) mancozeb (0.1mM), (H) maneb (0.1mM), (I) epoxiconazole (0.1mM) and (J) fluroxypyr methyl ester (0.1mM) treated SH-SY5Y cell mitochondria (n=3). (Blue line automatically generated during graph formation).

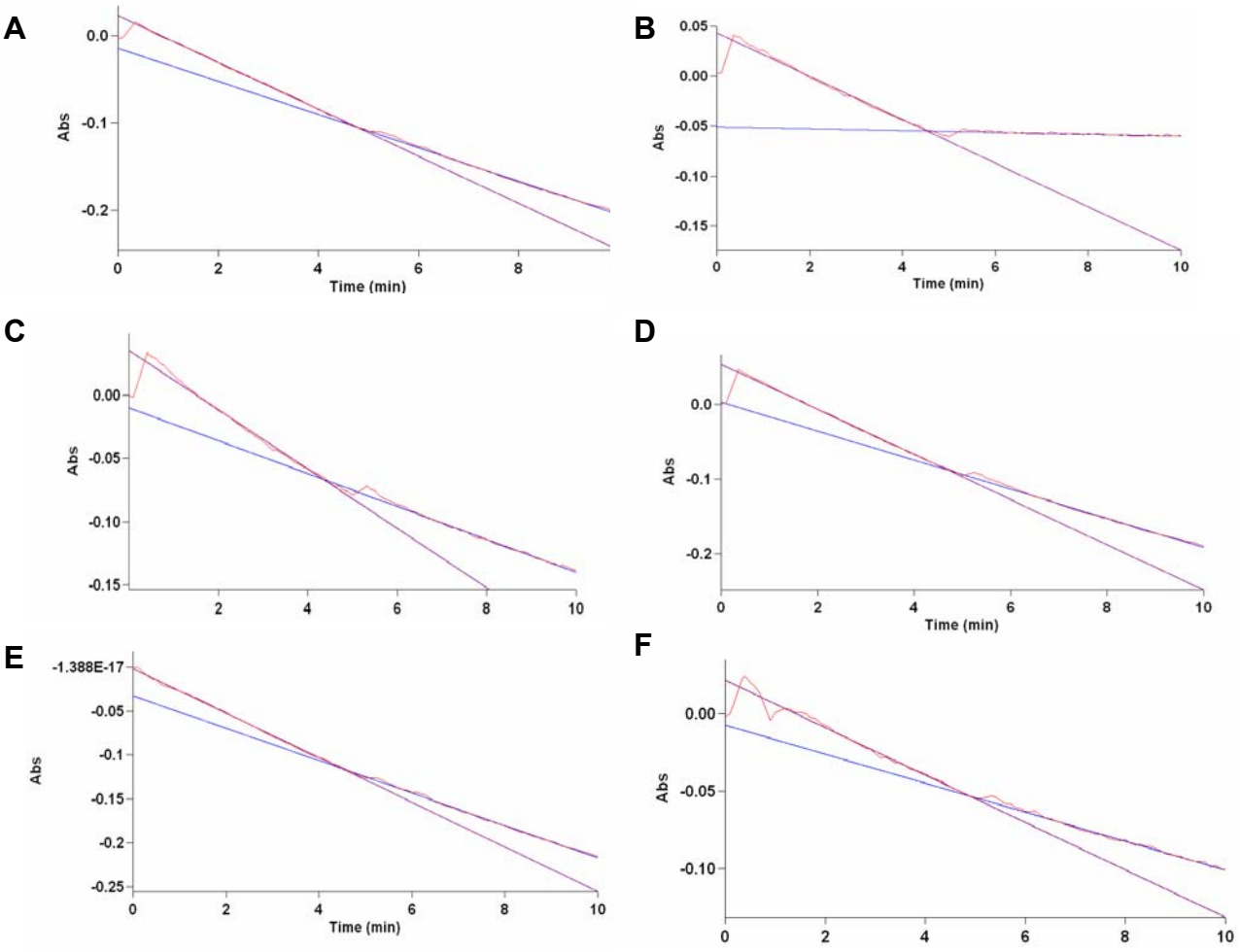

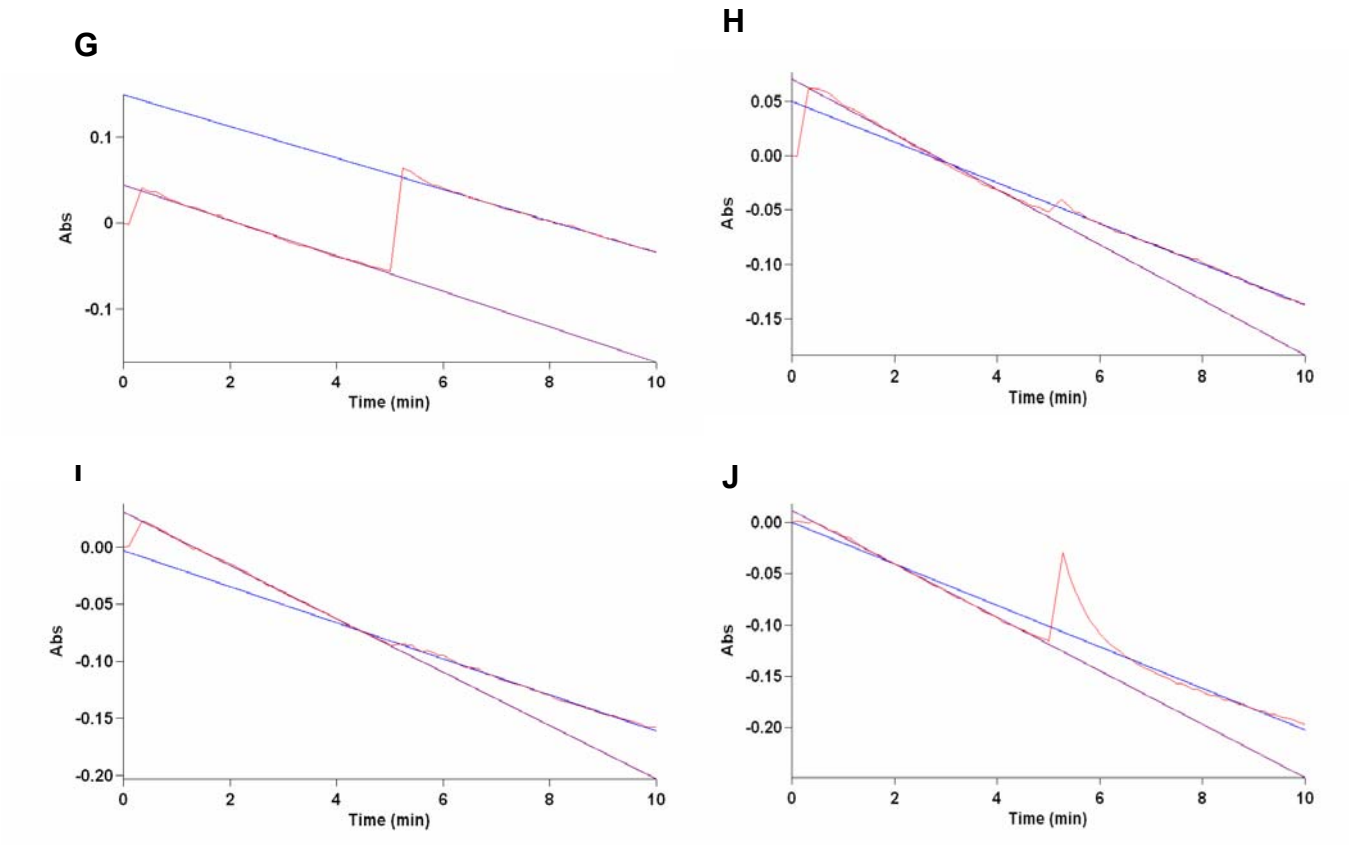
G
H
I
J
Abs
Time (min)

Acute mancozeb or maneb exposure can inhibit ATP production before major toxicity effects take effect. These chemicals inhibit and uncouple respiration at low doses and completely inhibit respiration at higher dose (0.03mM) (Domico *et al*., 2006). Although reports have suggested that maneb inhibits complex III (Zhang *et al*., 2003), data linking maneb or mancozeb with the inhibition of complex-I is still insufficient. Lower (0.001mM) or higher (1mM) doses of maneb or mancozeb had no significant effect on complex I or II activity. Complex II activity was unaffected after 1 hour exposure. Similarly, epoxiconazole and fluroxypyr methyl ester (FPM) had no effect on complex-I or II activity at 0.1mM after 1 hour exposure.

Although the underlying mechanisms causing the selective dopaminergic neuron death are not clear, mitochondrial complex I dysfunction has long been implicated in this process (Abou-Sleiman *et al*., 2006). Indeed, accidental exposure to MPTP provided the first evidence of complex I dysfunction in PD (Langston *et al*., 1983). Later on it was revealed that MPP+, an MPTP metabolite, inhibited complex I activity (Dauer and Przedborski, 2003). In this study, MPP+ was added to the reaction mixture containing SH-SY5Y mitochondrial extracts and whilst acutely it showed no effect at 0.04mM (see fig 6.1E), at 10nM and 100nM doses and incubated for 1 hour after which complex I/II activity was measured, results showed a dose response effect with significant reduction in complex I activity with 100nM dose, although the level of reduction was not as high as rotenone. Complex II activity was unaffected after 1 hour exposure (fig 6.2, table 6.2).

Fig 6.2: Mean CI/II activity in MPP+ treated SH-SY5Y mitochondria: Complex I (µmols of NADH oxidised/min) and II activity (µmols of DCPIP reduc/min) in isolated SH-SY5Y cells mitochondria after 1 hour incubation with MPP+ (10nM and 100nM) (n=3, ±SD, *p<0.05).

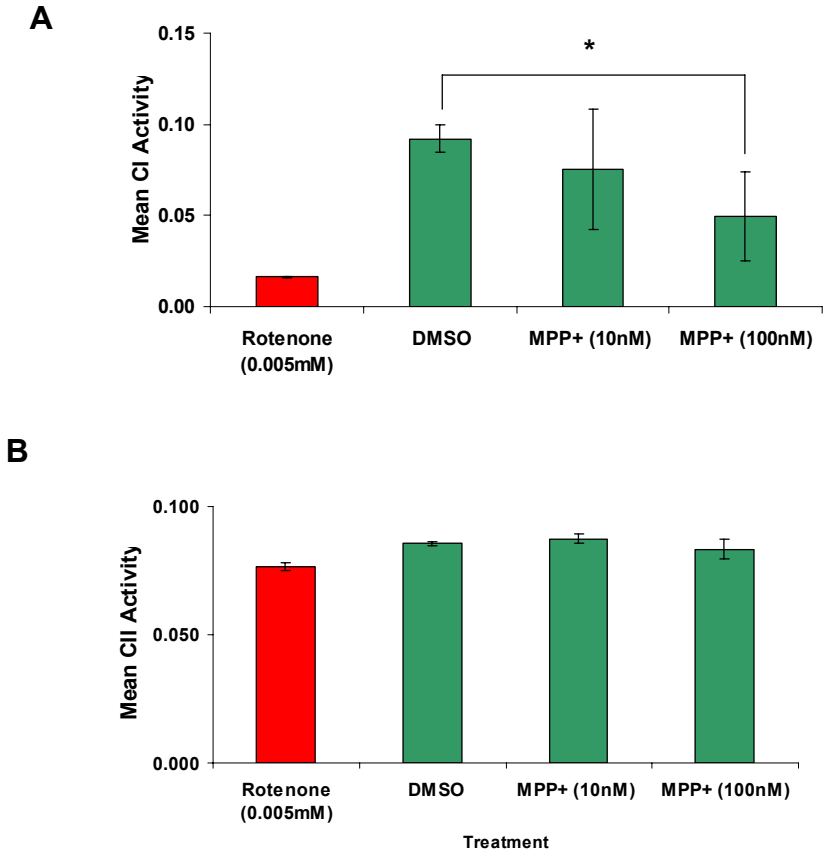

Table 6.2: Complex I and II activity measurement in MPP+ treated SH-SY5Y cells: Complex I (µmols of NADH oxidised/min) and II activity (µmols of DCPIP reduc/min) in isolated SH-SY5Y cells mitochondria after 1 hour incubation with MPP+ (10nM and 100nM) (n=3, ±SD, *p<0.05).

Sample	Conc.	Mean Complex I activity (µM/min)	Mean Complex I activity (µM/min)	CI/CII
Control (+ rotenone)	0.005mM	0.02±0.00	0.076±0.001	0.26
DMSO (0.1%)	-	0.09±0.007	0.086±0.0008	1.05
MPP+	10nM	0.08±0.033	0.087±0.001	0.92
MPP+	100nM	0.05±0.024*	0.083±0.003	0.60

Intracellularly, diquat undergoes redox cycling, producing superoxide anions (Saeed *et al*., 2001) but it is not known if it damages mitochondria through complex-I inhibition. Paraquat which is of the same dipyridyl class of compounds has been hypothesised to inhibit complex I (Fukushima *et al*., 1994) but despite structural similarities with paraquat, diquat may not share its mode of toxicity. Results showed that 1 hour diquat treatment at 0.001mM, 0.01mM and 0.1mM failed to significantly reduce (*p<0.05) complex I activity (fig 6.3 A, B) but the use of a higher dose (1mM) showed a time-dependent significant reduction in complex I activity (fig 6.4 A, B; table 6.3). Complex-I activity at 30, 45 and 60 minutes with 1mM diquat showed a percentage reduction of 17%±0.93, 52%±0.93 and 64%±1.11 respectively. Complex II activity was unaffected after 1 hour exposure.

Fig 6.3: Mean CI/II activity in Diquat treated SH-SY5Y mitochondria: (a) Complex I (µmols of NADH oxidised/min) and (b) II activity (µmols of DCPIP reduced/min) activity after 1 hour incubation with diquat at 0.001mM, 0.01mM and 0.1mM (n=3, ±SD, *p<0.05).

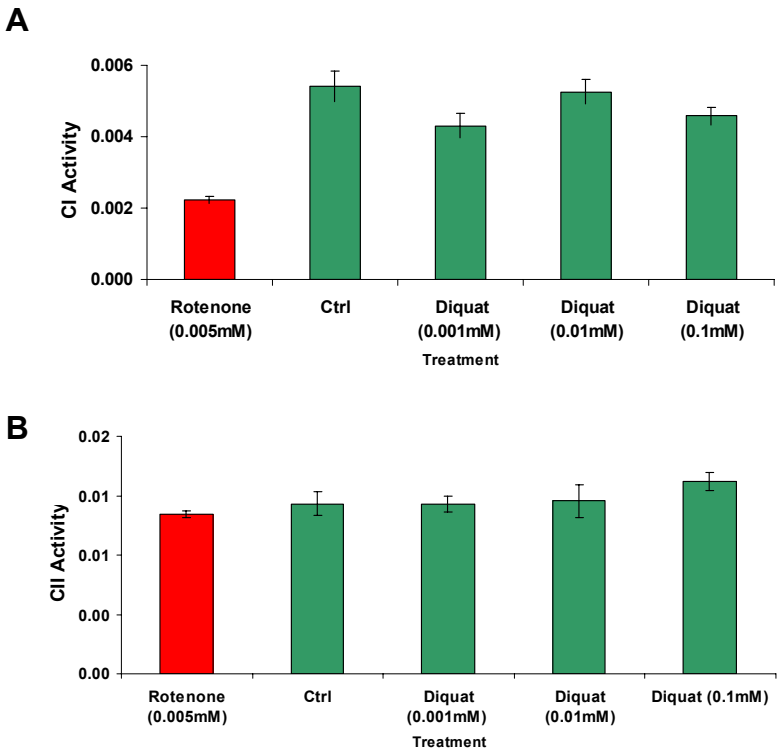

Fig 6.4: Mean CI/II activity in Diquat treated SH-SY5Y mitochondria: Complex I (µmols of NADH oxidised/min) (a) and II activity (µmols of DCPIP reduc/min) (b) activity after 15, 30, 45 and 60 minute incubation with diquat at 1mM (n=3, ±SD, *p<0.05).

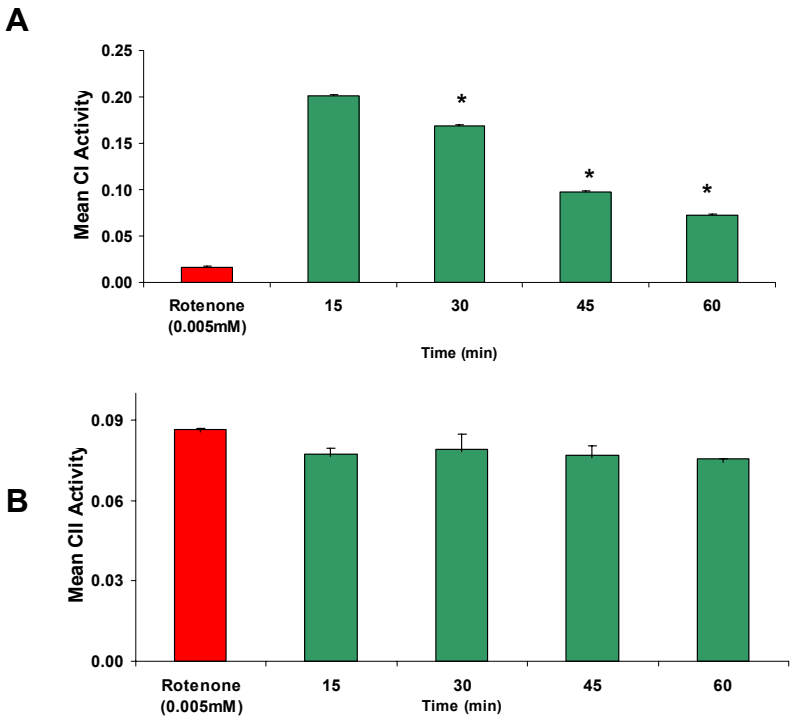

Table 6.3: Mean CI/II activity in diquat treated SH-SY5Y cells: Complex I (µmols of NADH oxidised/min) and II activity (µmols of DCPIP reduc/min) after 15, 30, 45 and 60 minute incubation with diquat at 1mM (n=3, ±SD, *p<0.05).

Sample	Conc.	Mean Complex I activity (µM/min)	Mean Complex II activity (µM/min)	CI/CII
Control (+ rotenone)	0.005mM	0.02±0.0008	0.086±0.001	0.23
Diquat (15min)	1mM	0.201±0.0009	0.077±0.002	2.61
Diquat (30min)	1mM	0.17±0.0006*	0.079±0.006	2.15
Diquat (45min)	1mM	0.097±0.0009*	0.077±0.003	1.27
Diquat (60min)	1mM	0.072±0.0011*	0.075±0.00	0.97

Chronic rotenone exposure has been linked with the increase of α-synuclein in SK-N-MC cells (Betarbet *et al*., 2006) and sub-lethal doses of rotenone in *Drosophila* cause selective loss of dopaminergic neurons inducing locomotor deficits (Coulom and Birman, 2004). In SH-SY5Y cells treated with selected toxins for a period of 5 weeks, complex-I activity was not significantly different from untreated samples but significantly higher than rotenone (0.005mM) dose used as a positive control (table 6.4). Complex-II activity remained unaltered.

Table 6.4: Chronic toxin exposure and complex I-II activity: Mean CI/II activity in chronically treated SH-SY5Y cells (5 Weeks exposure, diquat (0.01mM), MPP+ (0.01mM), mancozeb (0.01mM) and maneb (0.01mM) (n=3, ±SD, *p<0.05).

Sample	Conc. (mM)	Mean Complex I activity (µM/min)	Mean Complex II activity (µM/min)	CI/CII
Untreated	-	0.0050±0.0042	0.078±0.002	0.07
Rotenone	5nM	0.0048±0.0032	0.076±0.002	0.063
Diquat	0.01mM	0.0075±0.003	0.088±0.002	0.085
MPP+	0.01mM	0.0058±0.0034	0.081±0.004	0.07
Maneb	0.01mM	0.0046±0.0001	0.092±0.004	0.05
Mancozeb	0.01mM	0.0046±0.00002	0.090±0.004	0.05

6.1.3.2 Toxin exposure and mitochondrial distribution:

Mitochondria are dynamic organelles as they actively divide, fuse with one another and are actively transported (in neurons) throughout axons and dendrites (Hollenbeck and Saxton, 2005; Okamoto and Shaw, 2005). Their fusion and fission helps in maintaining their integrity, turnover, stabilisation and segregation (Westermann, 2002).

To investigate the effect of toxin exposure on mitochondrial distribution, SH-SY5Y cells were incubated with MitoTracker® Red CMXRos (Invitrogen) before 24 hour toxin treatment including H_20_2 (0.1mM), diquat (0.1mM), mancozeb (0.05mM), maneb (0.05mM), maneb (0.05mM), MPP+ (0.05mM) (fig 6.5, data not shown for maneb and MPP+), rotenone (0.05mM), epoxiconazole (0.05mM) and fluroxypyr ester (0.05mM) (fig 6.6). Results showed a higher number of cytoplasmic aggregates in treated cells compared with uniform distribution in untreated cells (data not statistically analysed). Cell viability was very low in H_20_2 treated cells (less than 5% of untreated cells) making estimation of mitochondrial distribution difficult to visualise. Nevertheless, remaining cells showed a marked reduction in overall staining highlighted by aggregates distributed throughout the cell body. Similar results were observed in rotenone, diquat, maneb and mancozeb treated cells. However, a lower percentage of aggregates were seen in epoxiconazole (0.05mM) and fluroxypyr ester (0.05mM) treated cells.

Aggregate formation in diquat treated cells was dose dependent. A relatively smaller number of stained bodies were seen with 0.001mM dose but their number increased when treated at 0.01mM and 0.1mM (fig 6.7). A similar effect was seen with rotenone treated cells (data not shown).

Fig 6.5: Mitochondrial localisation after toxin treatment: SH-SY5Y cells treatment with selected toxins after staining with MitoTracker® Red CMXRos. Viewed under fluorescent microscope (magnification x40, each image is representative of three independent fields).

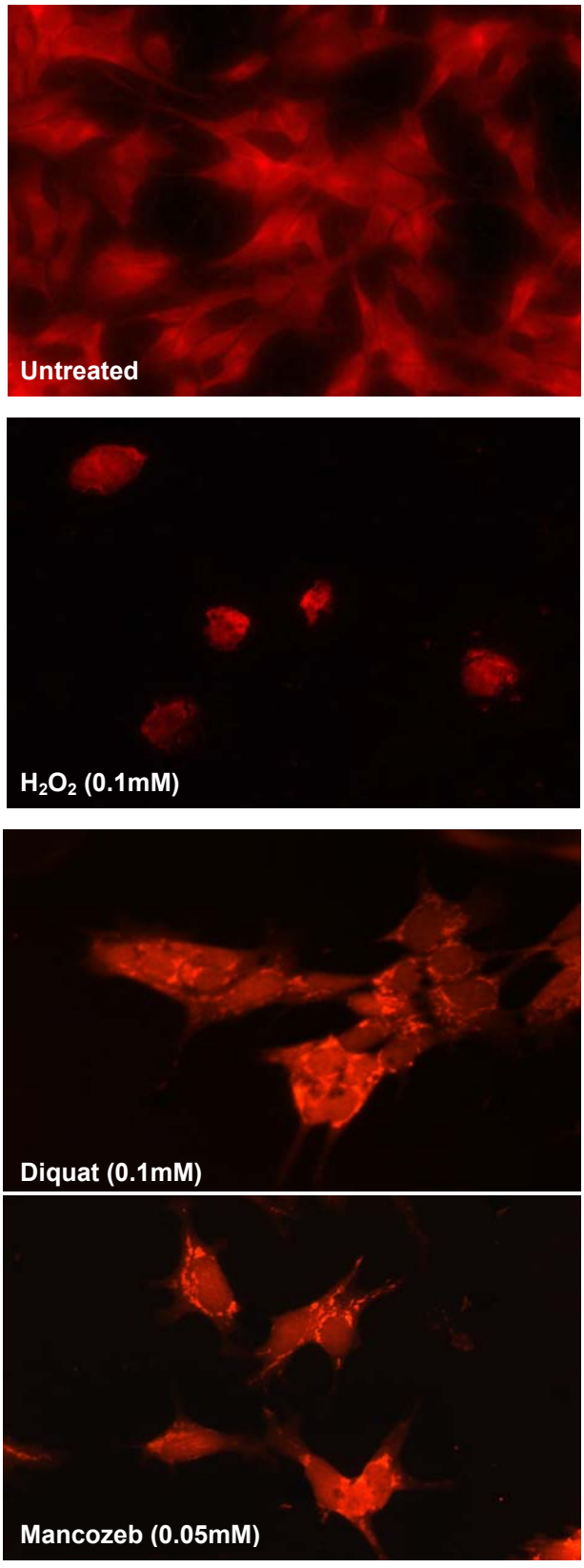

Fig 6.6: Mitochondrial localisation after toxin treatment: SH-SY5Y cells treatment with selected toxins after staining with MitoTracker® Red CMXRos (magnification x40, each image is representative of three independent fields).

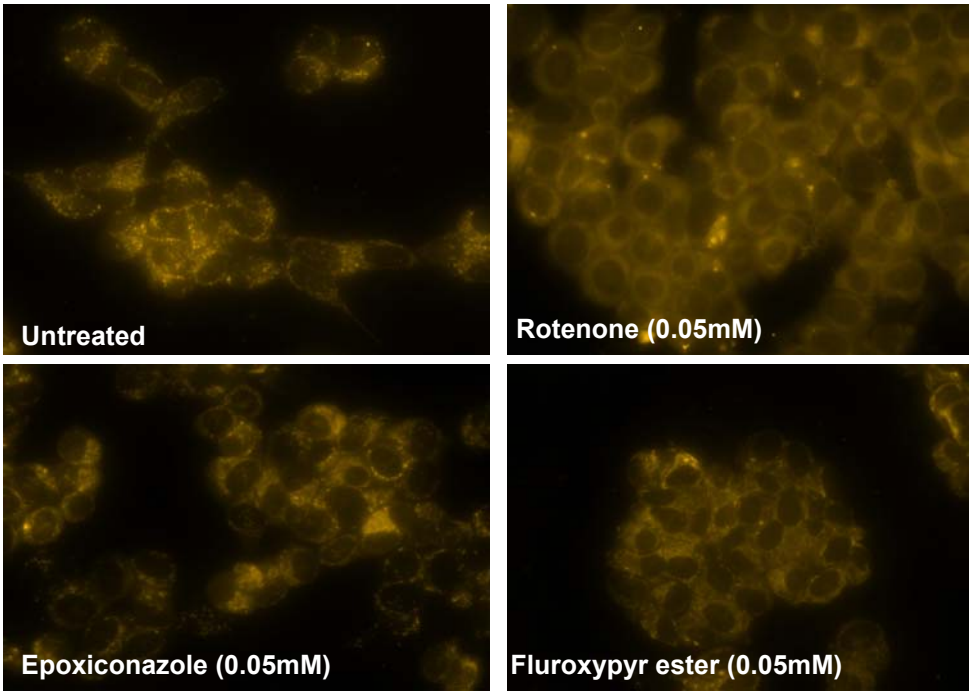

Fig 6.7: Mitochondrial localisation after diquat treatment: SH-SY5Y cells treatment with diquat showed the formation of mitochondrial aggregates in a dose-dependent manner (magnification x40, each image is representative of three independent fields).

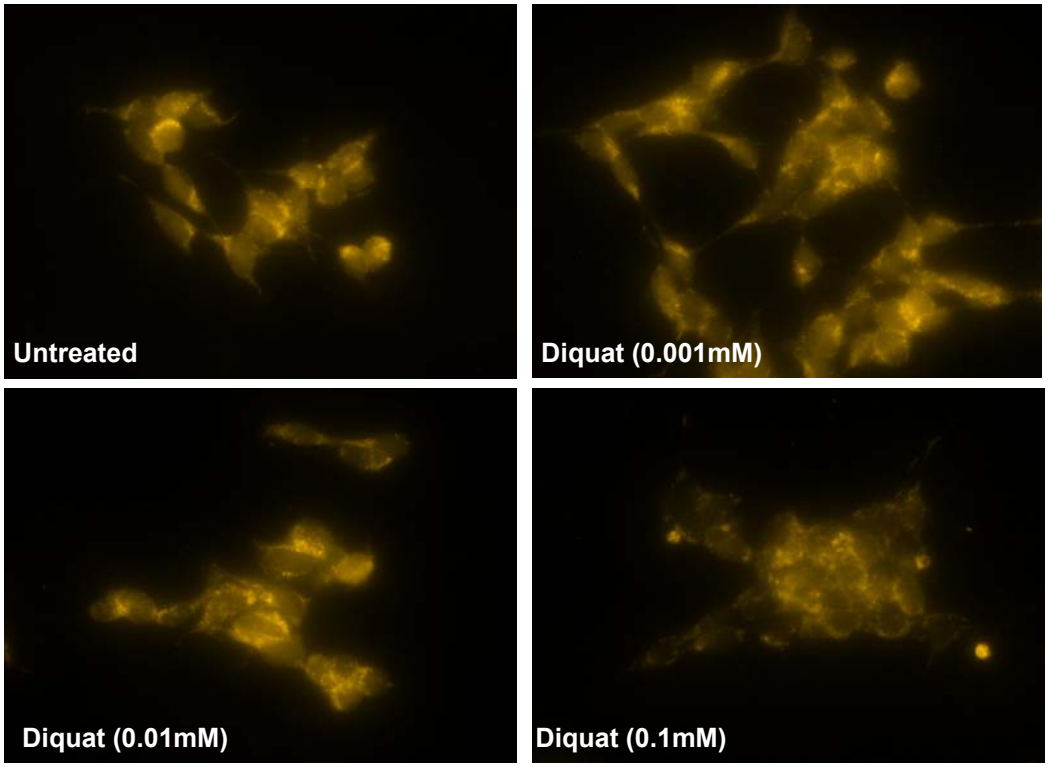

6.1.4 Discussion:

Changes in mitochondrial function are critical for cell survival as any deficiency, especially in the mitochondrial respiratory chain can cause reduced ATP synthesis, ROS generation leading to oxidative stress and mitochondrial depolarisation, all leading to cell-death (Drechsel and Patel, 2008). Ageing of the nervous system is often associated with mitochondrial dysfunction (Melov, 2004) and evidence accumulated over several years links mitochondrial dysfunction with PD. Indeed, 15–30% reduction in complex I activity in non-familial sporadic PD patients has been observed (Schapira *et al*., 1989). Both rotenone and MPP+ selectively inhibit complex I and produce several features of PD, thus providing evidence that oxidative stress and a complex I deficiency might underlie PD (Schmidt and Alam, 2006).

The quality of mitochondria extracted from cells heavily relies on the method used to break open the cells. The use of a hypotonic buffer provided a rich mitochondrial pellet which also helped minimise the rotenone-insensitive background activity. Freeze-thawing in hypotonic media provided an accurate complex-I activity measurement as this method gives maximum access of the substrate to its binding site on the inner mitochondrial membrane. Mitochondrial stability is affected by the buffer composition, therefore, supplementing it with ubiquinone-1 increased the rate of complex-I activity. Fatty acids cause the opening of the permeability transition pore so by using fatty-acid free BSA; rotenone sensitivity was increased (Birch-Machin *et al*., 1994).

The objective of this study was to investigate the role of complex I inhibition in SH-SY5Y cell-death induced by selected agrochemicals. Results showed that rotenone which is a potent mitochondrial complex I inhibitor successfully inhibited complex I activity almost immediately at 0.005mM. Previous studies have suggested its IC_{50} between 0.1nM and 100nM depending on the method and system used (Choi *et al*., 2008). Studies using a similar human neuroblastoma cell-line SK-N-MC have shown dose-dependent changes in oxidative damage, ATP depletion and cell-death (Sherer *et al*., 2003). It is suggested that inhibition of mitochondrial NADH dehydrogenase by rotenone is linked with a reduction in mitochondrial membrane

potential observed after mitochondrial injury followed by the release of cytochrome c into cytosol which leads to caspase-9 activation (Mattson, 2000). Indeed, data from this study shows a complete inhibition of complex I activity at 0.005mM and presence of aggregates after 0.05mM exposure. This coupled with a reduction in mitochondrial transmembrane potential (chapter 3, fig 3.21) shows hallmarks of early stage of the mitochondrial apoptotic pathway. Previous studies have shown changes in mitochondrial structure and function in response to acute rotenone exposure e.g. presence of 'donut'-shaped mitochondria in HeLa cells (Benard *et al*., 2007), fragmented morphology and reduced membrane potential in human fibroblasts after acute high-dose rotenone exposure (Mortiboys *et al*., 2008), mitochondrial fragmentation in rat cortical neurons (Barsoum *et al*., 2006) and swelling and decreased mitochondrial motility in fibroblasts (Pham *et al*., 2004).

MPP+ reduced CI activity in a dose-dependent manner showing no effect at 10nM but showing a 40% reduction at 100nM consistent with previous reports. It is accepted that complex I inhibition remains the main target of MPP+ action but alternative mechanisms like reduction in mitochondrial transmembrane potential (chapter 3, fig 3.21), inhibition of glycolysis, microtubule depolymerisation and oxidative stress also play part in its neurotoxicity (Cappelletti *et al*., 2005). Similar suggestions have been made by Choi *et al* (2008) who have shown through their study that dopaminergic neuron loss caused by MPP+ is not entirely dependent on CI inhibition. The analysis of mitochondrial structure was not possible with MitoTracker dye and it only gave a measure of mitochondrial distribution showing cells under stress with clumping around the nucleus compared with untreated cells which showed stained structures widely and thinly spread throughout the cell-body (fig 6.5).

Some studies have suggested that complex I activity of isolated mitochondrial *in vitro* may be inhibited by paraquat (Fukushima *et al*., 1994; Tawara *et al*., 1996). The suggestion that it shares structural similarity with MPP+ and therefore acts as a complex-I inhibitor has been questioned by researchers (Richardson *et al*., 2005). Studies using yeast and mammalian-cells show that paraquat is actively transported through the mitochondrial membrane where it is reduced to a radical cation by CI leading to the production of mitochondria-damaging superoxide (Cocheme and

Murphy, 2008) but its ability to reach the internal mitochondrial membrane and inhibit complex I in intact cells is still under investigation (Shimada *et al*., 1998). Data presented here support the argument that paraquat does not act as a complex I inhibitor as 1mM dose had no effect on either complex-I or II activities. Data from earlier experiments also suggested that paraquat (1mM) did not affect mitochondrial transmembrane potential after 24 hour exposure (see chapter 3, fig 3.21). These finding agree with the suggestion that oxidative stress, independent of complex-I inhibition may be critical in paraquat cytotoxicity (McCormack *et al.,* 2005; McCormack *et al.,* 2006). Although lower diquat doses (0.001-0.1mM) failed to have any effect, a 1mM dose of diquat caused a time-dependent reduction in complex-I activity (fig 6.4). Such a high dose can cause oxidative stress leading to a reduction in complex I activity rather than its direct inhibition. Intracellularly, diquat undergoes redox cycling, producing superoxide anions and resultant highly unstable diquat radical causes the formation of superoxide anion radical (Saeed *et al*., 2001). This continuous oxidation and reduction of diquat results in superoxide anion radicals reacting with each other and producing molecular oxygen and hydrogen peroxide (Jones & Vale, 2000). This effect cannot be explained in isolated mitochondria used in these experiments but data from mitochondrial staining (fig 6.7) suggests a change in mitochondrial distribution after 0.1mM treatment with increased aggregation compared with 0.001mM and 0.01mM doses. Given that diquat only causes complex I inhibition at 1mM and following extended time periods (cf rotenone), it is unclear from the current studies if diquat generates free radicals via the mitochondrial respiratory chain or elsewhere in the cell.

Previous data suggests that maneb, mancozeb, epoxiconazole and fluroxypyr methyl ester do not affect the mitochondrial transmembrane potential (MTP: chapter 3; fig 3.21) and results from this study indicate that complex-I and II activities are not affected by these chemicals either (fig 6.1). Depolarisation of mitochondria interferes with electron transport and respiration (Mookherjee *et al*., 2007); therefore it can be assumed that these chemicals do not directly lead to changes in intrinsic components of mitochondrial bioenergetics like mitochondrial membrane potential and ATP synthesis which in turn affects the mitochondrial transport and distribution. Minimal mitochondrial aggregation was observed compared with H_2O_2 (0.1mM) treatment which showed increased aggregation and a significant reduction in MTP.

Similar features have been observed in previous studies where H_2O_2 treatment changed mitochondrial structure and majority of the mitochondria were swollen and vacuolated (Polimeno *et al*., 2009). Indeed, excitotoxicity and oxidative stress can disrupt mitochondrial movement (Rintoul *et al*., 2003). This may indicate that maneb, mancozeb, epoxiconazole and fluroxypyr methyl ester cause cell death independently of mitochondria.

Chronic rotenone exposure can increase α-synuclein levels and cause selective loss of dopaminergic neurons in cell/drosophila-models (Betarbet *et al*., 2006; Coulom and Birman, 2004) and reduce mitochondrial movement in differentiated SH-SY5Y cells (Borland *et al*., 2008). Results from this study showed that chronic rotenone toxin exposure did not affect complex-I or II activity, and similarly none of the other agrochemicals tested affected the levels of complex I or II. Previous studies have measured mitochondrial bioenergetics and components like ATP levels which can be a consequence of complex I inhibition to see if its depletion can be detected after chronic rotenone exposure (5nM) in SK-N-MC cells (Betarbet *et al*., 2006). Cellular ATP levels were unchanged after 3–4 weeks suggesting minimal disturbance of mitochondrial function. Long term exposure of cells to agrochemicals would therefore not appear to affect mitochondrial energetics.

Neurons depend on correct mitochondrial dynamics to meet their high energy demands especially in axons and nerve terminals. Mitochondria are vital for calcium buffering and providing energy for maintaining the vesicular neurotransmitter pool. If any of the above chemicals directly disturb mitochondrial function, it can disrupt neuronal maintenance, function, localisation and active transport, which is required for delivery to sites of increased energy requirement (Van Laar and Berman, 2009). Vulnerable neurons can be more susceptible to slight changes in mitochondrial maintenance as suggested by studies showing that mitochondria cover smaller cytoplasmic area in the substantia nigra dopaminergic neurons compared with neighbouring non-dopaminergic neurons or those unaffected in PD such as ventral tegmental area neurons (Liang *et al*., 2007). Any disruption in mitochondrial dynamics may lead to a reduced distribution of healthy mitochondria within the axon or at the nerve terminal and cause an accumulation of damaged mitochondria leading

to stress and cell-death (Van Laar and Berman, 2009). With the exception of perhaps diquat, the agrochemicals tested do not appreciably influence mitochondrial function.

Chapter Seven: RT-PCR gene analysis of toxin treated SH-SY5Y cells

7.1.1 Introduction:

It is hypothesised that a complex pattern of environmental and genetic factors contribute to the development of idiopathic PD. Although polymorphisms (ubiquitin C-terminal hydrolase gene), deletions (*PARKIN, PINK1* and *DJ-1* genes), duplications/triplications (α-synuclein) and mutations (α-synuclein, *LRRK2*) account for a small percentage of PD cases (Conn *et al*., 2003), the role of these genetic risk factors can not be ignored. The selective vulnerability of nigral dopaminergic neurons and the widespread nature of PD pathology require an understanding of genetic factors which cause impairment of proteasomal activity, protein aggregation, mitochondrial bioenergetic dysfunction and cell-signalling leading to damage through oxidative stress (Borland *et al*., 2008).

Microarray-based gene expression profiling of isolated DA neurons from control and PD substantia nigra has shown the involvement of oxidative stress, mitochondrial and ubiquitin-proteasome dysfunction, programmed cell-death signalling events, down-regulation of *PARK* genes and changes in expression of genes related to ion channel and neurotransmitter (Elstner *et al*, 2009; Simunovic *et al*., 2009). Previous studies using cDNA microarrays to analyse SH-SY5Y cells after MPP+ toxicity have shown that changes in gene expression may control ER stress and mitochondrial dysfunction (Conn *et al*., 2003). Mandel *et al* (2000) analysed differential gene expression in MPTP treated mice for 5 days and noticed an increase in the expression of genes linked with oxidative stress, glutamate excitotoxicity, inflammation signal transduction molecules and proteins involved in cell-cycle regulation.

7.1.1.1 Aims:

The aim of this study was to investigate the effect of toxin treatment on the expression of genes related to a number of different factors which may have a role in PD pathogenesis derived from study of altered gene expression in isolated SN neurones in PD (Elstner *et al*., 2009). To better understand the mechanisms of cell death after toxin treatment and PD neurodegeneration, TaqMan® Custom Arrays were used to characterise the transcriptional response of SH-SY5Y cells to acute and chronic toxin treatment. TaqMan® Custom Arrays, a 384-well micro fluidic card

allowed 384 simultaneous real-time PCR reactions and did not require extensive liquid-handling robots or multichannel pipettors to fill the card. This method allowed efficient analysis of a large number of genes and quantification of their regulation by running multiple samples against gene expression targets pre-loaded into each well.

7.1.2 Methods:

Refer to materials and methods (section 2.5).

7.1.3 Results:

Expression of 48 genes (table 7.1, 7.2) was measured in appropriate control and treated samples. Genes were chosen on the basis of expression in cell death pathways and from analysis of nigral neurones in PD (Elstner *et al*, 2009). Two replicates per sample were assayed for each gene in a 384-well format plate. GAPDH was used as endogenous control gene and for data normalisation across samples. Normalisation of Ct values of each gene and determination of fold increase or decrease was measured by calculating the $2^{-\Delta\Delta Ct}$ value (Relative Quantification Method, Applied Biosystems 2008).

Table 7.1: Symbol and title of selected genes analysed through RT-PCR.

Symbol	Gene
SNCA	α-synuclein
PDXK	Pyridoxal (pyridoxine, vitamin B6) kinase
TRAPPC4	Trafficking protein particle complex 4
SRGAP2	Slit-robo GTPase activating protein
MT-ND2	Mitochondrially encoded NADH dehydrogenase 2
MT-ND1	Mitochondrially encoded NADH dehydrogenase 1
UCHL1	Ubiquitin carboxyl-terminal esterase L1
TH	Tyrosine hydroxylase
SLC6A3	Solute carrier family 6, member 3
GAD1	Glutamate decarboxylase 1
GBA	Glucosidase, beta, acid
ATG3	Autophagy related gene 3
ATG5	Autophagy related gene 5
BECN1	Beclin 1
GSTM1	Glutathione S-transferase Mu 1
GSTM5	Glutathione S-transferase Mu 5
RIPK1	Kinase, Protein kinase, Non-receptor serine/threonine protein kinase
BAX	BCL2-associated X protein
BID	BH3 interacting domain death agonist
BAK1	Bcl-2 homologous antagonist/killer
PARK7	DJ-1
NDUFAF1	NADH dehydrog. (ubiquinone) 1 alpha sub complex
COX7A2L	Cytochrome c oxidase subunit VIIa polypeptide 2 like
SDHB	Succinate dehydrogenase complex, subunit B
UBB	Ubiquitin B
NFKB1	Nuclear factor related to kapp beta A
SLC25A29	Solute carrier family 25, member 29
SLC25A42	Solute carrier family 25, member 42
IFI6	Interferon alpha-inducible protein 6
UQCRFS1	Ubiquinol-cytochrome c reductase, Rieske iron-sulfur polypeptide 1
TBP	Basal transcription factor
PSMB5	Proteasome (prosome, macropain) subunit, beta type, 5
FYN	Proto-oncogene tyrosine-protein kinase Fyn
DRD2	Dopamine receptor D2
PPP1R13B	Protein phosphatase 1, regulatory (inhibitor) subunit 13B

Table 7.2: Symbol and title of selected genes analysed through RT-PCR.

Symbol	Gene
C20orf111	Chromosome 20 open reading frame 111 (peroxide-inducible transcript 1)
PDCL3	Phosducin-like 3
DAD1	Defender against cell death 1
DNAJA1	DNAJ (Hsp40) homolog, subfamily A, member 1
HSP90AA1	Heat shock 90kDa protein 1
DNAJB6	DNAJ (Hsp40) homolog
DCTN3	Dynactin 3
RMND1	Required for meiotic nuclear division 1 homolog
VAMP4	Vesicle-associated membrane protein 4
PLTP	Phospholipid transfer protein
GSTM3	Glutathione S-transferase M3
PRDX3-H	Peroxiredoxin 3

7.1.3.1 Gene expression profile of SH-SY5Y cells after acute toxin exposure:

SH-SY5Y cells were treated with diquat (0.1mM), epoxiconazole (0.1mM), fluroxypyr methyl ester (0.1mM), mancozeb (0.1mM), maneb (0.1mM) and rotenone (0.01mM) for 24 hours and after sample preparation, gene expression was calculated. Results revealed a significant fold increase (*P<0.01) in genes like *SRGAP2, MT-ND1, GBA, PARK7, SNCA, IFI6, SLC25A42, FYN, DRD2, UBB, C20orf111* and *PPP1R13B* after acute toxin exposure. A significant reduction (*P<0.01) was observed in *GSTM1, RMND1* and *SLC6A3* (table 7.3, 7.4). The subset of genes, whose expression was found to be differentially affected as a result of acute toxin treatment are shown in tables 7.3 and 7.4. Overall, *SRGAP2, MT-ND1, IFI6, C20orf111,* and *PPP1R13B, SNCA* and *UBB*, showed relatively similar modes of expression (up or down-regulation of ±1.4fold) for the majority of compounds tested suggesting a common set of genes which change following acute exposure. It is of interest that two of these genes, *SNCA* and *UBB* are involved with Parkinson's disease and Lewy body formation and *MT-ND1* and *C20orf111* are associated with oxidative metabolism.

7.1.3.2 Gene expression profile of SH-SY5Y cells after chronic toxin exposure:

For chronic exposure lasting 4 weeks, SH-SY5Y cells were grown in medium supplemented with diquat (0.001mM), epoxiconazole (0.01mM), fluroxypyr methyl ester (0.01mM), mancozeb (0.001mM), maneb (0.001mM), rotenone (5nM) and MPP+ (0.01mM) for 4 weeks and after sample preparation, gene expression was calculated. Overall results showed a significant reduction (*P<0.01) in the expression

of *UCHL1, ATG3, BECN1, GSTM1, BAK1, PARK7, NFKB1, SLC25A29, TRAPC4, DCTN3, RMND1, SLC25A42* and significant (*P<0.01) increase in *SDHBH, RIPK1, GAD1* and *MT-ND1* (tables 7.5, 7.6). Genes showing relatively common expression (±1.4 fold) following chronic chemical exposure were *ATG3, BECN1, BAK1, RIPK1* (involved in autophagy and cell death pathways), *MT-ND1, SDHB, SLC25A29* (mitochondrial carnitine/acylcarnitine carrier protein) associated with mitochondrial function, and *GAD1* and *TRAPPC4* involved in neurotransmission. With the exception of *MT-ND1*, there were no genes which were significantly regulated in common between acute and chronic chemical exposure, and in the case of *MT-ND1*, exposure appears to cause a slight increase in gene expression.

Table 7.3, 7.4: Description of genes identified by whole genome expression after acute 24 hour toxin exposure: Tables 3 and 4 show gene symbols and fold change in expression of only those genes which appeared to be up or down-regulated after treatment with selected toxins. (Significant results shown in bold, n=5, *p<0.01).

Table 7.3:

Chemicals	*SRGAP2*	*MT-ND1*	*GBA*	*GSTM1*	*DJ-1*	*RMND1*	*SNCA*	*SLC6A3*
Diquat	***2.2****	***1.56****	***2.6****	***1.3****	***1.8****	0.74	1.6	1.3
Epoxiconazole	0.22	1.5	0.7	***0.63****	0.77	0.65	1.5	0.86
Fluroxypyr methyl ester	***1.87****	***1.8****	1.3	0.8	1.3	***0.36****	1.5	1.04
Mancozeb	2.07	1.3	1.3	***0.93****	1.6	0.5	0.9	0.7
Maneb	1.6	***1.6****	1.3	1.1	1.3	0.53	***1.9****	***0.45****
Rotenone	1.9	***1.6****	1.3	***0.78****	1.4	***0.36****	1.3	0.9

Table 7.4:

Chemicals	*IFI6*	*SLC25A42*	*FYN*	*DRD2*	*UBB*	*PDCL3*	*C20orf111*	*PPP1R13B*
Diquat	2.1	***1.8****	***1.7****	***1.5****	1.3	***1.6****	1.7	2.0
Epoxiconazole	1.9	1.1	0.9	0.8	***2.1****	1.1	***3.8****	1.5
Fluroxypyr methyl ester	1.9	***1.34****	***1.54****	***1.80****	***1.60****	1.2	1.6	***2.4****
Mancozeb	1.9	1.3	1.2	1.1	1.1	1.3	2.3	1.6
Maneb	***3.0***	1.4	0.9	0.8	1.9	1.3	2.5	1.6
Rotenone	1.6	***1.3****	***1.6****	1.7	1.4	1.3	1.7	2.1

Table 7.5, 7.6: Description of genes identified by whole genome expression after chronic 4 week toxin exposure: Tables 5 and 6 show gene symbols and fold change in expression of only those genes which appeared to be up or down-regulated after toxin treatment. Significant results shown in bold (n=5, *p<0.01) (- indicates undetermined values).

Table 7.5:

Chemicals	*UCHL1*	*ATG3*	*BECN1*	*GSTM1*	*BAK1*	*PARK7*	*NFKB1*	*SLC25A29*	*MT-ND1*
Diquat	***0.13****	***0.43****	***0.26****	***0.47****	***0.07****	***0.70****	***0.61****	***0.35****	1.02
Epoxiconazole	1.3	0.72	0.83	0.93	0.71	1.1	***1.31****	1.13	1.1
Fluroxypyr methyl ester	0.95	0.66	1.23	***0.56****	***0.47****	1.06	1.17	0.58	1.18
Mancozeb	***0.36****	***0.45****	***0.35****	***0.70****	***0.11****	0.84	-	0.6	1.34
Maneb	0.31	***0.28****	***0.13****	***0.52****	***0.07****	0.45	1.20	***0.24****	1.37
Rotenone	0.71	***0.45****	***0.36****	0.82	***0.18****	0.87	-	1.03	***1.37****
MPP+	0.30	***0.37****	***0.22****	0.93	***0.17****	0.63	1.16	0.41	1.44

Table 7.6:

Chemicals	*TBP*	*PDCL3*	*SDHB*	*RIPK1*	*TRAPPC4*	*DCTN3*	*RMND1*	*SLC25A42*	*GAD1*
Diquat	***4.13****	***0.49****	1.2	1.81	0.91	0.22	0.44	1.01	2.11
Epoxiconazole	-	***1.29****	***1.79****	1.2	0.87	-	-	0.96	1.63
Fluroxypyr methyl ester	1.67	1.2	2.50	***3.84****	0.95	1.3	1.27	0.85	1.1
Mancozeb	-	1.03	***1.98****	2.03	***0.42****	-	-	1.21	1.7
Maneb	***0.33****	0.77	1.45	1.32	***0.19****	***0.21****	***0.39****	0.87	1.34
Rotenone	-	1.1	***1.47****	1.45	***0.46****	-	-	1.03	***2.08****
MPP+	-	0.81	***1.71****	1.46	***0.23****	-	-	***0.80****	1.73

7.1.4 Discussion:

Accumulating evidence indicates the role of environmental toxins in the progression of PD but the precise mechanisms through which these chemicals cause cell-death remain elusive. To get a better insight into the events leading to SH-SY5Y cell death, gene expression after acute high dose (24h) and chronic lower dose (4 week) treatment was investigated.

Previous studies studying the effects of PD linked toxins like paraquat on SH-SY5Y cells have shown significant alterations in the expression of genes which code for p53, TNF receptors and ligands, caspases, Bcl-2, TRAFs, IAPs, CARDs and those related with DNA damage-response and anti-apoptotic responses (Moran *et al*., 2008). Acute diquat (0.1mM) exposure significantly increased the expression of various genes (table 7.3, 7.4) but not of those linked with protein aggregation and degradation (like α-synuclein, ubiquitin B, *PSMB5*), autophagy (*BECN1*, *ATG3, ATG5*) or apoptosis (*BAX, BID, BAK1*). *DJ-1* (PARK7) was the only PD-linked gene which showed a significant fold increase following diquat treatment; though *SNCA* showed a 1.6 fold non-significant increase. Previous studies have shown down-regulation of *DJ-1* in PD patient nigra (Simunovic *et al*., 2009) and involvement in signalling in response to oxidative stress (Hardy *et al*., 2006). Other genes which showed an increased expression included *SRGAP2* which is involved in brain development, induces neurite outgrowth and negatively regulates neuronal migration (Guerrier *et al*., 2009), MT-ND1 a NADH dehydrogenase which is a part of complex I (Lenaz *et al*., 2004), GBA which is involved in the synthesis of lysosomal enzyme beta-glucocerebrosidase (*GBA* mutations have been associated with an increased risk of PD; Nishioka *et al*., 2009), SLC25A42 which is involved in the transport of molecules over the mitochondrial membrane (Haitina *et al*., 2006), DRD2 (Dopamine receptor D2) which shows increased density in PD (Seeman and Niznik, 1990) and PDCL3 which is a member of the phosducin-like protein family involved in caspase activation during apoptosis (Wilkinson *et al*., 2004). In contrast chronic diquat exposure predominantly reduced expression of genes involved with autophagic (*ATG3, BECN1*) and apoptotic (*PDCL3, NFKB1*) responses along with a reduced expression of *GSTM1* and *SLC29A*, suggesting the potential of reduced capacity to respond to diquat exposure. Similarly, *UCHL-1* was significantly down

regulated after chronic exposure but showed no change after 24 hour exposure. UCHL1 is involved in protein (de)ubiquitination and converts polyubiquitin chains into monomeric ubiquitin molecules. If UCHL-1 expression and its subsequent levels are reduced, it may lead to reduction in the available pool of ubiquitin and reduced UPS activity (Bossers et al., 2009). Overall, altered gene expression following acute diquat exposure shows the presence of oxidative stress (as observed through changes in *GSTM1*) and involvement of mitochondria (as seen with an up-regulation of *MT-ND1*) which may indicate cells' compensatory response to decreased energy levels.

Han et al (2008) measured gene expression in liver tissues of male C57BL/6 mice treated with diquat over a number of different time points lasting up to 12 hours and also compared the expression patterns in antioxidant knockout mice. They found an increase in genes linked with stress response rather than those having obvious antioxidant functions. p53 target genes involved in genotoxic stress checkpoint response were significantly up-regulated. Comparison of these results with another study investigating *in vivo* changes in gene expression after paraquat exposure showed that expression of 38% of genes statistically altered by diquat in the liver was also changed after paraquat treatment (Edwards *et al*., 2003).

Rotenone, a complex I inhibitor, caused a significant increase in *MT-ND1* expression after both acute and chronic exposure. Whereas *SLC25A42* and *FYN* were up-regulated after acute exposure but showed no change after chronic treatment. Autophagy related genes *ATG3* and *BECN1* as well as *BAK1* and *TRAPPC4* (transport protein) were down-regulated after chronic exposure only, indicating similarities to diquat. This suggests that the expression response to elevated autophagic or apoptotic stress does not necessarily constitute an up-regulation of classical autophagic or apoptotic genes. Previously, Borland et al (2008) have shown that chronic rotenone exposure (50nM) only alters expression of a minority of genes which has no major effect on rotenone's mechanism of toxicity. They recorded an up-regulation of few mtDNA coded genes linked with mitochondrial electron transport chain but expression of nuclear DNA coded genes remained unaltered.

Dopaminergic neurodegeneration is a complex process containing a cascade of events that cannot be explained by changes in the gene expression of cell-death or

oxidative stress related genes. This is best explained with examples of maneb and mancozeb which have shown changes in expression of several proteins but an examination of their expression using RT-PCR has shown that only *GSTM1* was down-regulated after acute mancozeb treatment, whereas *SNCA, MT-ND1* and *IFI6* were significantly up-regulated after acute maneb exposure. Chronic exposure however showed significant down-regulation of cell-death related genes including *ATG3, BECN1, BAK1* (both mancozeb and maneb) and PD-linked gene *UCHL1* (mancozeb only). As with diquat and rotenone, cells appear to down-regulate expression of autophagic and apoptotic response genes and just like epoxiconazole, MPP+ and rotenone, up-regulation of *SDHB* in mancozeb treated cells may indicate cellular response to mitochondrial respiratory chain inhibition. Overall, mancozeb and maneb showed similar gene expression changes.

Acute epoxiconazole exposure significantly increased the expression of ubiquitin B (*UBB*) and *C20orf111* (peroxide-inducible transcript 1) but showed a reduction in *GSTM1* expression. The presence of up-regulated *UBB* expression may indicate a response to damaged proteins which epoxiconazole may induce and possible clearance via the ubiquitin proteasome system and it would be of interest to determine if there is altered activity and the presence of ubiquitinated proteins following epoxiconazole treatment. The presence of changes in *GSTM1* and *C20orf111* may indicate an oxidative stress response mechanism following epoxiconazole treatment which could contribute to protein damage. Chronic epoxiconazole exposure however showed no changes in these genes and only showed significantly altered expression of *NFKB1, PDCL3* and *SDHB* (all up-regulated).

Acute fluroxypyr methyl ester (FPM) exposure significantly increased the expression of *SRGAP2, MT-ND1, SLC25A42, FYN, DRD2, UBB* and *PPP1R13B* and only down-regulated RMND1 expression. These results parallel those of acute diquat exposure and may indicate a similar mechanism of action or alternatively a regulated response by SH-SY5Y cells to toxin exposure. Similar to diquat, maneb and mancozeb, chronic FPM exposure showed a significant reduction in *GSTM1* and *BAK1* as well as an increase in *RIPK1*, properties of which have been discussed in previous chapters, although the reduction in autophagic and apoptotic gene expression was not significantly altered.

After chronic MPP+ exposure only *SDHB* was up-regulated whereas other genes were down-regulated. SDHB is a component of complex II of the electron transport chain (Ishii *et al*., 1998) and its up-regulation may be indicative of cellular response to mitochondrial respiratory chain inhibition. This is interesting since MPTP/MPP+ treatment is known to cause mitochondrial dysfunction and ROS production although in this study we did not observe a significant change in *GSTM1* expression. Previous studies exploring the effects of MPTP or MPP+ have shown distinct patterns of gene expression. Conn et al (2001) have shown that MPP+ induced gene expression changes control mitochondrial dysfunction and ER stress. Other studies using cDNA microarray analysis to produce a MPP+ toxicity profile after 72 hour exposure showed up-regulation of *c-Jun*, a change which has been observed in mice striatum (Perez-Otano *et al*, 1998) and substantia nigra after MPTP intoxication (Nishi, 1997). In the current study, *ATG3, BECN1* and *BAK1* were down-regulated after chronic exposure. Proteins of BCL2 family are involved in toxin induced apoptosis. Studies have shown that MPP+ can cause BCL2 and BCL2L1 activation in SH-SY5Y cells (Offen *et al*., 1998) but others show no such effect (Veech *et al*., 2000).

Exposure of SH-SY5Y cells to MPP+ causes apoptotic death (Fall and Bennett, 1999) accompanied with an increased oxidative stress (Cassarino *et al*., 1997), activation of pro- and/or anti-apoptotic signalling pathways (Cassarino *et al*., 2000; Halvorsen *et al*., 2002), increased production of bcl-2 and bcl-XL (Dennis and Bennett, 2003; Veech *et al*., 2000) and Bax (Dennis and Bennett, 2003). Brill et al (2003) have shown that MPP+ induces apoptotic death through a process involving cytochrome c release (within 2-4 hours) and caspase-dependent DNA degradation between 12 to 24 hours after MPP+ exposure in SH-SY5Y cells. They suggest that complex I inhibition after acute MPP+ exposure leads to changes in the expression of multiple genes which may be linked with cell survival. They suggested that changes in gene expression depended on mitochondrial integrity and occurred hours before the appearance of apoptotic markers. In the current study, the changes seen following chronic MPP+ exposure where *ATG3, BECN1* and *BAK1* were down-regulated, may indicate a compensatory response to promote cell survival.

Results from gene and protein expression studies of post-mortem PD brains and in animal models have shown that expression changes occur in later stages of the disease when cell number is significantly lower and remaining cells are undergoing apoptosis or necrosis (Mandel *et al*., 2002). Therefore, early gene expression profile can reveal biochemical changes that lead to initial series of events that promote neurodegeneration. This could also involve novel growth factor genes and those related to prostaglandins, glucose metabolism-related proteins, cytochrome P450 etc which have been linked with events involved with neuronal cell-death (Grunblatt *et al*., 2001). Indeed, cDNA expression microarrays have been used in studies to detect early gene expression changes occurring within 3 to 24 hours after methamphetamine-induced DA neurodegeneration in mouse striatum (Cadet *et al*., 2001) or midbrain (Xie *et al*., 2002). These studies also reported an up-regulation of genes related to energy metabolism (*COX1, NADH2*), apoptosis, inflammation, growth factors, signalling, stress-response, oxidative stress and ion regulation (*SLC10A1, SLC9A3R1*). Some of these findings are similar to those observed in the current study which also showed changes in genes involved in processes like ATP generation (*MT-ND1, MT-ND2*), solute transport (*SLC25A29, SLC25A42*) and apoptosis (*BID, BAK1*).

Previous studies investigating the effect of chronic MPTP administration in animal models suggest that a cascade of events including changes in gene expression linked with inflammation, glucose and iron metabolism, cell cycle regulators and oxidative stress occurs and at the same time survival mechanisms including different trophic factors and anti-oxidant mechanism are activated including glutathione transferases, GDNF, IL-10 and cyclin B2 etc (Mandel *et al*., 2002). Results from this study showed no change in genes which may play a role in protection apart from *GSTM1* which was significantly down-regulated after chronic toxin exposure (table 7.5). Wang et al (2007) have reported similar results in a microarray study using midbrain-derived dopaminergic neuronal cells. Their data showed changes in molecular mechanisms common with the pathogenesis of PD. Their results suggested involvement of oxidative stress, apoptosis, signal transduction and iron binding after MPP+ induced toxicity. However, chronic MPP+ exposure in the current study failed to show significant change in expression of genes linked with apoptosis or signal transduction though changes in autophagy (*BECN1, ATG3, RIPK1, BAK1*) and

mitochondrial function (*SDHB, MT-ND1*) were altered. Only *TRAPPC4* which has a role in ER to Golgi vesicle mediated transport (Elstner *et al.,* 2009) showed down-regulation. In general, many of the genes altered in LBD midbrain neurones (Elstner *et al.*, 2009) appear to be altered by MPP+ exposure.

This study did not provide complete insight in precise sequence of events causing cell-death although provided some indication that mechanisms like apoptosis and autophagy may be down-regulated and processes like oxidative stress (as observed through changes in expression of *DJ-1, C20orf111* and *GSTM1*) and mitochondrial dysfunction (as noted by changes in *MT-ND1* and *SDHB*) play a major role in toxicity. It can be deduced from this study's results that changes observed here might interact with deleterious mechanisms already recognised to have a role in the toxin induced cell-death of SH-SY5Y cells including mitochondrial dysfunction, impairment of the UPS and involvement of apoptosis. Further work is required to explain the relationship between early gene changes and biochemical events that lead to late gene expression which are most likely to contribute towards DA neurodegeneration. SH-SY5Y cells are not primary neurons but from a neuroblastoma tumour lineage, therefore, it has been suggested that this may affect gene expression responses to sub-acute toxin exposure but they are very sensitive to rotenone/MPP+-induced neurotoxicity which is an advantage in the identification of early and subtle changes in gene expression and at the same time they provide a useful and readily available model for these experiments until human stem cell-derived DA neurons become widely available.

Chapter Eight: Differentiation of human embryonic neural precursor stem cells

8.1.1 Introduction:

Limited availability of human cells for both therapeutic and basic research is a major problem in the development of transplantation therapies for Parkinson's disease. Dopaminergic neurons could be used in cell replacement therapy (Lindvall *et al.,* 2001) or used for assessing the role of potential therapeutic agents in culture assays and if they were readily accessible, studies on cellular mechanisms involved in PD could be greatly facilitated. Previous studies have shown that human embryonic stem cells (hESCs) can divide indefinitely in culture. This makes them a valuable source of functional differentiated cells for cell replacement therapies as they can be induced to differentiate into cell types of all three germ layers *in vivo* and *in vitro* (Thomson *et al.,* 1998). Therefore, these differentiation systems can provide a simple experimental model for developing optimal cultures of midbrain dopaminergic neurones suited for implantation studies in animal models of PD. That is why a main objective in the clinical application of hESCs is the generation of midbrain dopaminergic neurons for cell transplantation therapy of Parkinson's disease (Freed *et al.,* 2002). They can also be useful in understanding the factors and mechanisms involved in cell proliferation, differentiation pathways, derivation and control of different cell-lineages and in screening assays (Trosko and Chang, 2009).

8.1.1.1 Aims:

Stable cell-lines derived from neuroectodermal, neuroendocrine or glial tumours and primary cultures (from embryonic rodent brain) are widely used in most *in vitro* studies. Tumour derived cell-lines provide an almost indefinite supply of cells for research but they have rapid growth rates in complete contrast to the adult CNS and are difficult to differentiate into stable cultures. Stable, often non-dividing cells can be derived from primary cultures but a continuous supply is needed in order to provide required amounts of tissue for research and testing. Since neuroblastoma cell-line SH-SY5Y is not derived from the CNS, it shows significant phenotypic differences to CNS dopaminergic neurones. This potential question can be addressed by developing stem cell-lines from human foetal material. This study aimed to overcome these limitations by deriving human Neural Precursor Cell (hNPC) lines and developing a simple culture system for the differentiation of hNPCs to neuronal

populations of cells, including the midbrain dopaminergic lineage characterised by the expression of different neuronal and dopaminergic markers.

8.1.2 Methods: Refer to materials and methods (section 2.6).

8.1.3 Results:

8.1.3.1 Differentiation of hNPSC into cells with dopaminergic-like phenotype:

Neurospheres showed continued growth in defined serum free medium for at least 30 weeks from all regions tested (telencephalon, medulla, mesencephalon) with the exception of spinal cord which failed to proliferate after 3-4 weeks. Expression of classical hNPC marker such as nestin, SOX2 and vimentin and incorporation of BrdU were positively identified in neurospheres. hNPC neurospheres easily adhered to the substrate and began sprouting processes when placed in serum containing medium. Undifferentiated neurospheres and 14 days differentiated cells were extracted in native lysis buffer and analysed through western blotting to check the level/presence of neuronal markers. Protein expression using western blotting of differentiated hNPC demonstrated the presence of readily detectable levels of several neuronal receptors (e.g. mGluR1) and transporters (e.g. DAT) along with intracellular signalling proteins.

Undifferentiated neurospheres stained positive for nestin (neural stem/progenitor cell marker) (fig 8.1, 8.2). Other results showed a high population (more than 70%) of Tuj1 and TH positive cells (fig 8.4a) demonstrating that neural cells can be successfully derived from proliferating neural progenitor cells. However, hNPCs differentiated for later experiments showed a lower percentage of TH positive cells (fig 8.4b). An approximation of relative numbers of Tuj-1 or TH-positive cells was made by counting the total number of DAPI and TH-positive cells with clear cell morphology. In addition, larger numbers of weakly positive cells and cells with unclear morphology were also observed. To determine whether these growth factors play a role in inducing neuronal differentiation, we compared differentiation of hESCs in the presence or absence of stem cell factor (SCF). No significant difference in the number of TH-positive cells was observed among the cells differentiated either with or without SCF. Overall immunocytochemical analysis showed the presence of

approximately 70% neurons as defined using neurone-specific beta-tubulin (Tuj-1), which could be directed to produce chemically defined neurones e.g. tyrosine hydroxylase (fig 8.3). Glial cell types were present with majority of cells being astrocytes (GFAP +ve) (fig 8.3) with small numbers (1-3%) of oligodendrocytes but with the presence of some nestin and BrdU +ve cells indicating dividing stem cells were still present.

Fig 8.1: Cultivation of neural stem cells. (A) Phase contrast image of 2 week-old midbrain neurospheres; (B) Neurospheres stained positive for stem cell marker nestin (yellow), (blue = DAPI nuclear stain); (C) Tuj-1 and (D) DAPI stained cells growing outwards from a neurospheres (40X magnification).

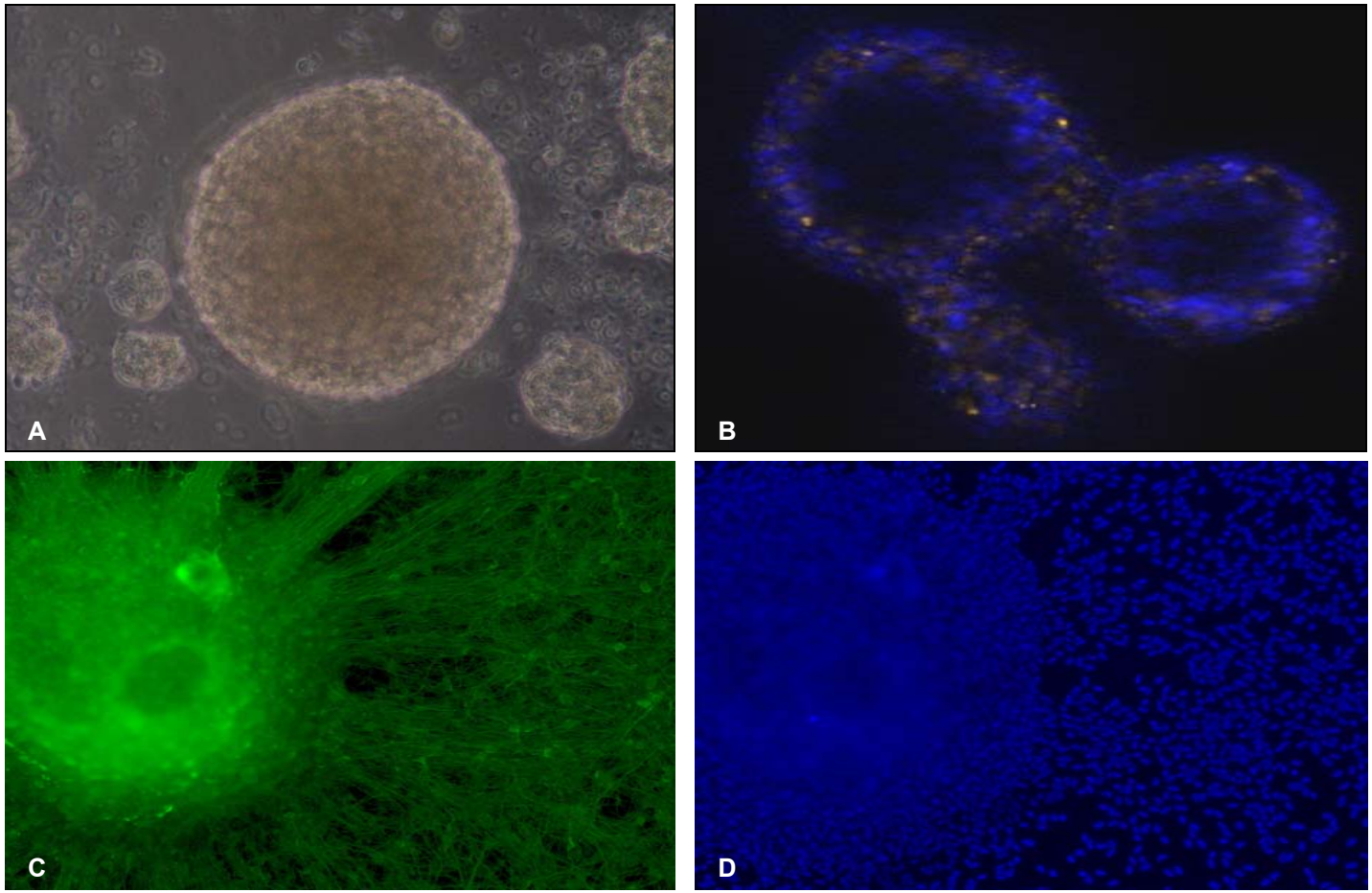

Fig 8.2: Immunocytochemical analysis of neurospheres. Neurospheres grown from single hNPCs on gelatine (A,B) or poly-L-lysine (C,D) coated slides for 14 days in DMEM/F12 supplemented with EGF, FGF2 and LIF. Neurospheres in all conditions show immunoreactivity to both nestin and SOX2, indicating that cells within the spheres are neural cells as defined by these markers (40X magnification).

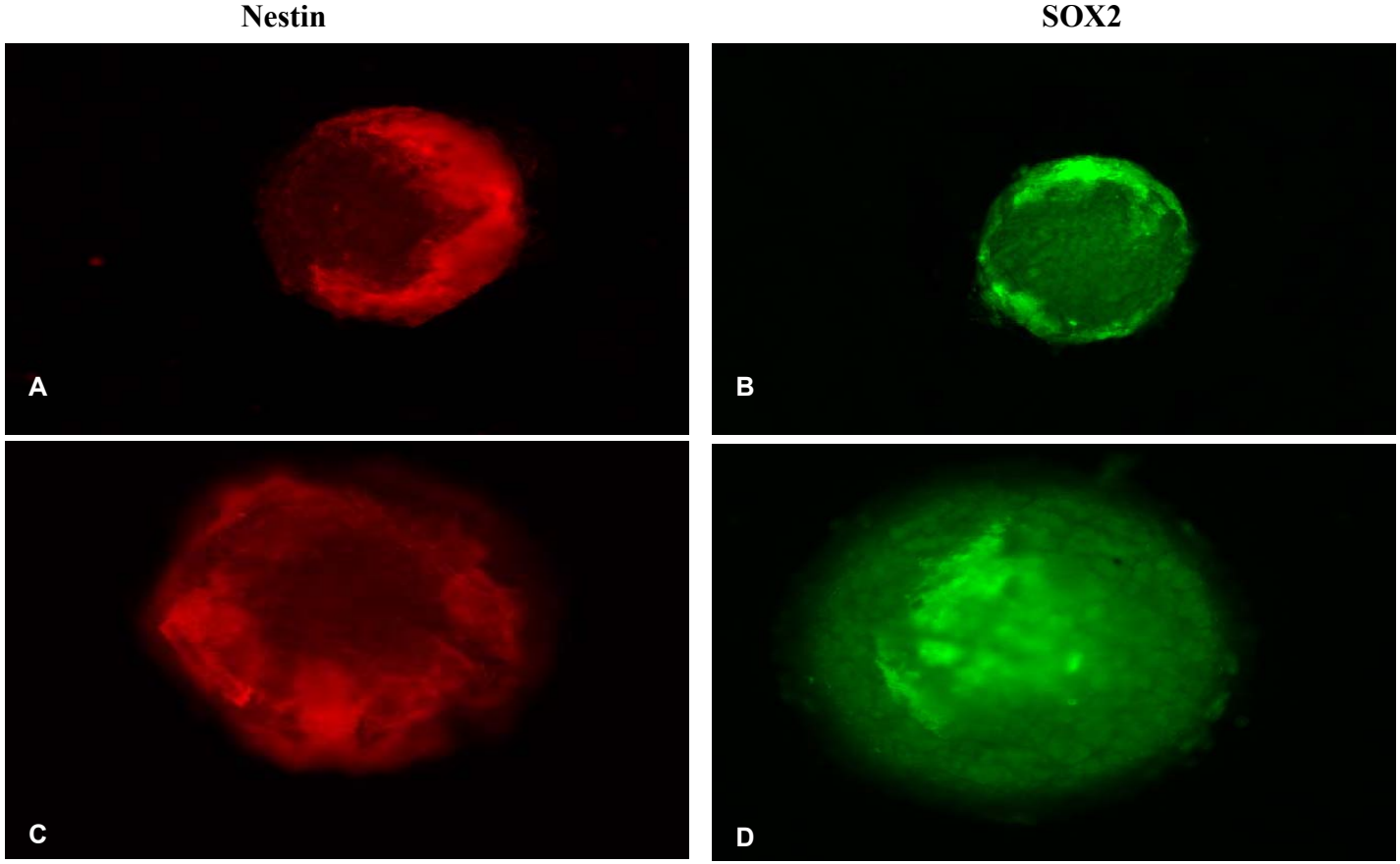

Fig 8.3: Immunocytochemical analysis of differentiated N969 cells. hNPCs positively stained for (A) TH, (B) Tuj-1, (C) Nestin and (D) GFAP (x10 magnification, each image is representative of three independent fields).

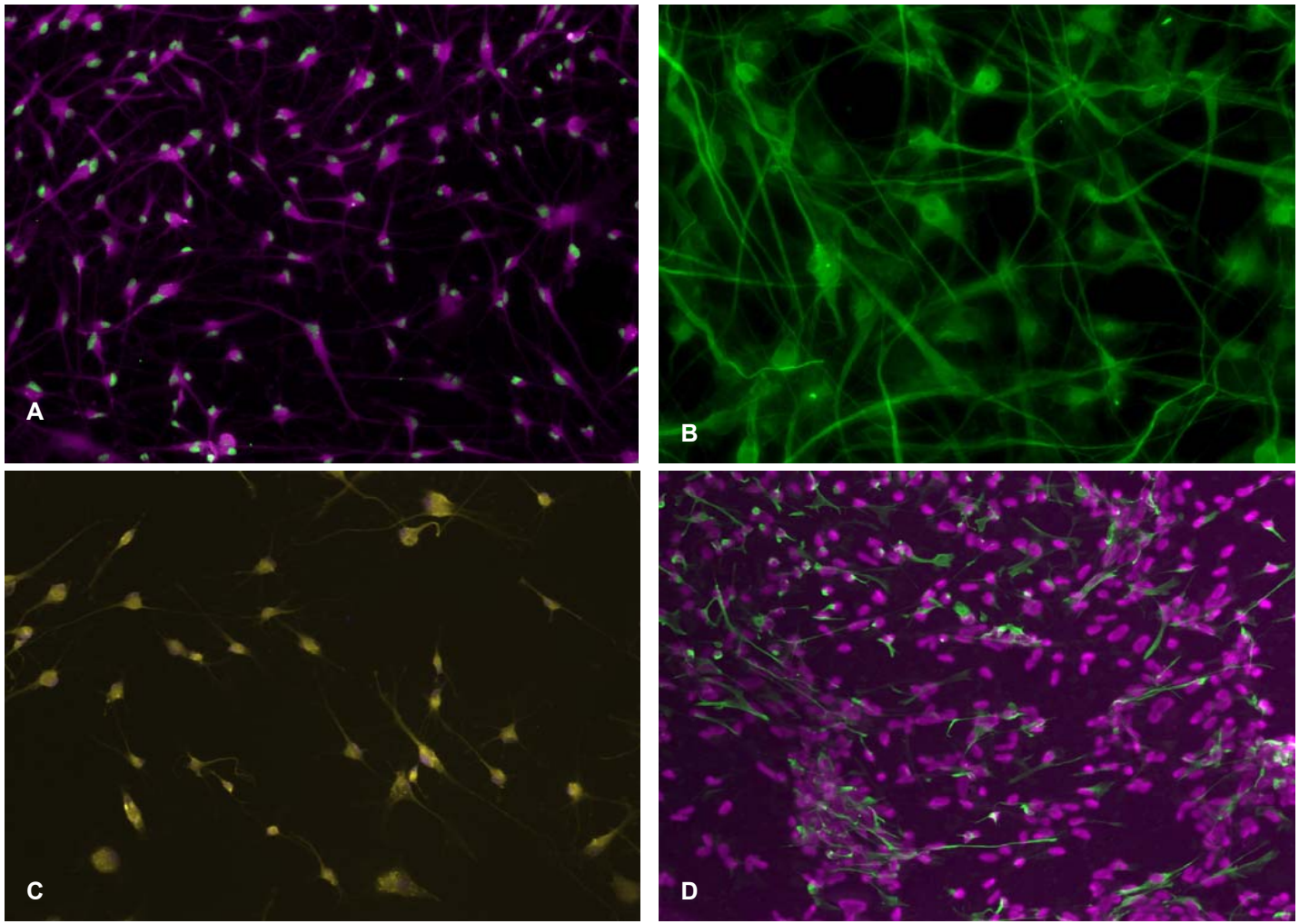

Fig 8.4: Percentage of TH and Tuj1 positive cells: (A) A high percentage of TH positive cells were present in differentiated cell population. (B) Percentage of cells expressing TH marker reduced with time (n = 3, ±SD).

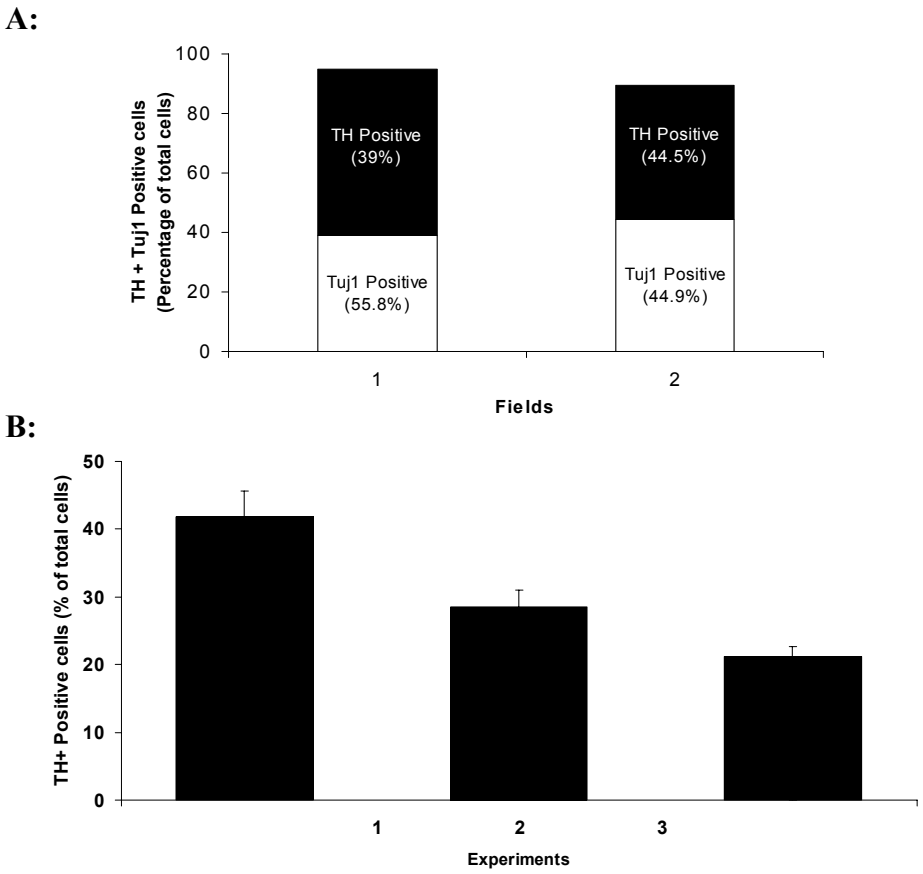

Protein expression using western blotting of differentiated hNPC demonstrated the presence of neural markers of specific receptors indicating the possibility of GABAergic, dopaminergic and glutamatergic neurones. A significantly higher level of tyrosine hydroxylase expression was noted in differentiated cells (fig 8.5A). Readily detectable levels of several neuronal receptors (e.g. GABA A Receptor γ 2 and G protein-coupled glutamate receptors 'mGluR1') and transporters (DAT) were detected (fig 8.5B). Detection of GABAergic marker GAD67 confirmed a heterogeneous population of differentiated cells. Proteins involved in the function of the presynaptic cholinergic neurons of the CNS like RAF kinase inhibitor protein (RKIP/PBP) or postsynaptic marker 'PSD95' were also detected and suggested advance differentiation with cells capable of forming synaptic contacts.

Fig 8.5: A) Protein analysis showing a high tyrosine hydroxylase levels in differentiated N969 cells. B) Expression of different neuronal markers in differentiated cells: hNPCs contain a range of neural markers of specific receptors indicating the possibility of mixed neuronal population.

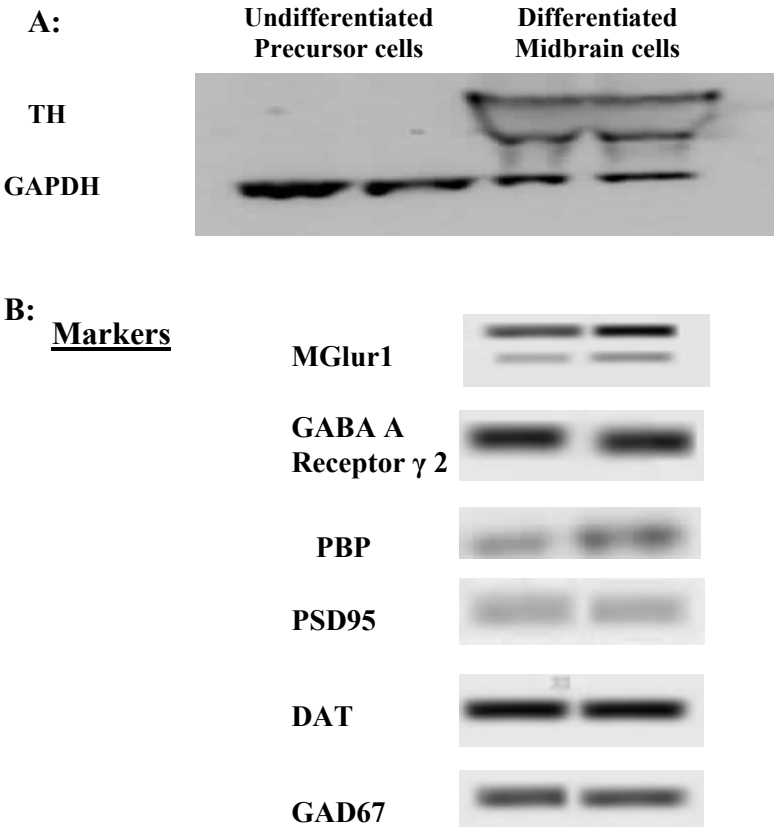

8.1.3.2 Toxin treatment:

N969 cells were induced to differentiate in 8 well chamber slides coated with poly-L-lysine. After 14 days, differentiated cells were treated with different chemicals for 24 hours (from 0.001mM-0.1mM) (fig 8.6), after which Alamar blue reduction was measured. Cytotoxicity screening showed that just like in SH-SY5Y cells, chemicals reduced cell-viability in a dose dependent manner. Maneb, mancozeb and rotenone caused significant reduction in viability at all three doses (0.1mM, 0.01mM and 0.001mM). Diquat, epoxiconazole and mecoprop-p caused significant toxicity at 0.01mM and 0.001mM, whereas MPTP and MPP+ were only toxic a1 0.1mM. Average percentage viability of hNPCs and SH-SY5Y cells were compared and results showed that hNPCs were marginally more sensitive to these toxins, especially at 0.1mM (table 8.1). Treated slides were fixed, stained and used for immunocytochemical analysis (fig 8.7). Co-staining and subsequent cell counts of TH and Tuj1 positive-cells showed that these toxins did not specifically target TH positive cells as no significant difference in the number of either marker was observed.

Fig 8.6: Effect of toxin treatment for 24 h on viability in differentiated midbrain precursor cells: Viability for each dose (0.001-0.1mM) is shown as percentage of untreated control. A) MPTP,B) MPP+, C) rotenone, D) diquat, E) maneb, F) mancozeb, G) epoxiconazole, H) mecoprop-p (n=3, difference from control was tested for statistical significance, * = *p* values<0.05 were accepted as significant).

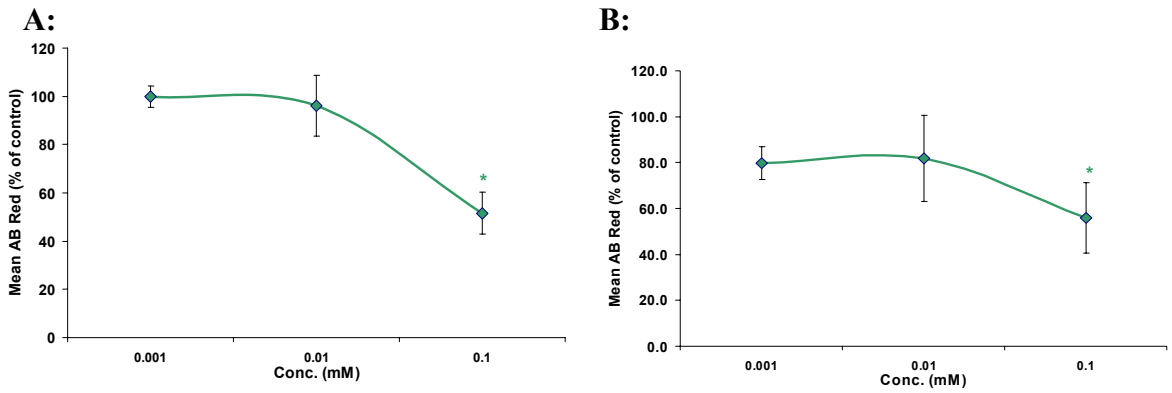

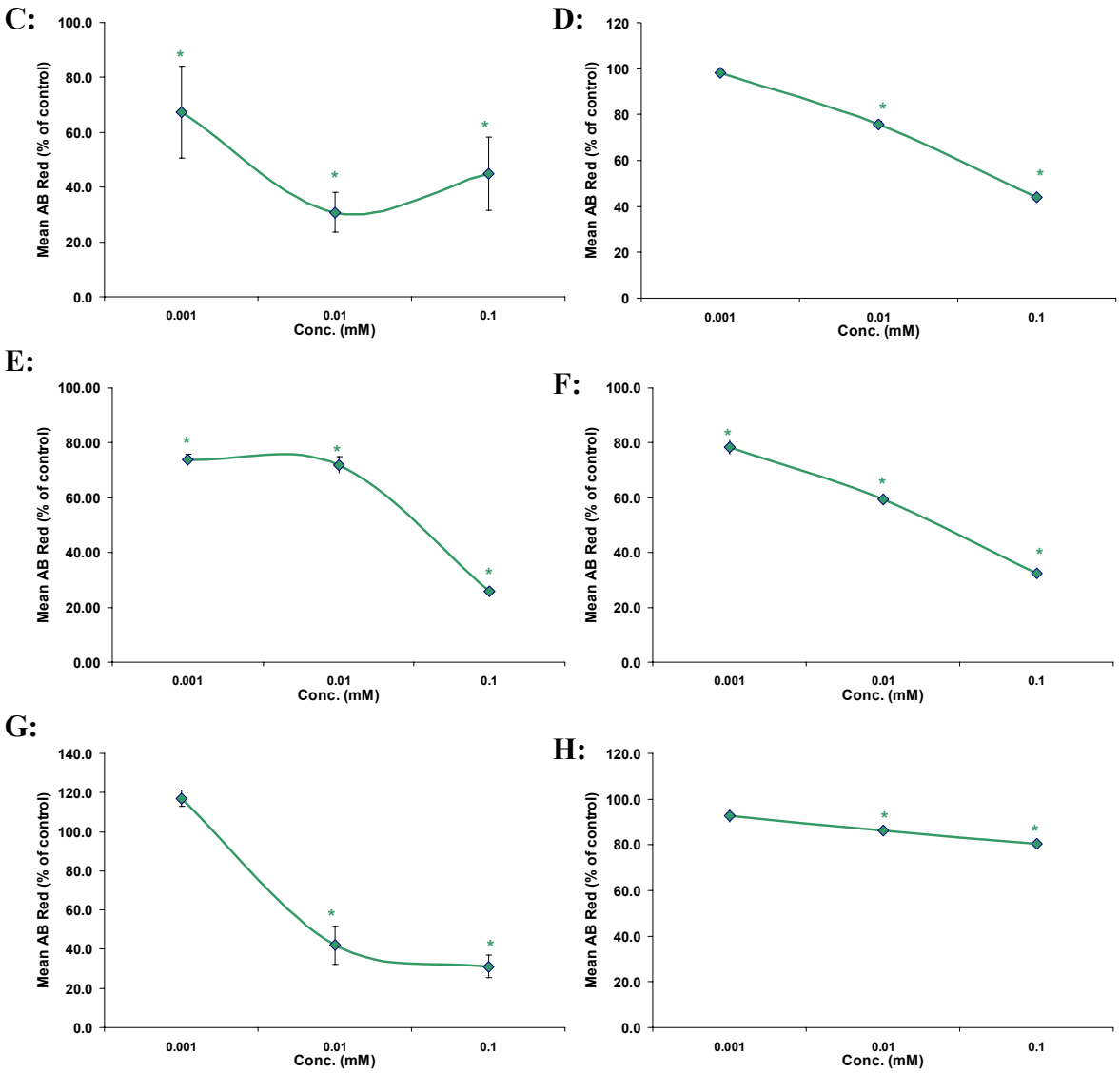

Table 8.1: Percentage viability comparison between SH-SY5Y cells and hNPCs after 24 hours toxin exposure: (Percentage of untreated control)

Toxin	Concentration (mM)					
	SH-SY5Y cells			Human Midbrain Cells		
	0.1	0.01	0.001	0.1	0.01	0.001
Rotenone	60	100	100	50	70	80
MPP+	80	95	100	50	80	80
MPTP	95	100	100	50	100	100
Diquat	45	100	100	45	75	100
Maneb	5	30	80	25	72	73
Mancozeb	5	20	90	30	60	80
Epoxiconazole	50	90	100	30	40	100
Fluroxypyr ester	40	85	100	75	75	90
Mecoprop methyl ester	85	100	100	80	85	100

Fig 8.7: Immunocytochemical staining of toxin treated cells: hNPCs were differentiated using standard protocol and then incubated with different toxins for 24 hours. Diquat (0.01mM) and mancozeb (0.01mM) treated slides were stained for TH and Tuj-1 markers (Each image representative of 3 different fields, Magnification = x10).

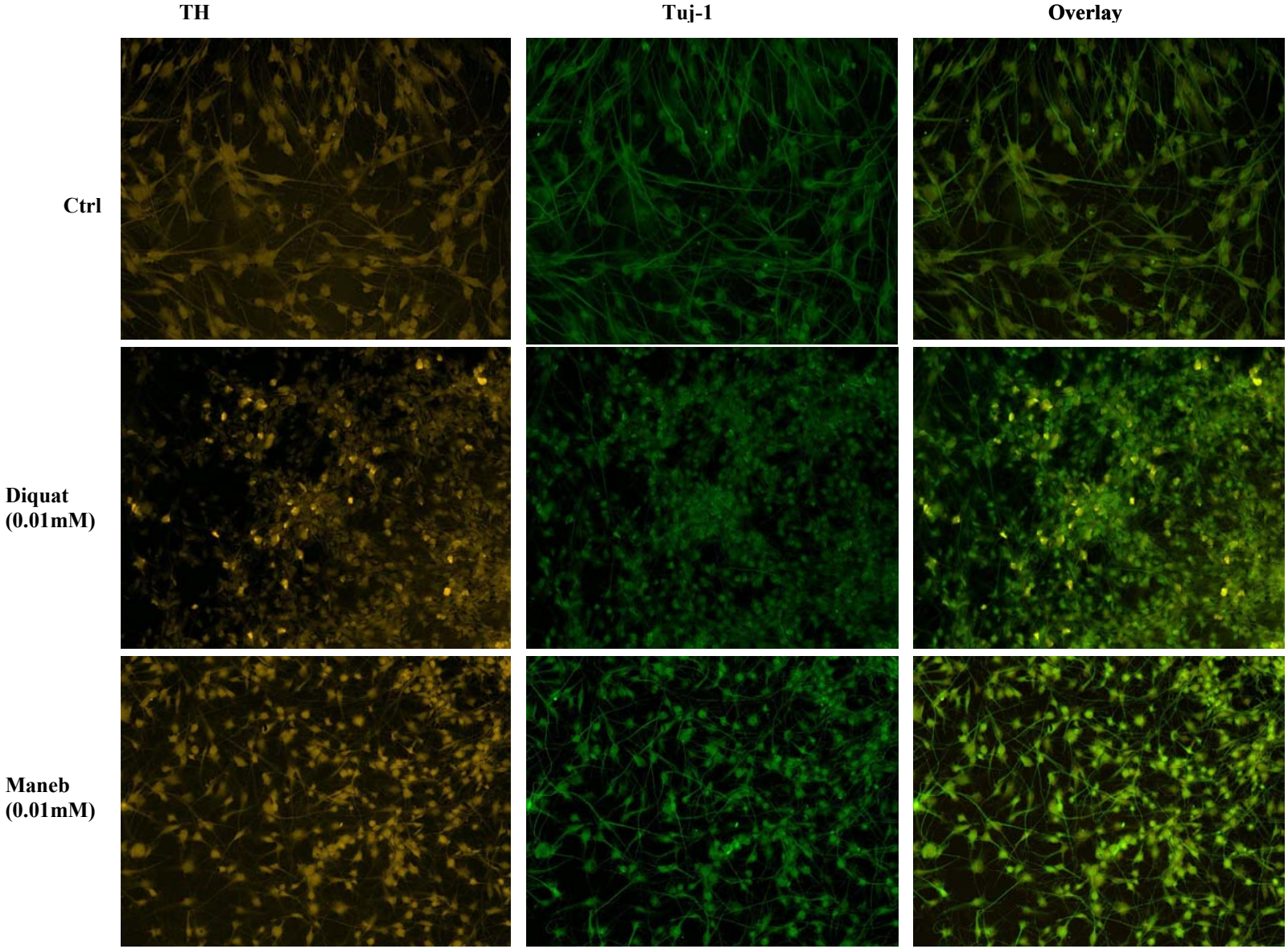

8.1.4 Discussion:

There are different ways to isolate hESCs and there are differences in the timing of cell derivation and the means by which cells are isolated. Therefore, characteristics and quality of resultant cells can differ but a similar pattern of stem cell markers is still exhibited in most cells. This study showed successful derivation of hNPC lines and undertook a preliminary evaluation of their suitability in neurotoxicology studies. Main findings suggest that these hNPC lines can be maintained for longer than 6 months in serum free defined media as 'neurosphere' cultures and can be successfully regrown from liquid nitrogen storage providing a long term supply from limiting amounts of starting material.

The neural lineages formed by this method of differentiation expressed specific markers of neural progenitors like SOX2 and nestin. We report that differentiated cells with a number of properties consistent with those of DA neurons can be efficiently generated from a hNPC line. Cells derived from this method are functionally and biochemically similar to normal dopaminergic neurons. Although further investigation is required to ensure other genetic or protein markers are expressed in these cells. The ultimate functional test of this would be to demonstrate dopamine release. The method used here resulted in the production of a high percentage of dopaminergic neuronal cells (fig 8.3E), which is essential for potential therapeutic application. These cultures can be induced to differentiate into neurones, astrocytes and oligodendrocytes by simple growth factor withdrawal and serum addition, or can be directed to differentiate into specific cell types (e.g. dopaminergic neurones) by addition of specific factors. Importantly, differentiation was not uniform and cell types other than non-dopaminergic cell types were present (fig 8.3A-D). Once differentiated, these cell lines are relatively stable and show minimal cell division over several weeks, express neuronal and glial antigens indicating the capacity to produce the normal repertoire of cells found in the CNS with the exception of microglia. We identified mature dopamine neuron markers including proteins directly involved in dopamine neurotransmitter biosynthesis and function, especially TH and DAT.

Protein expression in differentiated hNPC demonstrated the presence of different neural markers of specific receptors and specific neurotransmitter receptors. Once differentiated, cells maintained their phenotype for a considerably longer period of time *in vitro*. Examination of hNPCs over extended periods showed that dopaminergic characteristics of differentiated cells changed over time and cells did not stably express tyrosine hydroxylase marker (see fig 8.3F). This showed that the method needs to be further optimised so that characteristic markers in these cells can be maintained for prolonged periods of culture and an enriched population of a specific cell-type can be generated. More importantly, the presence of PBP and PSD95 suggests a synaptic contact between cells and they are capable of forming cellular networks as in the adult or even developing brain. hNPCs may therefore provide a suitable cell system to complement existing *in vitro* models used in toxicology.

The differentiated cells are killed by a range of known neurotoxins (kainic acid, data not shown) using doses which usually show little effect in tumour cell lines indicating that they may be more sensitive to toxins and providing a more accurate representation of the doses of compounds likely to have an effect *in vivo* in man. In this study toxicity screening using different chemicals has shown a dose-dependent reduction in cell-viability (see fig 8.5). When these results were compared to corresponding data from SH-SY5Y cells, it is noted that both cell-models show a similar pattern of toxicity with all chemicals but with hNPCs more vulnerable at higher doses like 0.01mM and 0.1mM (see table 8.1). Average Alamar blue reduction values from different experiments show slightly lower viability than that recorded with SH-SY5Y cells. It is possible that differences in response to toxins might be related to stage of cellular differentiation. A common problem of cell-models is that the *in vivo* environment cannot be mimicked by the using any cell-type or endpoint. Stem cells exist in their own unique niche. This microenvironment controls their proliferation and differentiation and factors like extracellular matrices and extracellular soluble signals play a part in generating a response to a toxic chemical.

By using growth factors which have clearly enabled differentiation of hNPCs into a mixed population containing tyrosine hydroxylase positive neurons, we have

tried to provide a microenvironment allowing cell to cell contacts in the hope that mimicking the *in vivo* niche could provide an accurate measure of the toxicity of these chemicals. Once cells are isolated from their niche and grown *in vitro*, their sensitivity to chemicals may change. This is one advantage of using a mixed cell-population compared with the homogeneous SH-SY5Y cell-line and may explain the increased vulnerability to different chemicals. The association between toxicants and neurological disorders has to be complemented by *in vivo* and *in vitro* experimental studies aimed at investigating the cellular and molecular mechanisms of toxicity. This study describes a method that can be used for the examination of the potential neurotoxic effects of pesticides in isolated dopaminergic neuronal systems.

Chapter Nine: Discussion

Duscussion:

The human neuroblastoma cell-line SH-SY5Y, which shows a dopaminergic phenotype, was successfully used as an *in vitro* model of dopaminergic neurones. Various aims were well supported by current findings. The fact that it is not derived from the CNS is often cited as a disadvantage because it can show significant differences to dopaminergic neurones derived from the CNS. Derivation of stem cells from human embryonic material and their successful differentiation into cells exhibiting neuronal phenotype and dopaminergic characteristics addressed the potential question of SH-SY5Y suitability. Presence of a mixed cell population gave a slightly more realistic picture of cell response to toxicity. In order to maintain the dopaminergic properties of these cells, future work should include immortalisation of these lines using c-myc or similar vectors. These cell lines could be characterised for their gene expression profile and compared to SH-SY5Y cells and adult dopaminergic neurones using assay of dopaminergic parameters and gene expression using real time Q-PCR and neurochemistry.

Activation of caspases has been widely reported during apoptosis induction in SH-SY5Y cells (Newhouse *et al*., 2004). Caspases are regarded as the primary mediator of apoptosis and they cleave various cellular proteins including PARP, which showed a dose and time related increase in expression. Reduction in toxicity with caspase-inhibitors like zVAD.fmk was minimal when compared with Nec-1 which provided complete protection against a number of different chemicals. Overall results from this study showed that PARP-1 induction was seen as a late event in agrochemical treated cells and treatment caused caspase independent cell death processes involving RIP. This study did not show any dose-related increase in caspase-3 levels and the use of caspase inhibitors failed to completely reduce toxicity. The absence of any effect of caspase inhibitors on this process for most agrochemicals with the exception of diquat, may suggest caspase independent induction of PARP-1. Assessment of cell death and apoptosis can be further facilitated by showing nuclear condensation, DNA fragmentation and perinuclear apoptotic bodies. These can be aided by using flow cytometry for nuclear pyknosis or TUNEL staining (if available) to show chromatin condensation and DNA strand breaks. Another area for future research is the identification of transcription factors and signalling intermediates in death pathways that are linked with toxin induced

apoptosis. These could include different signalling intermediates and transcription factors as well as those not directly associated with the apoptotic machinery but still interfere with apoptosis e.g. PI3K/Akt and mitogen-activated protein kinase signalling pathways (Franke *et al*., 1997; Fukunaga and Miyomoto, 1998).

Data from experiments designed to investigate the role of autophagy suggest that chaperone-mediated autophagy may be involved with diquat, maneb and mancozeb toxicity. Evidence of lysosomal accumulation after chemical treatment indicates that lysosome mediated CMA may become active to remove damaged organelles. Future studies using ultra-structural microscopy, biochemical techniques, pharmacological agents and fluorescent markers can further help in the detection of autophagy. Electron microscopy can be ideal for morphological characterisation and detection of electron-dense AVs with double membranes, mult-ivesicular and residual bodies (Larsen and Sulzer, 2002). Indeed, electron microscopy has been used to detect autophagy in cellular models of PD (Sulzer *et al*., 2000; Stefanis *et al*., 2001). Dyes like LysoSensor Yellow/Blue Dextran (which are degraded in lysosomes and endocytosed by cells) (Larsen and Sulzer, 2002) and auto-fluorescent monodansylcadaverine (MDC) exclusively stain AVs in both living and fixed neurons (Petersén *et al*., 2001b). Biochemical methods using radioactive amino acid labelling prior to autophagy induction can measure protein degradation at several time points (Gronostajski and Pardee, 1984). Biochemical markers such as acid phosphatase, cathepsins (Biederbick *et al*., 1995) and autophagosomal lactate dehydrogenase (LDH) (easily separated from cytosolic LDH through centrifugation) (Stromhaug *et al*., 1998) can be used as indicators of increased autophagy. The use of these methods would be of use in further characterising the cellular responses to chemical exposure.

In order to explore the effects of mitochondrial dysfunction on neuronal biochemistry and physiology, fluorescence imaging techniques, mitochondrial complex function, change in membrane potential and, since mitochondria are widely considered to be an important source of reactive oxygen species, ROS generation was measured and visualised (including classical inducers of ROS such as enhanced mitochondrial membrane potential and inhibition of complex I). Discharge of membrane potential has different consequences for the cell, including apoptosis

(Abramov *et al*., 2007). Cell viability in response to increased ROS generation depends on the efficiency of cellular antioxidant systems including glutathione activity. A deficit of anti-oxidative glutathione and lack of mitochondrial complex I and dopamine in nigral neurons has been reported (Perry *et al*., 1986). Its depletion can be an indicator of oxidative stress and impair neuronal viability. Therefore, a measurement of glutathione activity could complement data gathered from other experiments investigating ROS generation. Future studies can try to differentiate between cytosolic reactive oxygen species and that generated by the mitochondrial matrix as well as ROS that is accumulated intracellularly. This has been shown by Shaikh and Nicholson (2009) who observed accumulation of large amounts of intracellular ROS in rotenone treated cells which was not released into extracellular environment.

Mitochondria play a vital role in maintaining neuronal calcium homeostasis (Duchen, 2000). Future work should include measurement of intracellular calcium and calcium imaging, where the calcium response can be followed over a certain time period after toxin treatment to provide information about regulation of calcium signalling and if mitochondrial calcium stores are altered in cells with complex I defects. There is documented evidence of a chronic reduction in complex I activity affecting calcium signalling in SH-SY5Y cells. Indeed, rotenone exposure (lasting 2 weeks) exhibits unusual calcium dynamics suggesting that reduced complex I activity renders cells susceptible to calcium overload and cell death (Sherer *et al*., 2001).

Neurotoxic pesticides which specifically affect mitochondria may cause acute inhibition of mitochondrial enzymes and elevation in cellular iron levels through increased iron metabolism. However, it is unknown if raised iron levels in PD neurones lead to mtDNA mutations or elevated levels of reactive oxygen species. Therefore, future experiments should be directed to the understanding of the mechanisms that regulate cellular iron levels and antioxidant defences. This approach could include determining the iron content by mass spectrometry and observing the expression of iron homeostasis proteins. Parkinson's disease has been associated with accumulation of iron in redox-sensitive tissues like substantia nigra and hippocampal neurons (Hayflick, 2006). Normal substantia nigra contains higher iron

levels than in other brain regions but SN from PD patients contain even higher levels of accumulated iron than non-PD samples (Zecca *et al*., 2001). It has been suggested that primary changes in neuronal iron can lead to neurodegeneration in PD. Indeed, there is evidence of raised intraneuronal iron in single dopaminergic neurons which suggests an association between abnormal iron metabolism and PD (Oakley *et al*., 2007). Experiments using SH-SY5Y cells have also shown that iron induces cell death through oxidative stress (Aguirre *et al*., 2007).

Biochemical assays measuring complex I activity provided good correlations between cytotoxicity and complex I inhibitory activity. Acute toxin exposure had no effect on CI or CII activities. Similarly, chronic exposure had no effect on mitochondrial energetics. Future work may include experiments designed to achieve limited inhibition of the mitochondrial respiratory chain by administration of siRNA to dopaminergic cell cultures. Data form this current study can provide information about the chemicals and doses that affect mitochondrial function so that effects of acute or prolonged exposure can be measured. Addition of pesticides and selective mitochondrial inhibitors can be used to produce a toxicity dose response curve in the absence of siRNA administration. To determine if there is increased susceptibility and cell death in presence of low levels of siRNA, neurotoxins can be used to determine if the dose response curve is moved to the left indicating enhanced toxicity. A good candidate for siRNA knockdown is NDUFAF1, a mitochondrial protein which is the human homologue of *Neurospora crassa* complex I chaperone CIA30, considered to be involved in the process of complex I assembly. Indeed, its expression has been knocked down in previous studies using RNA interference to regulate the intra-mitochondrial amount of NDUFAF1 and reduce the amount and activity of complex I (Vogel *et al*., 2005).

Previous studies have shown an increase in cytochrome c oxidase (COX)-deficient neurons in PD substantia nigra (Bender *et al*., 2006) and abnormalities in the mitochondrial electron transport chain can be measured by evaluating the loss of COX activity in the presence of maintained succinate dehydrogenase (SDH) activity. SDH is encoded by the nuclear genome, whereas mtDNA encodes three catalytic subunits of COX. This effect has been visualised in previous studies where the presence of blue SDH staining and absence of brown COX staining indicates

respiratory chain deficiency (Reeve *et al*., 2008). Future experiments can determine if mtDNA mutations are increased in response to combination of siRNA knock down and pesticide administration (evaluated by COX/SDH staining).

Gene expression changes, as observed through real-time PCR, have provided an insight into the range of proteins or cell-signalling mechanisms that may have a role in toxin induced cell-death of SH-SY5Y cells. Studies should use time course studies to identify markers and potential therapeutic targets and show the temporal sequence of different events which underline cell-death. This could help separate the cell or stress responses from defence mechanisms or those causing general neurotoxicity. In future, experiments using laser capture micro-dissection can be applied to sections of substantia nigra from neuropathologically confirmed cases of PD and controls. Tissue samples required for these experiments can be obtained from Newcastle Brain Tissue Resource. This technique can allow the isolation of individual dopaminergic neurons from which RNA can be extracted and amplified. Once it has been labelled with dye it can be hybridised to whole genome microarrays. This approach can help identify classes and families of genes being expressed as functional units and generate data which can identify gene expression signatures behind pathological changes found in SN neurones of PD (Elstner *et al*, 2009).

In the present study, various parameters of toxicity were successfully measured, including cytotoxicity in SH-SY5Y cells and generation of cytotoxic levels which were used to study the effects of cell-signalling inhibitors on viability, measurement of mitochondrial transmembrane potential, ROS formation, inhibitory activity towards mitochondrial complex I/II, protein expression after acute and chronic toxin treatment and changes in gene expression. Acute toxicity can be evaluated by examination of end points that indicate effects on cellular organelles such as leakage of cell constituents into the medium (e.g. lactate levels), uptake of dyes into the cell and the formation of surface blebs. However, long term toxicity assessments are highly dependent on the relevant toxic end point.

Overall results from this study show involvement of ROS and mitochondrial dysfunction (which may well be interlinked) after toxin treatment but this needs

further examining since data from agrochemicals like diquat is inconclusive in showing whether free radical generation occurs via the mitochondrial respiratory chain. ROS such as superoxide anions and hydroxyl radicals are balanced by radical scavengers and antioxidant enzymes. Therefore, an imbalance favouring ROS generation can lead to lipid peroxidation with resultant membrane and DNA damage and subsequent cell death. Given that oxidative stress induces proteasomal dysfunction both mechanisms could interact and exacerbate toxicity. Most of the toxic responses observed in this project involve various biochemical events related to oxidative injury and signalling pathways. The characterisation of novel mechanisms involved with these toxins can contribute to an understanding of how environmental neurotoxins including agrochemicals might contribute to the incidence of PD.

Major limitations:

The major limitation of this study is the lack of in-depth study of precise mechanism of action of different toxins. The thesis is broad on several compounds and it does not go as deeply into one compound as perhaps is possible. A number of different cell death and signalling inhibitors were used but such pharmacological manipulation was not successful. In hindsight, inclusion of genetic manipulation at the expense of pharmacological manipulation could have given more favourable results. This could help answer the question of how extensive is the genetic contribution to disease and if there are different pathways with a general phenotype although with any long term manipulation such as siRNA knockdown may lead to compensatory changes in cells which may mask any significant effects. Another weakness may be the inclusion of several cell death mechanisms instead of choosing and focusing on one type. There is more scope for determination of lysosomal/autophagic pathway since studies on this system have indicated that this may be a major mechanism for some toxin exposures (e.g. MPTP). Lysosomal aggregation was observed after acute toxin exposures but more study is required to show whether such changes are productive or deleterious. Changes in protein expression along with gene expression data did not explain the role of different mutations and their mechanism and how they contribute to the development or progression of the disease. Gene expression study using RT-PCR needs to be repeated to provide a better data set, possibly complemented by the use of

microarrays to determine other pathways involved in the response to specific toxins. Immunocytochemical analysis showed distribution of different proteins but failed to show any aberrant deposition or aggregation, although this is not always seen in some forms of parkinsonism. Due to lack of time and facilities being at different location, the measurement of mitochondrial complexes was not carried in full detail. The project could have benefited from the measurement of all respiratory chain complexes and also by oxygen consumption by the respiratory chain. Stem cells are more likely to represent a stable neuronal phenotype even though they are probably still embryonic neurones. Due to delays in starting stem-cell work and longer period of their maintenance and differentiation and failure of full optimisation of protocol prevented a detailed study of their use.

Future directions:

Findings from this study can provide the basis for several areas of further research. These include the following:

- Although toxicity was measured in SH-SY5Y cells and differentiated stem cells, comparison with other neuronal cell-lines could also be beneficial. Human dopaminergic neuroblastoma (BE (2)-M17) or mesencephalon-derived dopaminergic neuronal cell line (MN9D) have been used in similar studies and could provide a more detailed collection of data. Previous studies have shown that MN9D are more sensitive to MPP+-induced toxicity (Choi et al., 1991).

- Other assays which can lead to a comprehensive study of these chemicals may include lactate dehydrogenase activity assay (for cell-death), fluorescence-activated cell sorter (FACS) analysis to identify apoptotic cells and to discriminate between necrosis and apoptosis, apoptosis detection kits for measuring cytochrome C release from mitochondria, caspase-3 and -9 assays to measure enzyme activity, ATP determination assays to identify if toxins cause ATP depletion, antioxidant enzyme activity (e.g. SOD) could be measured to give a clear picture of oxidative stress caused by different chemicals. Evaluation of neurite length and changes in cell size were not

quantitatively measured. Future experiments could measure these parameters as well as use techniques such as flow cytometry for observing changes in nuclear structure especially pyknosis.

- To study the relationship between α-synuclein and acute/chronic toxicity, cell lines stably transfected with wild-type or mutant α-synuclein could be used. Also, a more robust method of cell transfection needs to be adapted to ensure a higher percentage of siRNA knockdown. This study used lentiviral delivery method without great success. Therefore, stable transfection which may cause greater integration could be tried.

References

Aarsland D, Andersen K, Larsen JP, Lolk A, Nielsen H, Kragh- Sorensen P. Risk of dementia in Parkinson's disease: a community-based, prospective study. *Neurology*. 2001. 56:730–736

Abe K, Yoshida M, Usui T, Horinouchi S, Beppu T. Highly synchronous culture of fibroblasts from G2 block caused by staurosporine, a potent inhibitor of protein kinases. *Exp Cell Res* 1991; 192: 122–7.

Abbott RD, Ross GW, White LR, Sanderson WT, Burchfiel CM, Kashon M, Sharp DS, Masaki KH, Curb JD, Petrovitch H. Environmental, life-style, and physical precursors of clinical Parkinson's disease: recent findings from the Honolulu-Asia Aging Study. *J Neuro*l. 2003 Oct; 250 Suppl 3:III30-9.

Abeliovich, A., Schmitz, Y., Farinas, I., Choi-Lundberg, D., Ho, W.H., Castillo, P.E., Shinsky, N., Verdugo, J.M., Armanini, M., Ryan, A., et al. Mice lacking alpha-synuclein display functional deficits in the nigrostriatal dopamine system. *Neuron*, 2000; 25, 239–252.

Abeliovich A, Beal FM. Parkinsonism genes: culprits and clues. *J Neurochem*. 2006 Nov;99(4):1062-72.

Abou-Sleiman P.M., Healy D.G., Quinn N., Lees A.J., and Wood N.W. The role of pathogenic DJ-1 mutations in Parkinson's disease. *Ann. Neuro*l. 2003; 54, 283-286.

Abou-Sleiman PM, Muqit MM, Wood NW. Expanding insights of mitochondrial dysfunction in Parkinson's disease. *Nat Rev Neurosci*. 2006. 7:207–219.

Abramov AY, Scorziello A, Duchen MR. Three distinct mechanisms generate oxygen free radicals in neurons and contribute to cell death during anoxia and reoxygenation. *J Neurosci* 2007; 27: 1129–38.

Aebischer P, Tresco PA, Sagen J, Winn SR. Transplantation of microencapsulated bovine chromaffin cells reduces lesion-induced rotational asymmetry in rats. *Brain Res* 1991; 560:43– 49.

Aguirre P, Valdés P, Aracena-Parks P, Tapia V, Núñez MT. Upregulation of gamma-glutamate-cysteine ligase as part of the long-term adaptation process to iron accumulation in neuronal SH-SY5Y cells. *Am J Physiol Cell Physiol.* 2007 Jun;292(6):C2197-203

Aharon-Peretz J, Rosenbaum H, Gershoni-Baruch R. Mutations in the Glucocerebrosidase Gene and Parkinson's Disease in Ashkenazi Jews. *N Engl J Med*. 2004. 351:1972–1977.

Alam Z, Daniel S, Lees A, Marsden D, Jenner P, Halliwell B. A generalised increase in protein carbonyls in the brain in Parkinson's but not incidental Lewy body disease. *J Neurochem*. 1997; 69:1326–1329

Ali SF, Duhart HM, Newport GD, Lipe GW, Slikker W Jr. Manganese-induced reactive oxygen species: Comparison between Mn^{+2} and Mn^{+3}. *Neurodegeneration*. 1995. 4, 329–334.

Amstad PA, Yu G, Johnson GL, Lee BW, Dhawan S, Phelps DJ. Detection of caspase activation in situ by fluorochrome-labeled caspase inhibitors. *Biotechniques*. 2001 Sep;31(3):608-10, 612, 614

Andersen JK, Oxidative stress in neurodegeneration: cause or consequence? *Nat Med*. 2004 Jul;10 Suppl:S18-25. Review.

Anglade P, Vyas S, Javoy-Agid F, Herrero MT, Michel PP, Marquez J, et al. Apoptosis and autophagy in nigral neurons of patients with Parkinson's disease. *Histol Histopathol* 1997; 12: 25–31.

Aomi Y, Chen CS, Nakada K, Ito S, Isobe K, Murakami H, Kuno SY, Tawata M, Matsuoka R, Mizusawa H, Hayashi JI. Cytoplasmic transfer of platelet mtDNA from elderly patients with Parkinson's disease to mtDNA-less HeLa cells restores complete mitochondrial respiratory function. *Biochem Biophys Res Commu*n. 2001 Jan 12;280(1):265-73.

Archibald FS and Tyree C. Manganese poisoning and the attack of trivalent manganese upon catecholamines. *Arch. Biochem. Biophys*. 1987. 256, 638–650.

Arima K, Uéda K, Sunohara N, Hirai S, Izumiyama Y, Tonozuka-Uehara H, Kawai M. Immunoelectron-microscopic demonstration of NACP/alpha-synuclein-epitopes on the filamentous component of Lewy bodies in Parkinson's disease and in dementia with Lewy bodies. *Brain Res*. 1998 Oct 12;808(1):93-100.

Asker C, Wiman KG and Selivanova G. p53-induced apoptosis as a safeguard against cancer. Biochem *Biophys Res Commun.* 1999 Nov;265(1):1-6.

Autere J, Moilanen JS, Finnilä S, Soininen H, Mannermaa A, Hartikainen P, Hallikainen M, Majamaa K. Mitochondrial DNA polymorphisms as risk factors for Parkinson's disease and Parkinson's disease dementia. *Hum Genet*. 2004 Jun;115(1):29-35.

Bader, V., Ran Zhu, X., Lubbert, H., Stichel, C.C. Expression of DJ-1 in the adult mouse CNS. *Brain Res.* 2005; 1041, 102–111.

Bal A, Savasta M, Chritin M, Mennicken F, Abrous DN, Le Moal M, et al. Transplantation of fetal nigral cells reverses the increase of preproenkephalin mRNA levels in the rat striatum caused by 6-OHDA lesion of the dopaminergic nigrostriatal pathway: a quantitative in situ hybridization study. *Mol Brain Res*. 1993; 18:221–227.

Baligar, PN, Kaliwal, BB. Morphometric analysis of follicular growth and biochemical constituents in albino rats exposed to Mancozeb. *J Basic Clin Physiol Pharmacol*. 2004. 15: 241–262.

Bandopadhyay R, Kingsbury AE, Cookson MR, Reid AR, Evans IM, Hope AD, Pittman AM,Lashley T, Canet-Aviles R, Miller DW, McLendon C, Strand C, Leonard AJ, Abou-Sleiman PM,Healy DG, Ariga H, Wood NW, de Silva R, Revesz T, Hardy JA, Lees AJ. The expression of DJ-1 (PARK7) in normal human CNS and idiopathic Parkinson's disease. *Brain.* 2004. 127, 420–430.

Bárcia RN, Valle NS, McLeod JD. Caspase involvement in RIP-associated CD95-induced T cell apoptosis. *Cell Immunol.* 2003 Dec;226(2):78-85.

Barlow BK, Lee DW, Cory-Slechta DA, Opanashuk LA. Modulation of antioxidant defense systems by the environmental pesticide maneb in dopaminergic cells. *Neurotoxicology*. 2005. 26:63–75.

Barroso N, Campos Y, Huertas R, Esteban J, Molina JA, Alonso A, Gutierrez-Rivas E, Arenas J. Respiratory chain enzyme activities in lymphocytes from untreated patients with Parkinson disease. *Clin. Chem*. 1993. 39, 667–669.

Barsoum MJ, Yuan H, Gerencser AA, Liot G, Kushnareva Y, Gräber S, Kovacs I, Lee WD, Waggoner J, Cui J, White AD, Bossy B, Martinou JC, Youle RJ, Lipton SA, Ellisman MH,Perkins GA, Bossy-Wetzel E. Nitric oxide-induced mitochondrial fission is regulated by dynamin-related GTPases in neurons. *EMBO J*. 2006. 25, 3900–3911.

Bashkatova V, Alam M, Vanin A, Schmidt WJ, Chronic administration of rotenone increases levels of nitric oxide and lipid peroxidation products in rat brain, *Exp. Neurol.* 2004. 186: 235– 241.

Bauvy C, Gane P, Arico S et al. Autophagy delays sulindac sulfideinduced apoptosis in the human intestinal colon cancer cell line HT-29. *Exp Cell Res* 2001; 268:139-149.

Beal MF. Experimental models of Parkinson's disease. *Nat Rev Neurosci* 2001; 2:325–334.

Beck KE, De Girolamo LA, Griffin M, Billett EE. The role of tissue transglutaminase in 1-methyl-4-phenylpyridinium (MPP+)-induced toxicity in differentiated human SH-SY5Y neuroblastoma cells. *Neurosci Lett.* 2006 Sep 11;405(1-2):46-51

Belin AC, Westerlund M, Parkinson's disease: A genetic perspective, *FEBS Journal.* 2008; 275:1377–1383.

Benard G, Bellance N, James D, Parrone P, Fernandez H, Letellier T, Rossignol R. Mitochondrial bioenergetics and structural network organization. *J. Cell Sci. 2007*. 120, 838–848.

Bender A, Krishnan KJ, Morris CM, Taylor GA, Reeve AK, Perry RH, Jaros E, Hersheson JS, Betts J, Klopstock T, Taylor RW, Turnbull DM. High levels of mitochondrial DNA deletions in substantia nigra neurons in aging and Parkinson disease. *Nat Genet.* 2006 May;38(5):515-7.

Benecke R, Strümper P, Weiss H. Electron transfer complexes I and IV of platelets are abnormal in Parkinson's disease but normal in Parkinson-plus syndromes. *Brain*. 1993 Dec;116 (Pt 6):1451-63.

Beneke S, Bürkle A. Poly(ADP-ribosylation in mammalian ageing. *Nucleic Acids Res*. 2007;35(22):7456-65.

Berger NA, Sims JL, Catino DM and Berger SJ. Poly (ADP-ribose) polymerase mediates the suicide response to massive DNA damage: studies in normal and DNA-repair defective cells. *Princess Takamatsu Symp*., 1983. 13, 219–226.

Betarbet R, Sherer TB, MacKenzie G, Garcia-Osuna M, Panov AV, Greenamyre JT. Chronic systemic pesticide exposure reproduces features of Parkinson's disease. *Nat Neurosci* 2000; 3:1301–1306.

Betarbet R, Sherer TB, Greenamyre JT. Animal models of Parkinson's disease. *Bioessays.* 2002 Apr;24(4):308-18.

Betarbet R, Canet-Aviles RM, Sherer TB, Mastroberardino PG, McLendon C, Kim JH, Lund S, Na HM, Taylor G, Bence NF, Kopito R, Seo BB, Yagi T, Yagi A, Klinefelter G, Cookson

MR, Greenamyre JT.Intersecting pathways to neurodegeneration in Parkinson's disease: effects of the pesticide rotenone on DJ-1, alpha-synuclein, and the ubiquitin-proteasome system. *Neurobiol Dis*. 2006 May;22(2):404-20.

Bezard E, Gross CE, Fournier MC, Dovero S, Bloch B, Jaber M. Absence of MPTP-induced neuronal death in mice lacking the dopamine transporter. *Exp Neurol.* 1999 Feb;155(2):268-73.

BfR Expert Opinion No. 033/2006, Pesticide exposure and Parkinson's disease: BfR sees association but no causal relationship, 27 June 2006

Biederbick A., Kern H.F. and Elsasser H.P. Monodansylcadaverine (MDC) is a specific in vivo marker for autophagic vacuoles. *Eur. J. Cell Biol*. 1995. 66, 3-14.

Birch-Machin MA, Briggs HL, Saborido AA, Bindoff LA, Turnbull DM. An evaluation of the measurement of the activities of complexes I-IV in the respiratory chain of human skeletal muscle mitochondria. *Biochem Med Metab Biol*. 1994 Feb;51(1):35-42.

Blandini, F., Nappi, G., Greenamyre, J.T. Quantitative study of mitochondrial complex I in platelets of parkinsonian patients. *Mov. Disord.* 1998. 13, 11–15.

Blake CI, Spitz E, Leehey M, Hoffer BJ, Boyson SJ. Platelet mitochondrial respiratory chain function in Parkinson's disease. *Mov Disord.* 1997 Jan;12(1):3-8.

Blum D, Torch S, Lambeng N, Nissou M, Benabid AL, Sadoul R, Verna JM. Molecular pathways involved in the neurotoxicity of 6-OHDA, dopamine and MPTP: contribution to the apoptotic theory in Parkinson's disease. *Prog Neurobiol*. 2001; 65:135–172

Bondy SC. Intracellular calcium and neurotoxic events. *Neurotoxicol Teratol.* 1989 Nov-Dec;11(6):527-31. Review.

Bonifati V, Rizzu P, van Baren M et al., Mutations in the DJ-1 Gene Associated with Autosomal Recessive Early-Onset Parkinsonism. *Science*. 2003 Jan 10; 299(5604):256-9.

Borland MK, Trimmer PA, Rubinstein JD, Keeney PM, Mohanakumar K, Liu L, Bennett JP Jr. Chronic, low-dose rotenone reproduces Lewy neurites found in early stages of Parkinson's disease, reduces mitochondrial movement and slowly kills differentiated SH-SY5Y neural cells. *Mol Neurodegener.* 2008 Dec 29;3:21.

Bossers K, Meerhoff G, Balesar R, van Dongen JW, Kruse CG, Swaab DF, Verhaagen J. Analysis of gene expression in Parkinson's disease: possible involvement of neurotrophic support and axon guidance in dopaminergic cell death. *Brain Pathol*. 2009 Jan;19(1):91-107.

Bove J, Marin C, Bonastre M, Tolosa E. Adenosine A2A antagonism reverses levodopa-induced motor alterations in hemiparkinsonian rats. *Synapse*. 2002; 46:251–257.

Bove J, Prou D, Perier C, Przedborski S. 'Toxin-induced models of Parkinson's disease', *NeuroRx*. 2005 Jul;2(3):484-94.

Boya P, Gonzalez-Polo RA, Casares N, Perfettini JL, Dessen P, Larochette N, Metivier D, Meley D, Souquere S, Yoshimori T, Pierron G, Codogno P and Kroemer G. Inhibition of macroautophagy triggers apoptosis. *Mol. Cell. Biol.* 2005. 25: 1025–1040

Braak H, Del Tredici K, Rub U, de Vos RA, Jansen Steur EN, Braak E. Staging of brain pathology related to sporadic Parkinson's disease. *Neurobiol Aging* 2003; 24: 197–211.

Braak H, Ghebremedhin E, Rüb U, Bratzke H, Del Tredici K. Stages in the development of Parkinson's disease-related pathology. *Cell Tissue Res*. 2004 Oct;318(1):121-34.

Braak H, Rüb U, Jansen Steur EN, Del Tredici K, de Vos RA. Cognitive status correlates with neuropathologic stage in Parkinson disease. *Neurology*. 2005 Apr 26;64(8):1404-10.

Bredesen DE, Rao RV, Mehlen P. Cell death in the nervous system. *Nature*. 2006 Oct 19; 443 (7113):796-802.

Brill LB, Bennett JP Jr. Dependence on electron transport chain function and intracellular signaling of genomic responses in SH-SY5Y cells to the mitochondrial neurotoxin MPP(+). *Exp Neurol.* 2003 May;181(1):25-38.

Büeler H. Impaired mitochondrial dynamics and function in the pathogenesis of Parkinson's disease. *Experimental Neurology.* 2009. 218: 235–246

Buja LM, Eigenbrodt ML and Eigenbrodt EH. Apoptosis and necrosis: basic types and mechanisms of cell death. *Arch Pathol Lab Med.* 1993. 117:1208–1214.

Burke RE, Dauer WT, Vonsattel JPG. A Critical Evaluation of the Braak Staging Scheme for Parkinson's Disease. *Ann Neurol* 2008;64:485–491

Burns RS, LeWitt PA, Ebert MH, Pakkenberg H, Kopin IJ. The clinical syndrome of striatal dopamine deficiency. Parkinsonism induced by 1-methyl-4-phenyl-1,2,3,6-tetrahydropyridine (MPTP). *N Engl J Med*. 1985 May 30;312(22):1418-21

Butler D, Nixon RA, Bahr BA. Potential compensatory responses through autophagic/lysosomal pathways in neurodegenerative diseases. *Autophagy* 2006; 2: 234–7.

Cadet JL, Jayanthi S, McCoy MT, Vawter M, Ladenheim B. Temporal profiling of methamphetamineinduced changes in gene expression in the mouse brain: Evidence from cDNA array. *Synapse*. 2001. 41:40–48.

Calne DB, Chu NS, Huang CC, Lu CS, Olanow W. Magnesium and idiopathic parkinsonism: similarities and differences. *Neurology* 1994; 44:1583–6.

Calviello, G, Piccioni, E, Boninsegna, A et al. (2006): DNA damage and apoptosis induction by the pesticide Mancozeb in rat cells: involvement of the oxidative mechanism. *Toxicol Appl Pharmacol* 211: 87–96.

Canet-Avilés RM, Wilson MA, Miller DW, Ahmad R, McLendon C, Bandyopadhyay S, Baptista MJ, Ringe D, Petsko GA, Cookson MR. The Parkinson's disease protein DJ-1 is neuroprotective due to cysteine-sulfinic acid-driven mitochondrial localization. *Proc Natl Acad Sci U S A*. 2004 Jun 15;101(24):9103-8.

Cappelletti G, Surrey T, Maci R. The parkinsonism producing neurotoxin MPP+ affects microtubule dynamics by acting as a destabilising factor. *FEBS Lett.* 2005. 579:4781– 4786.

Carney EW, Schroeder R, Breslin WJ Developmental toxicity study in rats with fluroxypyr methylheptyl ester. *Teratology* 1995 Mar; 51(3):180.

Cash R, Raisman R, Ploska A, Agid Y. Dopamine D-1 receptor and cyclic AMP-dependent phosphorylation in Parkinson's disease. *J Neurochem*. 1987;49(4):1075-83.

Cassarino DS, Fall CP, Swerdlow RH, Smith TS, Halvorsen EM, Miller SW, Parks JP, Parker WD Jr, Bennett JP Jr. Elevated reactive oxygen species and antioxidant enzyme activities in animal and cellular models of Parkinson's disease. *Biochim Biophys Acta*. 1997 Nov 28;1362(1):77-86.

Cassarino DS, Halvorsen EM, Swerdlow RH, Abramova NN, Parker WD Jr, Sturgill TW, Bennett JP Jr. Interaction among mitochondria, mitogen-activated protein kinases, and nuclear factor-kappaB in cellular models of Parkinson's disease. *J Neurochem.* 2000 Apr;74(4):1384-92.

Cenci MA. Transcription factors involved in the pathogenesis of L-DOPA-induce d dyskinesia in a rat model of Parkinson's disease. *Amino Acids.* 2002;23(1-3):105-9.

Chae HJ, Kang JS, Byun JO, Han KS, Kim DU, Oh SM, Kim HM, Chae SW, Kim HR. Molecular mechanism of staurosporine-induced apoptosis in osteoblasts. *Pharmacol Res*. 2000 Oct;42(4):373-81.

Chalmers RM. Mitochondrial myopathy, parkinsonism and multiple mtDNA deletions in a Sephardic Jewish family. *Neurology*. 2002 Feb 26;58(4):670.

Chen G and Goeddel DV. TNF-R1 signaling: a beautiful pathway. *Science*. 2002. 296, 1634–1635.

Cheung ZH. The emerging role of autophagy in Parkinson's disease. *Mol Brain.* 2009 Sep 16;2(1):29

Chinta SJ, Andersen JK. Redox imbalance in Parkinson's disease. *Biochim. Biophys. Acta*. 2008; 1780, 1362–1367.

Chiueh C, Haung S, Murphy D. Enhanced hydroxyl radical generation by 20-methyl analog of MPTP: suppression by clorgyline and deprenyl. *Synapse*. 1992. 11:346–348

Choi HK, Won LA, Kontur PJ, Hammond DN, Fox AP, Wainer BH, et al. Immortalization of embryonic mesencephalic dopaminergic neurons by somatic cell fusion. *Brain Res* 1991;552:67–76.

Choi WS, Yoon SY, Oh TH, Choi EJ, O'Malley KL, Oh YJ. Two distinct mechanisms are involved in 6-hydroxydopamine- and MPP+- induced dopaminergic neuronal cell death: role of caspases, ROS, and JNK. *J. Neurosci. Res.* 1999. 57: 86-94.

Choi J., Sullards M.C., Olzmann J.A., Rees H.D., Weintraub S.T., Bosrwick D.E., Gearing M., Levey A.I., Chin L.S., and Li L. *J. Biol. Chem.* 2006; 281, 10816-10824.

Choi WS, Kruse SE, Palmiter RD, Xia Z Mitochondrial complex I inhibition is not required for dopaminergic neuron death induced by rotenone, MPP+, or paraquat. *Proc Natl Acad Sci U S A*. 2008. 30; 105(39):15136-41.

Chua CEL, Tang BL, α-synuclein and Parkinson's disease: the first roadblock. *J. Cell. Mol. Med*. 2006; 10 (4): 837-846.

Chung, K.K., Zhang, Y., Lim, K.L., Tanaka, Y., Huang, H., Gao, J., Ross, C.A., Dawson, V.L., Dawson, T.M. Parkin ubiquitinates the alpha-synuclein-interacting protein,synphilin-1: implications for Lewy-body formation in Parkinson disease. *Nat. Med.* 2001; 7, 1144–1150.

Clark IE, Dodson MW, Jiang C, Cao JH, Huh JR, Seol JH, Yoo SJ, Hay BA, Guo M. Drosophila pink1 is required for mitochondrial function and interacts genetically with parkin. *Nature*. 2006; 441, 1162–1166

Clements CM, McNally RS, Conti BJ, Mak TW, Ting JP. DJ-1, a cancer- and Parkinson's disease-associated protein, stabilizes the antioxidant transcriptional master regulator Nrf2. *Proc Natl Acad Sci U S A*. 2006 Oct 10;103(41):15091-6.

Cocheme HM, Murphy MP. Complex I is the major site of mitochondrial superoxide production by paraquat. *J Biol Chem.* 2008; 283 (4):1786–1798.

Cohen, G. Monoamine oxidase, hydrogen peroxide and Parkinson`s disease. *Adv. Neurol*. 1986. 45: 119-125.

Cohen JJ. Programmed cell death in the immune system. *Adv Immunol* 1991; 50:55–85.

Cookson MR, 'The biochemistry of Parkinson's disease'. *Annu Rev Biochem.* 2005; 74:29-52.

Colapinto M, Mila S, Giraudo S, Stefanazzi P, Molteni M and Rossetti C *et al.*, Alpha-synuclein protects SH-SY5Y cells from dopamine toxicity, *Biochem Biophys Res Commun*.2006. 349: 1294–1300.

Congress of the United States Office of Technology Assessment, 1995. Screening and testing chemicals in commerce. OTA-BP-ENV-166. Office of Technology Assessment,Washington<http://www.wws.princeton.edu/cgibin/byteserv.prl/~ota/disk1/1995/9553/9553.

Conn KJ, Ullman MD, Eisenhauer PB, Fine RE, Wells JM. Decreased expression of the NADH: Ubiquinone oxidoreductase (complex I) subunit 4 in 1-methyl-4- phenylpyridinium-treated human neuroblastoma SH-SY5Y cells. *Neurosci Lett.* 2001 Jun 29;306(3):145-8

Conn KJ, Gao WW, Ullman MD, McKeon-O'Malley C, Eisenhauer PB, Fine RE, Wells JM. Specific upregulation of GADD153/CHOP in MPP+ -treated SH-SH-SY5Y cells. *J. Neurosci. Res*. 2001. 68:755–760.

Conn KJ, Ullman MD, Larned MJ, Eisenhauer PB, Fine RE, Wells JM. cDNA microarray analysis of changes in gene expression associated with MPP+ toxicity in SH-SY5Y cells. *Neurochem Res*. 2003 Dec; 28(12):1873-81.

Conn KJ, Gao W, McKee A, Lan MS, Ullman MD, Eisenhauer PB, Fine RE & Wells JM. Identification of the protein disulfide isomerase family member PDIp in experimental Parkinson's disease and Lewy body pathology. *Brain Res* 2004; 1022, 164–172

Conway K. A., Harper J. D., and Lansbury P. T. Accelerated *in vitro* fibril formation by a mutant a-synuclein linked to early-onset Parkinson disease. *Nat. Med.* 1998. 4, 1318–1320.

Cork LC, Sternberger NH, Sternberger LA, Casanova MF, Struble RG, Price DL. Phosphorylated neurofilament antigens in neurofibrillary tangles in Alzheimer's disease. *J Neuropathol Exp Neurol.* 1986. 45:56–64.

Corsini, E, Birindelli, S, Fustinoni, S et al. Immunomodulatory effects of the fungicide Mancozeb in agricultural workers. *Toxicol Appl Pharmacol.* 2005. 208: 178–185.

Coulom H, Birman S. Chronic exposure to rotenone models sporadic Parkinson's disease in Drosophila melanogaster. *J Neurosci*. 2004. 24(48):10993-8.

Cregan,S.P., Dawson,V.L. and Slack,R.S. Role of AIF in caspase-dependent and caspase-independent cell death. *Oncogene*, 2004. 23, 2785–2796.

Cregan SP, MacLaurin JG, Craig CG, Robertson GS, Nicholson DW, Park DS and Slack RS. Bax-dependent caspase-3 activation is a key determinant in p53- nduced apoptosis in neurons. *J. Neurosci*. 1999. 19: 7860-7869

Crowther RA, Daniel SE, Goedert M. Characterisation of isolated alpha-synuclein filaments from substantia nigra of Parkinson's disease brain. *Neurosci Lett.* 2000 Oct 6;292(2):128-30.

Crotzer VL, Blum JS. Autophagy and intracellular surveillance: modulating MHC class II antigen presentation with stress. *Proc Natl Acad Sci USA* 2005; 102: 7779–80.

Cubells J.F., Rayport S., Rajendran G. and Sulzer D. Methamphetamine neurotoxicity involves vacuolation of endocytic organelles and dopamine-dependent intracellular oxidative stress. *J. Neurosci.* 1994. 14, 2260-2271.

Cuervo AM, Stefanis L, Fredenburg R, Lansbury PT, Sulzer D. Impaired degradation of mutant α-synuclein by chaperone-mediated autophagy. *Science* 2004; 305: 1292–5.

Darios F, Corti O, Lücking CB, Hampe C, Muriel MP, Abbas N, Gu WJ, Hirsch EC, Rooney T, Ruberg M, Brice A.Parkin prevents mitochondrial swelling and cytochrome c release in mitochondria-dependent cell death. *Hum Mol Genet.* 2003 Mar 1;12(5):517-26.

Dauer W, Przedborski S, 'Parkinson's Disease: Mechanisms and Models', *Neuron* 2003; 39, 889–909.

Davie CA. A review of Parkinson's disease. *British Medical Bulletin.* 2008; 86: 109-27

Davidson, W.S., Jonas, A., Clayton, D.F., George, J.M. Stabilization of alpha-synuclein secondary structure upon binding to synthetic membranes. *J. Biol. Chem*. 1998; 273, 9443–9449.

Dawson, T. M., and Dawson, V. L. Molecular pathways of neurodegeneration in Parkinson's disease. *Science.* 2003. *302*, 819–822.

Degterev, A., Huang, Z., Boyce, M., Li, Y., Jagtap, P., Mizushima, N., Cuny, G.D., Mitchison, T.J., Moskowitz, M.A., and Yuan, J. Chemical inhibitor of nonapoptotic cell death with therapeutic potential for ischemic brain injury. *Nat. Chem. Biol*. 2005. 1, 112–119.

Degterev, A., Hitomi, J., Germscheid, M., Ch'en, I.L., Korkina, O., Teng, X., Abbott, D., Cuny, G.D., Yuan, C., Wagner, G., *et al*. Identification of RIP1 kinase as a specific cellular target of necrostatins. *Nat. Chem. Biol.* 2008. 4, 313–321.

De Girolamo L. A., Billett E. E. and Hargreaves A. J. The effect of 1-methyl-4-phenyl-1,2,3,6-tetrahydropyridine on differentiating N2a cells. *J. Neurochem*. 2000. 75, 133-140.

De la Monte, S. M., Sohn, Y. K., Ganju, N., and Wands, J. R. P53- and CD95-ssociated apoptosis in neurodegenerative diseases. *Lab Invest*. 1998.78:401–411.

De Lau LML, Breteler MMB, 'Epidemiology of Parkinson's disease', *Lancet Neurol.* 2006 Jun; 5(6):525-35.

Deng H, Jankovic J, Guo Y, Xie W, Le W. Small interfering RNA targeting the PINK1 induces apoptosis in dopaminergic cells SH-SH-SY5Y. *Biochem Biophys Res Commun.* 2005 Dec 2;337(4):1133-8.

Dennis J, Bennett JP Jr. Interactions among nitric oxide and Bcl-family proteins after MPP+ exposure of SH-SY5Y neural cells II: exogenous NO replicates MPP+ actions. *J Neurosci Res*. 2003 Apr 1;72(1):89-97.

Devin A, Cook A, Lin Y et al. The distinct roles of TRAF2 and RIP in IKK activation by TNF-R1: TRAF2 recruits IKK to TNF-R1 while RIP mediates IKK activation. *Immunity.* 2000. 12: 419–429

Di Fonzo A, Wu-Chou YH, Lu CS, van Doeselaar M, Simons EJ, Rohé CF, Chang HC, Chen RS, Weng YH, Vanacore N, Breedveld GJ, Oostra BA, Bonifati V. A common missense variant in the LRRK2 gene, Gly 2385Arg, associated with Parkinson's disease risk in Taiwan. *Neurogenetics*. 2006 Jul;7(3):133-8.

Dick FD, 'Parkinson's disease and pesticide exposures', *British Medical Bulletin Advance Access,* 2007; 1-13.

Dickson DW, Braak H, Duda JE, Duyckaerts C, Gasser T, Halliday GM, Hardy JH, Leverenz JB, Tredici KD, ZK, and Litvan I. Neuropathological assessment of Parkinson's disease: refining the diagnostic criteria. *The Lancet Neurology*, 2009. 8(12): 1150-1157.

Dinis-Oliveira RJ, Remiaio F, Carmo H, Duarte JA, Sanchez Navarro A, Bastos ML, Carvalho F, Paraquat exposure as an etiological factor of Parkinson's disease *NeuroToxicology*. 2006 Dec; 27(6):1110-22.

Djavaheri-Mergny, M., Amelotti, M., Mathieu, J., Besancon, F., Bauvy, C., Souquere, S., Pierron, G., and Codogno, P. 2006. NF-κB activation represses tumor necrosis factor-α-induced autophagy. *J. Biol. Chem.* 281: 30373–30382.

Dobson, A. W., Erikson, K. M., and Aschner, M. Manganese neurotoxicity. *Ann. N Y Acad. Sci*. 2004. 1012, 115–128.

Domico LM, Zeevalk GD, Bernard LP, Cooper KR. Acute neurotoxic effects of mancozeb and maneb in mesencephalic neuronal cultures are associated with mitochondrial dysfunction. *Neurotoxicology.* 2006. 27:816–825.

Domico, L. M.; Cooper, K. R.; Bernard, L. P.; Zeevalk, G. D. Reactive oxygen species generation by the ethylene-bis-dithiocarbamate (EBDC) fungicide mancozeb and its contribution to neuronal toxicity in mesencephalic cells. *Neurotoxicology*. 2007 Nov;28(6):1079-91

Dong, B. Ferger, J.C. Paterna, D. Vogel, S. Furler, M. Osinde, J. Feldon and H. Bueler, Dopamine-dependent neurodegeneration in rats induced by viral vector-mediated overexpression of the parkin target protein, CDCrel-1, *Proc. Natl. Acad. Sci. U. S. A.* 2003.100: 12438–12443.

Drechsel DA, Patel M. Role of reactive oxygen species in the neurotoxicity of environmental agents implicated in Parkinson's disease. *Free Radic Biol Med.* 2008 Jun 1;44(11):1873-86.

Duchen MR. Mitochondria and calcium: from cell signaling to cell death. *J Physiol* 2000; 529 Pt 1: 57–68.

Dukhande, V. V., Malthankar-Phatak, G. H., Hugus, J. J., Daniels, C. K., and Lai, J. C. Manganese-induced neurotoxicity is differentially enhanced by glutathione depletion in astrocytoma and neuroblastoma cells. *Neurochem. Res*. 2006. 31, 1349–1357.

Dunn, W. A. Jr. Autophagy and related mechanisms of lysosome-mediated protein degradation. *Trends Cell Biol.* 1994. 4: 139–143.

Easton A, Guven K, de Pomerai DI. Toxicity of the Dithiocarbamate Fungicide Mancozeb to the Nontarget Soil Nematode, Caenorhabditis elegans. *J Biochem Mol Toxicol.* 2001;15(1):15-25.

Eberhardt O, Coelln RV, Kugler S, Lindenau J, Rathke-Hartlieb S, Gerhardt E, Haid S,Isenmann S, Gravel C, Srinivasan A, Bahr M, Weller M, Dichgans J, Schulz JB. Protection by synergistic effects of adenovirus-mediated X-chromosome-linked inhibitor of apoptosis and glial cell line-derived neurotrophic factor gene transfer in the 1-methyl-4-phenyl-1,2,3,6-tetrahydropyridine model of Parkinson's disease. *J Neurosci.* 2000 Dec 15;20(24):9126-34.

Eberhardt O, Schulz JB. Apoptotic mechanisms and antiapoptotic therapy in the MPTP model of Parkinson's disease. *Toxicol Lett.* 2003 Apr 4;139(2-3):135-51.
EC, 2005-Eurpean Commission Health & Consumer Protection, Review report for Mancozeb, SANCO/4058/2001 - rev. 4.3, 2005.

Edinger and Thompson, 2004 A.L. Edinger and C.B. Thompson, Death by design: apoptosis, necrosis and autophagy, *Curr. Opin. Cell Biol.* 2004. 16:663–669

Edwards MG, Sarkar D, Klopp R, Morrow JD, Weindruch R, Prolla TA. Age-related impairment of the transcriptional responses to oxidative stress in the mouse heart. *Physiol Genomics* 2003;13:119–127.

Ekstrand MI, Terzioglu M, Galter D, Zhu S, Hofstetter C, Lindqvist E, Thams S, Bergstrand A, Hansson FS, Trifunovic A, Hoffer B, Cullheim S, Mohammed AH, Olson L, Larsson NG. Progressive parkinsonism in mice with respiratory-chain-deficient dopamine neurons. *Proc Natl Acad Sci U S A.* 2007 Jan 23;104(4):1325-30

El-Agnaf O. M., Jakes R., Curran M. D., and Wallace A. (1998) Effects of the mutations Ala30 to Pro and Ala53 to Thr on the physical and morphological properties of alpha-synuclein protein implicated in Parkinson’s disease. *FEBS Lett* 1998. 440, 67–70.

Elmore S. Apoptosis: a review of programmed cell death. *Toxicol Pathol*. 2007;35(4):495-516.

Elstner M, Morris CM, Heim K, Lichtner P, Bender A, Mehta D, Schulte C, Sharma M, Hudson G, Goldwurm S, Giovanetti A, Zeviani M, Burn DJ, McKeith IG, Perry

RH, Jaros E,Krüger R, Wichmann HE, Schreiber S, Campbell H, Wilson JF, Wright AF, Dunlop M, Pistis G, Toniolo D, Chinnery PF, Gasser T, Klopstock T, Meitinger T, Prokisch H, Turnbull DM.Single-cell expression profiling of dopaminergic neurons combined with association analysis identifies pyridoxal kinase as Parkinson's disease gene. *Ann Neurol.* 2009 Dec;66(6):792-8.

Engel LS, Checkoway H, Keifer MC et al. Parkinsonism and occupational exposure to pesticides. *Occup Environ Med*. 2001; 58:582–589.

EPA Epoxiconazole fact sheet. United states Environmental Protection Agency, Office of Prevention, Pesticides and Toxic Substances 2006 (7505P).

EPA, 2005- EPA Mancozeb Facts, United States Environmental Protection Agency, Prevention, Pesticides and Toxic Substances (7508C), EPA 738-F-05-XX, Sep 2005.

Eskelinen, E. L., Illert, A. L., Tanaka, Y., Schwarzmann, G., Blanz, J., Von Figura, K. and Saftig, P. Role of LAMP-2 in lysosome biogenesis and autophagy. *Mol. Biol. Cell.* 2002. 13, 3355-3368.

Fabbri E, Capuzzo A. Cyclic AMP signaling in bivalve molluscs: an overview. *J Exp Zool A Ecol Genet Physiol*. 2010 Feb 1

Fahn S, Sulzer D. Neurodegeneration and Neuroprotection in Parkinson Disease. *The Journal of the American Society for Experimental NeuroTherapeutics.* 2004; 1:139–154.

Fall CP and Bennett Jr JP. MPP+ induced SH-SY5Y apoptosis is potentiated by cyclosporin A and inhibited by aristolochic acid. *Brain Research.* 1998. 811(1-2): 143-146

Fall CP, Bennett JP Jr. Characterization and time course of MPP+-induced apoptosis in human SH-SY5Y neuroblastoma cells. *J Neurosci Res.* 1999 Mar 1;55(5):620-8

Fallon, L., Moreau, F., Croft, B.G., Labib, N., Gu, W.J., Fon, E.A., 2002. Parkin and CASK/LIN-2 associate via a PDZ-mediated interaction and are co localized in lipid rafts and postsynaptic densities in brain. *J. Biol. Chem*. 2002; 277, 486–491.

Fan J, Ren H, Jia N, Fei E, Zhou T, Jiang P, Wu M, Wang G. DJ-1 decreases Bax expression through repressing p53 transcriptional activity. *J Biol Chem.* 2008 Feb 15;283(7):4022-30

Farrer M, Chan P, Chen R, Tan L, Lincoln S, Hernandez D, Forno L, Gwinn-Hardy K, Petrucelli L, Hussey J, Singleton A, Tanner C, Hardy J, Langston JW. Lewy bodies and parkinsonism in families with parkin mutations. *Ann Neurol*. 2001 Sep;50(3):293-300

Farrer MJ, Genetics of Parkinson disease: paradigm shifts and future prospects. *Nat Rev Genet* 2006; 7, 306–318.

Fawthrop, D. J., Boobis, A. R., and Davies, D. S. Mechanisms of cell death. *Arch. Toxicol.* 1991. 65, 437–444.

Feany MB, Bender WW. A Drosophila model of Parkinson's disease. *Nature*. 2000 Mar 23;404(6776):394-8.

Fearnley JM and Lees AJ. Ageing and Parkinson’s disease. *Brain*, 1991; 114 (5): 2283-2301

Fehrenbacher N, Bastholm L, Kirkegaard-Sørensen T, Rafn B, Bøttzauw T, *et al*. Sensitization to the lysosomal cell death pathway by oncogene-induced down-regulation of lysosome-associated membrane proteins 1 and 2. *Cancer Res.* 2008;68:6623–6633.

Fénelon G, Mahieux F, Huon R, Ziégler M. Hallucinations in Parkinson's disease: prevalence, phenomenology and risk factors. *Brain*. 2000 Apr;123 (Pt 4):733-45.

Fenelon G. Psychosis in Parkinson's disease: phenomenology, frequency, risk factors, and current understanding of pathophysiologic mechanisms. *CNS Spectr*. 2008. 13:18–25

Fernagut PO, Hutson CB, Fleming SM, Tetreaut NA, Salcedo J, Masliah E, Chesselet MF. Behavioral and histopathological consequences of paraquat intoxication in mice: effects of alpha-synuclein over-expression. *Synapse*. 2007; 61:991–1001

Ferraro E, Cecconi F. Autophagic and apoptotic response to stress signals in mammalian cells. *Arch Biochem Biophys.* 2007 Jun 15;462(2):210-9

Festjens *et al*., 2006 N. Festjens, T. Vanden Berghe and P. Vandenabeele, Necrosis, a well-orchestrated form of cell demise: signalling cascades, important mediators and concomitant immune response, *Biochim. Biophys. Acta.* 2006. 1757 (9–10): 1371–1387.

Fiskum, G., Starkov, A., Polster, B.M., Chinopoulos, C. Mitochondrial mechanisms of neural cell death and neuroprotective interventions in Parkinson's disease. *Ann. N. Y. Acad. Sci.* 2003. 991, 111–119.

Fleming SM, Jordan MD, Masliah E, Chesselet MF, Roos KP. Alterations in baroreceptor function in transgenic mice overexpressing human alpha synuclein. *Neurosci Abst* 2007;33:50e9.

Fornai F, Lenzi P, Gesi M, Ferrucci M, Lazzeri G, Capobianco L, de Blasi A, Battaglia G, Nicoletti F, Ruggieri S, Paparelli A. Similarities between methamphetamine toxicity and proteasome inhibition. *Ann N Y Acad Sci.* 2004 Oct;1025:162-70.

Forno LS, Sternberger LA, Sternberger NH, Strefling AM, Swanson K, Eng LF. Reaction of Lewy bodies with antibodies to phosphorylated and non-phosphorylated neurofilaments. *Neurosci Lett.* 1986. 64:253–258.

Franco JL, Posser T, Gordon SL, Bobrovskaya L, Schneider JJ, Farina M, Dafre AL, Dickson PW, Dunkley PR. Expression of tyrosine hydroxylase increases the resistance of human neuroblastoma cells to oxidative insults. *Toxicol Sci.* 2010 Jan; 113(1):150-7.

Frankhauser P, Grimmer Y, Bugert P, Deuschle M, Schmidt M, Schloss P. Characterization of the neuronal dopamine transporter DAT in human blood platelets, *Neurosci. Lett.* 2006. 399:197–201.

Franke TF, Kaplan DR, Cantley LC: PI3K: Downstream AKTion blocks apoptosis. *Cell* 1997;88:435–437.

Friedlander R. Apoptosis and caspases in neurodegenerative diseases. *N Engl J Med.* 2003. 348:1365–1375

Freed CR. Will embryonic stem cells be a useful source of dopamine neurons for transplant into patients with Parkinson's disease? *Proc Natl Acad Sci USA*. 2002; 99:1755–1757.

Fukuda T, Ewan L, Bauer M, Mattaliano RJ, Zaal K, Ralston E, *et al*. Dysfunction of endocytic and autophagic pathways in a lysosomal storage disease. *Ann Neurol* 2006; 59: 700–8.

Fuchs J, Mueller JC, Lichtner P, Schulte C, Munz M, Berg D, Wullner U, Illig T, Sharma M, Gasser T. The transcription factor PITX3 is associated with sporadic Parkinson's disease. *Neurobiol Aging* 2009 May;30(5):731-8

Fujiwara H, Hasegawa M, Dohmae N, Kawashima A, Masliah E, Goldberg MS, Shen J, Takio K, Iwatsubo T. alpha-Synuclein is phosphorylated in synucleinopathy lesions. *Nat Cell Biol.* 2002 Feb;4(2):160-4.

Fukunaga K, Miyamoto E: Role of MAP kinase in neurons. *Mol Neurobiol* 1998;16:79–95.

Fukushima T, *et al.* Mechanism of cytotoxicity of paraquat. III. The effects of acute paraquat exposure on the electron transport system in rat mitochondria. *Exp Toxicol Pathol.* 1994. 46:437–441.

Fujiwara et al., 2002 H. Fujiwara, M. Hasegawa, N. Dohmae, A. Kawashima, E. Masliah, M.S. Goldberg, J. Shen, K. Takio and T. Iwatsubo, alpha-Synuclein is phosphorylated in synucleinopathy lesions, *Nat. Cell Biol.* 4 (2002), pp. 160–164.

Gainetdinov RR, Fumagalli F, Jones SR, Caron MG. Dopamine transporter is required for in vivo MPTP neurotoxicity: evidence from mice lacking the transporter. *J Neurochem.* 1997 Sep;69(3):1322-5.

Galanaud JP, Elbaz A, Clavel J, Vidal JS, Correze JR, Alperovitch A, Tzourio C. Cigarette Smoking and Parkinson's Disease: A Case–Control Study in a Population Characterized by a High Prevalence of Pesticide Exposure. *Movement Disorder.* 2005; 20 (2): 181-189.

Galter D, Westerlund M, Carmine A, Lindqvist E, Sydow O & Olson L. LRRK2 expression linked to dopamine-innervated areas. *Ann Neurol* 2006; 59, 714–719.

Galvin, J. E., V. M.-Y. Lee, M. L. Schmidt, P.-H. Tu, T. Iwatsubo, and J. Q. Trojanowski. 1999. Pathobiology of the Lewy body (LB): Studies of purified LBs, monoclonal antibodies and LB-like inclusions in transgenic mouse models. In Advances in Neurology (G. Stern, Ed.), Vol. 80, pp. 313–324. Lippincott-Williams-Wilkins, New York.

Galvin JE. Interaction of alpha-synuclein and dopamine metabolites in the pathogenesis of Parkinson's disease: a case for the selective vulnerability of the substantia nigra. *Acta Neuropathol.* 2006; 112: 115–26.

Gandhi S, Muqit MM, Stanyer L, Healy DG, Abou-Sleiman PM, Hargreaves I, Heales S, Ganguly M, Parsons L, Lees AJ, Latchman DS, Holton JL, Wood NW, Revesz T. PINK1 protein in normal human brain and Parkinson's disease. *Brain.* 2006 Jul;129(Pt 7):1720-31.

Gandhi S, Wood, NW. Molecular pathogenesis of Parkinson's disease. *Human Molecular Genetics*, 2005, Vol 14, 18: 2749-2755.

Gao Y, Raj JU. SQ22536 and W-7 inhibit forskolin-induced cAMP elevation but not relaxation in newborn ovine pulmonary veins. *Eur J Pharmacol.* 2001 Apr 20;418(1-2):111-6.

Gao HM, Hong JS, Zhang W, Liu B. Distinct role for microglia in rotenone-induced degeneration of dopaminergic neurons. *J Neurosci* 2002;22:782–90.

Garthwaite DG, Thomas MR, Anderson H and Stodart H. Pesticide usage survey report 202. Arable crops in Great Britain 2004. National Statistics. Central Science Laboratory, Sand Sutton.

Gavin, C. E., Gunter, K. K., and Gunter, T. E. Manganese and calcium efflux kinetics in brain mitochondria. Relevance to manganese toxicity. *Biochem. J.* 1990. 266, 329–334.

Gerber GB, Léonard A, Hantson P. Carcinogenicity, mutagenicity and teratogenicity of manganese compounds. *Crit Rev Oncol Hematol.* 2002 Apr;42(1):25-34.

Germain M and Slack RS. Dining in with BCL-2: new guests at the autophagy table. *Clinical Science*. 2010. 118: 173–181

Giasson BI, Uryu K, Trojanowski JQ, Lee VM. Mutant and wild type human alpha-synucleins assemble into elongated filaments with distinct morphologies in vitro. *J Biol Chem*. 1999 Mar 19;274(12):7619-22.

Giasson BI, Murray IV, Trojanowski JQ, Lee VM. A hydrophobic stretch of 12 amino acid residues in the middle of alpha-synuclein is essential for filament assembly. *J Biol Chem*. 2001 Jan 26;276(4):2380-6.

Gibson, RM. (1999). Role of Apoptosis in Neuronal Toxicology . In: Roberts, RA *Apoptosis in Toxicology* . UK: Informa Healthcare. 145

Gibb WR, Lees AJ. The relevance of the Lewy body to the pathogenesis of idiopathic Parkinson's disease. *J Neurol Neurosurg Psychiatry*. 1988 Jun;51(6):745-52.

Giorgi M, D'Angelo V, Esposito Z, Nuccetelli V, Sorge R, Martorana A, Stefani A, Bernardi G, Sancesario G. Lowered cAMP and cGMP signalling in the brain during levodopa-induced dyskinesias in hemiparkinsonian rats: new aspects in the pathogenetic mechanisms. *Eur J Neurosci.* 2008 Sep;28(5):941-50

Gitler AD, Chesi A, Geddie ML, Strathearn KE, Hamamichi S, Hill KJ, Caldwell KA, Caldwell GA, Cooper AA, Rochet JC, Lindquist S. Alpha-synuclein is part of a diverse and highly conserved interaction network that includes PARK9 and manganese toxicity. *Nat Genet.* 2009 Mar;41(3):308-15.

Glinka Y, Gassen M, Youdim MB. Mechanism of 6-hydroxydopamine neurotoxicity. *J Neural Transm Suppl*. 1997; 50:55–66

Goedert M, Alpha-synuclein and neurodegenerative diseases. *Nat Rev Neurosci.* 2001 Jul;2(7):492-501

Goetz, A. K., Ren, H., Schmid, J. E., Blystone, C. R., Thillainadarajah, I., Best, D. S., Nichols, H. P., Strader, L. F., Wolf, D. C., Narotsky, M. G., et al. (2007). Disruption of

testosterone homeostasis as a mode of action for the reproductive toxicity of triazole fungicides in the male rat. Toxicol. Sci. 95, 227–239.

Golstein and Kroemer, 2007 P. Golstein and G. Kroemer, Cell death by necrosis: towards a molecular definition, *Trends Biochem. Sci.* 2007. 32:37–43

Gómez-Tortosa E, Newell K, Irizarry MC, Sanders JL, Hyman BT. alpha-Synuclein immunoreactivity in dementia with Lewy bodies: morphological staging and comparison with ubiquitin immunostaining. *Acta Neuropathol.* 2000 Apr;99(4):352-7.

Gomes A, Fernandes E, Lima JL. Fluorescence probes used for detection of reactive oxygen species. *Journal of Biochemical & Biophysical Methods* 2005;65:45–80.

Gonzales, D.H., *et al*. Biogenesis of mitochrondrial c-type cytochromes. *J. Bioenerg. Biomembr.* 1990. 22: 753-768.

González-Polo RA, Boya P, Pauleau AL, Jalil A, Larochette N, Souquère S, Eskelinen EL, Pierron G, Saftig P, Kroemer G. The apoptosis/autophagy paradox: autophagic vacuolization before apoptotic death. *J Cell Sci*. 2005 Jul 15;118(Pt 14):3091-102.

Gorell JM, Johnson CC, Rybicki BA, et al. The risk of Parkinson's disease with exposure to pesticides, farming, well water, and rural living. *Neurology*. 1998; 50: 1346-1350.

Gosal D, Ross OA, Toft M. Parkinson's disease: the genetics of a heterogeneous disorder. *Eur J Neurol*. 2006 Jun;13(6):616-27.

Greenamyre JT, Betarbet R, Sherer TB, The rotenone model of Parkinson’s disease: genes, environment and mitochondria. *Parkinsonism and Related Disorders*. 2003, 9: S59–S64.

Grimm S, Stanger BZ, Leder P. RIP and FADD: two ‘‘death domain’’-containing proteins can induce apoptosis by convergent, but dissociable, pathways, *Proc. Natl. Acad. Sci*. USA 1996. 93(20)10923-7

Gronostajski R.M. and Pardee A.B. Protein degradation in 3T3 and tumorigenic transformed 3T3 cells. *J. Cell Physiol*. 1984. 119, 127-132.

Gross A, McDonnell JM, Korsmeyer SJ. BCL-2 family members and the mitochondria in apoptosis. *Genes Dev.* 1999. 13:1899–1911.

Grote K, Niemann L, Selzsam B, Haider W, Gericke C, Herzler M, Chahoud I. Epoxiconazole Causes Changes in Testicular Histology and Sperm Production in the Japanese quail (Coturnix coturnix japonica). *Environ Toxicol Chem.* 2008 Jun 3:1.

Grunblatt E, Mandel S, Maor G, and Youdim MBH. Gene expression analysis in MPTP mice model of Parkinson’s disease using cDNA microarray. *J. Neurochem.* 2001. 78:1–12.

Guerrier S, Coutinho-Budd J, Sassa T, Gresset A, Jordan NV, Chen K, Jin WL, Frost A, Polleux F. The F-BAR domain of srGAP2 induces membrane protrusions required for neuronal migration and morphogenesis. *Cell.* 2009 Sep 4;138(5):990-1004

Gunter TE and D.R. Pfeiffer DR, Mechanisms by which mitochondria transport calcium, *Am. J. Physiol* 1990. 258, pp. C755–C786.

Gunter, T. E., Gavin, C. E., Aschner, M., and Gunter, K. K. Speciation of manganese in cells and mitochondria: A search for the proximal cause of manganese neurotoxicity. *Neurotoxicology*. 2006. 27, 765–776.

Haas RH, Nasirian HF, Nakano K, Ward D, Hill PR, Shults CW, Low platelet mitochondrial complex I and complex II/III activity in early untreated Parkinson's disease, *Ann. Neurol*. 1995. 37: 714–722.

Hague S.M., Rogaeva E., Hernandez D., Gulick C., Singleton A., Hanson M., Johnson J., Weiser R., Gallardo M., Ravina B., Gwinn-Hardy K., Crawley A., St George-Hyslop P.H., Lang A.E., Heutink P., Bonifati V., Hardy J.A., and Singleton A. *Ann. Neurol.* 2003; 54, 271-274.

Haitina T, Lindblom J, Renström T, Fredriksson R. Fourteen novel human members of mitochondrial solute carrier family 25 (SLC25) widely expressed in the central nervous system. *Genomics*. 2006 Dec;88(6):779-90.

Halliwell B, Gutteridge J (1999) Oxidative stress in PD. In: Halliwell B, Gutteridge J (eds) Free radicals in biology and medicine. Oxford University Press, New York pp 744–758

Halvorsen EM, Dennis J, Keeney P, Sturgill TW, Tuttle JB, Bennett JB Jr. Methypyridinium (MPP+)- and nerve growth factor-induced changes in pro- and anti-apoptotic signaling pathways in SH-SY5Y neuroblastoma cells. *Brain Res.* 2002 Oct 11;952(1):98-110.

Han ES, Muller FL, Pérez VI, Qi W, Liang H, Xi L, Fu C, Doyle E, Hickey M, Cornell J, Epstein CJ, Roberts LJ, Van Remmen H,Richardson A. The in vivo gene expression signature of oxidative stress. *Physiol Genomics*. 2008 Jun 12;34(1):112-26.

Hancock DB, Martin ER, Mayhew GM, Stajich JM, Jewett R, Stacy MA, Scott BL, Vance JM, Scott WK. Pesticide exposure and risk of Parkinson's disease: a family-based case-control study. *BMC Neurol*. 2008 Mar 28; 8:6

Hara T, Nakamura K, Matsui M, Yamamoto A, Nakahara Y, Suzuki-Migishima R, Yokoyama M, Mishima K, Saito I, Okano H, Mizushima N: Suppression of basal autophagy in neural cells causes neurodegenerative disease in mice. *Nature* 2006, 441:885-9.

Hardy J, Cai H, Cookson MR, Gwinn-Hardy K, Singleton A. Genetics of Parkinson's disease and parkinsonism. *Ann Neurol.* 2006 Oct;60(4):389-98.

Hartmann A, Hunot S, Michel PP, Muriel MP, Vyas S, Faucheux BA, Mouatt-Prigent A, Turmel H, Srinivasan A, Ruberg M, Evan GI, Agid Y, Hirsch EC: Caspase-3: A vulnerability factor and final effector in apoptotic death of dopaminergic neurons in Parkinson's disease. *Proc Natl Acad Sci USA* 2000;97:2875–2880.

Hartmann A, Troadec J-D, Hunot S et al.Caspase-8 Is an effector in apoptotic death of dopaminergic neurons in Parkinson's disease, but pathway inhibition results in neuronal necrosis. *J Neurosci.* 2001. 21:2247–2255

Hasegawa E, Takeshige K, Oishi T, Murai Y, Minakami S. 1-Methyl-4-phenylpyridinium (MPP+) induces NADH-dependent superoxide formation and enhances NADH-dependent lipid peroxidation in bovine heart submitochondrial particles. *Biochem Biophys Res Commun.* 1990 Aug 16;170(3):1049-55.

Hashimoto M., Hsu L. J., Xia Y., Takeda A., Sisk A., Sundsmo M., and Masliah E. Oxidative stress induces amyloid-like aggregate formation of NACP/alpha-synuclein in vitro. *Neuroreport.* 1999. 10, 717–721.

Hatcher JM, Pennell KD, Miller GW. Parkinson's disease and pesticides: a toxicological perspective. *Trends Pharmacol Sci.* 2008 Jun;29(6):322-9.

Hatano Y, Li Y, Sato K, Asakawa S, Yamamura Y, Tomiyama H, Yoshino H, Asahina M, Kobayashi S, Hassin-Baer S, Lu CS, Ng AR, Rosales RL, Shimizu N, Toda T, Mizuno Y,Hattori N. Novel PINK1 mutations in early-onset parkinsonism *Ann Neuro*l. 2004 Sep;56(3):424-7

Hayflick SJ. Neurodegeneration with brain iron accumulation: from genes to pathogenesis. *Semin Pediatr Neurol* 13: 182–185, 2006.

Haugarvoll K, Toft M, Skipper L, Heckman MG, Crook JE, Soto A, Ross OA, Hulihan MM, Kachergus JM, Sando SB, White LR,Lynch T, Gibson JM, Uitti RJ, Wszolek ZK, Aasly JO, Farrer MJ. Fine-mapping and candidate gene investigation within the PARK10 locus. *Eur J Hum Genet*. 2009 Mar;17(3):336-43.

Healy DG, Abou-Sleiman PM, Wood NW, Genetic causes of Parkinson's disease: UCHL-1. Cell *Tissue Res.* 2004 Oct; 318(1):189-94.

Heikkila RE., Hess A, Duvoisin RC. Dopaminergic neurotoxicity of 1-methyl-4-phenyl-1,2,3,6-tetrahydropyridine in mice. *Science*. 1984; 224, 1451-1453.

Hernan MA, Takkouche B, Caamano-Isorna F, Gestal-Otero JJ, 'A meta-analysis of coffee drinking, cigarette smoking, and the risk of Parkinson's disease', *Ann Neurol.* 2002 Sep;52(3):276-84.

Herrera FE, Zucchelli S, Jezierska A, Lavina ZS, Gustincich S, Carloni P. On the oligomeric state of DJ-1 protein and its mutants associated with Parkinson's Disease: a combined computational and in vitro study. *J Biol Chem*. 2007 May 15.

Hertzman C, Wiens M, Bowering D, Snow B & Calne D. Parkinson's disease: A case–control study of occupational and environmental risk factors. *Am J Ind Med*. 1990; 17, 349–355.

Hewitt PG, Perkins J, Hotchkiss SA. Metabolism of fluroxypyr, fluroxypyr methyl ester, and the herbicide fluroxypyr methylheptyl ester. I: during percutaneous absorption through fresh rat and human skin in vitro. *Drug Metab Dispos.* 2000 Jul;28(7):748-54.

Hewitt PG, Perkins J, Hotchkiss SA. Metabolism of fluroxypyr, fluroxypyr methyl ester, and the herbicide fluroxypyr methylheptyl ester. II: in rat skin homogenates. *Drug Metab Dispos*. 2000 Jul;28(7):755-9.

Hod Y., Pentyala S. N., Whyard T. C., El-Maghrabi M. R. Identification and characterization of a novel protein that regulates RNA-protein interaction. *J. Cell. Biochem*., 72: 435-444, 1999.

Hofer A, Berg D, Asmus F, Niwar M, Ransmayr G, Riemenschneider M, Bonelli SB, Steffelbauer M, Ceballos-Baumann A, Haussermann P, Behnke S, Kruger R, Prestel J, Sharma M, Zimprich A, Riess O, Gasser T. The role of alpha-synuclein gene multiplications

in early-onset Parkinson's disease and dementia with Lewy bodies. *J Neural Transm.* 2005 Sep;112(9):1249-54.

Hoglinger GU, Feger J, Annick P, Michel PP, Karine P, Champy P, et al. Chronic systemic complex I inhibition induces a hypokinetic multisystem degeneration in rats. *J Neurochem* 2003; 84:1–12.

Hollenbeck P. Products of endocytosis and autophagy are retrieved from axons by regulated retrograde organelle transport. *J. Cell Biol*. 1993. 121, 305-315.

Hollenbeck PJ, Saxton WM. The axonal transport of mitochondria. *J. Cell Sci.* 2005. 118, 5411–5419.

Holler N, Zaru R. Micheau O, Thome M, Attinger A, Valitutti S, Bodmer JL, Schneider P, Seed B, and Tschopp J. Fas triggers an alternative, caspase-8-independent cell death pathway using the kinase RIP as effector molecule. *Nat. Immunol.* 2000. 1, 489–495.

Holtz WA and O'Malley K. Parkinsonian mimetics induce aspects of unfolded protein response in death of dopaminergic neurons. *J. Biol. Chem*. 2003; 278: 19367–19377

Honig LS and Rosenberg RN. Apoptosis and neurologic disease. *Am. J. Med.*2000. 108:317–330.

Hosokawa N, Hara Y, Mizushima N: Generation of cell lines with tetracycline-regulated autophagy and a role for autophagy in controlling cell size. *FEBS Lett* 2006, 580:2623–2629

Hsu H, Huang J, Shu HB, Baichwal V, Goeddel DV. TNF-dependent recruitment of the protein kinase RIP to the TNF receptor-1 signaling complex. *Immunity*. 1996 Apr;4(4):387-96.

Hughes JT. Brain damage due to paraquat poisoning: a fatal case with neuropathological examination of the brain. *Neurotoxicology*. 1988; 9:243–248.

Huynh, D.P., Scoles, D.R., Ho, T.H., Del Bigio, M.R., Pulst, S.M Parkin is associated with actin filaments in neuronal and nonneural cells. Ann. Neurol. 2000; 48, 737–744.

Hwang DY, Fleming SM, Ardayfio P, Moran-Gates T, Kim H, Tarazi FI, Chesselet MF, Kim K. 3,4-dihydroxyphenylalanine reverses the motor deficits in Pitx3-deficient aphakia mice: behavioral characterization of a novel genetic model of Parkinson's disease. *J Neurosci.* 2005; 25:2132–2137

Iaccarino C, Crosio C, Vitale C, Sanna G, Carri MT, Barone P. Apoptotic mechanisms in mutant LRRK2-mediated cell death. *Hum Mol Genet.* 2007. 16:1319–1326.

IEH (2005) Pesticides and Parkinson's Disease — A Critical Review (Web Report W21), Leicester.

Imai, Y., Soda, M., Inoue, H., Hattori, N., Mizuno, Y., Takahashi, R., 2001. An unfolded putative transmembrane polypeptide, which can lead to endoplasmic reticulum stress, is a substrate of Parkin. *Cell*, 2001; 105, 891–902.

Imai Y, Soda M & Takahashi R. Parkin suppresses unfolded protein stress-nduced cell death through its E3 ubiquitin-protein ligase activity. *J Biol Chem*. 2000; 275, 35661–35664.

Imai Y, Soda M, Inoue H, Hattori N, Mizuno Y and Takahashi R. An unfolded putative transmembrane polypeptide, which can lead to endoplasmic reticulum stress, is a substrate of Parkin. *Cell.* 2001; 105: 891–902

Imai Y and Takahashi R. How do Parkin mutations result in neurodegeneration? *Curr. Opin. Neurobiol.* 2004; 14: 384–389

Inden M, Taira T, Kitamura Y, Yanagida T, Tsuchiya D, Takata K, Yanagisawa D, Nishimura K, Taniguchi T, Kiso Y, Yoshimoto K, Agatsuma T, Koide-Yoshida S, Iguchi-Ariga SM, Shimohama S, Ariga H. PARK7 DJ-1 protects against degeneration of nigral dopaminergic neurons in Parkinson's disease rat model. *Neurobiol Dis.* 2006 Oct;24(1):144-58.

Isenberg JS, Klaunig JE. Role of the mitochondrial membrane permeability transition (MPT) in rotenone-induced apoptosis in liver cells. *Toxicol Sci.* 2000 Feb;53(2):340-51.

Ishii N, Fujii M, Hartman PS, Tsuda M, Yasuda K, Senoo-Matsuda N, Yanase S, Ayusawa D, Suzuki K. A mutation in succinate dehydrogenase cytochrome b causes oxidative stress and ageing in nematodes. *Nature*. 1998 Aug 13;394(6694):694-7.

Jankovic J. Parkinson's disease: clinical features and diagnosis. *J. Neurol. Neurosurg. Psychiatry* 2008; 79: 368-376

Jablonicka, A, Polakova, H, Karelova, J, Vargová, M. Analysis of chromosome aberrations and sister-chromatid exchanges in peripheral blood lymphocytes of workers with occupational exposure to the mancozeb-containing fungicide Novozir Mn80. *Mutat Res*. 1989. 224: 143–146.

Javitch JA, D'Amato RJ, Strittmatter SM, Snyder SH. Parkinsonism-inducing neurotoxin, N-methyl-4-phenyl-1,2,3,6 -tetrahydropyridine: Uptake of the metabolite N-methyl-4-phenylpyridine by dopamine neurons explains selective toxicity. *Proc. Natl. Acad. Sci. U.S.A*. 1985. 82, 2173–2177.

Jellinger KA. Cell death mechanisms in Parkinson's disease. *J Neural Transm* . 2000. 107:1–29.

Jellinger KA. Cell death mechanisms in neurodegeneration. *J.Cell.Mol.Med.* 2001. 5(1): 1-17

Jenco, J.M., Rawlingson, A., Daniels, B., Morris, A.J. Regulation of phospholipase D2: selective inhibition of mammalian phospholipase D isoenzymes by alpha- and beta-synucleins. *Biochemistry* 1998; 37, 4901–4909.

Jenner, P. Oxidative mechanisms in nigral cell death in Parkinson's disease. *Mov. Disord*. 1998. 13 (Suppl. 1), 24-34

Jeon BS, Jackson-Lewis V, Burke RE. 6-Hydroxydopamine lesion of the rat substantia nigra: time course and morphology of cell death. *Neurodegeneration.* 1995 Jun;4(2):131-7.

Jia Z, Misra HP, Developmental exposure to pesticides zineb and/or endosulfan renders the nigrostriatal dopamine system more susceptible to these environmental chemicals later in life. *Neurotoxicology*. 2007. 28:727–735.

Jiang, H., Jiang, Q., Feng, J. Parkin increases dopamine uptake by enhancing the cell surface expression of dopamine transporter. *J. Biol. Chem*. 2004; 2004; 279, 54380–54386.

Jiang CC, Chen LH, Gillespie S, Kiejda KA, Mhaidat N, Wang YF, Thorne R, Zhang XD, Hersey P. Tunicamycin sensitizes human melanoma cells to tumor necrosis factor-related apoptosis-inducing ligand-induced apoptosis by up-regulation of TRAIL-R2 via the unfolded protein response. *Cancer Res.* 2007 Jun 15;67(12):5880-8.

Jiménez-Jiménez FJ, Mateo D & Giménez-Roldán S, Exposure to well water and pesticides in Parkinson's disease: A case–control study in the Madrid area. *Mov Disord,* 1992; 7, 149–152.

Jones GM, Vale JA. Mechanisms of Toxicity, Clinical Features, and Management of Diquat Poisoning: A Review. *Clinical Toxicology*, 2000. 38(2), 123–128.

Jonsson, G. Chemical neurotoxins as denervation tools in neurobiology. *Annu. Rev. Neurosci.* 1980; 3, 169–187.

Kabuta T, Furuta A, Aoki S, Furuta K, Wada K: Aberrant interaction between Parkinson disease-associated mutant UCH-L1 and the lysosomal receptor for chaperone-mediated autophagy. *J Biol Chem* 2008, 283:23731.

Kahle PJ, Neumann M, Ozmen L, Mu¨ ller V, Jacobsen H, Schindzielorz A, Okochi M, Leimer U, van der Putten H, Probst A, Kremmer E, Kretschman HA, Haass C. Subcellular localization of wild-type and Parkinson's disease-associated mutant a-synuclein in human and transgenic mouse brain. *J Neurosci* 2000;20: 6365–73.

Kalia, S.K., Lee, S., Smith, P.D., Liu, L., Crocker, S.J., Thorarinsdottir, T.E., Glover, J.R., Fon, E.A., Park, D.S., Lozano, A.M., 2004. BAG5 inhibits parkin and enhances dopaminergic neuron degeneration. *Neuron.* 2004. 44:931–945.

Kametaka S, Matsuura A, Wada Y, Ohsumi Y. Structural and functional analyses of APG5, a gene involved in autophagy in yeast. Gene. 1996 Oct 31;178(1-2):139-43.

Kanthasamy, A.G., Borowitz, J.L., Pavlakovic, G., and Isom, G.E. Dopaminergic neurotoxicity of cyanide: neurochemical, histological, and behavioural characterization. *Toxicology and applied pharmacology. 1994. 126*, 156-163.

Kataoka T, Budd RC, Holler N, Thome M, Martinon F, Irmler M, Burns K, Hahne M, Kennedy N, Kovacsovics M, Tschopp J. The caspase-8 inhibitor FLIP promotes activation of NF-kappaB and Erk signaling pathways. *Curr Biol.* 2000 Jun 1;10(11):640-8.

Kaufman RJ. Stress signaling from the lumen of the endoplasmic reticulum: coordination of gene transcriptional and translational control, *Genes Dev.*1999; 13: 1211–1233.

Keeny P, Xie J, Capaldi R, Bennett J Jr. Parkinson's disease brain mitochondrial complex I has oxidatively damaged subunits, is functionally impaired and misassembled. *J Neurosci Res.* 2006; 26:5256–5264

Kelliher, M.A. *et al.* The death domain kinase RIP mediates the TNF-induced NF-κB signal. *Immunity* 1998. 8, 297–303.

Kermer P, Liman J, Weishaupt JH, Bähr M. Neuronal apoptosis in neurodegenerative diseases: from basic research to clinical application. *Neurodegener Dis*. 2004;1(1):9-19

Kiffin, R., Christian, C., Knecht, E. and Cuervo, A. Activation of chaperone mediated autophagy during oxidative stress. *Mol. Biol. Cell*.2004. 1: 4829-4840.

Kiffin R, Kaushik S, Zeng M, Bandyopadhyay U, Zhang C, Massey AC, Martinez-Vicente M, Cuervo AM. Altered dynamics of the lysosomal receptor for chaperone-mediated autophagy with age. *J Cell Sci*. 2007 Mar 1;120(Pt 5):782-91.

Kim, S. J., Kim, J. E., and Moon, I. S. Paraquat induces apoptosis of cultured rat cortical cells. *Mol Cells.* 2004b. 17:102–107.

Kim YS, Morgan MJ, Choksi S, Liu ZG. TNF-Induced Activation of the Nox1 NADPH Oxidase and Its Role in the Induction of Necrotic Cell Death. *Molecular Cell*. 2007. 26, 675–687

Kirik D, Rosenblad C, Burger C, Lundberg C, Johansen TE, Muzyczka N, Mandel RJ, Bjorklund A. Parkinson-like neurodegeneration induced by targeted overexpression of alphasynuclein in the nigrostriatal system. *J Neurosci.* 2002; 22:2780–2791

Kirik D, Annett LE, Burger C, Muzyczka N, Mandel RJ, Bjorklund A, Nigrostriatal alpha-synucleinopathy induced by viral vector-mediated overexpression of human alpha-synuclein: a new primate model of Parkinson's disease. *Proc Natl Acad Sci U S A*. 2003 Mar 4;100(5):2884-9.

Kinumi, T., Kimata, J., Taira, T., Ariga, H., Niki, E. Cysteine-106 of DJ-1 is the most sensitive cysteine residue to hydrogen peroxide mediated oxidation in vivo in human umbilical vein endothelial cells. *Biochem. Biophys. Res. Commum*. 2004. 317, 722–728.

Kitada T, Asakawa S, Hattori N, Matsumine H, Yamamura Y, Minoshima S, Yokochi M, Mizuno Y, Shimizu N. Mutations in the parkin gene cause autosomal recessive juvenile parkinsonism. *Nature* 1998; 392:605–608.

Kitanaka, C. & Kuchino,Y. Caspase-independent programmed cell death with necrotic morphology. *Cell Death Differ.* 1999. 6, 508–515.

Kitao, Y. Imai, K. Ozawa, A. Kataoka, T. Ikeda, M. Soda, K. Nakimawa, H. Kiyama, D.M. Stern, O. Hori, K. Wakamatsu, S. Ito, S. Itohara, R. Takahashi and S. Ogawa, Pael receptor induces death of dopaminergic neurons in the substantia nigra via endoplasmic reticulum stress and dopamine toxicity, which is enhanced under condition of parkin inactivation, *Hum. Mol. Genet.* 2007.16: 50–60.

Klionsky DJ, Emr SD. Autophagy as a regulated pathway of cellular degradation. *Science*. 2000 Dec 1;290 (5497):1717-21.

Klionsky DJ, Cregg JM, Dunn WA Jr, Emr SD, Sakai Y, Sandoval IV, Sibirny A, Subramani S, Thumm M, Veenhuis M, Ohsumi Y. A unified nomenclature for yeast autophagy-related genes. *Dev. Cell.* 2003. 5: 539–545.

Kluck, R. M.; Bossy-Wetzel, E.; Green, D. R.; Newmeyer, D. D. The release of cytochrome c from mitochondria: a primary site for Bcl-2 regulation of apoptosis. *Science*. 1997. 275:1132–1136.

Ko HS, von Coelln R, Sriram SR, Kim SW, Chung KK, Pletnikova O, Troncoso J, Johnson B, Saffary R, Goh EL, Song H, Park BJ, Kim MJ, Kim S, Dawson VL, Dawson TM. Accumulation of the authentic parkin substrate aminoacyl-tRNA synthetase cofactor, p38/JTV-1, leads to catecholaminergic cell death. *J. Neurosci*. 2005; 25, 7968–7978.

Koller, W., Vetere-Over7eld, B., Gray, C., et al. Environmental risk factors in Parkinson's disease. *Neurology*. 1990, 40; 1218-1221.

Komatsu, M. *et al.* Impairment of starvation-induced and constitutive autophagy in Atg7-deficient mice. *J. Cell Biol.* 2005. 169, 425–434.

Komatsu M, Waguri S, Chiba T, Murata S, Iwata J, Tanida I, Ueno T, Koike M, Uchiyama Y, Kominami E, Tanaka K: Loss of autophagy in the central nervous system causes neurodegeneration in mice. *Nature* 2006, 441:880-884

Kopin IJ. Features of the dopaminergic neurotoxin MPTP. *Ann N Y Acad Sci.* 1992 May 11;648:96-104.

Kowall NW, Hantraye P, Brouillet E, Beal MF, McKee AC, Ferrante RJ. MPTP induces alpha-synuclein aggregation in the substantia nigra of baboons. *Clin Neurosci Neuropathol* 2000; 11:211–3.

Krajewski S, Krajewska M, Ellerby LM, Welsh K, Xie Z, Deveraux QL, Salvesen GS, Bredesen DE, Rosenthal RE, Fiskum G, Reed JC. Release of caspase-9 from mitochondria during neuronal apoptosis and cerebral ischemia. *Proc Natl Acad Sci USA*. 1999 May 11;96(10):5752-7.

Kramer ML, Schulz-Schaeffer WJ. Presynaptic alpha-synuclein aggregates, not Lewy bodies, cause neurodegeneration in dementia with Lewy bodies. *J Neurosci*. 2007; 27:1405–1410

Kroemer G, Jäättelä M. Lysosomes and autophagy in cell death control. *Nat Rev Cancer.* 2005 Nov;5(11):886-97

Krohn, A. J., Wahlbrink, T., and Prehn, J. H. Mitochondrial depolarization is not required for neuronal apoptosis. *J. Neurosci.*1999.19: 7394-7404.

Kruger R, Kuhn W, Muller T, et al. Ala30Pro mutation in the gene encoding alpha-synuclein in Parkinson's disease. *Nat Genet* 1998;18:106 –108.

Kuma, A., Hatano, M., Matsui, M., Yamamoto, A., Nakaya, H., Yoshimori, T., Ohsumi, Y., Tokuhisa, T., and Mizushima, N. The role of autophagy during the early neonatal starvation period. *Nature*. 2004. 432: 1032–1036.

Kunchithapautham K, Rohrer B: Apoptosis and autophagy in photoreceptors exposed to oxidative stress. *Autophagy.* 2007, 3:433–441

Kundu M, Thompson CB. Macroautophagy versus mitochondrial autophagy: a question of fate? *Cell Death Differ.* 2005 Nov;12 Suppl 2:1484-9.

Kushnareva Y, Murphy AN, Andreyev A. Complex I-mediated reactive oxygen species generation: modulation by cytochrome c and NAD(P)+ oxidation-reduction state. *Biochem. J.* 2002; 368, 545–553

Lai BCL, Marion, SA, Teschke K, Tsui JKC. Occupaional and environmental risk factors for Parkinson's disease. *Parkinsonism and Related Disorders.* 2002, 8: 297-309.

Lambeth, J.D. NOX enzymes and the biology of reactive oxygen. *Nat. Rev. Immunol.* 2004. 4, 181–189.

Langston, J.W., Ballard, P., Tetrud, J.W., Irwin, I. Chronic Parkinsonism in humans due to a product of meperidine-analog synthesis. *Science* 1983; 219, 979–980.

Langston JW, Forno LS, Tetrud J, Reeves AG, Kaplan JA, Karluk D. Evidence of active nerve cell degeneration in the substantia nigra of humans years after 1-methyl-4-phenyl-1,2,3,6-tetrahydropyridine exposure. *Ann Neurol* 1999;46:598–605.

Larsen KE, Sulzer D. Autophagy in neurons: a review. *Histol Histopathol.* 2002; 17(3):897-908.

Lazebnik YA, Kaufmann SH, Desnoyers S, Poirier GG, Earnshaw WC. Cleavage of poly(ADP-ribose) polymerase by a proteinase with properties like ICE. *Nature*. 1994 Sep 22;371(6495):346-7.

Lee, CH. and Chung, JH. The hCds1 (Chk2)-FHA Domain Is Essential for a Chain of Phosphorylation Events on hCds1 That Is Induced by Ionizing Radiation. *J. Biol. Chem.*2001. 276, 30537–30541

Lee HJ, Khoshaghideh F, Patel S, Lee SJ. Clearance of alpha-synuclein oligomeric intermediates via the lysosomal degradation pathway. *J Neurosci.* 2004 Feb 25;24(8):1888-96.

Lee HS, Park CW and Kim,YS. MPP+ increases the vulnerability to oxidative stress rather than directly mediating oxidative damage in human neuroblastoma cells. *Exp. Neurol*. 2000. 165, 164–171.

Lee FJ, Liu F, Genetic factors involved in the pathogenesis of Parkinson's disease, *Brain Res Rev*. 2008 Aug;58(2):354-64.

Lee CS, Park SY, Ko HH, Song JH, Shin YK, Han ES. Inhibition of MPP+-induced mitochondrial damage and cell death by trifluoperazine and W-7 in PC12 cells. *Neurochem Int.* 2005 Jan;46(2):169-78

Lehmann RG, Lickly LS, Lardie TS, Miller JH, Baldwin WS, Significance of metabolites to plants. *Weed Res*. 1991. 31 (6):347-356.

Lehmann RG, Miller JR and Cleveland CB. Fate of fluroxypyr in water. *Weed Res.* 1993. 33:197–204.

Lenaz G, Baracca A, Carelli V, D'Aurelio M, Sgarbi G, Solaini G. Bioenergetics of mitochondrial diseases associated with mtDNA mutations. *Biochim Biophys Acta.* 2004 Jul 23;1658(1-2):89-94.

Leroy E, Boyer R, Auburger G, Leube B, Ulm G, Mezey E, Harta G, Brownstein MJ, Jonnalagada S, Chernova T, Dehejia A, Lavedan C, Gasser T, Steinbach PJ, Wilkinson KD, Polymeropoulos MH. The ubiquitin pathway in Parkinson's disease. *Nature*. 1998 Oct 1;395(6701):451-2.

Lesage S, Brice A. Parkinson's disease: from monogenic forms to genetic susceptibility factors. Hum Mol Genet. 2009 Apr 15;18(R1):R48-59

Lesage S, Condroyer C, Lannuzel A, Lohmann E, Troiano A, Tison F, Damier P, Thobois S, Ouvrard-Hernandez AM, Rivaud-Péchoux S, Brefel-Courbon C, Destée A, Tranchant C, Romana M, Leclere L, Dürr A, Brice A. Molecular analyses of the LRRK2 gene in European and North-African autosomal dominant Parkinson's disease. *J Med Genet.* 2009 Apr 8.

Levine, B. & Yuan, J. Autophagy in cell death: an innocent convict? *J. Clin. Invest.* 2005. 115: 2679–2688.

Levine B, Kroemer G. Autophagy in the pathogenesis of disease. *Cell.* 2008 Jan 11; 132(1):27-42.

Levy, B. S., and Nassetta, W. J. Neurologic effects of manganese in humans: A review. *Int. J. Occup. Environ. Health*. 2003. 9, 153–163.

Levy OA, Malagelada C, Greene LA. Cell death pathways in Parkinson's disease: proximal triggers, distal effectors, and final steps. *Apoptosis.* 2009 Apr;14(4):478-500.

Li W, Yuan XM, Ivanova S, Tracey KJ, Eaton JW and Brunk UT, 3-Aminopropanal, formed during cerebral ischaemia, is a potent lysosomotropic neurotoxin. *Biochem. J.* 2003. 371:429–436

Li J, Spletter ML, Johnson DA, Wright, LS, Svendsen CN, and Johnson JA. Rotenone-induced caspase 9/3-independent and -dependent cell death in undifferentiated and differentiated human neural stem cells. *J. Neurochem.* 2005. 92, 462–476.

Li Y, Sun L, Cai T, Zhang Y, Lv S, Wang Y, Ye L. alpha-Synuclein overexpression during manganese-induced apoptosis in SH-SY5Y neuroblastoma cells. *Brain Res Bull.* 2010 Mar 16;81(4-5):428-33.

Lin Y, Choksi S, Shen HM, Yang QF, Hur GM, Kim YS, Tran JH, Nedospasov SA, Liu ZG. Tumor necrosis factor-induced nonapoptotic cell death requires receptor-interacting protein-mediated cellular reactive oxygen species accumulation. *J. Biol. Chem.* 2004.279:10822–10828.

Liang XH, Kleeman LK, Jiang HH, Gordon G, Goldman JE, Berry G, Herman B, Levine B. Protection against fatal Sindbis virus encephalitis by Beclin, a novel Bcl-2-interacting protein. *J. Virol.* 1998. 72: 8586–8596.

Liang XH, Jackson S, Seaman M, Brown K, Kempkes B, Hibshoosh H, Levine B. Induction of autophagy and inhibition of tumorigenesis by beclin 1. *Nature*. 1999. 402, 672–676.

Liang CL, Wang TT, Luby-Phelps K, German DC. Mitochondria mass is low in mouse substantia nigra dopamine neurons: implications for Parkinson's disease. *Exp. Neurol.* 2007. 203, 370–380.

Lindvall O, Hagell P. Cell therapy and transplantation in Parkinson's disease. *Clin Chem Lab Med* 2001; 39:356– 361.

Liou HH, Tsai MC, Chen CJ, Jeng JS, Chang YC, Chen SY, Chen RC. Environmental risk factors and Parkinson's disease: A case-control study in Taiwan. *Neurology*. 1997; 48, 1583-1588.

Liu Y, Fallon L, Lashuel HA, Liu Z, Lansbury PT Jr. The UCH-L1 gene encodes two opposing enzymatic activities that affect alpha-synuclein degradation and Parkinson's disease susceptibility. *Cell*. 2002. 111, 209–218.

Lo Bianco C, Ridet JL, Schneider BL, Deglon N, Aebischer P. alpha -Synucleinopathy and selective dopaminergic neuron loss in a rat lentiviral-based model of Parkinson's disease. *Proc Natl Acad Sci U S A*. 2002 Aug 6;99(16):10813-8.

Lo RY, Tanner CM, Albers KB, Leimpeter AD, Fross RD, Bernstein AL, McGuire V, Quesenberry CP, Nelson LM, Van Den Eeden SK. Clinical features in early Parkinson's disease and survival. *Arch Neurol.* 2009; 66(11): 1353-58.

Lockhart PJ, Lincoln S, Hulihan M, Kachergus J, Wilkes K, Bisceglio G, Mash DC, Farrer MJ. DJ-1 mutations are a rare cause of recessively inherited early onset Parkinsonism mediated by loss of protein function. *J Med Genet.* 2004 Mar;41(3):e22.

Lockshin and Zakeri, 2004a R.A. Lockshin and Z. Zakeri, Apoptosis, autophagy, and more, *Int. J. Biochem. Cell Biol.* 2004. 36: 2405–2419

Lotharius J, O'Malley KL. The parkinsonism-inducing drug 1-methyl-4-phenylpyridinium triggers intracellular dopamine oxidation. A novel mechanism of toxicity. *J Biol Chem* 2000;275:38581–8.

Lowe J, McDermott H, Landon M, Mayer RJ, Wilkinson KD. Ubiquitin carboxyl-terminal hydrolase (PGP 9.5) is selectively present in ubiquitinated inclusion bodies characteristic of human neurodegenerative diseases. *J. Pathol.* 1990. 161, 153–160.

Lum JJ, Bauer DE, Kong M, Harris MH, Li C, Lindsten T, Thompson CB. Growth factor regulation of autophagy and cell survival in the absence of apoptosis. *Cell.* 2005. 120, 237–248.

Luoma P, Melberg A, Rinne JO, Kaukonen JA, Nupponen NN, Chalmers RM, Oldfors A, Rautakorpi I, Peltonen L, Majamaa K, Somer H, Suomalainen A. Parkinsonism, premature menopause, and mitochondrial DNA polymerase gamma mutations: clinical and molecular genetic study. *Lancet.* 2004 Sep 4-10;364(9437):875-82.

LysoTracker® and LysoSensor™ Probes, Molecular Probes®, Invitrogen detection technologies

Mandel S, Grünblatt E, Youdim M. cDNA microarray to study gene expression of dopaminergic neurodegeneration and neuroprotection in MPTP and 6-hydroxydopamine models: implications for idiopathic Parkinson's disease. *J Neural Transm Suppl.* 2000;(60):117-24.

Mandel S, Grünblatt E, Maor G, Youdim MB. Early and late gene changes in MPTP mice model of Parkinson's disease employing cDNA microarray. *Neurochem Res.* 2002 Oct;27(10):1231-43

Mann VM, Cooper JM, Krige D, Daniel SE, Schapira AH, Marsden CD. Brain, skeletal muscle and platelet homogenate mitochondrial function in Parkinson's disease. *Brain*. 1992 Apr;115 (Pt 2):333-42.

Mann VM, Cooper JM, Daniel SE, Srai K, Jenner P, Marsden CD, Schapira AH. Complex I, iron, and ferritin in Parkinson's disease substantia nigra. *Ann Neurol.* 1994 Dec;36(6):876-81.

Manning-Bog AB, McCormack AL, Li J, Uversky VN, Fink AL, Di Monte DA. The herbicide paraquat causes up-regulation and aggregation of alpha-synuclein in mice: paraquat and alpha-synuclein. *J Biol Chem.* 2002 Jan 18;277(3):1641-4

Maria Fimia, G., Stoykova, A., Romagnoli, A., Giunta, L., Di Bartolomeo, S., Nardacci, R., Corazzari, M., Fuoco, C., Ucar, A., Schwartz, P., *et al*. Ambra1 regulates autophagy and development of the nervous system. *Nature*. 2007. 447: 1121–1125.

Martin LJ, Pan Y, Price AC et al. Parkinson's disease alpha-synuclein transgenic mice develop neuronal mitochondrial degeneration and cell death. *J Neurosci.* 2006. 26:41–50

Martınez, M., Martı´nez, N., Herna´ndez, A. I., and Ferra´ndiz, M. L. Hypothesis: Can N-acetylcysteine be beneficial in Parkinson's disease? *Life Sci.* 1999. 64, 1253–1257.

Marshall LE, Himes RH. Rotenone inhibition of tubulin selfassembly. *Biochim Biophys Acta* 1978; 543:590 –594.

Masliah E, Rockenstein E, Veinbergs I, Mallory M, Hashimoto M, Takeda A, Sagara Y, Sisk A, Mucke L. Dopaminergic loss and inclusion body formation in alpha-synuclein mice: implications for neurodegenerative disorders. *Science.* 2000 Feb 18;287(5456):1265-9.

Mata, I. F., Lockhart, P. J. & Farrer, M. J. Parkin genetics: one model for Parkinson's disease. *Hum. Mol. Genet*. 2004; 13, R127–R133.

Mattson MP. Apoptosis in neurodegenerative disorders. *Nat Rev Mol Cell Biol*. 2000. 1:120–129.

Mattson MP, Magnus T. Ageing and neuronal vulnerability. *Nat Rev Neurosci.* 2006 Apr;7(4):278-94.

Mattson, M. P. Neuronal life-and-death signaling, apoptosis, and neurodegenerative disorders. *Antioxid. Redox Signal.* 2006. 8:1997–2006.

McCormack AL, Thiruchelvam M, Manning-Bog AB, Thiffault C, Langston JW, Cory-Slechta DA, Di Monte DA. Environmental risk factors and Parkinson's disease: selective degeneration of nigral dopaminergic neurons caused by the herbicide paraquat. *Neurobiol Dis.* 2002 Jul;10(2):119-27.

McCormack, A. L., and Di Monte, D. A. Effects of L-dopa and other amino acids against paraquat-induced nigrostriatal degeneration. *J. Neurochem*. 2003. 85, 82–86.

McCormack, A. L., Atienza, J. G., Johnston, L. C., Andersen, J. K., Vu, S., and Di Monte D. A. Role of oxidative stress in paraquat-induced dopaminergic cell degeneration. *J. Neurochem.* 2005. 93:1030–1037.

McCormack AL, Atienza JG, Langston JW, DiMonte DA. Decreased susceptibility to oxidative stress underlies the resistance of specific dopaminergic cell populations to paraquat-induced degeneration. *Neuroscience*. 2006. 141:929–937.

McGeer PL, Itagaki S, Boyes BE, McGeer EG. Reactive microglia are positive for HLA-DR in the substantia nigra of Parkinson's and Alzheimer's disease brains. *Neurology* 1988; 38:1285–91.

Meco G, Bonifati V, Vanacore N, Fabrizio E. Parkinsonism after chronic exposure to the fungicide maneb (manganese ethylene-bis-dithiocarbamate). *Scand J Work Environ Health.* 1994 Aug;20(4):301-5.

Meley, D., Bauvy, C., Houben-Weerts, J.H., Dubbelhuis, P.F., Helmond, M.T., Codogno, P., and Meijer, A.J. AMPactivated protein kinase and the regulation of autophagic proteolysis. *J. Biol. Chem.* 2006. 281: 34870–34879.

Melov, S. Modeling mitochondrial function in aging neurons. *Trends Neurosci*. 2004. 27, 601–606.

Menendez J, Bastida F. Use of adjuvant-enhanced formulations to increase bipyridylium-herbicide effectiveness. *Commun Agric Appl Biol Sci.* 2004;69(3):61-5.

Meredith GE, Totterdell S, Petroske E, Santa Cruz K, Callison RC, Lau YS. Lysosomal malfunction accompanies alpha-synuclein aggregation in a progressive mouse model of Parkinson's disease. *Brain Res* 2002; 956: 156–65.

Meredith G, Halliday GM, Totterdell S, 'A critical review of the development and importance of proteinaceous aggregates in animal models of Parkinson's disease: new insights into Lewy body formation'. *Parkinsonism and Related Disorders* 2004; 10:191–202.

Meredith GE, Sonsalla PK, Chesselet MF. Animal models of Parkinson's disease progression. *Acta Neuropathol.* 2008 Apr;115(4):385-98.

Metzler DF. Health impact of organics in groind water. *Am J Public Health* 1982; 72:1375-84.

Miller DW, Hague SM, Clarimon J, Baptista M, Gwinn-Hardy K, Cookson MR, Singleton AB. alpha-Synuclein in blood and brain from familial Parkinson disease with SNCA locus triplication. *Neurology* 2004; 62:1835–1838.

Mills, PK, Yang, R, Riordan, D. Lymphohematopoietic cancers in the United Farm Workers of America (UFW), 1988–2001. *Cancer Causes Control*. 2005. 16: 823–830.

Mitsumoto A, Nakagawa Y. DJ-1 is an indicator for endogenous reactive oxygen species elicited by endotoxin. *Free Radic Res*. 2001 Dec;35(6):885-93.

Mizuno Y, Hattori N, Kubo S, Sato S, Nishioka K, Hatano T, Tomiyama H, Funayama M, Machida Y, Mochizuki H. Progress in the pathogenesis and genetics of Parkinson's disease. *Philos Trans R Soc Lond B Biol Sci.* 2008 Jun 27; 363(1500):2215-27.

Mizushima N. Autophagy: process and function. *Genes Dev.* 2007 Nov 15;21(22):2861-73

Mochizuki H, Goto K, Mori H, Mizuno Y: Histochemical detection of apoptosis in Parkinson's disease. J Neurol Sci 1996; 137:120–123.

Mogi A, Togari A, Kondo T, Mizuno Y, Komure O, Kuno S, Ichinose H, Nagatsu T. Caspase activities and tumor necrosis factor receptor R1 (p55) level are elevated in the substantia nigra from Parkinsonian brain. *J Neural Transm*. 2000. 107:335–341.

Molina-Jimenez *et al*., 2005 M.F. Molina-Jimenez, M.I. Sanchez-Reus, M. Cascales, D. Andres and J. Benedi, Effect of fraxetin on antioxidant defense and stress proteins in human neuroblastoma cell model of rotenone neurotoxicity. Comparative study with myricetin and *N*-acetylcysteine, *Toxicol. Appl. Pharmacol.*2005.209:214–225

Mookherjee P, Quintanilla R, Roh MS, Zmijewska AA, Jope RS, Johnson GV. Mitochondrial-targeted active Akt protects SH-SY5Y neuroblastoma cells from staurosporine-induced apoptotic cell death. *J Cell Biochem.* 2007 Sep 1;102(1):196-210.

Moore, D.J., Zhang, L., Troncoso, J., Lee, M.K., Hattori, N., Mizuno, Y., Dawson, T.M., Dawson, V.L. Association of DJ-1 and parkin mediated by pathogenic DJ-1 mutations and oxidative stress. Hum. *Mol. Genet.* 2005; 14, 71–84.

Moran LB, Croisier E, Duke DC, Kalaitzakis ME, Roncaroli F, Deprez M, Dexter DT, Pearce RKB, Graeber MB, Analysis of alpha-synuclein, dopamine and parkin pathways in neuropathologically conWrmed parkinsonian nigra. *Acta Neuropathol* 2007; 113:253–263.

Morrison RS and Kinoshita Y. The role of p53 in neuronal cell death. *Cell Death and Differentiation*. 2000. 7, 868 -879

Moran JM, Gonzalez-Polo RA, Ortiz-Ortiz MA, Niso-Santano M, Soler G, Fuentes JM. Identification of genes associated with paraquat-induced toxicity in SH-SY5Y cells by PCR array focused on apoptotic pathways. *J Toxicol Environ Health A*. 2008;71(22):1457-67.

Mortiboys, H., Thomas, K.J., Koopman,W.J., Klaffke, S., Abou-Sleiman, P., Olpin, S.,Wood, N.W., Willems, P.H., Smeitink, J.A., Cookson, M.R., Bandmann, O. Mitochondrial function and morphology are impaired in parkin-mutant fibroblasts. *Ann. Neurol*. 2008. 64, 555–565.

Muqit MM, Gandhi S, Wood NW. Mitochondria in Parkinson disease: back in fashion with a little help from genetics. *Arch Neurol.* 2006 May; 63(5):649-54.

Murakami T, Shoji M, Imai Y, Inoue H, Kawarabayashi T, Matsubara E, Harigaya Y, Sasaki A, Takahashi R and Abe K. Pael-R is accumulated in Lewy bodies of Parkinson's disease. *Ann. Neurol*. 2004; 55: 439–442

Murphy, D.D., Rueter, S.M., Trojanowski, J.Q., Lee, V.M. Synucleins are developmentally expressed, and alphasynuclein regulates the size of the presynaptic vesicular pool in primary hippocampal neurons. *J. Neurosci.* 2000; 20, 3214–3220.

Najim al-Din, A.S., Wriekat, A., Mubaidin, A., Dasouki, M. and Hiari, M. Pallido-pyramidal degeneration, supranuclear upgaze paresis and dementia: Kufor-Rakeb syndrome. *Acta Neurol. Scand*., 1994; 89, 347–352.

Nakamura K, Kitamura Y, Tsuchiya D, Inden M and Taniguchi T. In vitro neurodegeneration model: dopaminergic toxin-induced apoptosis in human SH-SY5Y cells. *International Congress Series*. 2004. 1260:287– 290

Narendra D, Tanaka A, Suen DF, Youle RJ, Parkin is recruited selectively to impaired mitochondria and promotes their autophagy. *J. Cell Biol.* 2008. 183, 795–803.

Navarro A, Boveris A, Bández MJ, Sánchez-Pino MJ, Gómez C, Muntané G, Ferrer I. Human brain cortex: mitochondrial oxidative damage and adaptive response in Parkinson disease and in dementia with Lewy bodies. *Free Radic Biol Med*. 2009 Jun 15; 46(12):1574-80

Neumar RW, Xu YA, Gada H, Guttmann RP, Siman R. Cross-talk between calpain and caspase proteolytic systems during neuronal apoptosis. *J Biol Chem*. 2003 Apr 18;278(16):14162-7.

Newhouse K, Hsuan SL, Chang SH, Cai B, Wang Y, Xia Z. Rotenone-induced apoptosis is mediated by p38 and JNK MAP kinases in human dopaminergic SH-SY5Y cells. *Toxicol Sci.* 2004 May;79(1):137-46.

Ni B, Wu X, Du Y,Su Y, Hamilton-Byrd E, Rockey PK, Rostech P, Poirier GG, Paul SM. Cloning and expression of a rat brain interleukin-1b-converting enzyme (ICE) related protease (IRP) and its possible role in apoptosis of cultured cerebellar granule neurons. *J Neurosci* 1997.17:1561–1569.

Nicholson DW, Ali A, Thornberry NA, Vaillancourt JP, Ding CK, Gallant M, Gareau Y, Griffin PR, Labelle M, Lazebnik YA, *et al*. Identification and inhibition of the ICE/CED-3 protease necessary for mammalian apoptosis. *Nature*. 1995 Jul 6;376(6535):37-43.

Niesink JM, de Vries J, Hollinger MA. Toxicology: Principles and Applications. Boca Raton: CRC Press, 1996.

Nikam S, Nikam P, Ahaley SK and Ajit V Sontakke AV. Oxidative stress in Parkinson's disease. *Indian Journal of Clinical Biochemistry,* 2009. 24 (1) 98-101

Niki T, Takahashi-Niki K, Taira T, Iguchi-Ariga SM, Ariga H.DJBP: a novel DJ-1-binding protein, negatively regulates the androgen receptor by recruiting histone deacetylase complex, and DJ-1 antagonizes this inhibition by abrogation of this complex. *Mol Cancer Res.* 2003 Feb;1(4):247-61.

Nishi, K. Expression of c-Jun in dopaminergic neurons of the substantia nigra in 1-methyl-4-phenyl-1,2,3,6-tetrahydropyridine (MPTP)-treated mice. *Brain Res.* 1997. 771:133–141.

Nishioka K, Vilariño-Güell C, Cobb SA, Kachergus JM, Ross OA, Wider C, Gibson RA, Hentati F, Farrer MJ. Glucocerebrosidase mutations are not a common risk factor for Parkinson disease in North Africa. *Neurosci Lett. 2*009 Nov 27.

Nixon, R. A., S. E. Lewis, and C. A. Marotta. Posttranslational modification of neurofilament proteins by phosphate during axoplasmic transport in retinal ganglion cell neurons. *J. Neurosci.* 1987. 7: 1145–1158.

Nixon RA, Wegiel J, Kumar A, Yu WH, Peterhoff C, Cataldo A, Cuervo AM: Extensive involvement of autophagy in Alzheimer disease: an immuno-electron microscopy study. *J Neuropathol Exp Neurol* 2005, 64:113–122

Nuti A, Ceravolo R, Dell'Agnello G, Gambaccini G, Bellini G, Kiferle L, Rossi C, Logi C, Bonuccelli U, Environmental factors and Parkinson's disease: a case-control study in the Tuscany region of Italy. *Parkinsonism and Related Disorders.* 2004; 10: 481–485.

Oakley AE, Collingwood JF, Dobson J, Love G, Perrott HR, Edwardson JA, Elstner M, Morris CM. Individual dopaminergic neurons show raised iron levels in Parkinson disease. *Neurology*. 2007 May 22;68(21):1820-5

Oda T, Kosuge Y, Arakawa M, Ishige K and Ito Y. Distinct mechanism of cell death is responsible for tunicamycin-induced ER stress in SK-N-SH and SH-SY5Y cells. *Neuroscience Research.* 2008. 60(1):29-39.

Offen D, Beart PM, Cheung NS, Pascoe CJ, Hochman A, Gorodin S, Melamed E, Bernard R, Bernard O. Transgenic mice expressing human Bcl-2 in their neurons are resistant to 6-hydroxydopamine and 1-methyl-4-phenyl-1,2,3,6- tetrahydropyridine neurotoxicity. *Proc Natl Acad Sci U S A*. 1998 May 12;95(10):5789-94.

Okamoto, K., Shaw, J.M. Mitochondrial morphology and dynamics in yeast and multicellular eukaryotes. *Annu. Rev. Genet*. 2005. 39, 503–536.

Olanow CW, Agid Y, Mizuno Y, Albanese A, Bonuccelli U, Damier P, De Yebenes J, Gershanik O, Guttman M, Grandas F, Hallett M, Hornykiewicz O, Jenner P, Katzenschlager R, Langston WJ, LeWitt P, Melamed E, Mena MA, Michel PP, Mytilineou C, Obeso JA, Poewe W, Quinn N, Raisman-Vozari R, Rajput AH, Rascol O, Sampaio C, Stocchi F. Levodopa in the treatment of Parkinson's disease: current controversies. *Mov Disord.* 2004 Sep;19(9):997-1005. Review.

Olsson M, Nikkhah G, Bentlage C, Björklund A. Forelimb akinesia in the rat Parkinson model: differential effects of dopamine agonists and nigral transplants as assessed by a new stepping test. *J Neurosci.* 1995 May;15(5 Pt 2):3863-75.

Onyango IG. Mitochondrial Dysfunction and Oxidative Stress in Parkinson's Disease. *Neurochem Res.* 2008. 33:589–597

Orth M, Tabrizi SJ. Models of Parkinson's disease. *Mov Disord.* 2003 Jul;18(7):729-37.

Ostrerova, N., Petrucelli, L., Farrer, M., Mehta, N., Choi, P., Hardy, J., Wolozin, B. alpha-Synuclein shares physical and functional homology with 14-3-3 proteins. *J. Neurosci.* 1999; 19, 5782–5791.

O¨ztap E, Topal A. A cell protective mechanism in a murine model of Parkinson's disease. *Turk J Med Sci* 2003; 33: 295–9.

Pant, H. C., and Veeranna. Neurofilament phosphorylation. Biochem. *Cell Biol.* 1995. 73: 575–592.

Pankratz N, Foroud T., Genetics of Parkinson disease. *NeuroRx.* 2004 Apr;1(2):235-42.

Park JY, Lansbury PT Jr. Beta-synuclein inhibits formation of alpha-synuclein protofibrils: a possible therapeutic strategy against Parkinson's disease. *Biochemistry.* 2003 Apr 8;42(13):3696-700.

Park J, Lee SB, Lee S, Kim Y, Song S, Kim S, Bae E, Kim J, Shong M, Kim JM, Chung J. Mitochondrial dysfunction in Drosophila PINK1 mutants is complemented by parkin. *Nature*. 2006; 441, 1157–1161

Park S, Stacy M. Non-motor symptoms in Parkinson's disease. *J Neurol.* 2009. 256 (Suppl 3):S293–S298

Parker Jr., W.D., Parks, J.K., Swerdlow, R.H. Complex I deficiency in Parkinson's disease frontal cortex. *Brain Res.* 2008. 1189, 215–218.

Patil C and Walter P, Intracellular signaling from the endoplasmic reticulum to the nucleus: the unfolded protein response in yeast and mammals, *Curr. Opin. Cell Biol.* 2001, 13: 349–355

Pattingre, S., Tassa, A., Qu, X., Garuti, R., Liang, X.H., Mizushima, N., Packer, M., Schneider, M.D., and Levine, B. Bcl-2 antiapoptotic proteins inhibit Beclin 1-dependent autophagy. *Cell*. 2005. 122: 927–939.

Penn, A.M., Roberts, T., Hodder, J., Allen, P.S., Zhu, G., Martin, W.R. Generalized mitochondrial dysfunction in Parkinson's disease detected by magnetic resonance spectroscopy of muscle. *Neurology*. 1995. 45: 2097–2099.

Perez-Otano I., Mandelzys A and Morgan JI. MPTP Parkinsonism is accompanied by persistent expression of a delta- FosB-like protein in dopaminergic pathways. *Brain Res. Mol. Brain Res*. 1998. 53:41–52.

Perry TL, Yong VW: Idiopathic Parkinson's disease, progressive supranuclear palsy and glutathione metabolism in the substantia nigra of patients. *Neurosci Lett* 1986;67:269–274.

Petersén A., Larsen K.E., Behr G.G., Romero N., Przedborski S., Brundin P. and Sulzer D. Expanded CAG repeats in exon 1 of the Huntington's disease gene stimulate dopamine-mediated striatal neuron autophagy and degeneration. *Hum. Mol*. 2001b. *Genet*. 10,1243-1254.

Petiot A, Ogier-Denis E, Blommaart EF, Meijer AJ, Codogno P. Distinct classes of phosphatidylinositol 3'-kinases are involved in signaling pathways that control macroautophagy in HT-29 cells. *J Biol Chem*. 2000 Jan 14;275(2):992-8.

Petit A, Kawarai T, Paitel E, Sanjo N, Maj M, Scheid M, Chen F, Gu Y, Hasegawa H, Salehi-Rad S, Wang L, Rogaeva E, Fraser P, Robinson B, St George-Hyslop P, Tandon A. Wild-type PINK1 prevents basal and induced neuronal apoptosis, a protective effect abrogated by Parkinson disease-related mutations. *J Biol Chem.* 2005 Oct 7;280(40):34025-32.

Petrovitch H, Ross GW, Abbott RD, Sanderson WT, Sharp DS, Tanner CM, Masaki KH, Blanchette PL, Popper JS, Foley D, Launer L, White LR. Plantation work and risk of Parkinson disease in a population-based longitudinal study. *Archives of Neurology*. 2002 Nov; 59(11):1787-92

Petrozzi L, Ricci G, Giglioli NJ, Siciliano G, Mancuso M. Mitochondria and neurodegeneration. *Biosci Rep*. 2007 Jun;27(1-3):87-104.

Petrucelli L, O'Farrell C, Lockhart PJ, Baptista M, Kehoe K, Vink L, Choi P, Wolozin B, Farrer M, Hardy J, Cookson MR. Parkin protects against the toxicity associated with mutant alpha-synuclein: proteasome dysfunction selectively affects catecholaminergic neurons. *Neuron.* 2002 Dec 19;36(6):1007-19.

Pham, N.A., Richardson, T., Cameron, J., Chue, B., Robinson, B.H. Altered mitochondrial structure and motion dynamics in living cells with energy metabolism defects revealed by real time microscope imaging. *Microsc. Microanal.* 2004.10, 247–260.

Piacentini M, Evangelisti C, Mastroberardino PG, Nardacci R, Kroemer G. Does prothymosin-alpha act as molecular switch between apoptosis and autophagy? *Cell Death Differ* 2003;10: 937–9.

Pickford, F., Masliah, E., Britschgi, M., Lucin, K., Narasimhan, R., Jaeger, P. A., Small, S., Spencer, B., Rockenstein, E., Levine, B. and Wyss-Coray, T. The autophagy-related protein beclin 1 shows reduced expression in early Alzheimer disease and regulates amyloid β accumulation in mice. *J. Clin. Invest*. 2008. 118, 2190-2199.

Plowey ED, Cherra SJ 3rd, Liu YJ, Chu CT. Role of autophagy in G2019S-LRRK2-associated neurite shortening in differentiated SH-SY5Y cells. *J Neurochem*. 2008 May;105(3):1048-56.

Plun-Favreau H, Klupsch K, Moisoi N, Gandhi S, Kjaer S, Frith D, Harvey K, Deas E, Harvey RJ,McDonald N, Wood NW, Martins LM, Downward J. The mitochondrial protease HtrA2 is regulated by Parkinson's disease-associated kinase PINK1. *Nat Cell Biol.* 2007 Nov;9(11):1243-52.

Polimeno L, Pesetti B, Lisowsky T, Iannone F, Resta L, Giorgio F, Mallamaci R, Buttiglione M, Santovito D, Vitiello F, Mancini ME, Francavilla A. Protective effect of augmenter of liver regeneration on hydrogen peroxide-induced apoptosis in SH-SY5Y human neuroblastoma cells. *Free Radic Res*. 2009 Sep; 43 (9):865-75

Polyak K, XiaY,Zweier JL, Kinzler KW andVogelstein B. A model for p53- induced apoptosis. *Nature*. 1997. 389: 300- 305

Polymeropoulos MH, Lavedan C, Leroy E, Ide SE, Dehejia A, Dutra A, Pike B, Root H, Rubenstein J, Boyer R, Stenroos ES, Chandrasekharappa S, Athanassiadou A, Papapetropoulos T, Johnson WG, Lazzarini AM, Duvoisin RC, Di Iorio G, Golbe LI, Nussbaum RL. Mutation in the alpha-synuclein gene identified in families with Parkinson's disease. *Science*. 1997 Jun 27;276(5321):2045-7.

Posmantur, R., R. L. Hayes, C. E. Dixon, and W. C. Taft. Neurofilament 68 and neurofilament 200 protein levels decrease after traumatic brain injury. *J. Neurotrauma*. 1994. 11: 533–545.

Presgraves SP**,** Ahmed T**,** Borwege S**,** Joyce JN. Terminally differentiated SH-SY5Y cells provide a model system for studying neuroprotective effects of dopamine agonists. *Neurotox. Res*. 2004. 5:579-598.

Priyadarshi A, Khuder SA, Schaub EA, Shrivastava S, A meta-analysis of Parkinson's disease and exposure to pesticides. *Neurotoxicology*. 2000 Aug; 21(4):435-40.

Priyadarshi A, Khuder SA, Schaub EA, Priyadarshi SS. Environmental risk factors and Parkinson's disease: a metaanalysis. *Environ Res.* 2001 Jun; 86(2):122-7.

Przedborski, S., Kostic, V., Jackson-Lewis, V., Naini, A.B., Simonetti, S., Fahn, S., Carlson, E., Epstein, C.J., Cadet, J.L. Transgenic mice with increased Cu/Zn-superoxide dismutase activity are resistant to N-methyl-4-phenyl-1,2,3,6-tetrahydropyridine-induced neurotoxicity. *J. Neurosci.* 1992. 12, 1658-1667.

Przedborski S, Levivier M, Jiang H, Ferreira M, Jackson-Lewis V, Donaldson D, Togasaki DM. Dose-dependent lesions of the dopaminergic nigrostriatal pathway induced by intrastriatal injection of 6-hydroxydopamine. *Neuroscience*. 1995 Aug;67(3):631-47.

Przedborski S, Vila M, MPTP: a review of its mechanisms of neurotoxicity, *Clinical Neuroscience Research* 2001; 1:407–418.

Przedborski S, Pathogenesis of nigral cell death in Parkinson's disease. *Parkinsonism and Related Disorders* 2005; 11:S3–S7.

Przedborski S, Ischiropoulos H. Reactive oxygen and nitrogen species: weapons of neuronal destruction in models of Parkinson's disease. *Antioxid Redox Signal.* 2005 May-Jun;7(5-6):685-93

Pyle A, Foltynie T, Tiangyou W, Foltynie T, Tiangyou W, Lambert C, Keers SM, Allcock LM, Davison J, Lewis SJ, Perry RH, Barker R, Burn DJ, Chinnery PF. Mitochondrial DNA haplogroup cluster UKJT reduces the risk of PD. *Ann Neurol* 2005; 57:564–567.

Pyo JO, Jang MH, Kwon YK, Lee HJ, Jun JI, Woo HN, Cho DH, Choi B, Lee H, Kim JH, Mizushima N, Oshumi Y, Jung YK. Essential roles of Atg5 and FADD in autophagic cell death: dissection of autophagic cell death into vacuole formation and cell death. *Biol Chem* 2005. 280: 20722–20729.

Qin ZH, Wang Y, Kegel KB, Kazantsev A, Apostol BL, Thompson LM, Yoder J, Aronin N, DiFiglia M: Autophagy regulates the processing of amino terminal huntingtin fragments. *Hum Mol Genet* 2003, 12:3231–3244

Ramachandiran S, Hansen JM, Jones DP, Richardson JR, Miller GW. Divergent mechanisms of paraquat, MPP+, and rotenone toxicity: oxidation of thioredoxin and caspase-3 activation. *Toxicol Sci.* 2007 Jan;95(1):163-71.

Ramirez A, Heimbach A, Gründemann J, Stiller B, Hampshire D, Cid LP, Goebel I, Mubaidin AF, Wriekat AL, Roeper J, Al-Din A, Hillmer AM, Karsak M, Liss B, Woods CG, Behrens MI, Kubisch C. Hereditary parkinsonism with dementia is caused by mutations in ATP13A2, encoding a lysosomal type 5 P-type ATPase. *Nat Genet*. 2006 Oct;38(10):1184-91.

Rajput AH, Uitti RJ, Stern W & Laverty W Early onset Parkinson's disease in Saskatchewan: Environmental considerations for etiology. *Can J Neurol Sci*, 1986; 13, 312–316.

Ramaker C, Marinus J, Stiggelbout AM, et al. Systematic evaluation of rating scales for impairment and disability in Parkinson's disease. *Mov Disord* 2002; 17:867–76.

Ray DE: Pesticides derived from plants and other organisms. In *Handbook of Pesticide Toxicology*. Edited by: Hayes WJ Jr, Laws ER Jr. New York, NY: Academic Press; 1991:2-3.

Reeve AK, Krishnan KJ, Turnbull D. Mitochondrial DNA mutations in disease, aging, and neurodegeneration. *Ann N Y Acad Sci*. 2008 Dec;1147:21-9.

Reinhardt HC, Yaffe MB. Kinases that control the cell cycle in response to DNA damage: Chk1, Chk2, and MK2. *Curr Opin Cell Biol.* 2009 Apr;21(2):245-55.

Relative Quantification, Applied Biosystems 7300 Real-Time PCR System, Applied Biosystems 7500 & 7500 Fast Real-Time PCR System. Applied Biosystems, 2008.

Ren Y, Zhao J, Feng J. Parkin binds to α / ßtubulin and increases their ubiquitination and degradation. *J Neurosci* 2003; 23:3316 –3324.

Resh MD. Fyn, a Src family tyrosine kinase. *Int J Biochem Cell Bio*l. 1998 Nov;30(11):1159-62

Richardson JR, Quan Y, Sherer TB, Greenamyre JT, Miller GW. Paraquat neurotoxicity is distinct from that of MPTP and rotenone. *Toxicol Sci.* 2005 Nov;88(1):193-201

Rintoul, G.L., Filiano, A.J., Brocard, J.B., Kress, G.J., Reynolds, I.J. Glutamate decreases mitochondrial size andmovement in primary forebrain neurons. *J.Neurosci*. 2003. 23, 7881–7888.

Ritz B, Yu F. Parkinson's disease mortality and pesticide exposure in California 1984-1994. *Int J Epidemiol.* 2000 Apr; 29(2):323-9.

Rivlin-Etzion M, Marmor O, Heimer G, Raz A, Nini A, Bergman H. Basal ganglia oscillations and pathophysiology of movement disorders. *Curr Opin Neurobiol.* 2006 Dec;16(6):629-37

Roberg K, Relocalization of cathepsin D and cytochrome *c* early in apoptosis revealed by immunoelectron microscopy. *Lab. Invest.* 2001.81: 149–158

Roberg K, Johansson U and Öllinger K. Lysosomal release of cathepsin D precedes relocation of cytochrome *c* and loss of mitochondrial transmembrane potential during apoptosis induced by oxidative stress. *Free Radic. Biol. Med.* 1999. 27:1228–1237

Rodríguez M, Barroso-Chinea P, Abdala P, Obeso J, González-Hernández T. Dopamine cell degeneration induced by intraventricular administration of 6-hydroxydopamine in the rat: similarities with cell loss in parkinson's disease. *Exp Neurol.* 2001 May;169(1):163-81.

Ross RA, Spengler BA, Biedler JL. Coordinate morphological and biochemical interconversion of human neuroblastoma cells. *J Natl Cancer Inst.* 1983 Oct;71(4):741-7.

Ryu EJ, Harding HP, Angelastro JM, Vitolo OV, Ron D and Greene LA. Endoplasmic reticulum stress and the unfolded protein response in cellular models of Parkinson's disease. *J. Neurosci*. 2002; 22: 10690–10698

Saatman, K. E., D. I. Graham, and T. K. McIntosh. The neuronal cytoskeleton is at risk after mild and moderate brain injury. *J. Neurotrauma.* 1998. 15: 1047–1058.

Saeed SA, Wilks MF, Coupe M. Acute diquat poisoning with intracerebral bleeding. *Postgrad Med J.* 2001 May;77(907):329-32.

Saftig P, Wouter Beertsen W and Eeva-Liisa Eskelinen E. LAMP-2 A control step for phagosome and autophagosome maturation. *Autophagy*. 2008. 4:4, 510-512; 16

Sakamoto M, Uchihara T, Hayashi M, Nakamura A, Kikuchi E, Mizutani T, Mizusawa H, Hirai S. Heterogeneity of nigral and cortical Lewy bodies differentiated by amplified triple-labeling for alpha-synuclein, ubiquitin, and thiazin red. *Exp Neurol*. 2002 Sep;177(1):88-94.

Sakata, E., Yamaguchi, Y., Kurimoto, E., Kikuchi, J., Yokoyama, S., Yamada, S., Kawahara, H., Yokosawa, H., Hattori, N., Mizuno, Y., et al., 2003. Parkin binds the Rpn10 subunit of 26S proteasomes through its ubiquitin-like domain. *EMBO Rep.* 2003; 4, 301–306.

Sakhi S, Sun N, Wing LL, Mehta P and Schreiber SS. Nuclear accumulation of p53 protein following kainic acid-induced seizures. *NeuroReport*. 1996. 7: 493-496

Samii A, Nutt JG, Ransom BR. Parkinson's disease. *Lancet*. 2004; 363(9423):1783-93

Sarkar, S., Perlstein, E.O., Imarisio, S., Pineau, S., Cordenier, A., Maglathlin, R.L., Webster, J.A., Lewis, T.A., O'Kane, C.J., Schreiber, S.L., et al. 2007. Small molecules enhance autophagy and reduce toxicity in Huntington's disease models. *Nat. Chem. Biol.* 3: 331–338.

Saporito M.S., Thomas B.A., Scott R.W., MPTP activates c-Jun NH2-terminal kinase (JNK) and its upstream regulatory kinase MKK4 in nigrostriatal neurons *in vivo*. *J. Neurochem.*, 2000. 75: 1200-1208.

Sauer H, Oertel WH. Progressive degeneration of nigrostriatal dopamine neurons following intrastriatal terminal lesions with 6-hydroxydopamine: a combined retrograde tracing and immunocytochemical study in the rat. *Neuroscience.* 1994 Mar;59(2):401-15.

Satake W, Nakabayashi Y, Mizuta I, Hirota Y, Ito C, Kubo M, Kawaguchi T, Tsunoda T, Watanabe M, Takeda A, Tomiyama H, Nakashima K, Hasegawa K, Obata F, Yoshikawa T, Kawakami H, Sakoda S, Yamamoto M, Hattori N, Murata M,Nakamura Y, Toda T. Genome-wide association study identifies common variants at four loci as genetic risk factors for Parkinson's disease. *Nat Genet*. 2009 Dec;41(12):1303-7

Satoh MS, Lindahl T. Role of poly(ADP-ribose) formation in DNA repair. *Nature.* 1992 Mar 26;356(6367):356-8.

Schapira, A.H., Cooper, J.M., Dexter, D., Jenner, P., Clark, J.B., Marsden, C.D. Mitochondrial complex I deficiency in Parkinson's disease. *Lancet.* 1989 Jun 3;1(8649):1269

Schapira AH, Mann VM, Cooper JM, Dexter D, Daniel SE, Jenner P, Clark JB, Marsden CD. Anatomic and disease specificity of NADH CoQ1 reductase (complex I) deficiency in Parkinson's disease. *J Neurochem*. 1990; 55:2142–2145

Schapira AH, Cooper JM, Dexter D, Clark JB, Jenner P, Marsden CD. Mitochondrial complex I deficiency in Parkinson's disease. *J Neurochem*. 1998 Mar;54(3):823-7.

Schapira AH. Present and future drug treatment for Parkinson's disease. J Neurol Neurosurg Psychiatry. 2005 Nov;76(11):1472-8.

Schapira A. Mitochondrial disease. *Lancet*. 2006; 368:70–82

Schapira AH. Etiology of Parkinson's disease. *Neurology*. 2006; 66:S10–S23

Schapira AH. Mitochondrial dysfunction in Parkinson's disease. *Cell Death Differ.* 2007; 1-5.

Schlaepfer, W. W. Neurofilaments: Structure, metabolism and implications in disease. *J. Neuropathol. Exp. Neurol*. 1987. 46:117–129.

Schmidt, W. J., and Alam, M. Controversies on new animal models of Parkinson's disease pro and con: The rotenone model of Parkinson's disease (PD). *J. Neural Transm. Suppl.* 2006. 273–276.

Schober A. Classic toxin-induced animal models of Parkinson's disease: 6-OHDA and MPTP. *Cell Tissue Res*. 2004 Oct;318(1):215-24.

Seaton, T.A., Cooper, J.M., Schapira, A.H.V. Free radical scavengers protect dopaminergic cell lines from apoptosis induced by complex I inhibitors. *Brain Res*. 1997. 777, 110-/118.

Seeman P and Niznik HB. Dopamine receptors and transporters in Parkinson's disease and schizophrenia. *FASEB J.* 1990 Jul;4(10):2737-44.

Seidler A, Hellenbrand W, Robra B-P, Vieregge P, Nischan P, Joerg J, Oertel WH, Ulm G & Schneider E. Possible environmental, occupational, and other etiologic factors for Parkinson's disease: A case–control study in Germany. *Neurolog*. 1996, 46, 1275–1284.

Sellbach AN, Boyle RS, Silburn PA, Mellick GD. Parkinson's disease and family history. *Parkinsonism Relat Disord.* 2006 Oct;12(7):399-409.

Semchuk KM, Love EJ, Lee RG. Parkinson's disease and exposure to rural environmental factors: a population based case-control study. *Can J Neurol Sci*. 1991 Aug; 18(3):279-86.

Seo JH, Rah JC, Choi SH, Shin JK, Min K, Kim HS, Park CH, Kim S, Kim EM, Lee SH, Lee S, Suh SW, Suh YH. Alpha-synuclein regulates neuronal survival via Bcl-2 family expression and PI3/Akt kinase pathway. *FASEB J.* 2002 Nov;16(13):1826-8

Sgado P, Alberi L, Gherbassi D, Galasso SL, Ramakers GM, Alavian KN, Smidt MP, Dyck RH, Simon HH (2006) Slow progressive degeneration of nigral dopaminergic neurons in postnatal Engrailed mutant mice. *Proc Natl Acad Sci USA* 103:15242–15247

Shaikh SB, Nicholson LF. Effects of chronic low dose rotenone treatment on human microglial cells. *Mol Neurodegener.* 2009 Dec 31;4:55

Shendelman S, Jonason A, Martinat C, Leete T and Abeliovich A. DJ-1 is a redox-dependent molecular chaperone that inhibits α-synuclein aggregate formation, *PLoS Biol.* 2004. 2:362

Sherer TB, Trimmer PA, Borland K, Parks JK, Bennett JP Jr, Tuttle JB. Chronic reduction in complex I function alters calcium signaling in SH-SY5Y neuroblastoma cells. *Brain Res.* 2001 Feb 9;891(1-2):94-105.

Sherer TB, Betarbet R, Stout AK, Lund S, Baptista M, Panov AV, Cookson MR, Greenamyre JT. An in vitro model of Parkinson's disease: linking mitochondrial impairment to altered alpha-synuclein metabolism and oxidative damage. *J Neurosci* 2002; 22:7006–15.

Sherer, T. B.; Betarbet, R.; Testa, C. M.; Seo, B. B.; Richardson, J. R.; Kim, J. H.; Miller, G. W.; Yagi, T.; Matsuno-Yagi, A.; Greenamyre, J. T. Mechanism of toxicity in rotenone models of Parkinson's disease. *J. Neurosci.* 2003. 23:10756–10764.

Sherer TB, Kim JH, Betarbet R, Greenamyre JT. Subcutaneous rotenone exposure causes highly selective dopaminergic degeneration and α-synuclein aggregation. *Exp Neurol*. 2003; 179:9 –16.

Shimada H, Hirai K, Simamura E, Pan J. Mitochondrial NADH-quinone oxidoreductase of the outer membrane is responsible for paraquat cytotoxicity in rat livers. *Arch Biochem Biophys.*1998. 351:75–81.

Shimura, H., Hattori, N., Kubo, S., Mizuno, Y., Asakawa, S., Minoshima, S., Shimizu, N., Iwai, K., Chiba, T., Tanaka, K., et al. Familial Parkinson disease gene product, parkin, is a ubiquitin–protein ligase. *Nat. Genet*. 2000; 25, 302–305.

Shimura, H., Schwartz, D., Gygi, S.P., Kosik, K.S. CHIP-Hsc70 complex ubiquitinates phosphorylated tau and enhances cell survival. *J. Biol. Chem.* 2004; 279, 4869–4876.

Shimizu K, Ohtaki K, Matsubara K, Aoyama K, Uezono T, Saito O, Suno M, Ogawa K, Hayase N, Kimura K, Shiono H. Carrier-mediated processes in blood--brain barrier penetration and neural uptake of paraquat. *Brain Res.* 2001 Jul 6;906(1-2):135-42.

Shinbo, Y., Taira, T., Niki, T., Iguchi-Ariga, S.M., Ariga, H., 2005. DJ-1 restores p53 transcription activity inhibited by Topors/p53BP3. *Int. J. Oncol.* 2005; 26, 641–648.

Shiraishi T, Yoshida T, Nakata S, Horinaka M, Wakada M, Mizutani Y, Miki T, Sakai T. Tunicamycin enhances tumor necrosis factor-related apoptosis-inducing ligand-induced apoptosis in human prostate cancer cells. *Cancer Res*. 2005 Jul 15;65(14):6364-70.

Shukla Y, Taneja P, Arora A, Sinha N. Mutagenic potential of Mancozeb in Salmonella typhimurium. *J Environ Pathol Toxicol Oncol*. 2004;23(4):297-302.

Shults CW. Lewy bodies. *Proc Natl Acad Sci U S A.* 2006 Feb 7;103(6):1661-8.

Sian J, Dexter D, Jenner P, Marsden C. Decreased in nigral glutathione in Parkinson's disease. *Br J Pharmacol*. 1991;104:281

Sik Kim J, Wie Cho E, Won Chung H, Gyu Kim I. Effects of Tiron, 4,5-dihydroxy-1,3-benzene disulfonic acid, on human promyelotic HL-60 leukemia cell differentiation and death. *Toxicology*. 2006. 223 (1-2): 36-45

Silvestri L, Caputo V, Bellacchio E, Atorino L, Dallapiccola B, Valente EM, Casari G. Mitochondrial import and enzymatic activity of PINK1 mutants associated to recessive parkinsonism. *Hum Mol Genet.* 2005 Nov 15;14(22):3477-92

Sim CH, Lio DS, Mok SS, Masters CL, Hill AF, Culvenor JG, Cheng HC. C-terminal truncation and Parkinson's disease-associated mutations down-regulate the protein serine/threonine kinase activity of PTEN-induced kinase-1. *Hum Mol Genet*. 2006 Nov 1;15(21):3251-62.

Simón-Sánchez J, Martí-Massó JF, Sánchez-Mut JV, Paisán-Ruiz C, Martínez-Gil A, Ruiz-Martínez J, Sáenz A, Singleton AB, López de Munain A, Pérez-Tur J. Parkinson's disease due to the R1441G mutation in Dardarin: a founder effect in the Basques. *Mov Disord* 2006; 21:1954-9.

Simsiman, G. V., Daniel, T. C., and Chesters, G. (1976). Diquat and endothall: Their fates in the environment. *Residue Rev*. 62, 131–174.

Simunovic F, Yi M, Wang Y, Macey L, Brown LT, Krichevsky AM, Andersen SL, Stephens RM, Benes FM, Sonntag KC. Gene expression profiling of substantia nigra dopamine neurons: further insights into Parkinson's disease pathology. *Brain*. 2009 Jul;132(Pt 7):1795-809.

Singleton AB, Farrer M, Johnson J, Singleton A, Hague S, Kachergus J, Hulihan M, Peuralinna T, Dutra A, Nussbaum R, Lincoln S, Crawley A, Hanson M, Maraganore D, Adler C, Cookson MR, Muenter M, Baptista M, Miller D, Blancato J, Hardy J, Gwinn-Hardy K. alpha-Synuclein locus triplication causes Parkinson's disease. *Science*. 2003 Oct 31;302(5646):841.

Škárka L and Oštadál B. Mitochondrial membrane potential in cardiac myocytes. *Physiol Res. 2005*.51:425-434.

Smeyne RJ, Jackson-Lewis V, The MPTP model of Parkinson's disease, *Molecular Brain Research* 2005; 134: 57– 66.

Smigrodzki R, Parks J, Parker WD. High frequency of mitochondrial complex I mutations in Parkinson's disease and aging. *Neurobiol Aging*. 2004 Nov-Dec;25(10):1273-81.

Smith LL. Mechanism of paraquat toxicity in the lung and its relevance to treatment. *Hum Toxicol* 1987;6:31–6.

Smith WW, Jiang H, Pei Z et a.Endoplasmic reticulum stress and mitochondrial cell death pathways mediate A53T mutant alpha-synuclein-induced toxicity. *Hum Mol Genet*. 2005. 14: 3801–3811.

Smith WW, Margolis RL, Li X, Troncoso JC, Lee MK, Dawson VL, Dawson TM, Iwatsubo T, Ross CA. Alpha-synuclein phosphorylation enhances eosinophilic cytoplasmic inclusion formation in SH-SY5Y cells. *J Neurosci.* 2005 Jun 8;25(23):5544-52.

Song X, Ehrich M, 'Cytotoxic effects of MPTP on SH-SY5Y human neuroblastoma cells'. *Neurotoxicology*. 1997;18(2):341-53.

Song DD, Shults CW, Sisk A, Rockenstein E, Masliah E. Enhanced substantia nigra mitochondrial pathology in human alpha-synuclein transgenic mice after treatment with MPTP. *Exp Neurol.* 2004 Apr;186(2):158-72.

Spillantini MG, Crowther RA, Jakes R, Hasegawa M, Goedert M. alpha-Synuclein in filamentous inclusions of Lewy bodies from Parkinson's disease and dementia with lewy bodies. *Proc Natl Acad Sci U S A*. 1998 May 26;95(11):6469-73.

Stacy M. Sleep disorders in Parkinson's disease: epidemiology and management. *Drugs Aging.* 2002. 19:733–739

Stadelmann C, Deckwerth TL, Srinivasan A, Bancher C, Bruck W, Jellinger K, Lassmann H: Activation of caspase-3 in single neurons and autophagic granules of granulovacuolar degeneration in Alzheimer's disease: evidence for apoptotic cell death. *Am J Pathol* 1999, 155:1459–1466

Staropoli, J.F., McDermott, C., Martinat, C., Schulman, B., Demireva, E., Abeliovich, A.. Parkin is a component of an SCF-like ubiquitin ligase complex and protects postmitotic neurons from kainate excitotoxicity. *Neuron*. 2003. 37, 735–749.

Stavrovskaya IG, Kristal BS. The powerhouse takes control of the cell: is the mitochondrial permeability transition a viable therapeutic target against neuronal dysfunction and death? *Free Radic Biol Med*. 2005; 38:687–697

Stefanis L., Larsen K.E., Rideout H.J., Sulzer D. and Greene L.A. Expression of A53T mutant, but not wild type, a-synuclein in PC12 cells induces alterations of the ubiquitin-dependent degradation system, loss of dopamine release, and autophagic cell death. *J. Neurosci.* 2001. 21, 9549-9560.

Stern M, Dulaney E, Gruber SB, Golbe L, Bergen M, Hurtig H, Gollomp S & Stolley P The epidemiology of Parkinson's disease. A case–control study of young-onset and old-onset patients. *Arch Neurol.* 1991; 48: 903–907.
Strauss KM *et al.* Loss of function mutations in the gene encoding Omi/HtrA2 in Parkinson's disease. *Hum Mol Genet*, 2005. 14: 2099–2111

Stromhaug P.E., Berg T.O., Fengsrud M. and Seglen P.O. Purification and characterization of autophagosomes from rat hepatocytes. *Biochem. J.* 1998. 335, 217-224.

Sumimoto H, Ueno N, Yamasaki T, Taura M, Takeya R. Molecular mechanism underlying activation of superoxide-producing NADPH oxidases: roles for their regulatory proteins. *Jpn J Infect Disease. 2004. 57:S24–S25*

Sulzer D., Bogulavsky J., Larsen K.E., Karatekin E., Kleinman M., Turro N., Krantz D., Edwards R., Greene L.A. and Zecca L. Neuromelanin biosynthesis is driven by excess cytosolic catecholamines not accumulated by synaptic vesicles. *Proc. Natl. Acad. Sci*. 2000. 97, 11869-11874.

Suntres, Z. E. Role of antioxidants in paraquat toxicity. *Toxicology.* 2002. 180:65-77.

Swerdlow RH, Parks JK, Davis JN, Cassarino DS, Trimmer PA, Currie LJ, Dougherty J, Bridges WS, Bennett JP, Wooten GF, Parker WD. Matrilineal inheritance of complex I dysfunction in a multigenerational Parkinson's disease family. *Ann Neurol*. 1998 Dec;44(6):873-81.

Swerdlow RH, Parks JK, Cassarino DS, Binder DR, Bennett JP Jr, Di Iorio G, Golbe LI, Parker WD Jr. Biochemical analysis of cybrids expressing mitochondrial DNA from Contursi kindred Parkinson's subjects. *Exp Neurol.* 2001 Jun;169(2):479-85.

Taira, T., Saito, Y., Niki, T., Iguchi-Ariga, S.M.M., Takahashi, K., Ariga, H. DJ-1 has a role in antioxidative stress to prevent cell death. *EMBO Rep*. 2004. 5, 213–218.

Takahashi RN, Rogerio R, Zanin M. Maneb enhances MPTP neurotoxicity in mice. *Res Commun Chem Pathol Pharmacol* 1989;66:167–70.

Takahashi N, Miner LL, Sora I, Ujike H, Revay RS, Kostic V, Jackson-Lewis V, Przedborski S, Uhl GR. 'VMAT2 knockout mice: heterozygotes display reduced amphetamine-conditioned reward, enhanced amphetamine locomotion, and enhanced MPTP toxicity'. *Proc Natl Acad Sci U S A*. 1997 Sep 2;94(18):9938-43.

Takahashi RN, Rogerio R, Zanin M. Maneb enhances MPTP neurotoxicity in mice. *Res Commun Chem Pathol Pharmacol* 1989;66:167–70.

Takahashi-Niki, K., Niki,T., Taira, T., Iguchi-Ariga, S.M.M., Ariga, H., 2004. Reduced anti-oxidative stress activities of DJ-1 mutants found in Parkinson's disease patients. *Biochem. Biophys. Res. Commun.* 320, 389–397.

Takeyama, N., Tanaka, T., Yabuki, T., and Nakatani, T. The involvement of p53 in paraquat-induced apoptosis in human lung epithelial-like cells. *Int. J. Toxicol*. 2004. 23:33–40.

Talpade, D. J.; Greene, J. G.; Higgins Jr., D. S.; Greenamyre, J. T. In vivo labeling of mitochondrial complex I (NADH:ubiquinone oxidoreductase) in rat brain using [(3)H]dihydrorotenone. *J. Neurochem*. 2000. 75:2611–2621

Tan EK, Khajavi M, Thornby JI, Nagamitsu S, Jankovic J, Ashizawa T. Variability and validity of polymorphism association studies in Parkinson's disease. *Neurology*. 2000 Aug 22;55(4):533-8.

Tan JM, Dawson TM. Parkin blushed by PINK1. *Neuron* 2006;50: 527−9.

Tassa A, Roux MP, Attaix D, Bechet DM: Class III phosphoinositide 3-kinase-Beclin1 complex mediates the amino acid-dependent regulation of autophagy in C2C12 myotubes. *Biochem J* 2003, 376:577–586

Tatton W.G., Olanow C.W., Apoptosis in neurodegenerative diseases: the role of mitochondria. *Biochem. Biophys. Acta*, 1999. 1410: 195- 214.

Tatton N.A., Increased caspase-3 and BAX immunoreactivity accompanying nuclear GAPDH translocation and neuronal apoptosis in Parkinson´s disease. *Exp. Neurol., 2000.* 166: 29-43.

Tatton WG, Chalmers-Redman R, Brown D, Tatton N. Apoptosis in Parkinson's disease: Signals for neuronal degradation. *Ann Neurol.* 2003. 53 (Suppl 3):S61–S70. Discussion S70–62.

Tawara T, *et al.*Effects of paraquat on mitochondrial electron transport system and catecholamine contents in rat brain. *Arch Toxicol*. 1996. 70:585–589.

Taxvig C, Hass U, Axelstad M, Dalgaard M, Boberg J, Andeasen HR, Vinggaard AM. Endocrine-disrupting activities in vivo of the fungicides tebuconazole and epoxiconazole. *Toxicol Sci*. 2007 Dec;100(2):464-73.

Testa CM, Sherer TB, Greenamyre JT. Rotenone induces oxidative stress and dopaminergic neuron damage in organotypic substantia nigra cultures. *Brain Res Mol Brain Res*. 2005 Mar 24;134(1):109-18.

Tetrud JW, Langston JW, Redmond DE Jr, Roth RH, Sladek JR, Angel RW. MPTP-induced tremor in human and non-human primates. *Neurology*. 1986; 36(Suppl 1):308.

Thiruchelvam M, Brockel BJ, Richfield EK, Baggs RB, Cory-Slechta DA. Potentiated and preferential effects of combined paraquat and maneb on nigrostriatal dopamine systems: environmental risk factors for Parkinson's disease? *Brain Res* 2000;873:225–34.

Thiruchelvam M, Richfield EK, Goodman BM, Baggs RB, Cory-Slechta DA. Developmental exposure to the pesticides paraquat and maneb and the Parkinson's disease phenotype. *Neurotoxicology* 2002;23: 621–33.

Thomas MR & Wardman OL. Pesticide Usage Survey Report 150.Review of usage of pesticides in agriculture and horticulture throughtout Great Britain 1986-1996. Pesticide Usage Survey Group. Central Science Laboratory, York.

The Pesticide Manual 10th Edition, British Crop Protection Council/Royal Society of Chemistry, 1994.

Thome M, Schneider P, Hofmann K, Fickenscher H, Meinl E, Neipel F, Mattmann C, Burns K, Bodmer JL, Schröter M, Scaffidi C, Krammer PH, Peter ME, Tschopp J. Viral FLICE inhibitory proteins (FLIPs) prevent apoptosis induced by death receptors. *Nature.* 1997 Apr 3;386(6624):517-21.

Thomson JA, Itskovitz-Eldor J, Shapiro SS et al. Embryonic stem cell lines derived from human blastocysts. *Science* 1998;282:1145–1147.

Trimmer PA, Smith TS, Jung AB and Bennett Jr JP. Dopamine neurons from transgenic mice with a knockout of thep53 gene resist MPTP neurotoxicity. *Neurodegeneration*. 1996. 5: 233-239

Trimmer, P.A., Borland, M.K., Keeney, P.M., Bennett Jr., J.P., Parker Jr., W.D. Parkinson's disease transgenic mitochondrial cybrids generate Lewy inclusion bodies. *J. Neurochem.* 2004. 88, 800–812.

Trosko JE, Chang CC. Factors to consider in the use of stem cells for pharmaceutic drug development and for chemical safety assesmant. *Toxicology*. 2009 Nov 27. [Epub ahead of print]

Tsai YC, Fishman PS, Thakor NV, Oyler GA. Parkin facilitates the elimination of expanded polyglutamine proteins and leads to preservation of proteasome function. *J Biol Chem.* 2003 Jun 13;278(24):22044-55.

Tsang MM and Trombetta LD, The protective role of chelators and antioxidants on mancozeb-induced toxicity in rat hippocampal astorcytes, *Toxicology and Industrial Health* 2007; 7: 459–470.

Twelves D, Perkins KS, Counsell C. Systematic review of incidence studies of Parkinson's disease. *Mov Disord*. 2003 Jan;18(1):19-31. Review

Uéda K, Fukushima H, Masliah E, Xia Y, Iwai A, Yoshimoto M, Otero DA, Kondo J, Ihara Y, Saitoh T. Molecular cloning of cDNA encoding an unrecognized component of amyloid in Alzheimer disease. *Proc Natl Acad Sci U S A*. 1993 Dec 1;90(23):11282-6

Ueda, S., Masutani, H., Nakamura, H., Tanaka, T., Ueno, M., and Yodoi, J. Redox control of cell death. *Antioxid. Redox Signal* 2002. 4:405–414.

Ulusoy A, Bjorklund T, Hermening S and Kirik D. In vivo gene delivery for development of mammalian models for Parkinson's disease. *Experimental Neurology.* 2008; 209 (1):89-100.

United States Environmental Protection Agency Pesticides Fact Sheets.

Uversky VN, Li J, Fink AL. Pesticides directly accelerate the rate of alpha-synuclein fibril formation: a possible factor in Parkinson's disease. *FEBS Lett.* 2001 Jul 6;500(3):105-8

Uversky, V. N. Neurotoxicant-induced animal models of Parkinson's disease: understanding the role of rotenone, maneb and paraquat in neurodegeneration. *Cell Tissue Res.* 2004. 318:225–241.

Vaccari A, Ferraro L, Saba P, Ruiu S, Mocci I, Antonelli T, *et al*. Differential mechanisms in the effects of disulfiram and diethyldithiocarbamate intoxication on striatal release and vesicular transport of glutamate. *J Pharmacol Exp Ther* 1998; 285:961–7.

Vaccari A, Saba P, Mocci I, Ruiu S, Dithiocarbamate Pesticides Affect Glutamate Transport in Brain Synaptic Vesicles. *JPET* 1999;288:1–5.

Vaccari A, Saba P, Mocci I, Ruiu S, Dithiocarbamate Pesticides Affect Glutamate Transport in Brain Synaptic Vesicles. *JPET* 1999;288:1–5.

Valente EM., Salvi S., Ialongo T, Marongiu R, Elia A E, Caputo V, Romito L, Albanese A, Dallapiccola B and Bentivoglio AR. PINK1 mutations are associated with sporadic early-onset parkinsonism. *Ann. Neurol*. 2004; 56, 336–341.

Valente EM, Abou-Sleiman PM, Caputo V, Muqit MM, Harvey K, Gispert S, Ali Z, Del Turco D, Bentivoglio AR, Healy DG, Albanese A, Nussbaum R, González-Maldonado R, Deller T, Salvi S, Cortelli P, Gilks WP, Latchman DS, Harvey RJ, Dallapiccola B, Auburger G, Wood NW. Hereditary early-onset Parkinson's disease caused by mutations in PINK1. *Science.* 2004a May 21;304(5674):1158-60.

Van der Walt JM, Nicodemus KK, Martin ER, Scott WK, Nance MA, Watts RL, Hubble JP, Haines JL, Koller WC, Lyons K, Pahwa R, Stern MB, Colcher A, Hiner BC, Jankovic J, Ondo WG, Allen FH, Goetz CG, Small GW, Mastaglia F, Stajich JM, McLaurin AC, Middleton LT, Scott BL, Schmechel DE, Pericak-Vance MA, Vance JM. Mitochondrial polymorphisms significantly reduce the risk of Parkinson disease. *Am J Hum Genet.* 2003 Apr;72(4):804-11.

Van Laar VS and Berman SB. Mitochondrial dynamics in Parkinson's disease. *Experimental Neurology*. 2009. 218(2):247-56

Vanacore N, Nappo A, Gentile M, Brustolin A, Palange S, Liberati A, S. Di Rezze, G. Caldora, M. Gasparini, F. Benedetti, V. Bonifati, F. Forastiere, A. Quercia, G. Meco.

Evaluation of risk of Parkinson's disease in a cohort of licensed pesticide users. *Neurol Sci.* 2002. 23:S119–S120.

Vasseur S, Afzal S, Tardivel-Lacombe J, Park DS, Iovanna JL, Mak TW, DJ-1/PARK7 is animportant mediator of hypoxia-induced cellularm responses. *Proc. Natl. Acad. Sci. U.S.A*. 2009 106, 1111–1116.

Veech GA, Dennis J, Keeney PM, Fall CP, Swerdlow RH, Parker WD Jr, Bennett JP Jr. Disrupted mitochondrial electron transport function increases expression of anti-apoptotic bcl-2 and bcl-X(L) proteins in SH-SY5Y neuroblastoma and in Parkinson disease cybrid cells through oxidative stress. *J. Neurosci. Res.* 2000. 61:693–700.

Vellai T, Autophagy genes and ageing. *Cell Death and Differentiation*. 2009. 16, 94–102

Venero JL, Beck KD, Hefti F. 6-Hydroxydopamine lesions reduce BDNF mRNA levels in adult rat brain substantia nigra. *Neuroreport*. 1994; 5:429–432.

Ventimiglia R, Lau L, Kinloch RA, Hopkins A, Karran EH, Petalidis LP, and Ward RW. Role of Caspases in Neuronal Apoptosis. *Drug Development Research. 2*001.52:515–533

Vila M, Vukosavic S, Jackson-Lewis V, Neystat M, Jakowec M, Przedborski S. Alpha-synuclein up-regulation in substantia nigra dopaminergic neurons following administration of the parkinsonian toxin MPTP. *J Neurochem*. 2000 Feb;74(2):721-9.

Viswanath V, Wu Y, Boonplueang R, Chen S, Stevenson FF, Yantiri F, Yang L, Beal MF, Andersen JK. Caspase-9 activation results in downstream caspase-8 activation and bid cleavage in 1-methyl-4-phenyl-1,2,3,6-tetrahydropyridine-induced Parkinson's disease. *J Neurosci.* 2001 Dec 15;21(24):9519-28

Vogel RO, Janssen RJ, Ugalde C, Grovenstein M, Huijbens RJ, Visch HJ, van den Heuvel LP, Willems PH, Zeviani M, Smeitink JA, Nijtmans LG. Human mitochondrial complex I assembly is mediated by NDUFAF1. *FEBS J.* 2005 Oct;272(20):5317-26.

Vogiatzi T, Xilouri M, Vekrellis K, Stefanis L: Wild type alpha-synuclein is degraded by chaperone-mediated autophagy and macroautophagy in neuronal cells. *J Biol Chem* 2008, 283:23542.

Volles MJ & Lansbury PT, Vesicle permeabilization by protofibrillar alpha-synuclein is sensitive to Parkinson's disease-linked mutations and occurs by a pore-like mechanism. *Biochemistry* 2002 Apr 9; 41(14):4595-602.

von Coelln R, Thomas B, Savitt JM, Lim KL, Sasaki M, Hess EJ, Dawson VL, Dawson TM. Loss of locus coeruleus neurons and reduced startle inparkin null mice. *Proc Natl Acad Sci USA* 2004; 101:10744–10749.

Wajant, H., Pfizenmaier, K., and Scheurich, P. Tumor necrosis factor signaling. *Cell Death Differ*. 2003. 10, 45–65.

Wang J, Xu Z, Fang H, Duhart HM, Patterson TA, Ali SF. Gene expression profiling of MPP+ treated MN9D cells: a mechanism of toxicity study. *Neurotoxicology*. 2007 Sep;28(5):979-87

Watabe M, Nakaki T. Rotenone induces apoptosis via activation of bad in human dopaminergic SH-SY5Y cells. *J Pharmacol Exp Ther.* 2004 Dec;311(3):948-53.

Webb JL, Ravikumar B, Atkins J, Skepper JN, Rubinsztein DC. Alpha-synuclein is degraded by both autophagy and the proteasome. *J Biol Chem* 2003; 278: 25009–13.

Westerlund M, Hoffer B, Olson L. Parkinson's disease: exit toxins; enter genetics. *Prog Neurobiol*. 2010 Feb 9;90(2):146-56.

Westermann, B. Merging mitochondria matters: cellular role and molecular machinery of mitochondrial fusion. *EMBO Rep*. 2002. 3, 527–531.

Wider C & Wszolek K. Clinical genetics of Parkinson's disease and related disrders. *Parkinsonism and related disorders.* 2007; 13, S229-S232.

Willingham S, Outeiro TF, DeVit MJ, Lindquist SL, Muchowski PJ. Yeast genes that enhance the toxicity of a mutant huntingtin fragment or alpha-synuclein. *Science*. 2003 Dec 5;302(5651):1769-72.

Wilkinson JC, Richter BW, Wilkinson AS, Burstein E, Rumble JM, Balliu B, Duckett CS. VIAF, a conserved inhibitor of apoptosis (IAP)-interacting factor that modulates caspase activation. *J Biol Chem.* 2004 Dec 3;279(49):51091-9.

Withers G. S., George J. M., Banker G. A., and Clayton D. F. Delayed localization of synelfin (synuclein, NACP) to presynaptic terminals in cultured rat hippocampal neurons. *Dev. Brain Res.*1997. 99, 87–94.

Wood SJ, Wypych J, Steavenson S, Louis JC, Citron M, Biere AL. alpha-synuclein fibrillogenesis is nucleation-dependent. Implications for the pathogenesis of Parkinson's disease. *J Biol Chem.* 1999 Jul 9;274(28):19509-12.

Wood-Kaczmar A, Gandhi S, Wood NW. Understanding the molecular causes of Parkinson's disease. *Trends Mol Med.* 2006 Nov;12(11):521-8.

Wredenberg A, Wibom R, Wilhelmsson H, Graff C, Wiener HH, Burden SJ, Oldfors A, Westerblad H, Larsson NG. Increased mitochondrial mass in mitochondrial myopathy mice. *Proc Natl Acad Sci U S A*. 2002 Nov 12;99(23):15066-71

Wright JM, Keller-Byrne J. Environmental determinants of Parkinson's disease. *Arch Environ Occup Health*. 2005 Jan-Feb; 60(1):32-8.

Wullner, U., Lo¨schmann, P.-A., Schulz, J.B., Schmid, A., Dringen, R., Eblen, F., Turski, L., Klockgether, T. Glutathione depletion potentiates MPTP and MPP+ toxicity in nigral dopaminergic neurones. *NeuroReport*. 1996. 7, 921-923.

Xie T, Tong L, Barrett T, Yuan J, Hatzidimitriou G, McCann UD, Becker KG, Donovan DM, Ricaurte GA. Changes in gene expression linked to methamphetamine-induced dopaminergic neurotoxicity. *J. Neurosci.* 2002. 22: 274–283.

Xu J, Kao SY, Lee FJ, Song W, Jin LW, Yankner BA. Dopamine-dependent neurotoxicity of alpha-synuclein: a mechanism for selective neurodegeneration in Parkinson disease. *Nat Med*. 2002 Jun;8(6):600-6.

Xu Z, Cawthon D, McCastlain KA, Slikker W Jr, Ali SF. Selective alterations of gene expression in mice induced by MPTP. *Synapse.* 2005 Jan;55(1):45-51.

Xu, J., Zhong, N.,Wang, H., Elias, J.E., Kim, C.Y., Woldman, I., Pifl, C., Gygi, S.P., Geula, C., Yankner, B.A., 2005. The Parkinson's diseaseassociated DJ-1 protein is a transcriptional co-activator that protects against neuronal apoptosis. *Hum. Mol. Genet*. 2005; 14, 1231–1241.

Xue L, Fletcher GC, and Aviva M. Tolkovsky1Autophagy Is Activated by Apoptotic Signalling in Sympathetic Neurons: An Alternative Mechanism of Death Execution. *Molecular and Cellular Neuroscience*. 1999; 14:180–198

Yamada M, Iwatsubo T, Mizuno Y, Mochizuki H. Overexpression of alpha-synuclein in rat substantia nigra results in loss of dopaminergic neurons, phosphorylation of alpha-synuclein and activation of caspase-9: resemblance to pathogenetic changes in Parkinson's disease. *J Neurochem*. 2004 Oct;91(2):451-61

Yamaguchi H, Shen J. Absence of dopaminergic neuronal degeneration and oxidative damage in aged DJ-1-deficient mice. *Molecular Neurodegeneration*. 2007; 2:10.

Yang Y, Nishimura I, Imai Y, Takahashi R, Lu B.Parkin suppresses dopaminergic neuron-selective neurotoxicity induced by Pael-R in Drosophila.*Neuron*. 2003 Mar 27;37(6):911-24.

Yang W, Tiffany-Castiglioni E. Paraquat-induced apoptosis in human neuroblastoma H-SY5Y cells: involvement of p53 and mitochondria. *J Toxicol Environ Health.* 2008;71(4):289-99.

Yang Q, She H, Gearing M, Colla E, Lee M, Shacka JJ, Mao Z. Regulation of neuronal survival factor MEF2D by chaperone-mediated autophagy. *Science*. 2009 Jan 2;323(5910):124-7

Yoritaka A, Hattori N, Uchida K, Tanaka M, Stadtman E, Mizuno Y. Immunohistochemical detection of 4-hydroxynonenal protein adducts in Parkinson disease. *Proc Natl Acad Sci USA*. 1996; 93:2696–2701

Yue Z., Horton A., Bravin M., DeJager P.L., Selimi F., and Heintz N. A novel protein complex linking the d2 glutamate receptor and autophagy: implications for neurodegeneration in Lurcher mice. *Neuron*. 2002. 35: 921-933.

Yue, Z., Jin, S., Yang, C., Levine, A. J. & Heintz, N. Beclin 1, an autophagy gene essential for early embryonic development, is a haploinsufficient tumor suppressor. *Proc. Natl Acad. Sci. USA*. 2003. 100:15077–15082

Yokota T, Sugawara K, Ito K, Takahashi R, Ariga H, Mizusawa H. Down regulation of DJ-1 enhances cell death by oxidative stress, ER stress, and proteasome inhibition. *Biochem Biophys Res Commun.* 2003 Dec 26;312(4):1342-8.

Zakeri Z, Bursch W, Tenniswood M, Lockshin RA. Cell death: programmed, apoptosis, necrosis, or other? *Cell Death Differ.* 1995 Apr;2(2):87-96

Zarranz JJ, Alegre J, Gomez-Esteban JC, et al. The new mutation, E46K, of alpha-synuclein causes Parkinson and Lewy body dementia. *Ann Neurol* 2004; 55:164 –173.

Zamzami N, Susin SA, Marchetti P, Hirsch T, Gomez-Monterrey I, Castedo M and Guido K, Mitochondrial control of nuclear apoptosis. *Journal of Experimental Medicine* 1996, 183: 1533–1544

Zecca L, Gallorini M, Schunemann V, Trautwein AX, Gerlach M, Riederer P, Vezzoni P, Tampellini D. Iron, neuromelanin and ferritin content in the substantia nigra of normal subjects at different ages: consequences for iron storage and neurodegenerative processes. *J Neurochem. 2001.* 76: 1766–1773

Zhang, Y., Gao, J., Chung, K.K., Huang, H., Dawson, V.L., Dawson, T.M. Parkin functions as an E2-dependent ubiquitin–protein ligase and promotes the degradation of the synaptic vesicle-associated protein, CDCrel-1. *Proc. Natl. Acad. Sci. U. S. A.* 2000b; 97, 13354–13359.

Zhang J, Fitsanakis VA, Gu G, Jing D, Ao M, Amarnath V, Montine TJ. Manganese ethylene-bis-dithiocarbamate and selective dopaminergic neurodegeneration in rat: a link through mitochondrial dysfunction. *J Neurochem*. 2003; 84:336–346

Zhang XD, Gillespie SK, Hersey P. Staurosporine induces apoptosis of melanoma by both caspase-dependent and -independent apoptotic pathways. *Mol Cancer Ther.* 2004 Feb;3(2):187-97

Zhao H, Piwnica-Worms H. ATR-mediated checkpoint pathways regulate phosphorylation and activation of human Chk1. *Mol Cell Biol.* 2001 Jul;21(13):4129-39.

Zheng, W., and Zhao, Q. Iron overload following manganese exposure in cultured neuronal, but not neuroglial cells. *Brain Res*. 2001. 897, 175–179.

Zhou Y, Shie FS, Piccardo P, Montine TJ, Zhang J. Proteasomal inhibition induced by manganese ethylene bis-dithiocarbamate: relevance to Parkinson's disease. *Neuroscience*. 2004. 128:281–291.

Zhou W, Zhu M, Wilson MA, Petsko GA, Fink AL. The oxidation state of DJ-1 regulates its chaperone activity toward alpha-synuclein. *J Mol Biol.* 2006 Mar 3;356(4):1036-48.

Zhou C, Huang Y, Shao Y, May J, Prou D, Perier C, Dauer W, Schon EA, Przedborski S. The kinase domain of mitochondrial PINK1 faces the cytoplasm. *Proc Natl Acad Sci U S* A. 2008 Aug 19;105(33):12022-7

Fig
Immunocyto
mical stainir
toxin tre
cells hN

Zhu JH, Horbinski C, Guo F, Watkins S, Uchiyama Y, Chu CT. Regulation of autophagy by extracellular signal-regulated protein kinases during 1-methyl-4-phenylpyridinium-induced cell death. *Am J Pathol*. 2007 Jan;170(1):75-86

Zoratti M and Szabo I, The mitochondrial permeability transition. *Biochimica et Biophysica Acta* 1995. 1241:139–176